# PROTON AND PHOSPHORUS SPECTROSCOPY OF HYPOXIC, ISCHAEMIC AND HAEMORRHAGIC PERINATAL BRAIN INJURY

CAROL J. PEDEN

DOCTOR OF MEDICINE

UNIVERSITY OF EDINBURGH.

1996



## DECLARATION

This thesis was composed by me and is based on work conducted at the Magnetic Resonance Unit in the Royal Postgraduate Medical School and Hammersmith Hospital. All magnetic resonance spectroscopy examinations were performed by a team of researchers. I was a key member of the team for the examinations reported here: I drew up the protocols for these studies and developed the hypotheses on which they were based; I was responsible for the clinical management of all the patients while in the magnetic resonance unit; Dr. D. Menon and I, selected all monitoring and ventilation equipment used, and modified it as necessary with the help of Dr. A. Hall; I helped set up and run the magnet system for each patient examination; I was solely responsible for the analysis of the paediatric proton data and for the presentation of that data, and was helped in the analysis of the phosphorus data by Dr. I.J. Cox.

Carol J. Peden.

March 1994.

CONTENTS


Page

i ABSTRACT

ii AIMS

iii LIST OF ABBREVIATIONS

iv ACKNOWLEDGEMENTS

1. THE DEVELOPMENT OF CLINICAL SPECTROSCOPY: AN HISTORICAL REVIEW

9. MAGNETIC RESONANCE SPECTROSCOPY

10. Physical Principles of Magnetic Resonance Spectroscopy

23. The phosphorus spectrum

27. The proton spectrum

31. Localization techniques

41. Technical Methods

53. HYPOXIA AND ISCHAEMIA IN THE NEWBORN INFANT

54. Hypoxia and ischaemia in the newborn infant: the clinical problem

61. Hypoxic-ischaemic injury to the brain: biochemistry

66. Magnetic resonance spectroscopy and hypoxic-ischaemic damage to the human brain

72. Sedation, anaesthesia and monitoring.

77. Clinical Methods

85. In vivo and in vitro CNS tumour studies

87. RESULTS

90. Monitoring equipment

92. Proton spectroscopy

109. Phosphorus spectroscopy.
125. Localized phosphorus spectra.
129. Proton and phosphorus spectroscopy.

134. DISCUSSION.
140. Proton spectroscopy.
150. Phosphorus spectroscopy.
155. Proton and phosphorus spectroscopy.
158. Conclusions.

REFERENCES

APPENDICES

conqueror

## ABSTRACT

Proton magnetic resonance spectroscopy was investigated as a non-invasive technique to observe biochemical changes in the brains of children who had sustained perinatal hypoxic, ischaemic and haemorrhagic brain injury.

Methods:

Proton spectra were acquired from the centre of the brain in premature infants, and from the parieto-occipital region in older children. Phosphorus spectra were also collected and compared with the proton spectra. Unlocalized phosphorus spectra were acquired at different repetition times. Some children had localized phosphorus spectroscopy examinations with two and four dimensional chemical shift imaging. The children were between 33 weeks post-conceptional age and four years and three months postnatal age at the time of their initial spectroscopy examination. The ability of early proton spectroscopy to predict outcome was considered in relation to the clinical neurological state at eighteen months or more. Because certain assumptions were made about the proton spectra (e.g. no $T_2$ measurements were made), proton spectra were acquired from adults with central nervous system tumours. At surgery, biopsies were taken from the tumours and from normal brain and were analysed with in vitro spectroscopy, histology and established biochemical techniques. The metabolite ratios were compared with those from the in vivo spectra. Modifications were made to commercially available monitoring and ventilation equipment to provide the same standards of care within the magnetic field for sick patients, as on the neonatal or intensive care units.

Results:

All the proton spectra had peaks attributable to N-Acetyl aspartate (NAA), choline containing compounds (Cho) and creatine plus phosphocreatine (Cr). The NAA/Cho and NAA/Cr peak height ratios increased with age, while the Cho/Cr ratio decreased. The NAA/Cr ratios were significantly decreased in all children with an abnormal neurological outcome when compared with the NAA/Cr ratios from children with a normal outcome. The NAA/Cho ratios were significantly decreased in those children with a moderate outcome but not in those with a severe neurological outcome. There were no significant changes in the Cho/Cr ratios.

The phosphorus spectra showed changes; phosphocreatine (PCr) to inorganic phosphate (Pi) decreased after injury and there was a marked increase in pH in the children with the poorest outcome. The apparent $T_1$ of Pi was increased in the first month after birth in the children with a severe outcome. Few changes were seen with localized phosphorus spectroscopy in children who had focal lesions. Phosphorus spectra returned to normal within weeks of birth, while the proton spectra remained abnormal.

The adult tumour proton spectra compared well with the in vitro spectra and histology of the biopsies. The concentrations changes of metabolites in vivo, were consistent with the measurements made with established biochemical techniques.

Discussion:

Hypoxic-ischaemic injury produced changes in the proton spectrum from neonatal brain. These changes persisted with time. Some of these changes correlated with outcome. Phosphorus spectra showed acute changes in response to injury, but the changes resolved within weeks. NAA is located in neurons; the decrease in NAA could be due to failure of neurons to develop normally, or to areas of neuronal loss and gliosis resulting from hypoxic-ischaemic damage. Phosphorus spectra may return to normal because neurons and glia have similar phosphorus metabolite ratios. Proton spectroscopy combined with magnetic resonance imaging, may become a useful technique for studying the anatomy and biochemistry of the brain in children who have suffered brain injury.

## AIMS

1. To use proton and phosphorus magnetic resonance spectroscopy as non-invasive methods of observing biochemical changes produced in neonatal brain by hypoxic and ischaemic injury.

2. To develop a safe and easily applicable system for monitoring and ventilating critically ill neonates, as well as adults, for prolonged periods within a magnetic resonance system.

3. To observe the changes in proton spectra of brain that are associated with normal development and ageing from premature infants to adults.

4. To validate our proton spectra through comparison with clinical examination, other established imaging and neurological monitoring techniques, and in vitro spectra.

5. To compare the changes seen in the proton spectra from neonatal brain with later neurological outcome, and to evaluate the potential of proton spectroscopy for predicting outcome after neonatal hypoxic-ischaemic injury.

6. To explore further some aspects of phosphorus spectroscopy, particularly the effects, if any, of hypoxia and ischaemia on $T_1$ relaxation effects in phosphorus spectra.

7. To use phosphorus chemical shift imaging in neonates and infants, and to compare this technique with magnetic resonance imaging and unlocalized phosphorus spectroscopy.

8. To compare phosphorus magnetic resonance spectroscopy with proton magnetic resonance spectroscopy as a means of studying the abnormal infant brain.

## LIST OF ABBREVIATIONS

| | |
|---|---|
| ATP | adenosine triphosphate |
| $^{13}C$ | $^{13}$ carbon |
| CHESS | chemical shift selective |
| Cho | choline containing compounds |
| Cr | creatine and phosphocreatine |
| CSI | chemical shift imaging |
| CT | computerised axial tomography |
| 2D, 4D | two dimensional, four dimensional |
| 2,3DPG | 2,3 diphosphoglycerate |
| DRESS | depth resolved surface coil spectroscopy |
| EEG | electroencephalography |
| $^{19}F$ | $^{19}$ fluorine |
| FID | free induction decay |
| GABA | γ aminobutyric acid |
| g | gauss |
| $^{1}H$ | proton |
| ISIS | image selected in vivo spectroscopy |
| Lac | lactate |
| MESA | multi echo stimulated acquisition |
| MR | magnetic resonance |
| MRI | magnetic resonance imaging |
| MRS | magnetic resonance spectroscopy |
| $^{23}Na$ | $^{23}$ sodium |
| NAA | N-acetylaspartate |
| NAAG | N-acetylaspartyl glutamate |
| NMR | nuclear magnetic resonance |
| $^{31}P$ | $^{31}$ phosphorus |

| | |
|---|---|
| PCr | phosphocreatine |
| PCA | post-conceptual age |
| PDE | phosphodiester |
| pHe | extracellular pH |
| pHi | intracellular pH |
| Pi | inorganic phosphate |
| PME | phosphomonoester |
| PNA | post-natal age |
| ppm | parts per million |
| PRESS | point resolved spectroscopy |
| RF | radio frequency |
| SPARS | spatially resolved spectroscopy |
| STEAM | stimulated echo |
| T | Tesla |
| TE | echo time |
| TR | repetition time |
| US | ultrasound |
| VSE | volume selective excitation |

## ACKNOWLEDGEMENTS

I would like to thank the following for the help and encouragement they have offered during the preparation of this thesis: all the staff at the NMR Unit , Hammersmith Hospital, in particular Dr Ian Young and Dr David Bryant; Professor David Gadian, Dr Neville Goodman, and my husband, Robin Smith. Funding for my post as a clinical research fellow was from the Medical Research Council.

# THE DEVELOPMENT OF CLINICAL SPECTROSCOPY AN HISTORICAL REVIEW

The phenomenon of nuclear magnetic resonance (NMR) was first described in 1946 by Felix Bloch and coworkers at Stanford University, and Edward Purcell and coworkers at Harvard, work that won both of them the Nobel prize for physics in 1952. During the next thirty years magnetic resonance spectroscopy (MRS) was widely used as an analytical tool in chemistry to analyse small homogeneous samples in the laboratory. This non-invasive non-destructive technique provided structural and conformational analysis of complex molecules in vitro; however, the widespread application of spectroscopy to analyse living tissue in biochemistry and medicine was to take much longer.

Shortly after the first NMR experiments were performed (Bloch, Purcell 1946), Bloch produced a proton signal from his finger: this was the first NMR signal from living tissue. During the next decade other researchers produced data from animal and human tissues (Odeblad et al 1956, Singer 1959). In these early studies the proton nucleus was used because of its high isotopic abundance, its high receptivity and its relevance to organic structure determination. The magnetic resonance signal was detected from small samples at relatively low fields (e.g. 0.67 Tesla (T) in Odeblad's experiment).

It was not until the early 1970s (Hoult et al 1974), when high field superconducting magnets and Fourier transform techniques were developed, that NMR became widely used to analyse samples of tissue, and the potential of in vivo spectroscopy began to be realised.

Initial work concentrated on the phosphorus nucleus because the resonances seen in the phosphorus spectrum, namely, adenosine triphosphate (ATP), phosphocreatine (PCr) and inorganic phosphate (Pi), are compounds central to the bioenergetic state of living cells, and intracellular pH can be obtained from the frequency of the inorganic phosphate signal. However, the relatively small number of observable compounds

visible and the physiological mechanisms that exist to correct abnormal phosphorus metabolism, ultimately limit the value of $^{31}P$ MRS for metabolic studies.

In the 1970s, $^{31}P$ spectra were obtained from isolated cells showing that ATP, PCr and 2,3 diphosphoglycerate (DPG) could be detected. Moon and Richards (1973) measured intracellular pH from the chemical shift of the inorganic phosphate and 2,3(DPG) resonances in human and rabbit red blood. Other groups used similar techniques (Ogawa et al 1978, Shulman et al 1979), for example Ogawa et al (1978) measured rapid changes in the pH of E. coli suspensions in response to increased oxygen concentrations.

In 1974 Hoult and his colleagues in Oxford described the measurement of phosphorus metabolites in intact rat muscle; the ratio of phosphocreatine to inorganic phosphate varied with stimulation of the muscle, and the pH decreased as the muscle aged. They saw the potential of $^{31}P$ MRS in biological systems, stating that it could yield information about metabolite levels, turnover, interactions and compartmentation (Hoult et al 1974).

These experiments were exciting demonstrations of the ability of MRS to examine intact tissue, measure intracellular pH and monitor metabolic interactions and reaction rates, but further development of the in vivo technique was limited by the design and the size of the magnet and by the deterioration of the tissue under study during the experiment.

In the next few years magnet design improved and the magnet bores were widened; new radiofrequency coils were developed and new methods of localization, namely surface coils (Ackerman et al, 1980), were used in phosphorus spectroscopy. It became possible to maintain isolated organs in good physiological condition within the bore of a magnet and changes in metabolite concentrations could be monitored during physiological stimuli and pathological insults.

In 1973 Lauterbur published a paper describing an NMR method for studying the

spatial distribution of molecules within a sample. This principle is the basis for magnetic resonance imaging, developments in which were later to be closely linked to improvements in, and the wider application of, clinical spectroscopy.

In 1978 Chance and coworkers produced the first $^{31}P$ MRS from intact animal brain. A mouse was placed, anaesthetized and inverted, in a conventional NMR spectrometer (with an 18mm bore) and its head surrounded by a radiofrequency coil. $^{31}P$ MRS signals of the head, from brain and overlying muscle, showed peaks for ATP, PCr and Pi. Acute hypoxia decreased PCr and pH, and increased Pi. The in vivo spectra had a lower inorganic phosphate concentration than spectra obtained from freeze-clamped brain tissue. A similar observation was made by Ackerman and coworkers (1980); they used surface coils to study different regions of the animal and localised metabolic changes induced by ischaemia were measured. They commented that MRS was ideally suited to the study of brain metabolism because of the difficulties in accurate analysis by freeze extraction methods of a tissue that is so sensitive to short periods of hypoxia or ischaemia.

This type of experiment, observing changes produced in the phosphorus spectrum by a variety of insults, demonstrated different responses in different types of tissue. Norwood and colleagues (1979) found, in studies of perfused rodent brain, that ATP and phosphocreatine declined simultaneously, whereas in skeletal muscle ATP concentration did not decline until phosphocreatine was almost completely depleted.

In 1981, a year after magnetic resonance imaging became practicable in the human body, Ross and coworkers described a phosphorus magnetic resonance spectroscopy study of a patient with McArdle's syndrome using a simple surface coil. This report was the first application of spectroscopy to clinical disease and was therefore a landmark in the development of spectroscopy. There have been many subsequent studies of human muscle, especially by Radda and his colleagues in Oxford and Chance and his coworkers in Philadelphia. The human muscle studies can be broadly divided into two groups: those that observe changes in metabolism in diseased muscle; and

those that follow metabolic changes produced in normal muscle by stresses such as exercise, ischaemia and starvation (Radda et al 1989).

Spectroscopy was recognised as a means of monitoring therapy, illustrated in reports such as that by Griffiths et al (1983), who observed with a surface coil the progression of a rhabdomyosarcoma on a hand during chemotherapy. This application has since been widely used to observe the changes in tumour metabolism produced by different treatments.

These early studies on humans were particularly suited to the high field magnets in use at the time (1.6T-2.5T), which had clear bore sizes of only 18-25cm. This restricted studies to those practicable in such a small space: on the upper and lower limbs of adults and the brains of newborn infants.

The first neonatal phosphorus magnetic resonance studies were carried out at University College Hospital in London (Cady et al 1983) and showed a decrease in brain PCr and a rise in Pi after severe birth asphyxia. At about the same time, similar studies were being performed by another group of workers in Philadelphia (Younkin et al 1984) Further studies by both groups confirmed these early findings and showed correlations between the degree of changes in the phosphorus spectra and subsequent outcome (Azzopardi et al 1989b).

Although there have been spectroscopy studies of paediatric liver, most of the spectroscopic work in infants and children has been done on the brain. As well as changes resulting from hypoxia and ischaemia, spectral abnormalities are found in CNS tumours and metabolic disorders (Bottomley 1989a).

With the rapid development of magnetic resonance imaging from 1980 onwards came improvement in magnet design, localization techniques and the design of receiver coils. These advances were applied to spectroscopy. Most spectroscopic studies up to this time had been with surface coil localization. These types of coil were ideal for studies

of muscle or the unlocalized studies of infant brain. However, to examine organs within the body such as the heart or liver, or to study specific regions of an organ, more sophisticated localization techniques were required. The application of the magnetic field gradients used for imaging achieved this. The technical requirements for spectroscopy are different from imaging and so different types of pulse sequence are used. Three of the more common sequences are depth resolved surface coil spectroscopy (DRESS), chemical shift imaging (CSI) and image selected in vivo spectroscopy (ISIS). None of these localization techniques is clearly the best under all circumstances and they remain championed by their own enthusiasts. Localization techniques are discussed further in another section of this thesis.

In 1983 Bottomley et al reported the combination of magnetic resonance imaging and spectroscopy for the study of anatomy, biochemistry and metabolism at 1.5T in a 1m bore magnet. The $^{31}P$ and $^{13}C$ spectra were acquired with surface coils using a DRESS localization technique to produce spectra from the brain of an adult. Bottomley subsequently used this localization technique to produce spectra from infarcted myocardium and showed similar changes resulting from ischaemia to those seen previously in muscle and neonatal brain (Bottomley et al 1987a).

Clinical proton spectroscopy took much longer to develop than phosphorus as it is technically more demanding. Proton MRS allows visualization of a large number of resonances, but the large number of metabolites present within a smaller chemical shift dispersion can make peak assignment difficult. Because the frequency dispersion is directly related to magnetic field strength the problem of resolution is much more marked at field strengths in clinical use, i.e. less than 2.35T. The two principal resonances in the proton spectrum are from water and fat. The concentration of body water (about 40M) provides the signal for the high quality images produced by MRI, but spectroscopists are interested in the signal from other metabolites, present at concentrations of less than 5mM. To see these, the water and fat resonances must be suppressed.

An in vivo high resolution proton MRS spectrum was acquired from a sample of

human dystrophic muscle in 1982 (Edwards et al, 1982), but small concentrations of metabolites could not be discerned because of low spectral resolution and the presence of large water and fatty acid residues. In 1983 Behar and colleagues reported the acquisition of high resolution proton spectra with excellent signal to noise from rat brain in vivo. They recorded an increase in lactate concentration with hypoxia. The other principal metabolites seen in the in vivo spectra were phosphocholine, phosphocreatine, creatine, N-acetylaspartate and glutamate; there were no obvious changes in the size of these metabolite peaks during the hypoxic insult.

In 1985 Bottomley and colleagues were the first group to report clinical proton spectra from intact tissue within a whole body magnet. They recorded localized and water suppressed proton spectra of human brain and muscle in vivo, using the DRESS technique. These spectra showed only a few resonances; better resolution of metabolite resonances was achieved later by combining water suppression with volume selective techniques such as spatially resolved spectroscopy (SPARS) (Luyten and den Hollander 1986), stimulated echo (STEAM) (Frahm et al 1987), and image selected in vivo spectroscoy (ISIS) (Hanstock et al 1988).

The first reported proton spectra from human brain showed peaks that were assigned to N-acetylaspartate (NAA), choline containing compounds (Cho), creatine plus phosphocreatine (Cr) and lipid-$CH_2$-resonances (Bottomley et al 1985). High resolution proton spectra from normal volunteers at 1.5T subsequently identified other metabolites; acetate, γ-aminobutyrate, glutamine, glutamate, aspartate, taurine, lactate and inositols (Frahm et al 1989a). Later in the same year Frahm et al (1989b) reported on the relaxation times of the metabolite signals seen in human brain spectra and the regional differences in concentration of these metabolites.

Other studies showed abnormal amounts of lactate in the brains of patients after cerebral infarction (Luyten et al 1987). Bruhn and colleagues (1989) described a patient with acute cerebral infarction who had complete loss of NAA and markedly elevated lactate. They suggested that the loss of NAA might represent neuronal death. Work on proton

spectroscopy, especially of the human brain, continues at a great pace. Many other studies will be discussed in the relevant sections of this thesis.

The other nuclei accessible for human MRS studies are $^{13}$carbon ($^{13}$C), $^{23}$sodium ($^{23}$Na) and $^{19}$fluorine ($^{19}$F). Spectroscopy of all three has produced interesting results but they have not yet received the widespread attention given to phosphorus and proton spectroscopy. Lactate, glutamate, aspartate and alanine can be visualised with $^{13}$C MRS, but it is expensive as a $^{13}$C labelled substrate (e.g. $^{13}$C glucose) is usually given intravenously because of the low natural isotopic abundance of $^{13}$C. $^{13}$C spectroscopy has produced very interesting information on carbohydrate metabolism but most of this work is confined at present to a small number of laboratories, such as that of Shulman and coworkers (Shulman et al 1990). $^{23}$Na MRS can distinguish intracellular from extracellular Na using dysprosium (generally in chelated form), an agent that alters the chemical shift of extracellular $^{23}$Na. However this has not been used in humans partly because of concerns about toxicity. There is very little natural fluorine in the body and so $^{19}$F spectroscopy is normally performed to detect introduced fluorocompounds such as the fluorinated anaesthetic agents (Menon et al 1990 b).

The development and application of MRS has been much slower than for MRI, the technique that has made such a dramatic impact on medical imaging in the last decade. There are several reasons for this. MRS must be performed at high field strengths (typically 1.5T or above) to achieve adequate spectral resolution. Greater magnetic field homogeneity is required and this often prolongs the setting up time for each patient. The regions of study must be larger for MRS than for MRI, as spectroscopy examines metabolites present at low concentrations, while MRI uses the 40M signal from water to produce images. Because of this, signal acquisition takes longer for MRS as a large number of repetitions must be averaged to achieve an adequate signal to noise ratio. MRS provides biochemical information not images, and therefore requires a knowledge of the relevant biochemistry to interpret any changes.
Some of the most successful applications of MRS to date, have been to observe

changes in metabolism produced by intervention or stress. These may be provoked during the study, such as the response of the liver to a fructose infusion, or may have already occurred, for example after neonatal hypoxic-ischaemic brain injury. MRS can be used to observe these changes noninvasively. Many of the clinical problems for which MRS could be of great value, such as the response to therapy of the critically ill patient in an intensive care unit or operating theatre, are not yet possible because of practical problems. Until there are dramatic changes in magnet design, size and shielding, this type of study must remain for the future. At present MRS remains described as a "potentially powerful clinical tool"; I hope this thesis may in some small way contribute to the realisation of that potential.

# MAGNETIC RESONANCE SPECTROSCOPY:

## PHYSICAL PRINCIPLES ; SPECTRA; LOCALIZATION TECHNIQUES; TECHNICAL METHODS

The basis of nuclear magnetism.

All atomic nuclei have charge due to protons, and mass due to protons and neutrons. In addition, the nuclei of some atoms possess spin, a property that may be visualised as a rotation of the nucleus about an axis. When a nucleus has even numbers of both protons and neutrons the pairs of protons and neutrons align so that their spins cancel out. Spin exists for a nucleus (isotope) only when it contains an odd (unpaired) proton, an odd neutron, or both. Just as the flow of electrons in a wire loop produces a magnetic field (Fig.1), the rotation of the charged protons in a spinning nucleus produces a local magnetic field (Fig.2). The nucleus therefore behaves like a miniature bar magnet.

Behaviour of NMR sensitive nuclei in a magnetic field.

When NMR sensitive nuclei (nuclei with a spin) are placed in a static magnetic field (the $B_0$ field), they tend to align themselves with the field. This axis is arbitrarily labelled 'Z'. About half of the nuclei align parallel to the field and the other half antiparallel to it (Fig.3). The nuclei in the antiparallel state are at a higher energy level, resulting in a small excess of nuclei in the lower energy parallel state, and a small net magnetization parallel to the $B_0$ field. It is this small excess of nuclei in the parallel state (typically of the order of $1\text{-}2/10^6$) that is of interest. Since such a small proportion of available nuclei are responsible for the NMR phenomenon, and since the energy transitions involved are small, magnetic resonance is inherently an insensitive technique, and for in vivo studies can only detect substances present in millimolar concentrations or above.

The resonant frequency of a nucleus and its determinants.

When aligned with the field, the nuclei continue to spin, and at the same time their axes rotate around the Z axis, a combination of movements that is termed precession: the same movement as a spinning top in the earth's gravitational field (Fig.4). The frequency of nuclear precession ($\upsilon$) depends on two variables: the gyromagnetic ratio

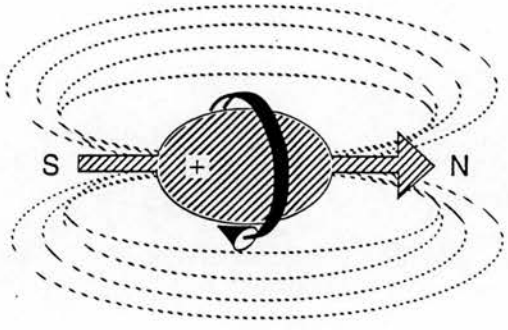



Fig.1 Diagrammatic representation of current flowing through a coil and producing an electromagnetic field. N and S in this and subsequent diagrams represent the north and south poles of the magnet.

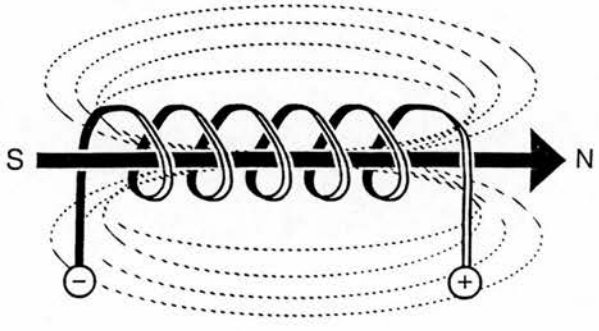



Fig.2 Diagrammatic representation of a spinning atomic nucleus. Movement of the positively charged protons produces a magnetic field, causing the nucleus to behave like a tiny bar magnet.

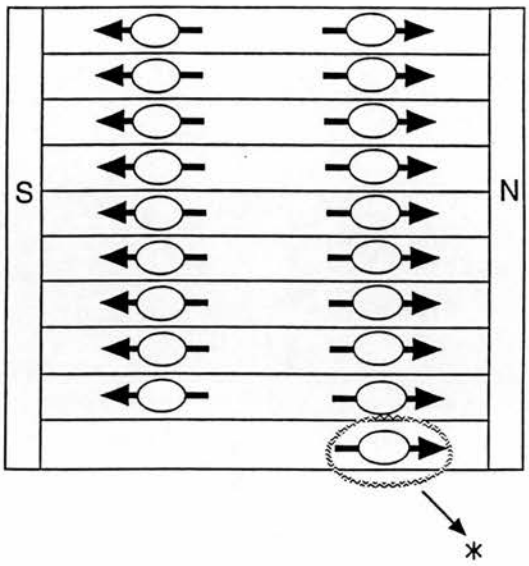



Fig.3 Diagrammatic representation of NMR-sensitive nuclei aligned in a magnetic field. Nuclei are aligned either parallel or antiparallel to the field. A small excess of nuclei (1-2/$10^6$) are parallel to the field (*), and are responsible for the NMR phenomenon.

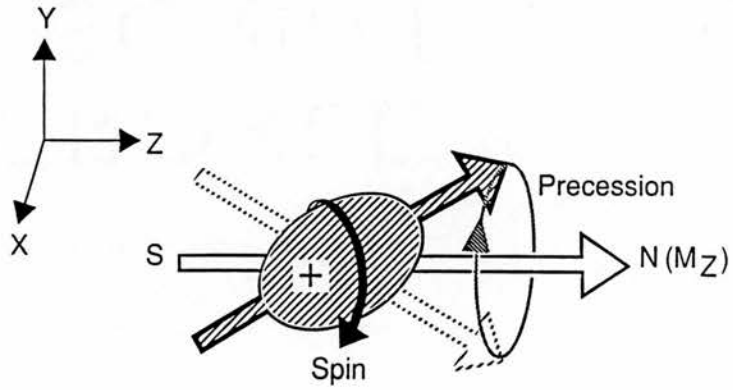



Fig.4 Behaviour of an NMR sensitive nucleus aligned with a magnetic field. The nucleus spins on its own axis, and precesses about the magnetic axis.

($\gamma$), which is specific for each isotope, and the strength of the magnetic field ($B_0$):

$$\upsilon = \gamma.B_o/2\pi$$

Thus, each nucleus has a characteristic or resonant frequency at a given magnetic field strength (Table 1). The specificity of this frequency enables the selection of a particular nucleus for study.

Excitation of nuclei by a second magnetic field and the production of the NMR signal.

When such a population of nuclei is subjected intermittently to a second time dependent magnetic field ($B_1$), oscillating at the resonant frequency of the nucleus and orientated at right angles to the static magnetic field ($B_0$), (a radiofrequency [RF] pulse), they tend to flip away from their longitudinal alignment and produce a net coherent magnetization in a plane at right angles to the Z axis (the XY plane) (Fig. 5). Depending on the strength and duration of the pulse of the resonant RF field, the nuclei can be rotated from their equilibrium position of alignment with Z to any angle to the main magnetic field. Pulses which rotate the total resultant magnetization (M) from Z to the XY plane are called $90^o$ or $\pi/2$ pulses, and a pulse which inverts the magnetization is a $180^o$ or $\pi$ pulse. The magnetization in the XY plane is still precessing around the Z axis, and decays with time after each exciting pulse. A stationary loop of wire in the presence of such a nucleus would therefore be subjected to a changing magnetic field, and consequently have current induced within it (Fig. 6). This current would have a decaying sinusoidal waveform, whose frequency is the same as the frequency of nuclear precession, the resonant frequency ($\upsilon$). The current represents the NMR signal, or the free induction decay (FID), and can be subjected to Fourier transformation, a mathematical manipulation which allows the frequency content to be analysed. The time domain signal (FID) representing signal strength as a function of time is transformed to a frequency domain representing signal strength versus frequency. This results in a spectrum (Fig. 6).

## TABLE 1.

| NUCLEUS | SPIN QUANTUM NO. | RESONANCE FREQUENCY AT 1.6T IN MHz | NATURAL ABUNDANCE % | RELATIVE SENSITIVITY AT CONSTANT FIELD |
|---|---|---|---|---|
| $^{1}H$ | 1/2 | 68.0 | 99.98 | 100 |
| $^{13}C$ | 1/2 | 17.2 | 1.1 | $1.6 \times 10^{-2}$ |
| $^{19}F$ | 1/2 | 60.18 | 100.0 | 83.0 |
| $^{23}Na$ | 3/2 | 18.02 | 100.0 | 9.3 |
| $^{31}P$ | 1/2 | 27.5 | 100.0 | 6.6 |

TABLE 1: spin quantum number, resonant frequency at 1.6 T, natural abundance and relative sensitivity at constant field for $^{1}H$, $^{13}C$ $^{19}F$, $^{23}Na$ and $^{31}P$ .

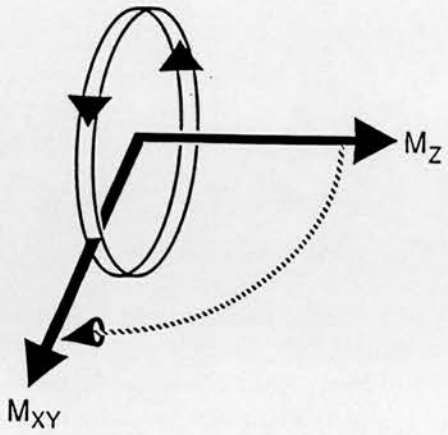



Fig.5 Application of an oscillating ($B_1$) field causes the magnetization along 'Z' to flip into the XY plane, where it continues to precess around the Z axis.

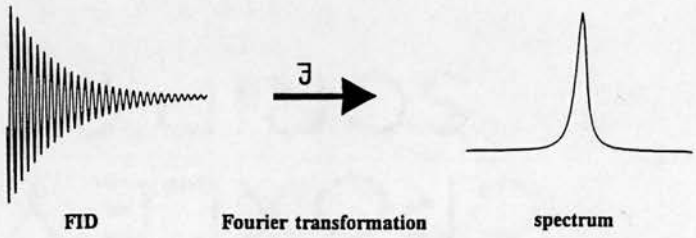



Fig.6 The decaying sinusoidal waveform on the left is the free induction decay (FID) and represents the current induced in a copper wire palaced in the vicinity of an excited nucleus (as in Fig.5). Fourier transformation of the FID results in a spectrum where intensity is plotted against frequency.

Effects of chemical structure on resonant frequency: the chemical shift ($\delta$).

The frequency of a given signal depends on the nucleus studied and the strength of the magnetic field that it experiences. What makes NMR a powerful chemical tool is that the magnetic field experienced by each individual nucleus is subtly modified by the effects of electrons around it; this causes a slight change in resonant frequency when chemical composition changes. Thus the proton spectrum from water is a single line because the two hydrogen nuclei within each water molecule have the same chemical environment (Fig.7). The proton spectrum from acetic acid has two peaks, each from protons in their own chemical environments (Fig.8). The position of each peak on the horizontal axis is usually expressed as displacement from the resonance of an internal or external reference compound and is termed chemical shift. The chemical shift ($\delta$) is usually expressed as parts per million (ppm) of the reference frequency, which allows comparison of chemical shifts at different field strengths. In addition, the area of each peak is related to the number of protons contributing to a particular resonance; thus NMR in the form of MRS can provide quantitative chemical information.

Factors affecting signal to noise ratio of a spectrum.

The signal to noise ratio can be measured from the spectrum.

Factors which affect the signal to noise ratio include;

(a). the nucleus being studied and the concentration of the nuclei present.

(b). the $B_o$ field strength.

(c). the volume of the sample (spectral resolution within small volumes will be better than that obtained for larger volumes in the absence of localization, but a smaller volume results in a reduction in signal to noise ratio).

(d). the design of the radiofrequency coil (Hoult and Richards 1976).

(e). line broadening which will be increased by inhomogeneities in the static magnetic field.

(f). relaxation phenomena ($T_1$ and $T_2$)

(g). the time for which the spectra are accumulated: several free induction decays may need to be averaged to produce a spectrum with useful amounts of signal in relation to

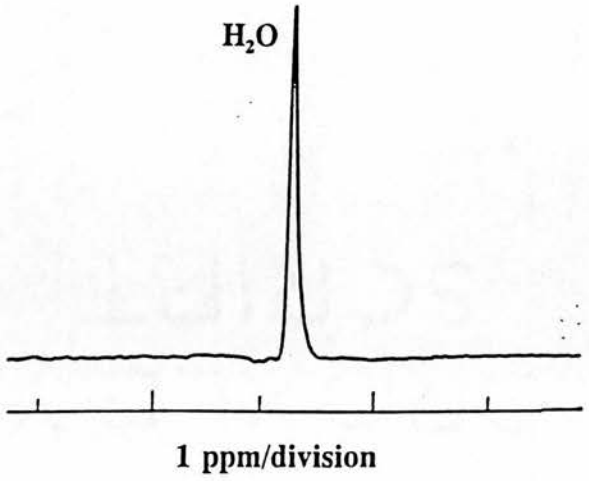



Fig.7 Proton spectrum of water. All the protons are in a similar chemical environment and produce a single resonance.

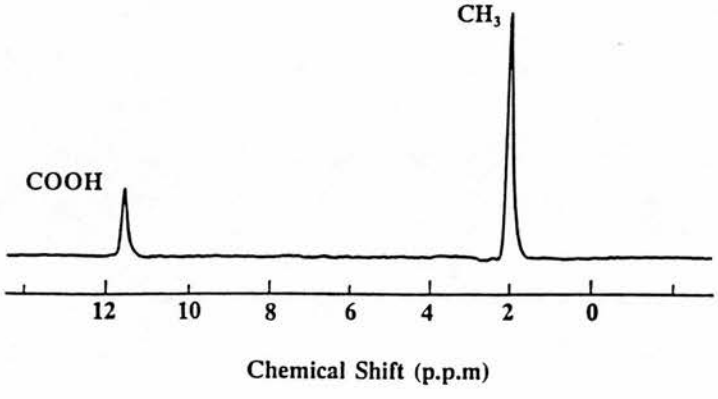



Fig.8 Proton spectrum of acetic acid. Protons in the methyl ($CH_3$) group are in a different chemical environment from those in the carboxyl (-COOH) group, resulting in two separate resonances. Since there are three times as many methyl as carboxyl protons, the $CH_3$ resonance is three times the intensity of the -COOH resonance.

background noise, especially when the nucleus studied is present in low concentrations. Signal varies directly with the number of scans, as noise is random it tends to cancel itself out with an increasing number of acquisitions so signal/noise varies as the square root of the number of scans.
Taking all these factors into account the signal to noise ratio is approximately equal to 2.5 x signal height/ peak to peak noise.

The relaxation times $T_1$ and $T_2$.

After the radiofrequency pulse is switched off the magnetization decays; the newly established magnetization in the XY plane disappears (transversal relaxation) and the magnetization along the Z axis recovers (longitudinal relaxation) (Fig.9). The time that it takes for the Z component magnetization to recover is described by the longitudinal relaxation time or time constant for exponential recovery $T_1$. The energy is dispersed from the nuclei to their surroundings; hence this decay is also known as spin-lattice relaxation. If the time between successive radiofrequency pulses is short, nuclei with a long $T_1$ will recover incompletely between excitations, resulting in decreasing amounts of signal, a process termed saturation (Fig.10). This can be used to measure $T_1$ variables for different signals.

The time taken for the transverse magnetization in the XY plane to decay is characterized by the spin-spin relaxation time, $T_2$ (Fig.11). When $T_2$ is long the signal decays more slowly. $T_2$ and $T_1$ can be used to provide a measure of the mobility of the environment of a given nucleus, $T_2$ increasing with increasing molecular mobility, and decreasing with molecular restriction. In practice most biologically significant NMR signals are those that arise predominantly from small mobile molecules. The signals from larger molecules have short $T_2$ values (i.e. decay very rapidly) and tend not to be picked up, or to be seen as a broad line which is lost during the processing of the spectrum.

After the RF pulse is switched off the protons develop different precession frequencies

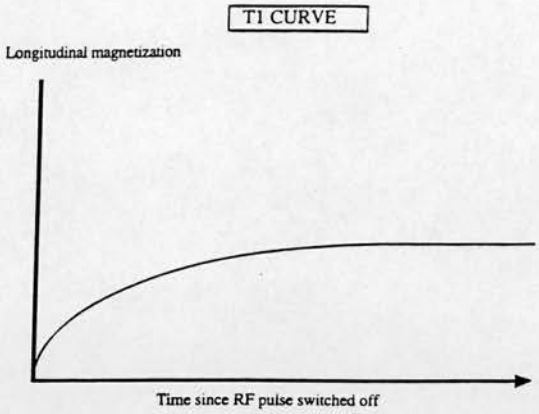



Fig. 9. Plot of the longitudinal magnetization against time after the radiofrequency pulse is switched off. The time that it takes for the Z component magnetization to recover is described by the spin-lattice relaxation time, $T_1$, the time constant for exponential recovery.

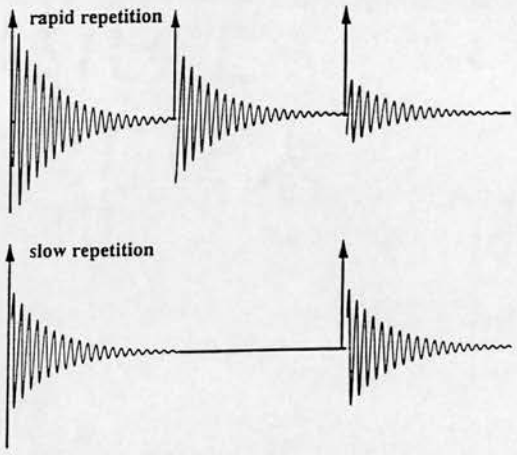



Fig. 10. Effect of repetition time (TR) on signal levels. Successive excitations are denoted by vertical arrows. In (i) the TR is short, recovery of magnetization between succesive pulses is incomplete and signal from successive pulses is attenuated. In (ii) the long TR allows complete recovery of magnetization and signal strength is maintained with successive pulses.

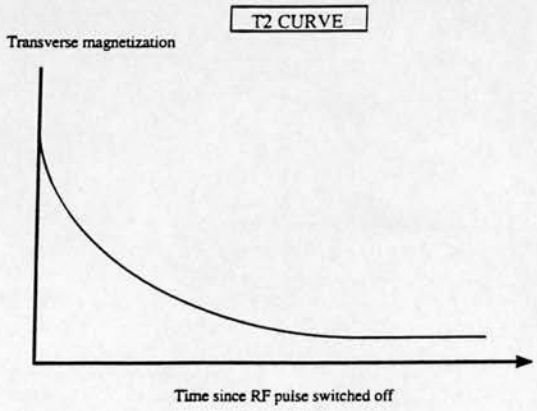



Fig. 11. Plot of the transverse magnetization against time after the radiofrequency pulse is switched off. The time taken for the transverse magnetization in the XY plane to decay is characterized by the spin-spin relaxation time, $T_2$.

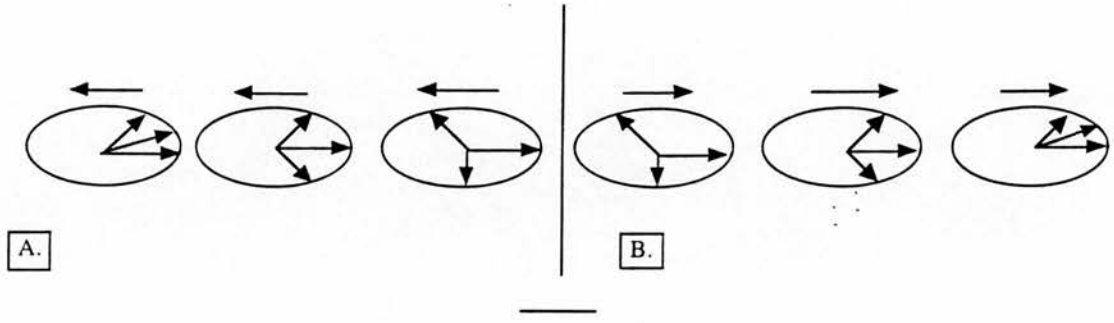
because of local magnetic field inhomogeneities and the influence of small unevenly distributed magnetic fields from neighbouring nuclei. As the nuclei fan out owing to their different precession frequencies, transverse magnetization decreases. The effects of magnetic field inhomogeneities remain constant over the period of data acquisition, their contribution to signal decay or phase coherence can be reversed by using a special pattern of RF pulses to recall the original signal as a 'spin echo' (Fig 12).

The factors determining $T_1$ and $T_2$ are numerous, but $T_1$ and $T_2$ are most sensitive to the degree of molecular motion of the sample. In solids and at low temperatures, there is little molecular motion and $T_1$ may be many seconds (s), while $T_2$ is only microseconds (μs). In liquids and at higher temperatures they are almost equal, both being about two seconds for water. $T_2$ can never be longer than $T_1$, and if the ratio of $T_2$ to $T_1$ approaches unity the sample may be assumed to be relatively liquid. These differences in relaxation times are used in MRI to create different appearances of areas such as grey and white matter in the human brain.

Spin-spin coupling:

The spins of two nuclei close together can interact, affecting the energy state of each other. We will call the two nuclei A and X as is convention. In a large population of molecules containing these two nuclei almost half the spins will be in a slightly higher energy state and the other half in a slightly lower energy state. This means that for the A nuclei for example, half will be at one energy level and half at another. The signals from the A nuclei are therefore split roughly 50:50 into two distinct but close spectral lines (Fig. 13). The separation of the two components of peak A is a constant known as $J$, the spin spin coupling constant, which is measured in Hz as it is independent of magnetic field strength. The splitting of the two components of peak A is therefore also known as $J$ splitting.

Spin-spin coupling can occur when two nuclei are bonded together or when the spin interaction is transmitted through intervening chemical bonds. Coupling patterns have




After the RF pulse is switched off, the protons dephase (A). The 180º pulse causes them to precess in the opposite direction and so they rephase (B).

Fig.12 The contribution of magnetic field inhomogeneities to signal decay can be reversed by using a 180º pulse which causes the nuclei to precess in the opposite direction and rephase; this is known as a spin echo sequence.

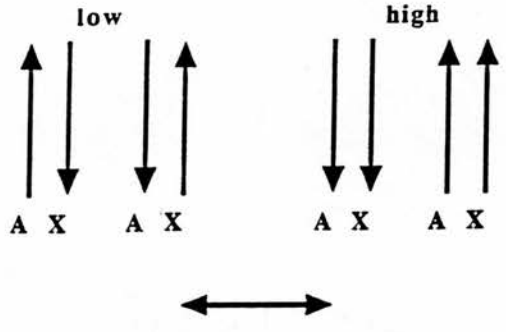



Fig.13 This illustrates the four possible spin states that exsist for two coupled nuclei A and X, both of spin 1/2. The + 1/2 and -1/2 energy states are represented by upward-pointing and downward-pointing arrows respectively.

been used to identify compounds within a spectrum. Spectra can be divided into two groups, first order and second order, on the basis of spin-spin coupling characteristics. First order spectra occur when the frequency differences between the resonances of the nuclei involved in spin-spin coupling are much smaller than the chemical shift; second order spectra occur when that is not the case. Spectra can be simplified and peak assignments made by spin decoupling (Gadian 1982).

## THE PHOSPHORUS SPECTRUM.

The phosphorus spectrum shown in figure 14 is from the brain of a normal infant, five days old. The peaks seen are from the three phosphate groups of ATP ($\gamma$, $\alpha$, $\beta$), phosphomonoesters (PME), phosophodiesters (PDE), inorganic phosphate (Pi) and phosphocreatine (PCr).

Most ATP is complexed to magnesium ($Mg^{2+}$) ions and the degree of ion binding affects the chemical shift of ATP. The signal from the $\gamma$-phosphate group of ATP may contain a contribution from the $\beta$-phosphate group of ADP. The $\alpha$-phosphate group signal at -7.5 ppm may contain contributions from ATP and ADP; a shoulder on this peak is characteristic of the phosphate signals from $NAD^+$ and NADH. An estimate of the concentrations of the various components of the three ATP peaks is made by comparing their areas, on the basis that the $\beta$-ATP peak is solely ATP.

The peak at 0 ppm is from phosphocreatine. This signal is used as a reference for the other chemical shifts of the spectrum. Phosphocreatine has a pKa of about 4.6 and its resonance frequency is insensitive to pH changes within the normal physiological range.

The chemical shift of the inorganic phosphate (Pi) peak is used to measure intracellular pH as its frequency is especially sensitive to pH in the physiological range (Petroff et al 1985). Inorganic phosphate exists mainly as $HPO_4^{2-}$ and $H_2PO^{4-}$ at about neutral pH. If there were no interchange between these two groups then the spectrum would have two distinct peaks. However, in solution the two species exchange with each other very rapidly and the resulting spectrum has a single peak, the chemical shift of which is determined by the relative amounts of each ion species.

The main problem with this method of measuring pH in clinical spectroscopy is the dependence on a reference which is normally phosphocreatine. In extreme tissue

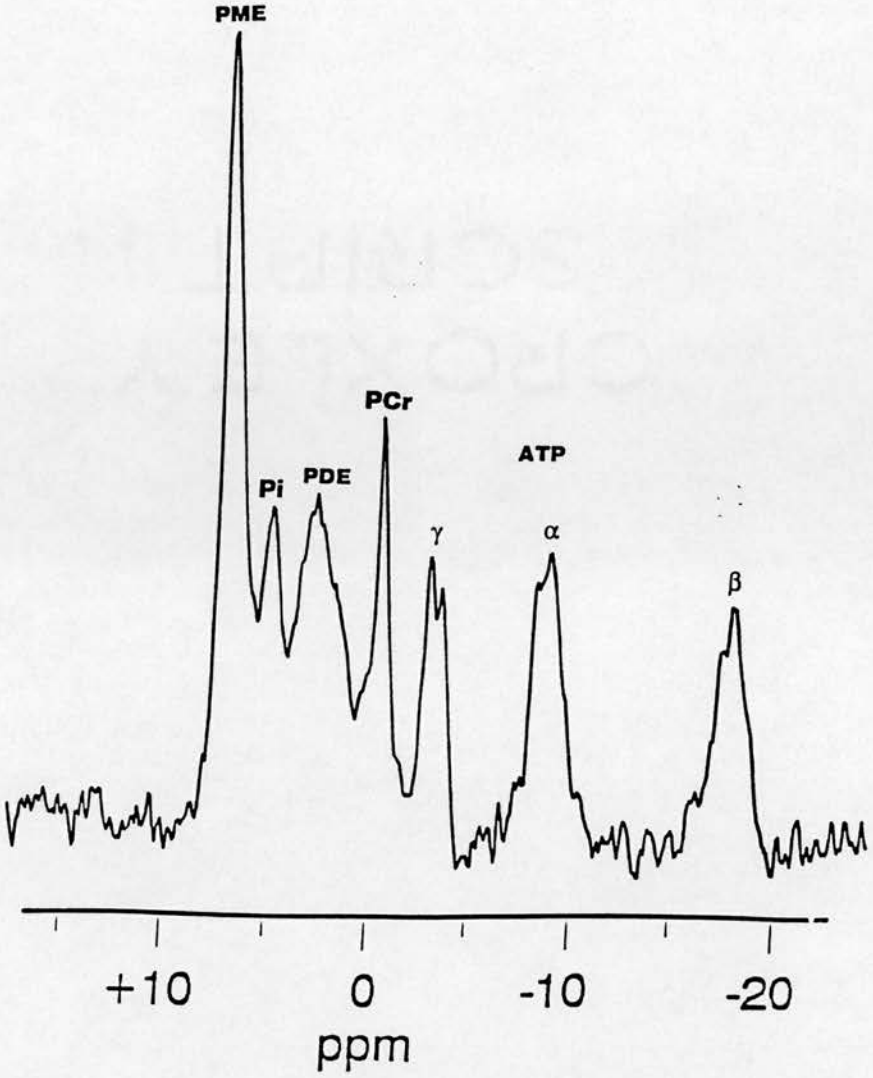



Fig.14 Unlocalized phosphorus spectrum from the brain of an infant (DT) with a normal neurological outcome, born at 38 weeks post conceptional age (PCA) and five days old at the time of examination. The phosphorus spectrum was acquired at 27.5MHz, at a repetition time (TR) of 5s with a 128 data collects. For this and subsequent phosphorus spectra no vertical scaling has been applied. The peaks seen on the spectrum are as follows: phosphomonoesters (PME), inorganic phosphate (Pi), phosphodiesters (PDE), phosphocreatine (PCr), and the three peaks ($\gamma$, $\alpha$, $\beta$) of adenosine triphosphate (ATP). The metabolite ratios of this spectrum are: PCr/Pi, 1.3; PME/PDE, 1.2; PCr/$\beta$ATP, 1.0 and the pH is 7.05.

Chemical shifts are expressed in the dimensionless units of parts per million (ppm) and are independent of the magnitude of the $B_0$ field. The chemical shift is obtained from the difference between the shielding constants of the sample and of the reference nucleus. Most clinical spectra are presented with the low frequency signals (from nuclei that are more shielded than the reference nucleus) to the right of the reference nucleus with a negative chemical shift. All spectra presented in this thesis conform to that convention.

damage little phosphocreatine remains and the peak is poorly defined. In this situation the accuracy of the pH measurement decreases as its biochemical relevance increases. The accuracy of the measurement under less extreme circumstances is thought to be about 0.04 to 0.1 pH unit, when the signal-to noise ratio is 3 or more, and up to 0.14 pH unit or more, with a signal-to noise ratio of 1-3, even for narrow line widths (Madden et al 1991). The Pi peak may be broad or split into two components, which implies that Pi is in two different environments, each with a slightly different pH (Busby et al 1978). This may be useful clinically. For example, within the sample there may be a region of healthy tissue with a normal pH, next to a region of dying cells with an acidic pH.

In phosphorus spectra from neonates the dominant peak is at about 7ppm (Fig. 14). This peak is within the phosphomonoester region (PME), and decreases markedly with age. In contrast, the peak at around 2ppm, in the phosphodiester region (PDE), is small in the neonatal spectrum (Fig. 14) and much larger in adult brain. The changes in these peaks with age will be considered further in the discussion.

The areas under the peaks in the spectrum can be used for the measurement of concentration ratios only if all the peaks are fully relaxed (that is, long enough repetitition times have been used to allow the magnetization to return to its equilibrium value). There is often not enough time for this during a clinical examination. If this criterion is not fulfilled then correction factors must be applied to express relative concentrations accurately.

Hope and coworkers (1984) used a range of pulse intervals and showed that by 20s relaxation was almost complete in all the peaks except PME. They predicted from a computer model that the fully relaxed signal from PME would be 7% greater at full relaxation than at 20s. They then derived correction factors, or saturation factors, by dividing the peak area at 20s by the peak area at 2s (adding 7% for PME). These saturation factors have been referred to subsequently by many other investigators, and little further investigation has been done on the effects of disease on them. This has

important implications, as the measurement of absolute and relative concentrations may be inaccurate if the saturation factors are altered by the disease process.

Spectral analysis

In vivo spectra are much more difficult to analyse than in vitro spectra, as the peaks are usually not well separated and are not on a flat baseline. Peak areas can be estimated in four ways (Meyer et al 1988):

(a). Peak height is easy to measure. Because it is a single measurement at the peak centre it may be less susceptible to distortion by neighbouring peaks than computer integration techniques. However, peak heights only reflect areas if the widths are the same.

(b). Triangulation: using a paper plot of the spectrum straight lines are drawn through a peak to fit it to a triangular shape; the area of the triangle is then calculated from its dimensions.

(c). Computer integration of the spectrum: a 'gate' is defined around each peak using two cursors on a computer screen and the integral of the spectrum between these two points is computed. Peak overlap means that the integral line has no straight horizontal position between the two peaks.

(d). Computer fitting of the spectrum using for example a Lorentzian fitting routine is the most accurate way available at present of analysing spectra.

## THE PROTON SPECTRUM

The proton spectrum is more complex than the phosphorus spectrum as there are many more resonances which can be detected within a small chemical shift range. The proton nucleus is the most sensitive nucleus (after tritium) and is present in almost all biological compounds. The much greater sensitivity of the proton nucleus than the phosphorus nucleus (100: 6.6) offers a 15-fold increase in signal to noise ratio, or a reduction by a factor of 225 ($15^2$) in signal averaging time at the same magnetic field strength. However, the number of molecules detectable and the greater sensitivity make it difficult to resolve the many overlapping resonances in the proton spectrum (Fan et al 1986). Also, the spectrum is dominated by an enormous water peak (about 80M proton signal) that must be suppressed to visualise the other metabolites, present in only millimolar concentrations (Fig.15).

The spectrum shown in figure 16a is from the brain of a patient with an intracerebral tumour. The spectrum in figure 16b is an in vitro spectrum from a biopsy of the same tumour. These two spectra illustrate the difference in resolution between proton spectra currently available clinically at 1.6T, and those acquired at the much higher field strengths (500 MHz in this example) and more ideal conditions of the laboratory. In vitro systems may run all night to acquire one spectrum, which is obviously not possible clinically. Although some MR system manufacturers are marketing clinical proton spectroscopy software programmes to operate on 1.0T magnet systems, most clinical proton spectroscopy studies have been performed at field strengths of 1.5T or more to achieve adequate resolution of the spectrum.

The principal resonances in the proton spectrum from human brain are from N-acetylaspartate (NAA, 2.02ppm), choline-containing compounds such as phosphorylcholine and glycerophosphorylcholine (Cho, 3.2ppm), and creatine and phosphocreatine (Cr, 3.0ppm; see figure 16a).

N-acetylaspartate (NAA) usually gives the largest metabolite peak in the water-

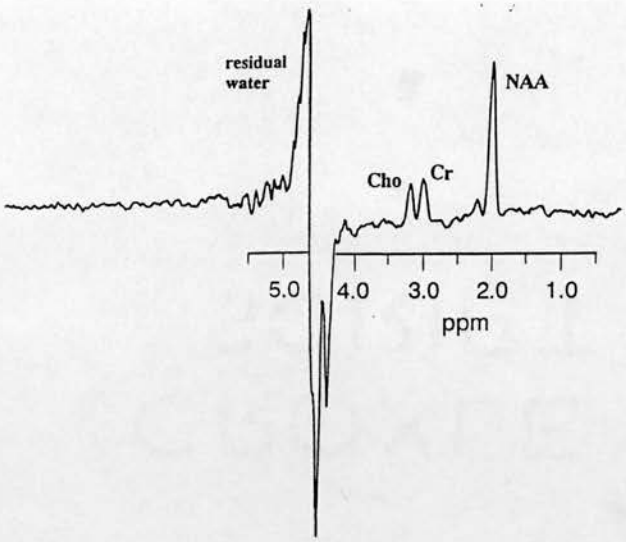



Fig.15 Proton spectrum of the brain acquired from an $8mm^3$ voxel in the parietal region of an adult volunteer. The complex resonance on the left arises from tissue water that has been suppressed by a factor of about 200 to allow visualisation of metabolites present in millimolar concentrations.

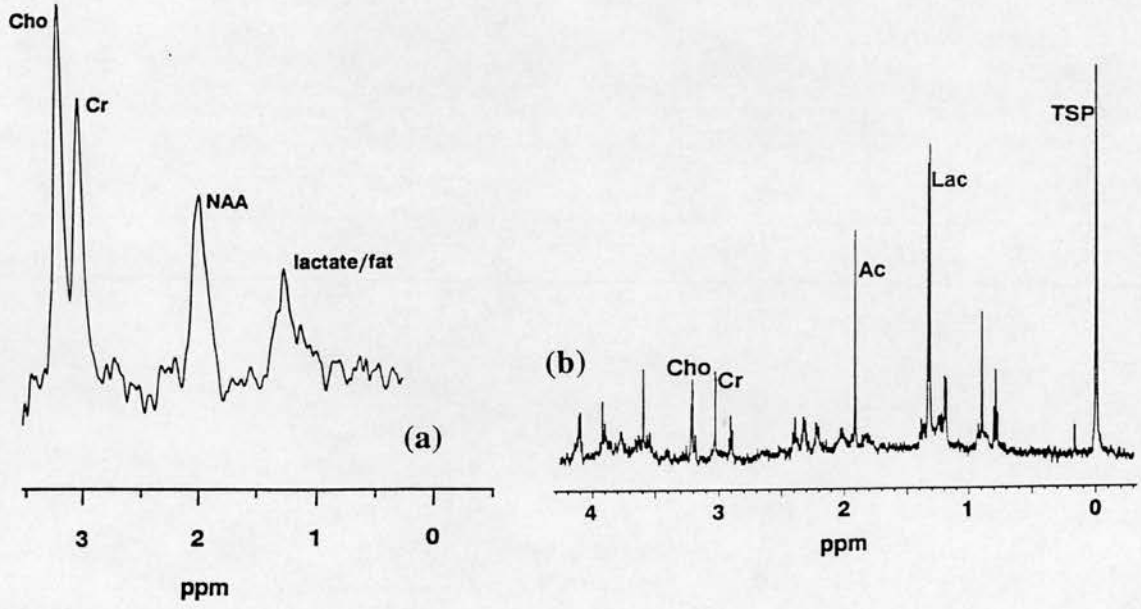



Fig. 16.

(a) Proton spectrum acquired from a $64cm^3$ volume, composed mainly of tumour, in the brain off a patient awaiting intracerebral surgery. The spectrum was acquired in vivo at 1.6T. The peaks seen in this spectrum are from N-acetylaspartate (NAA), choline containing compounds (Cho), creatine and phosphocreatine (PCr), and a peak which could be due to lactate or fat (Lac/fat). The NAA/Cho and NAA/Cr ratios are very much lower than those from the normal brain spectrum shown above.
(b) Proton spectrum acquired from a biopsy of the same tumour, taken at surgery. This spectrum was generated in vitro at 500MHz. The differences in the resolution of the two spectra are very obvious.

suppressed proton spectrum. Before clinical proton spectroscopy little attention was paid to NAA, and there were only a few reports of disorders involving NAA. Very high NAA concentrations are found in the urine, blood and brain of children with Canavan's disease, a rare autosomal recessive leukodystrophy which results in severe mental retardation, hypotonia and premature death (Austin et al 1991). As yet, little is known about the function of this amino acid derivative but it appears to be found primarily within neurons. Nadler and Cooper (1972) showed that NAA is localized in neurons by comparing NAA levels in whole brain with levels in tumours of the central nervous system. These glial cell tumours showed virtually no NAA. Insults to the brain resulting in neuronal loss cause a decrease in NAA concentration (Koller et al 1984; Bruhn et al 1989).

NAA may be a storage form of aspartate, because it has no effect on amino acid receptors, is not incorporated into peptides and is very mobile. Its mobility is the main reason for the sharp peak seen in clinical spectra (Birken and Oldendorf 1989). Alternatively NAA may be a breakdown product of another compound such as N-acetyl-aspartyl-glutamic acid (NAAG). NAAG and other compounds are known to contribute to the NAA peak seen in human spectra (Frahm et al 1989 a and b) and the actual concentration of NAA is thought to be 30-40% less than that suggested by the size of the NAA peak in the proton spectrum (Hanstock et al 1989). Brain contains an enzyme that catalyzes the synthesis of NAA from acetyl-CoA and L-aspartic acid; the distribution of this enzyme is similar to that of NAAG and therefore NAA may be a precursor of NAAG. The breakdown pathways of NAA are not yet well defined, although one route is breakdown by an acylase to aspartic acid and acetate (Birken and Oldendorf 1989).

In clinical spectra there may also be a large lipid peak at about 1.3ppm, which can be reduced by good spatial localization. Unfortunately, the lipid signal overlaps the position of the lactate resonance, and no conclusion should be made about the lactate concentration unless the fat peak is adequately suppressed. Other resonances that may be seen include glutamate and γ-aminobutyrate (GABA), glutamine, aspartate, taurine,

alanine and inositols (Narayana et al 1989; Frahm et al 1989 a and b, Gadian et al 1986). Some of these resonances, namely glutamine, GABA, aspartate, taurine and inositol, are difficult to identify at field strengths around 1.5T, and their presence has been confirmed by phantom studies (Frahm et al 1989 a and b).

Many proton spectra are no longer first-order spectra at 1.5T, where the typical *J* splitting of 5-10Hz corresponds to 0.1-0.15ppm and therefore often approaches the chemical shift difference of coupled spins. The result is complex lineshapes that overlap other multiplets. Taurine, for example at high fields, displays two multiplets for the N-$CH_2$ and S-$CH_2$ groups at 3.2 and 3.4 ppm. However, for clinical studies at 1.5T these two multiplets collapse into a broad resonance peaked at 3.3 ppm. Inositol produces several signals in high field spectra, only one of which is seen at 1.5T at an echo time of 50ms; at the echo time usually used in our experiments, 270ms, there is almost no signal. These resonances come and go according to the echo time used.

Narayana et al (1989 ) reported that the concentration of NAA was consistently higher in grey than in white matter, and the concentrations determined using the in vivo MR technique were greater than values previously determined by extraction techniques. One possible reason for the higher value obtained with in vivo spectroscopy is the overlap of the resonances of glutamate and γ-aminobutyrate and other N-acetyl containing compounds with the NAA resonance at 2.02ppm. Compounding difficulties in determining concentration are the $T_1$ and $T_2$ relaxation effects. The need to use factors to correct for $T_1$ and $T_2$ effects applies to all metabolites in the proton spectrum and, as mentioned previously, to the phosphorus signals also.

The $T_1$ and $T_2$ relaxation times for several regions of the normal adult human brain have been established by Frahm and colleagues (1989b), but at the time of this study no data were available on proton $T_1$ and $T_2$ times in spectra of immature brain.

## LOCALIZATION TECHNIQUES

Excellent quality spectra giving valuable clinical information can be obtained without localization; indeed there is a valid argument for using little or no localization for studies of global ischaemia or trauma in the brain. The substantial sensitivity advantage of acquiring spectra from unlocalized brain, compared with much smaller localized volumes, can outweigh the clinical value of observing the spatial distribution of such disorders and the reduction in signal to noise ratio incurred. However, to examine discrete lesions within organs, or to observe tissue heterogeneity, localization techniques are required.

Data acquisition with a surface coil is the easiest and most sensitive method available to localize chemical information from superficial tissues, but the study of internal organs using a surface coil is more difficult. In animal work, internal organs can be examined by exposing the organ surgically and placing the surface coil directly on it. This is not possible for human spectroscopy; one of the important advantages of spectroscopy in man is that it is non-invasive. Other localization methods have therefore been developed. In these techniques either radiofrequency, static or time dependent magnetic field gradients are used to improve the control and definition of the region under study. Localization techniques can be grouped on this basis into three general categories:

(a). Static spatial gradients used in the main magnetic field e.g topical magnetic resonance.
(b). Spatial gradients used in the radiofrequency excitation or detection fields e.g surface coil and rotating frame zeugmatography/ imaging.
(c). Pulsed spatial gradients at audio frequencies (i.e. the gradients used for MRI) e.g. volume selective excitation, depth resolved surface spectroscopy, image selected in vivo spectroscopy, spatially resolved spectroscopy, stimulated echo sequence and two to four dimensional chemical shift imaging.

Reviews of the different localization methods are given by Aue (1986), Bottomley

(1987c) and more recently in the Spectroscopy chapter by Matson and Weiner in "Magnetic Resonance Imaging" (eds. Stark and Bradley 1992).

(a). Methods using static focusing of $B_0$ (Gordon et al 1980, Oberhaensli et al 1987) apply the fact that high-resolution spectra can be obtained only in a volume with high $B_0$ homogeneity (topical magnetic resonance). Special gradient coils produce an approximately spherical volume of homogeneous magnetic field in regions close to the centre of the magnet. Outside this region the spectral lines are broadened and do not contribute much signal. The volume selected by this technique is roughly spherical and cannot be shaped to fit an anatomical structure or to select a particular region of abnormality. Using a focused $B_0$ field means that the patient must be moved every time a new volume is studied. This technique is rarely used now.

(b). The simplest form of localization uses surface coils. Small circular flat coils are positioned on the surface of the body directly over the organ to be studied (Ackerman et al 1980, Cady et al 1983, Bottomley et al 1983). The surface coil is an RF antenna consisting of coplanar loops of wire. In the simplest experiment the surface coil receives signals from an adjacent, approximately hemispherical volume. The signal intensity received is not uniform within the hemisphere; signals near the surface are received at full strength and deeper signals attenuated. Surface coil localization can be used to study superficial tissues such as muscle or adipose tissue as it provides optimal sensitivity for these. However, the high sensitivity to surface tissue can result in significant contamination of the spectrum if internal organs are studied.

Rotating frame imaging or rotating frame zeugmatography uses varying radiofrequency gradients to select multiple volumes (Cox and Styles 1980). A set of data accumulations are collected, in which the length of a transmitter pulse is incremented for each accumulation, then two dimensional Fourier transformation yields a matrix where chemical shift is represented along one axis and spatial position along the other. Thus each spectrum corresponds to a sample region bounded by $B_1$-isocontour

surfaces of the surface coil.

The main problem with the $B_1$ gradient methods is that the surface-coil $B_1$-isocontours curve back to the plane of the surface coil so it is difficult to avoid contamination of the region of interest by signals from surface layers of tissue.

(c). When accurate three dimensional discrimination is required, methods that combine selective radiofrequency pulses with $B_o$ gradients are the best choice. These techniques are particularly suitable for clinical MR as spectroscopic data can be correlated with a magnetic resonance image.

DRESS - 'depth resolved surface coil spectroscopy' uses a single selective excitation pulse in the presence of a pulsed magnetic field gradient to excite a flat plane of nuclei parallel to the plane of a surface coil (Bottomley et al 1984). DRESS is spatially restricted by the surface coil sensitivity profiles to disc-shaped volumes whose radii increase with depth. The signal is not usually homogeneous across the selected volumes, which can result in the shape and size of the actual selected volumes varying dramatically from the idealized profile. This technique, when first developed, offered controllable signal localization in one dimension. However it has been superceded by other methods which offer much better signal localization in directions orthogonal to the slice selective gradient, and less signal loss during the delay following selective excitation.

To examine the whole brain, RF coils must surround the head. This reduces the sensitivity attainable with surface coils but provides flexibility and convenience. The brain is imaged and then a volume of interest selected. The spectrometer settings, including radiofrequency power and field homogeneity, are then optimized for this volume of interest.

There are a number of techniques used to select the volume of interest; all have a selection sequence and then an observation sequence. Planes in an object are selected

by the application of frequency selective RF pulses in the presence of linear $B_0$ gradients. A key feature of these methods is that the magnetic gradients that produce high resolution proton images are also used to define the spectroscopic volumes (Fig. 17).

There are problems with pulsed magnetic field gradients. The spectrum is usually measured after a sequence of gradient pulses which can result in a residual magnetic field gradient, caused partly by the inductance of the gradient coil system but mainly by the induced eddy currents in the magnet and probe structure. These currents have relatively long time constants and cause loss of spectral resolution. Inductance of the gradient coils can be removed by cancellation, by overdriving the gradient waveform with a negative overshoot upon removal of the gradient pulses, or by compensation with data processing. The effect of eddy currents can be reduced by introducing a delay time between the selection and observation which should be kept short compared to the $T_1$ of the measured MR signals. Newer magnetic resonance systems have 'screened' gradients to minimise the induction of eddy currents. We did not have screened gradients during the studies presented in this thesis.

ISIS - image selected in vivo spectroscopy (Ordidge et al 1986) uses selective RF pulses in combination with linear magnetic field gradients. It allows a spectrum to be obtained from a well defined cube positioned by reference to a magnetic resonance image. The cube can be varied in size and position and is selected by eight sequences of three selective inversion pulses with three orthogonal field gradients followed by a 90-degree acquisition pulse. A spin-echo is not used, avoiding signal loss due to $T_2$ effects. Therefore ISIS has been particularly useful for nuclei with short $T_2$ values, such as $^{31}P$.

Luyten et al's (1986a) method (SPARS -spatially resolved spectroscopy) avoids strong broadband RF pulses in the presence of $B_0$ gradients. It preserves longitudinal magnetization in the volume of interest and destroys observable magnetization

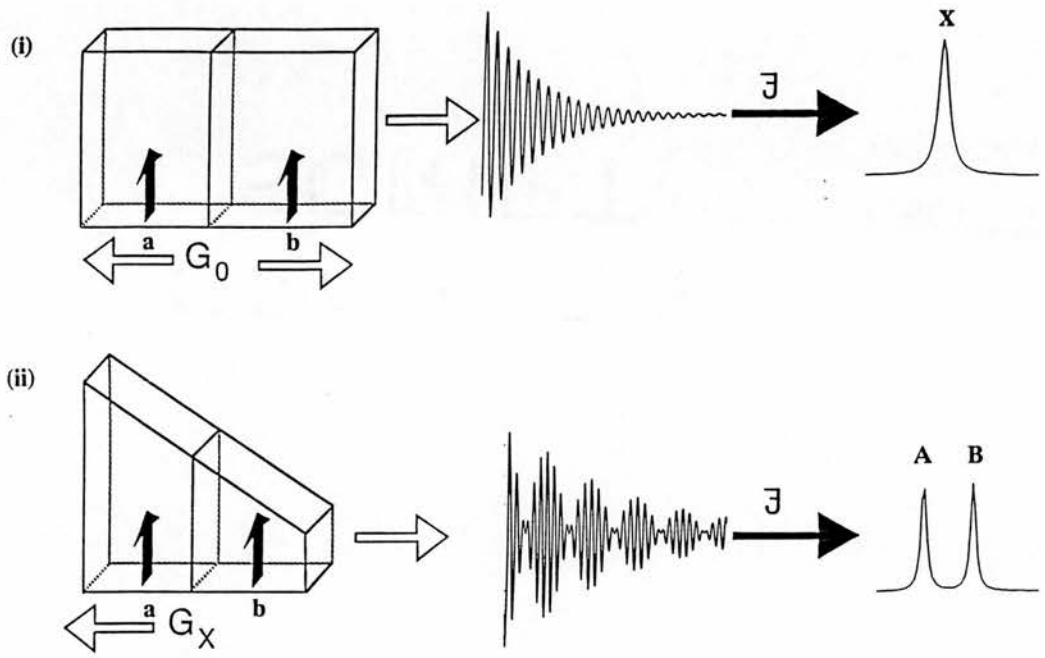



Fig.17 Principles of spatial localization using magnetic field gradients. In (i) the magnetic field is uniform and objects (a) and (b) experience the same field strength, and consequently produce a single resonance (X). In (ii) there is a gradient in the magnetic field (Gx). Object (a) experiences a higher magnetic field than object (b) resulting in two separate resonances (A) and (B). This difference in frequency thus encodes spatial information in the spectrum.

elsewhere. Because the selection sequence uses an echo technique, considerable losses in sensitivity occur for compounds with short $T_2$ values. Luyten et al (1986a) observed proton metabolites in human brain after applying a 1331-2662 sequence for water suppression after volume selection by SPARS.

The most accepted techniques for single volume proton spectroscopy are STEAM (stimulated echo sequence, Frahm et al 1989 a and b) and PRESS (point resolved spectroscopy, Bottomley 1987 b). Both methods produce good spatial localization and incorporate water suppression. The gradient waveforms used for STEAM are optimized for three factors: generation of a stimulated echo, dephasing of unwanted echo responses and reduction of signal attenuation due to motion and diffusion. The STEAM sequence is represented in Fig.18. It is simple and robust but produces only about half the possible signal from thc voxel of interest. The PRESS localization experiment consits of a 90-180-180 sequence, with each RF pulse being a frequency selective pulse applied in the presence of an orthogonal gradient. Unlike STEAM, PRESS retains the full signal from the voxel of interest but the 180-degree pulses need to be both slice selective and refocusing.

Water suppression techniques. The STEAM and PRESS sequences incorporate water suppression and spatial localization. The chemical shift selective, or CHESS, pulses precede the rest of the sequence and excite the unwanted water resonance which is then cancelled out by the subsequent gradients. The CHESS pulses excite spins within only a narrow frequency range around the water signal and so there is little degradation of the rest of the spectrum.

An alternative water suppression is a binomial pulse (Hore et al 1983). This pulse sequence incorporates many of the properties needed for an effective solvent suppression sequence, which include being easy to programme and use and an insensitivity to $B_1$ inhomogeneity.

In our proton experiments, three frequency selective 180$^o$ pulses in the presence of

Fig. 18. Stimulated echo sequence (STEAM) Frahm et al 1989, incorporating water suppression and spatial selection. CHESS = chemical shift selective. TE = echo time.

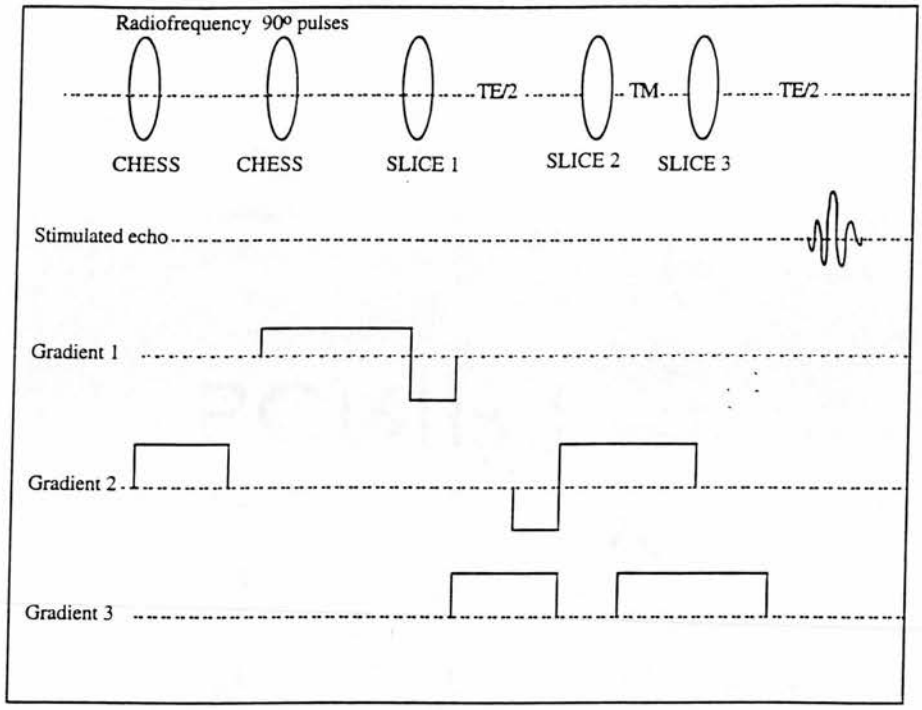
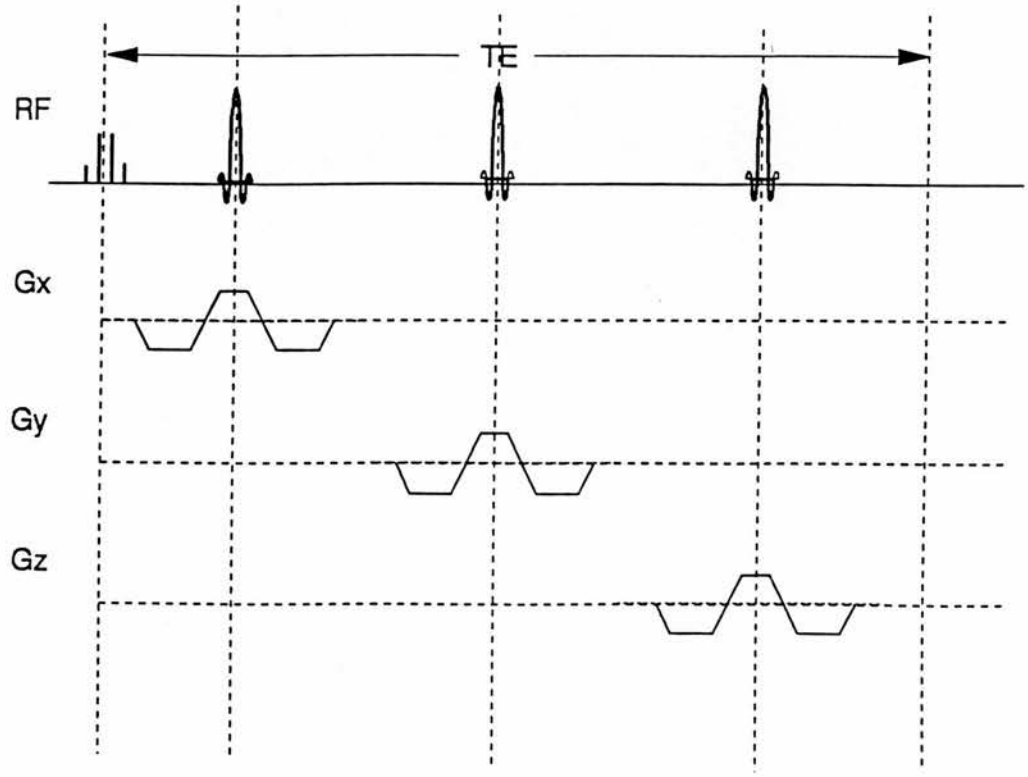



Fig. 19 The localization technique used for our proton spectroscopy used three frequency selective 180° pulses in the presence of gradients Gx, Gy, and Gz combined with a 1331 water suppression sequence. This method is known as multi echo spectroscopic acquisition or MESA (Lampmann et al 1986).



gradients Gx, Gy and Gz were combined with the $1\bar{3}3\bar{1}$ water suppression sequence (Fig.19). This method is known as multi echo spectroscopic acquisition or MESA (Lampmann et al 1986). Problems with the $1\bar{3}3\bar{1}$ binomial pulse, which include the fact that there is a non-linear excitation of the $B_1$ field, have been discussed by Morris et al (1986).

Chemical shift imaging (CSI); (two, three or four dimensional ) uses $B_0$ gradients to obtain spectra simultaneously from multiple regions (Brown et al 1982). A pulsed gradient is used to encode positional information in the initial phase of the free induction decay, which does not affect the resonant frequency distribution in space after the gradient has been turned off. By sampling the free induction decay after a gradient pulse, information about spatial variation can be separated from information about frequencies. The net effect is to measure the Fourier transform of the spatial and frequency distribution function of the spins which gives the spatial distribution of frequencies (chemical shifts) over the sample.

Four-dimensional chemical shift imaging generates a single four-dimensional data matrix encoding the three spatial coordinates (x,y,z) and the complete chemical shift range ($\delta$) for every volume element within that data set (Hall et al 1985). First, a non-selective radiofrequency pulse is used to excite the spins, which then evolve under the influence of three time-dependent magnetic field gradients applied along x, y and z (Fig. 20). The amplitude of the gradients is varied systematically in equal increments, the number of increments determining the digital definition of the corresponding spatial dimension. Chemical shift information is obtained by detecting the signal without any field gradient, and the final 4D matrix is assembled from the signal acquired for different combinations of magnitudes of Gx, Gy, and Gz (Fig.21).

The clinical applications of chemical shift imaging were first demonstrated by Bailes et al (1987) in human liver. More recent results for multidimensional experiments have been demonstrated in human brain for $^{31}P$ (Coutts et al 1989) and proton spectroscopy

Fig. 20. Schematic diagram for chemical shift imaging. TR = repetition time. TD = time delay. TA = acquisition time

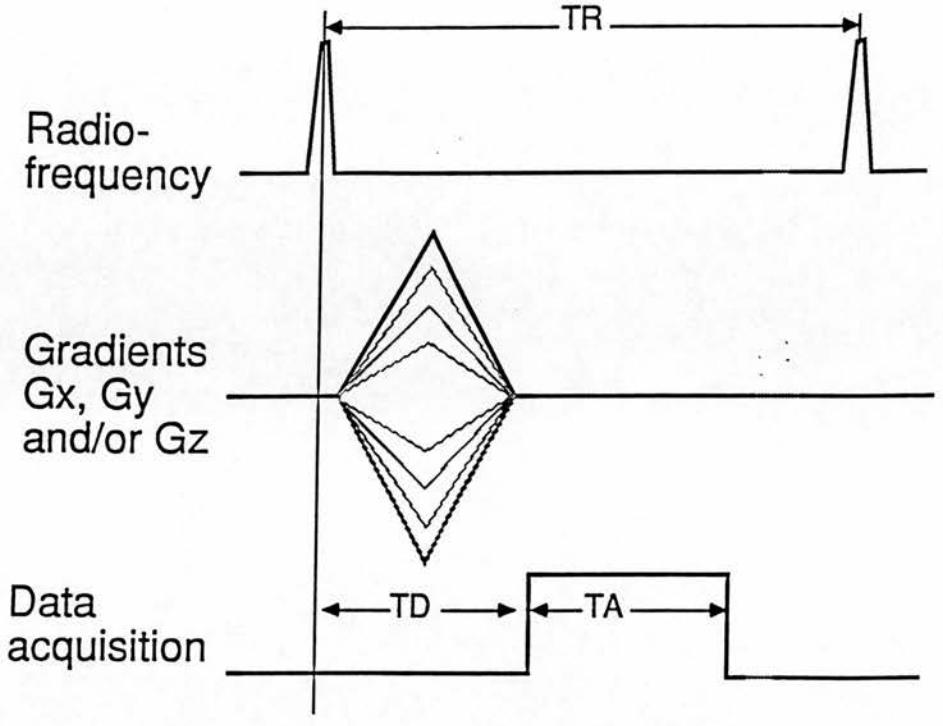
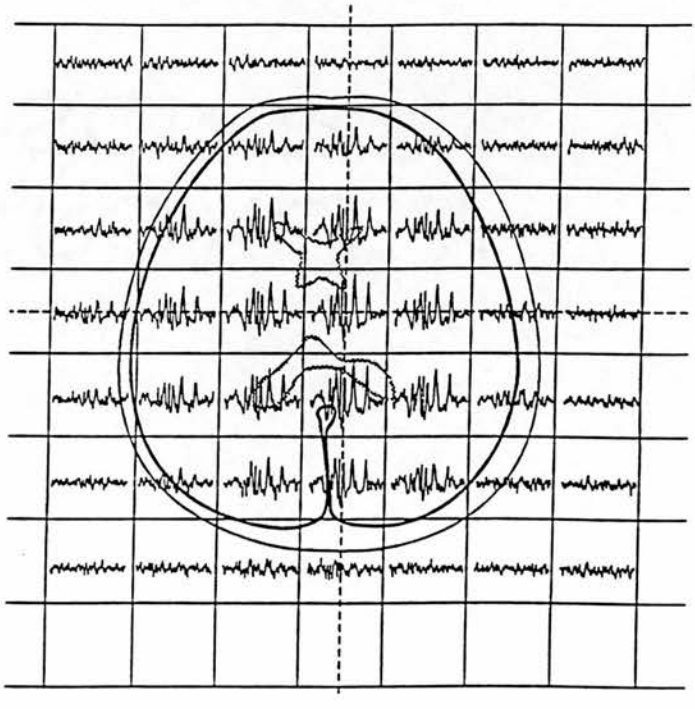



Fig. 21. One plane from a $^{31}P$ four-dimensional chemical shift image of the brain. $^{31}P$ MR spectra are simultaneously acquired from multiple voxels whose spatial location are shown above on an outline of a transverse image of the brain.



(Sargentoni et al 1992) . The data can be displayed in image format, "metabolite maps", which may be more easily interpreted by clinicians than spectra.

These studies were performed in a 1m bore magnet, operating at 1.6 Tesla (T), constructed by Oxford Magnet Technology Limited and developed for use as a spectroscopy system by the Picker Research Laboratory, GEC (Fig. 22). The resonant frequency for $^{31}P$ was 27.5 MHz and for $^{1}H$ was 68.0 MHz.

Setting-up procedures

The magnetic resonance system was calibrated by optimizing magnetic field homogeneity, "shimming", and then acquiring images and spectra from phantoms (usually 50 ml (10M) phosphoric acid) achieving linewidths of the order of 20 Hz. Before studying a patient a calibration of the $B_1$ field was performed (Fig. 23).

An individual patient protocol was written before commencing an examination, which took into account the clinical condition of the child, the time available, the nucleus to be studied and the localization technique and repetition times to be used.

All patients were checked for ferromagnetic material, and monitoring equipment was attached before they were put into the magnet bore. Their head was placed in a saddle-shaped transmit coil. The transmitter coil consisted of two rectangular-shaped turns of copper tubing approximately 39cm long by 34cm wide (Fig. 22). The coil produced a $90^0$ pulse from a trapezoidal radiofrequency wave of 150μs duration. It could be tuned for protons (68.0 MHz) or phosphorus (27.5MHz). The use of a separate saddle transmit coil produced a uniform pulse angle.

A variety of saddle receive coils were used depending on the particular spectroscopy examination, for example see Fig. 24. The receive coil was connected either to a high input impedance, low noise, preamplifier for operation at 27.5MHz, or to a low impedance preamplifier at 68MHz, allowing optimal operation at either frequency. Coupling between the transmit and receive coils was minimized by positioning at right

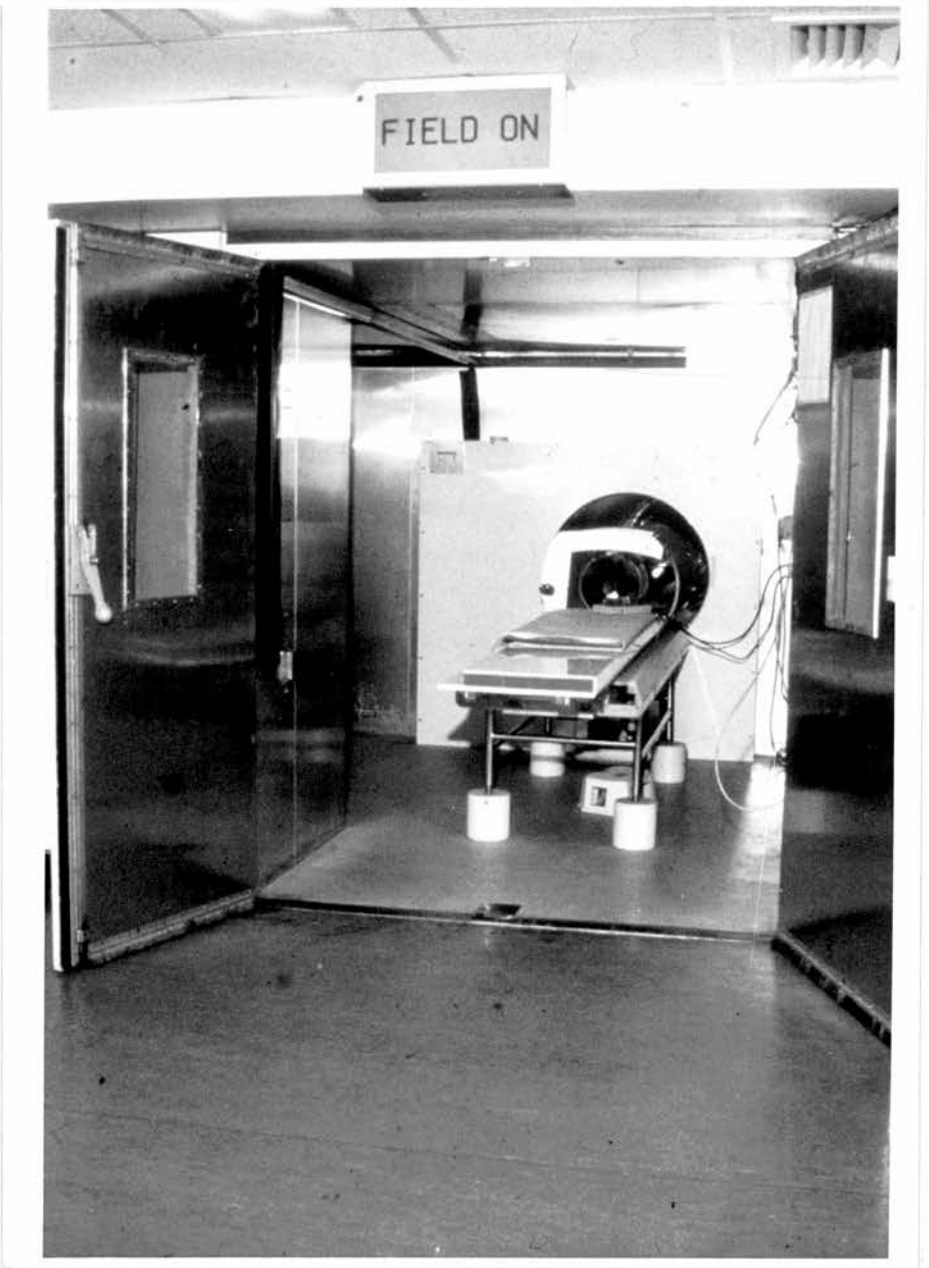



Fig. 22 Our 1.6T prototype magnet system. The doors, shown open, form part of the radiofrequency screen surrounding the magnet and are closed when a patient is in the system. The arrow indicates the transmitter coil.

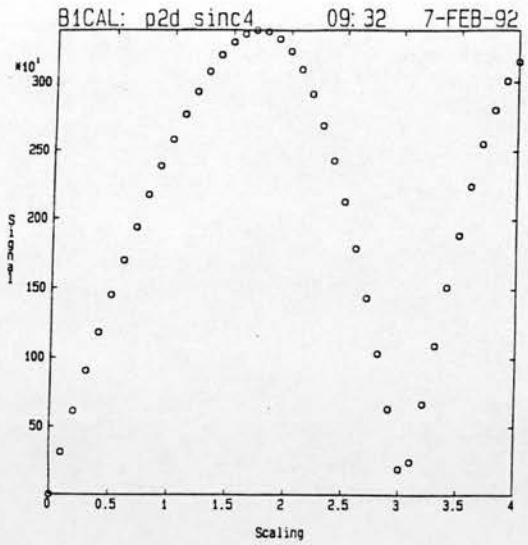



Fig. 23. A calibration of the $B_1$ field was performed before each patient examination. The point of intersection of the sine wave with the X-axis (in this case 3.05) was taken as the $B_1$ scaling factor for the examination.

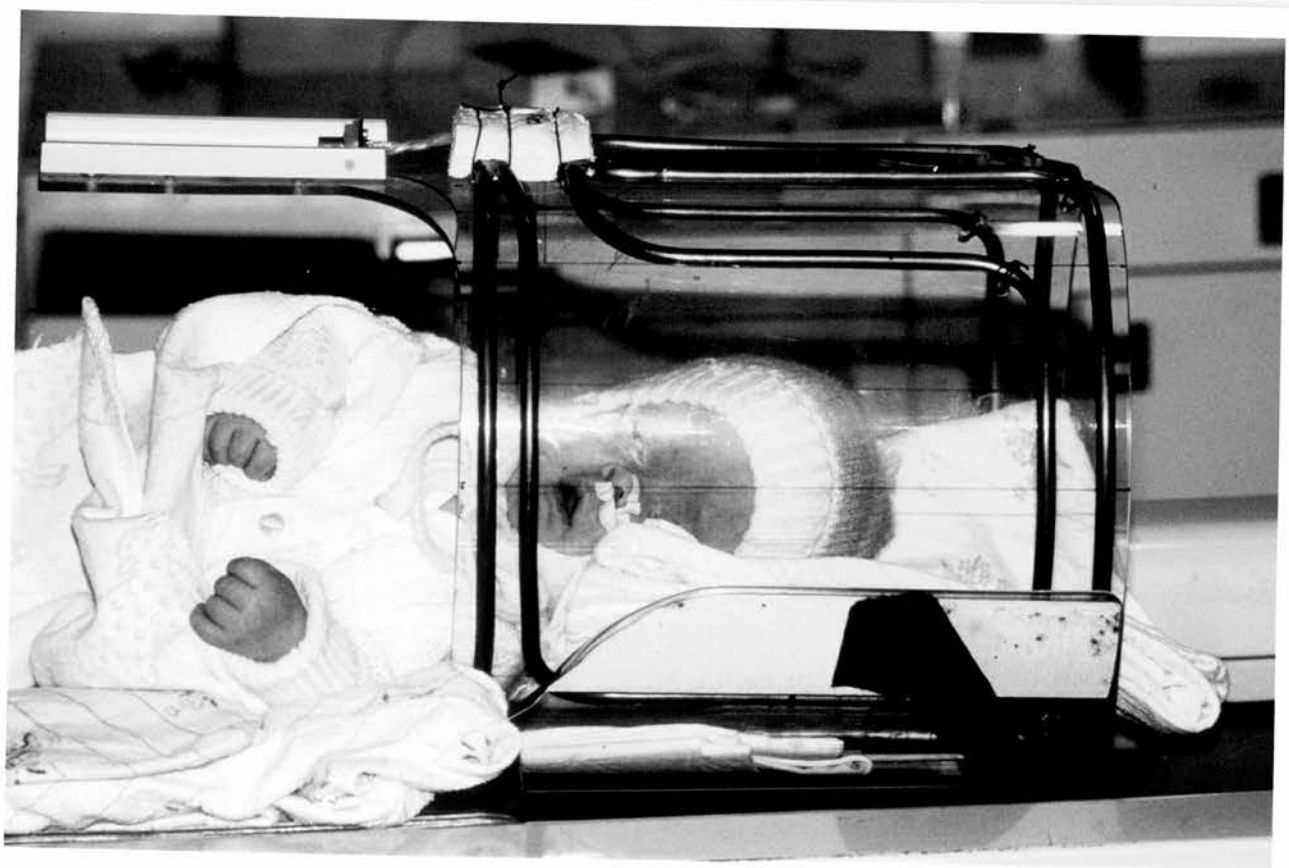


Fig. 24. A saddle shaped receive coil surrounding the head of an abnormal infant with hydrocephalus.

angles to each other and electronic decoupling. The pulse angle was measured using a search coil. The pulse angle was estimated by comparing the voltage induced in a small probe located outside the transmitter coil, when loaded with a patient, with that produced when using a known pulse angle (90°) for a phantom.

At the time of these studies the gradient coils were not actively shielded and so sequences with conservative TE's were used to minimise eddy currents.

PHOSPHORUS SPECTROSCOPY

Saddle shaped enveloping receiver coils of different sizes were used to enclose the children's heads (Fig. 24). Magnetic field inhomogeneities were reduced by shimming manually on the proton signals of water and fat. On average, shimming achieved a linewidth at half the peak height of the water resonance of 20-30 Hz for the whole head. Before spectroscopy, proton images were obtained in three perpendicular planes (with partial saturation sequences); these could be used subsequently to relate the child's anatomy to a spectral co-ordinate system, and to locate any anatomical lesions that may have caused spectral abnormalities.

Phosphorus spectra were collected using radiofrequency pulses of width 200μs at half height. Typically a pulse angle of 45° was used. Phase cycling was used to reduce artifacts.

A simple pulse and collect sequence was used for examinations in which signal was obtained from the whole sensitive volume without a specific localising technique. $^{31}P$ spectra were acquired from the whole volume of the child's head within the receive coil using the pulse-collect sequence with 32, 64, 128 or 256 data collections. The number of data collections depended on the repetition time. A repetition time of 5s was used in every examination but if the child was settled and more time was available 0.5s, 1s, 10s and 20s repetition times were also used. This enabled studies of the saturation effects of the different metabolites. Saturation effects for each signal were measured by comparing signal heights with different repetition times (TR) to give an indication of $T_1$ values.

The unlocalized spectra were processed with convolution difference filters and exponential difference filters of 1ms and 60ms in the time domain.

Some children were studied with two dimensional localised phosphorus spectroscopy. The sequence used to obtain phase-encoded data was shown in Fig. 20. To obtain a

two dimensional data set (spatial frequency and time) the amplitude of the phase encoding gradient was increased through 16 values. There were 1024 points in each of the 16 lines of data measured 64 times with phase cycling (Hoult and Richards 1975) to reduce artifacts. The repetition time of the sequence was 1s and the total acquisition time was about 20 minutes. The half width of the $B_1$ pulse was 200μs, the delay to start of sampling 3.1ms and sampling time 409.6ms, the length of the phase-encoding gradient 2ms and its maximum time integral 0.1 cycles/min.

The data were processed by filtering, a 2D Fourier transformation and manual zero order phase correction. An exponential filter was used along the time dimension and a cosine function along the spatial frequency dimension, which reduced the blurring of the slice profile, but increased its width to 16mm.

The 3.1ms delay to the start of sampling (Fig. 20) means that the data set is incomplete which results in a baseline artifact in the spectra. This artifact was reduced by including a spin echo in the sequence (Brown et al 1982).

When time permitted some children had 4D CSI performed. The pulse sequence used is illustrated in Fig. 20. The trapezoidal RF pulse lasted 250 μs and had sufficient bandwidth to irradiate the whole $^{31}P$ spectrum. Spatial localization was achieved with gradient phase encoding in three dimensions, as described previously. Three orthogonal gradient pulses (with a baseline duration 2ms, maximum gradient strength 0.75mT/m for a 4cm nominal voxel size) in the z, y, x directions were applied simultaneously, immediately after the radiofrequency pulse, to encode the time-domain signal spatially. The signal was then collected 3.1ms after the radiofrequency pulse in the absence of a gradient field. The amplitude of each gradient pulse was incremented through eight individual values (512 permutations in total). Each voxel position was identified by the co-ordinates z, y, x. The z axis of the co-ordinate system was along the long axis of the magnet; the y-axis vertical and the x-axis horizontal as defined previously.

The 4D CSI data sets were processed using spatial and temporal filtering, Fourier transformation and manual zero and first order phase correction. An exponential filter was applied in the time domain. A cosine filter was applied in each of the spatial frequency dimensions which reduced artifacts arising from insufficient digitization for discrete Fourier transformation in the spatial domain, but caused some signal from each voxel to be smeared out with resultant overlap of signal from neighbouring voxels (voxel smearing or overlap).

pH was measured from the chemical shift of inorganic phosphate relative to phosphocreatine using the following pH titration curve (Taylor et al 1983)

$$pH = 6.75 + \log (\delta\text{-}3.27)/(5.69\text{-}\delta)$$

Measurement of peak areas in our $^{31}P$ spectra.

In our spectra metabolite ratios are used as a form of quantification. Peak areas were used for analysis of the phosphorus spectra. The peaks were measured with a computer integration programme (Sun Workstations) by one observer who did not know the patient's outcome. The peak areas were measured by dropping perpendiculars to a baseline common to the full spectrum (Fig. 25a) . To show the effects of different methods of measurement the peak area was also measured with a line across the minimum points of the peak for two of the spectra (Fig. 25b). Unless otherwise stated, results are presented from spectra filtered with 1ms and 60 ms exponential difference filters and peaks analysed by dropping a perpendicular to a common baseline.

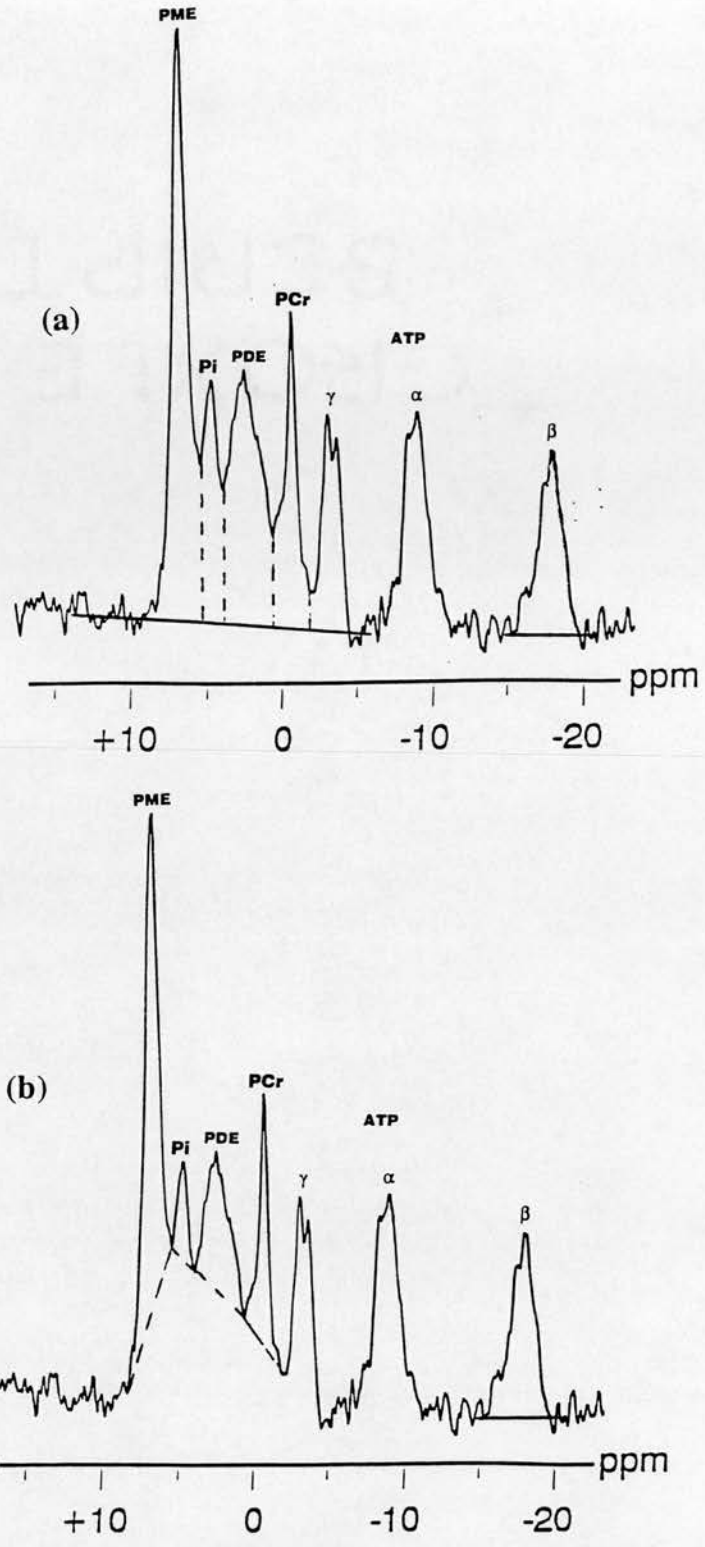



Fig. 25. Two methods of calculating the peak areas from a phosphorus spectrum, using a computer integration programme (Sun Workstations), are shown.
(a) The peak areas were defined by perpendiculars dropped to a baseline common to the full spectrum. This method was the one used throughout this thesis unless otherwise stated.
(b) The peak areas were defined by a line drawn across the minimum points of the peak.

The patients were placed in the magnet bore within a saddle shaped transmit receive coil tuned for protons at 68.0MHz. Shimming was done by optimizing the proton FID (mainly water, with some contribution from fat) by adjusting x, y and z, first-order shim coils. Proton line widths of the order of 30Hz were achieved only after 20 to 30 minutes of shimming.

Magnetic resonance imaging using a spin echo sequence (TR 500/ TE 22) was performed first in at least two orthogonal planes, to locate the region for spectroscopic study. To minimize spectral variability, spectra were acquired, when possible, from the same region in each infant. When we began these studies our technical capability was such that the smallest achievable volume of interest was $64cm^3$; in the smallest infants (PCA < 38w) this volume inevitably filled most of the brain. As our technical capability improved we were able to reduce the volume of interest to $27cm^3$. In the older infants and children the aim was to place a 27 - $64cm^3$ voxel at midventricular level in the parieto-occipital region (Fig. 27).

There were several reasons for choosing this latter region:
(a). Shimming is easier than in the frontal lobes
(b). Inclusion of, and contamination by, skull fat is avoided.
(c). The parieto-occipital region is commonly damaged in all types and patterns of hypoxic-ischaemic brain injury (O'Brien et al 1979) and includes the parasagittal distribution of injury described by Volpe and Pasternak (1977) and the laminar cortical necrosis described by Hawes and Mishkin (1972).

Spectroscopic localization was achieved by the MESA sequence (Lampman et al 1986) using multiple spin echoes with slice selective $180^o$ gradient pulses in three orthogonal planes (x, y, z) (see Fig.19). Shimming was then performed on the volume of interest

Fig. 26. Magnetic resonance image (SE 500/22) showing a 27cm$^3$ volume of interest for proton spectroscopy placed centrally in the brain of a premature infant.

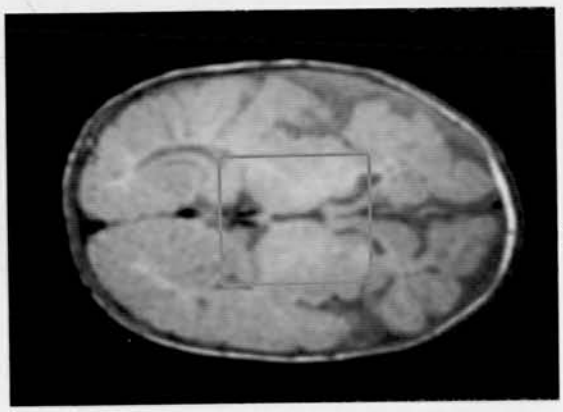
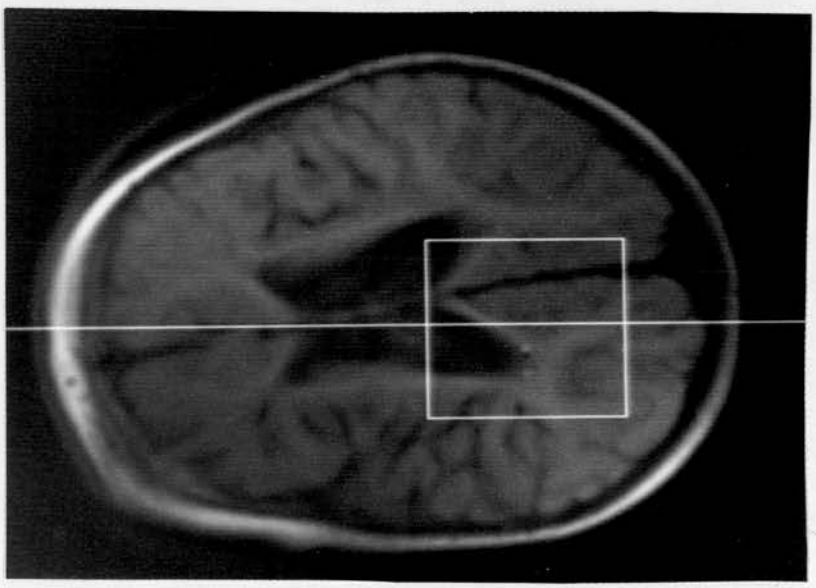


Fig. 27. A magnetic resonance image (SE 500/22) showing a 64cm$^3$ volume of interest for proton spectroscopy at mid-ventricular level in the parieto-occipital region of a full term infant.



to optimise magnetic field homogeneity in this volume. To see the other solute protons (about 10mM) the multiple spin echo sequence incorporated a binomial pulse (1331) to suppress the proton signal from water (about 80M).

The time to the start of the data collection, the echo time, was 270 ms. This time was chosen to allow observation of the proton coupled lactate doublet and to minimise eddy current effects before data collection. The repetition time was 2000 ms and 128 data collections were made. When time allowed a repetition time of 5000ms with 64 data collections was also used. These spectra were used to estimate saturation factors. In several cases a TE of 135ms was also used to assess $T_2$ effects.

Spectra were processed using an exponential line broadening filter of 120 ms. The line widths of the NAA, Cho and Cr peaks varied between patients because of differences in magnetic field homogeneity, but were similar for each individual patient. Field inhomogeneity broadens all the peaks to the same extent in the proton spectrum because the proton spectral area under study is very narrow (this does not apply to the phosphorus spectrum); therefore, peak heights were used in the assessment of metabolite ratios. The peak height was measured from a line drawn between the minimum points of each peak to the maximum height of the peak. The minimum points of the peak were at the known location of that compound e.g. the centre of the NAA peak at 2.02 ppm (Fig. 28). The base of the peak was not usually parallel to the baseline because of imperfections in water suppression as the 80M proton signal coming from body water must be suppressed in order to see other metabolite concentrations present only in millimolar concentrations.

The signal intensity ratios obtained were influenced by the water suppression sequence used, which effectively reduced the Cho and Cr signals in relation to NAA. This was reproducible from one examination to another and did not affect the overall analysis. The spectra were analysed without knowledge of the patient's outcome. As an assessment of the error of the peak height measurement, ten proton spectra were analysed by four individuals. The results were averaged to obtain a mean and standard

deviation, to give an indication of the error of measurement.

To compare the predictive ability of the metabolite ratios with outcome groups, the values for the control and normal children were grouped together and compared with the values for the moderate and severe outcome groups. Children classified as "other' were not included in the statistical analysis. For the group of infants born at term and examined within four weeks of birth, age was not considered as a complicating factor and so the metabolite ratios for the groups were compared using a Student's two sample *t* test (Stat-view).

To statistically compare all the metabolite ratios for all the children at different ages was more difficult. Advice was taken from statisticians. The following statistical analysis was kindly undertaken by Dr C. Day. As the observations were not made at specified times for each patient the results could not be analysed by multi-variate analysis of variance for different measures; the statistical analysis had to take into account the fact that the variables changed with post-conceptional age. Therefore two separate transformations of each of the variables were made. For NAA/Cho and NAA/Cr the first transformation was to divide the variable by the age. For Cho/Cr the variable was transformed by multiplying by age. This was done because NAA/Cho and NAA/Cr increase with age and Cho/Cr decreases with age. The second transformation of each of the original variables was derived by performing an ordinary linear regression of the original variable against age using only the data from normal and control patients. This produced a formula for calculating the expected value of the variable for the specified age based on the normal and control populations. This was then used to standardise the actual value of the variable obtained. This then gave us ten variables: three unchanged variables (NAA/Cr, NAA/Cho and Cho/Cr); three variables with a simple transformation, either a product or quotient of age; a standardised version of each variable, and age itself. These ten variables were then offered to a step-wise discriminate function analysis using three classes. The normals and controls were grouped together and there was a moderate and a severe outcome group,the adult values were omitted (SAS programme: SAS Institute Inc. Cary, NC, USA) .

This analysis showed that age was not a discriminant factor in the analysis of the data, therefore a Chi squared test with Yates' correction was applied to all children in the normal/control and severe outcome groups. Two by two tables were constructed to test the null hypothesis that there is no difference between the two outcome groups with NAA/Cho metabolite ratios $> 1.0$ and $<1.0$; with NAA/Cr metabolite ratios $> 1.5$ and $< 1.5$; and Cho/Cr ratios $> 1.5$ and $< 1.5$. To test the null hypothesis that the metabolite ratios show no significant differences between the normal/control and moderate outcome groups Fisher's exact test was used as the 2x2 tables had cells with $> 80\%$ of values less than 5.

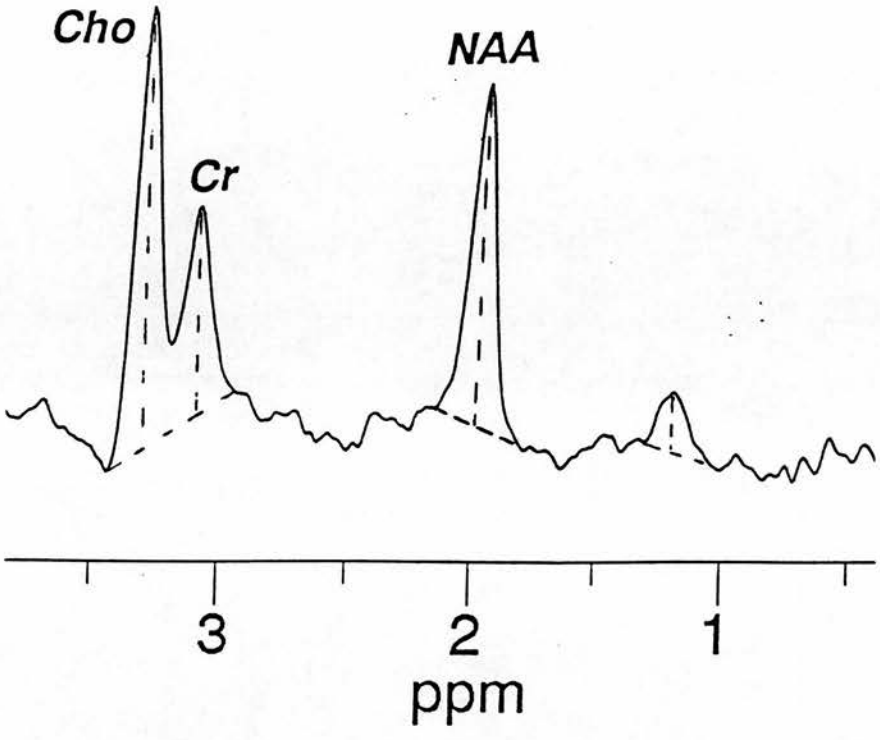



Fig. 28. Peak heights were used in the assessment of metabolite ratios for the proton spectra. The peak height was measured for the proton spectra perpendicular to a line drawn between the minimum points of each peak.

**HYPOXIA AND ISCHAEMIA IN THE NEWBORN INFANT:**
THE CLINICAL PROBLEM; BIOCHEMISTRY; MAGNETIC RESONANCE SPECTROSCOPY; MONITORING DURING MRS; CLINICAL METHODS

## HYPOXIA AND ISCHAEMIA IN THE NEWBORN INFANT: THE CLINICAL PROBLEM

Intrapartum asphyxia and its cerebral sequelae are the most important cause of neonatal brain injury. About six hundred full term infants die or become seriously disabled in the United Kingdom each year. The clinical damage is produced by a combination of hypoxia, on its own well tolerated by the neonatal brain, and hypoperfusion. The term hypoxic-ischaemic encephalopathy (HIE) is used to describe specific neurological abnormalities in a term infant following an hypoxic-ischaemic insult (Sarnat and Sarnat 1976).

The incidence of post-asphyxial encephalopathy is thought to be between 2 - 9% of live births in full term infants (Hill 1991, Levene et al 1985); moderate and severe post-asphyxial encephalopathy occurs in 1.1 and 1.0 per 1000 infants (Levene et al 1985). One quarter of these infants had shown intra-uterine growth retardation (Levene at al 1985). The incidence of asphyxial injury in premature babies is much higher (Volpe 1989). Among term newborns with hypoxic-ischaemic encephalopathy Finer et al suggested in 1981that 7% will die within the first 30 days and 28% of survivors will have significant neurological handicap. In a later study Robertson and Finer (1985) follwed these children to 3.5 years and found that while the prognosis for those children with severe HIE was very poor, chidren with mild HIE were likely to have a normal outcome. Outcome for children with moderate HIE was more difficult to predict.

The main injury to the neurons in perinatal asphyxia is due to a lack of oxygen. The perinatal brain is deprived of oxygen by two mechanisms; hypoxaemia, a decrease in the amount of oxygen in the blood to below the level required to maintain normal cellular function; and ischaemia, a decrease in the blood supply to below the level required to maintain normal cellular function (Vanucci 1990). The hypoxic-ischaemic

may result from impaired placental gas exchange or blood flow (Scher et al 1991), or may occur postnatally as a result of neonatal respiratory or cardiac compromise. Postnatal insults usually account for only 10% of infants with HIE (Brown et al 1974).

Neurons do not necessarily die during the asphyxial insult itself; the insult initiates cascades of processes that operate for a considerable time after the event and lead to neuronal death (Vannucci 1990, Gluckman and Williams 1992, Blennow et al 1994). The biochemical aspects are discussed in detail in the following section "Hypoxic-ischaemic injury to the brain: biochemistry."

The neuropathological features of HIE vary considerably with the gestational age of the infant and the nature of the insult (Barkovich and Truwit 1989). Selective neuronal necrosis is the most common variety of injury observed in neonatal HIE and refers to necrosis of neurons in characteristic, though often widespread distribution (Towbin 1970, Grunnet et al 1974). Other types of asphyxic pathological damage in the brain have been broadly divided into two groups depending on whether the child was full term or premature. In the full term newborn there is arterial boundary zone necrosis, particularly parasagittal injury and subcortical leukomalacia, as well as subarachnoid haemorrhages and necrosis of brain stem nuclei (Barkovich 1992). In the premature newborn there is periventricular haemorrhagic infarction, periventricular/intraventricular haemorrhage and periventricular leukomalacia (Banker and Larroche 1962, Fenichel 1990, Levene 1987, DeVries et al 1988).

Periventricular leukomalacia develops in the brains of premature infants in response to asphyxia in vascular watershed regions. Inadequate perfusion through the deep medullary arteries of the immature brain causes infarction particularly in the anastomotic areas between ventriculopetal medullary arteries and branches of ventriculofugal

choroidal arteries (Takashima and Tanaka 1978). In premature infants the cerebral cortex is spared the effects of ischaemia because of its rich leptomeningeal arterial supply. By term the deep medullary arteries have developed more effective anastomotic pathways but the leptomeningeal vasculature has regressed, exposing the subcortical region. The incidence of periventricular leukomalacia, as diagnosed with real time ultrasound, is 7.5% in infants of birthweight of 1500g or less (Levene et al 1983).

The dominant role of oxygen deprivation in the pathogenesis of selective neuronal injury is indicated by a variety of experimental and clinical observations (Norman 1978, Larroche 1977). However, the reasons for the selective vulnerability of neuronal groups in the central nervous system have remained largely undefined. Circulatory factors are likely to be invoved as neuronal injury is greater in vascular border zones. Neurons in deep cortical layers and particularly in the depths of sulci are especially affected. When adjacent white matter is also affected the classic pattern of subcortical leukomalacia is seen pathologically. As much of the injury in selective neuronal necrosis is not in a strictly vascular distribution it suggests that other factors are involved. The neurons in the brain that are most sensitive to hypoxic injury are in contact with synaptic terminals containing excitatory amino acids and the histologic appearance of acute brain degeneration following hypoxic-ischaemic damage is identical to that following glutamate-induced damage at NMDA binding sites (Ikonomidou et al 1989). It is possible that the regional vulnerability to oxygen deprivation may be related to the regional accumulation of excitotoxic amino acids, as well as calcium and oxygen free radicals (Vannucci 1990, Gluckman and Williams 1992, Blennow et al 1994). The areas of damage in newborn infants with profound hypoxic-ischaemic injury also correlate closely (with the exception of the hippocampus) with areas that are undergoing active myelination (Barkovich 1992).

Cerebral oedema is seen in the brain of premature and term infants after asphyxia and is both cytotoxic and vasogenic.

As the neurological damage depends on the age of the infant at the time of the injury, so does the resulting clinical syndrome. Premature infants with periventricular leukomalacia show extreme irritability: they are 'stiff' and have poor limb and trunk tone when examined at 40 weeks' postconceptual age. Sarnat and Sarnat (1976) graded the range of clinical signs after asphyxia in full term infants as mild, moderate and severe. These groupings have been modified by others, but we have used the Sarnat and Sarnat classification.

Infants with mild encephalopathy are irritable and jittery when stimulated; they appear to be 'hyperalert'. They have mild abnormalities of tone, particularly hypotonia of the trunk and neck. Limb reflexes are normal or slightly increased; clinically apparent seizures do not occur. The duration of mild encephalopathy ranges from one and a half hours to seven days according to different studies (Sarnat and Sarnat 1976, Levene et al 1985, Amiel-Tison and Ellison 1986). Infants with moderate encephalopathy are lethargic and irritable. Tone may be reduced or increased and the pattern may change, initial hypotonia becoming hypertonia. Tone may be markedly different between arms and legs; this is thought to be because of cortical border-zone injury. Seizures are common, usually occurring in the second 24 hours (Sarnat and Sarnat 1976, Levene et al 1985, Amiel-Tison and Ellison 1986). Sarnat and Sarnat (1976) found that these infants showed abnormal behaviour for a mean of 4.7 days. There is usually evidence of recovery by the end of the first week of life and deaths in this group are rare. Infants with severe hypoxic-ischaemic encephalopathy are comatose and severely hypotonic; they may never breathe adequately on their own. Seizures are frequent and may be prolonged. The most severely affected infants may have no seizure activity and an

isoelectric EEG. They have few reflexes apart from sluggish pupillary responses and doll's eye movements. Twenty four to 72 hours is a critical time: some infants will continue to deteriorate and die; others will begin to show signs of improvement (Sarnat and Sarnat 1976, Levene et al 1985, Amiel-Tison and Ellison 1986).

There are many definitions of birth asphyxia and none of them is accepted by everyone: this makes the planning of clinical studies and the comparison of treatments difficult. Criteria used to define birth asphyxia are a delay in establishing spontaneous respiration, a depressed Apgar score, cord blood acidosis, cardiotocograph abnormalities and clinical signs in the infant (Sarnat and Sarnat 1976, Levene et al 1985, Amiel-Tison and Ellison 1986). The Sarnat and Sarnat criteria are used at the Hammersmith Hospital where this study was undertaken, although much of the other information was also collected from most of the infants studied.

Investigations:

The diagnosis of birth asphyxia is made mainly on clinical signs; additional investigations add to the knowledge gained by clinical examination, exclude complications and may help in observing progress. To diagnose an infant as having hypoxic-ischaemic encephalopathy there must be a history of a significant hypoxic-ischaemic insult. In the experimental animal situation this is easy, but identification of a clinical episode can be difficult. It may be antenatal and asymptomatic in the mother, or it may be perinatal but unrecorded or undetected with available monitoring. Similar hypoxic-ischaemic events may have different effects in different neonates, raising the question; what is a significant hypoxic-ischaemic event?

The need to establish a prognosis is very important in neonatal medicine. In the very severely damaged child (Sarnat and Sarnat grade III hypoxic-ischaemic

encephalopathy) there are three possible outcomes: brain death, a persistent vegetative state, and survival with disabilities (Coulter 1987). For the first two outcomes, decisions to continue support or to withdraw treatment may be necessary. "Survival with disabilities" ranges from children who have spastic quadriplegia, are cortically blind and have very little cerebral function, to those who have only mild motor difficulties and a normal IQ (Coulter 1987). Parents are extremely anxious to know what life holds for them and their child. Neonatologists therefore continue to seek noninvasive methods for investigating the brain.

Cranial ultrasound through the open anterior fontanelle is the commonest method for investigating structural abnormalities in the newborn brain (Babcock and Ball 1983, Kreussner et al 1984). This is noninvasive and can be done repeatedly on the ward without moving the infant. It is particularly useful for investigating periventricular haemorrhage, common in preterm infants. Studies have shown that only the largest bleeds seem to cause permanent damage and that the most important cause of disability in the surviving preterm infants is extensive cystic leukomalacia resulting from hypoxic ischaemic brain injury (De Vries et al 1985). Ultrasound is not so useful for the detection of selective neuronal injury or for parasagittal injury because the cortical and brain stem lesions are too restricted or too peripheral to be visualised (Volpe 1987).

Magnetic resonance imaging is another established technique for examination of the brain of infants (Barkovich et al 1995, Keeney et al 1991). It can be used for further observation of lesions detected by cranial ultrasound (McArdle et al 1987, Rutherford et al 1994) or for follow-up examinations after the fontanelles have closed (Barkovich 1992, Barkovich and Truwit 1989). It offers better soft tissue definition than CT, and as there is no radiation hazard it can be used more frequently. A problem with MRI for the early examination of the neonatal brain is the high content of normal free water which makes damaged tissue less easy to detect than in older children (Barkovich and

Truwit 1989). MRI changes that have been associated with a poor outcome are diffuse injury, hyperintensity in the periventricular areas on $T_2$ weighted images and signs of periventricular leukomalacia (Johnson et al 1987). Repeated ultrasound in the neonatal period allows early identification of infants with a good or poor prognosis, but MRI can detect the precise site and extent of any lesions and allow their evolution to be followed (Rutherford et al 1994).

Seizures are common in asphyxiated infants and up to 50% are not manifested clinically, so continuous electroencephalography (EEG) monitoring is used. The EEG can be monitored in the neonatal intensive care unit (Eyre et al 1983) and it seems that early and continuous use of the EEG improves its prognostic significance (Watanabe et al 1980). Although seizures are a significant finding, the degree of background EEG abnormality is as important for determining prognosis. Hellstrom-Westas et al (1992) found the efficiency of the EEG (in the form of cerebral function monitoring) applied during the first six hours of life to predict good (normal trace) and poor (isoelectric or extremely low voltage) outcome to be 91%. Other researchers have also found a strong prognostic significance for EEG recording in the neonatal period (Watanabe et al 1980, Eyre 1988). EEG abnormalities associated with a poor prognosis include isoelectric recordings and periodic patterns (Sarnat and Sarnat 1976).

Auditory, visual and somatosensory evoked responses are used to record the brains response to an external stimulus; they are used to test the maturity and integrity of sensory pathways from the sense organ or nerve to the cortex. Auditory evoked potentials have been shown to correlate with a poor neurodevelopmental outcome if the abnormality persists once the infant has left the intensive care unit (Stockard et al 1983). Somatosensory evoked potentials have proved difficult to record even in healthy neonates, there is significant intra and inter subject variability (Blair 1971) and a high false negative rate (Gorke 1986).

Doppler ultrasound measures the velocity of cerebral blood flow noninvasively in infants with an open anterior fontanelle; it can show changes in flow velocity on repeated measurements but cannot measure absolute flow. Changes in an index of resistance, the Pourcelot Resistive Index (Pourcelot 1976), measured from the anterior cerebral artery may reflect cerebral vascular resistance, and this in turn has been reported to change in a variety of intracranial conditions such as perinatal asphyxia (Bada 1979, Archer et al 1986) and middle cerebral artery infarction (Messer 1991).

Treatment

At present there is little proven treatment available to limit the damage to the brain of the asphyxiated infant. Therapy is directed at resuscitation and support of the respiratory and cardiovascular systems, with the aim of preventing further hypoxic or hypotensive injury. Specific treatment of the brain includes the prevention of seizures with antiepileptic drugs, the control of intracranial hypertension with hyperventilation, and the use of drugs such as the corticosteroids, mannitol and barbiturates. Mannitol briefly reduces intracranial pressure; the benefits of corticosteroids and the barbiturates are unproven and controversial.

Research into ways of limiting brain damage is now directed at halting the cellular mechanisms of neuronal injury by calcium and the excitotoxic amino acids, glutamate and aspartate. The early animal work with calcium antagonists was encouraging (Vaagenes et al 1984) but clinical results to date have been disappointing (The European Study Group on Nimodipine in Severe Head Injury 1994). Studies continue on the N-methyl D-aspartate antagonists that block the action of the excitotoxic amino acids, and for a means of halting the cascade of damaging cellular reactions that result in hypoxic-ischaemic encephalopathy. These new methods of treatment are discussed in greater detail in the next section.

## HYPOXIC - ISCHAEMIC INJURY TO THE BRAIN: BIOCHEMISTRY

The brain uses 20% of total body oxygen consumption: 40% of this for maintaining cellular integrity, and 60% for the propagation of nerve potentials. The energy is generated by the breakdown of adenosine triphosphate (ATP) to adenosine diphosphate (ADP) and inorganic phosphate (Pi). Most of the ATP comes from oxidative phosphorylation in the mitochondria and the rest from glycolysis in the cytoplasm. If the delivery of oxygen and essential substrates is reduced by hypoxia or ischaemia, ATP production decreases but utilisation continues: ATP depletion results. This is the central event in hypoxia and ischaemia. Without ATP the gradients of ions and other molecules cannot be maintained across the cell membrane; intracellular communication stops, and macromolecules break down (Siesjo 1992 a and b, Siesjo 1988). The energy failure triggers a chain of reactions that may ultimately lead to cell death, although some of the damaging events may not occur until after reperfusion or reoxygenation (Siesjo 1988).

Currently it is believed that at least eight different categories of mechanism are involved in the multifactorial process which occurs during severe hypoxia and ischaemia, and after return of spontaneous circulation (Safar 1993, Siesjo 1988, Siesjo 1992 a and b) These can be divided into those occurring during global hypoxia and ischaemia (energy failure, ionic pump failure, excitotoxicity, calcium shifts and tissue acidosis) and those occurring during reperfusion (inflammation, oxygen delivery and perfusion, extracerebral organization and free radical activity).

The major breakdown of ionic homeostasis occurs when PCr and ATP concentrations approach zero. At that time the movement of ions across cell membranes down their ionic gradients is no longer matched by their return transport by the ATP-dependent pumps and there is a sudden increase in membrane permeability (Ekholm et al 1992).

### Acidosis and hyperglycaemia

During ischaemia glucose metabolism is switched from the aerobic phosphorylation

pathway to the anaerobic glycolytic pathway, which results in the accumulation of cellular lactate and a decrease in pH. Ischaemia causes an increase in lactate concentration that is approximately linear for the first 60 seconds (Nordstrom and Siesjo 1978). In complete ischaemia, the eventual lactate values correspond closely to the preischaemic stores of glucose and glycogen. Hypoglycaemia reduces tissue lactate (Ljunggren et al 1974) and hyperglycaemia increases it (Smith et al 1986). Since anaerobic glycolysis is the dominant cause of acidosis during ischaemia, a correlation can be expected between the amount of lactate accumulated and the decrease in intracellular pH (pHi); evidence suggests that pHi during ischaemia decreases purely as a function of lactate concentration (Smith et al 1986). This is not so for extracellular pH, which stabilises after a slight decrease. The reasons for this lack of proton equilibration are not known, but changes in extracellular pH do not reflect changes in intracellular pH (Murdoch and Hall 1990).

It is firmly established that conditions promoting the anaerobic metabolism of glucose to lactate in the ischaemic brain dramatically enhance ischaemic brain damage (Siesjo 1988). Features of this damage are oedema and fits. After long periods of ischaemia, hyperglycaemia causes immediate brain damage; after shorter periods of ischaemia the damage occurs after a delay that may be as long as 24 hours. The oedema that develops after ischaemia is more pronounced in hyperglycaemia, and recovery, if it occurs, is much more prolonged. Lactate concentrations of 16-20 mmol/kg are considered to be the threshold above which tissue damage occurs (Plum 1983). There are several mechanisms by which high concentrations of lactate cause neuronal injury; these include necrosis of endothelial cells with swelling and rupture of astrocytes, denaturation and inactivation of proteins including enzymes, suppression of the regeneration of $NAD^+$, and production of oxygen free radicals (Welsh et al 1982).

Excitotoxicity and calcium

Failure of Na/K -ATPase leads to increased concentrations of free glutamate and aspartate, excitatory amino acids (Lipton and Rosenberg 1994). These amino acids are normally cleared from the extracellular space by sodium-dependent, high-affinity

uptake systems and moved into astrocytes and neurons by transporters. Any defect that impairs the ability of cells to maintain the sodium gradient may cause the high-affinity glutamate-uptake system to fail (Lipton and Rosenberg 1994). Glutamate is the principal excitatory neurotransmitter in the brain, in pathologic conditions activation of glutamate receptors may mediate neuronal injury or death. This type of injury appears to be mediated by excessive influx of calcium into neurons through ionic channels triggered by activation of glutamate receptors (Choi 1985). Excessive amounts of intracellular calcium contribute to the overstimulation of normal processes, damaging neurons.

The first sign of glutamate toxicity, which develops within minutes after exposure to glutamate, is neuronal swelling (Choi et al 1987). This acute toxicity is dependent on the entry of excessive amounts of sodium and chloride ions, together with water into the cell, but it does not necessarily lead to cell death (Choi 1987). The acute toxicity associated with exposure to glutamate can be blocked by the the removal of sodium or chloride from the extracellular medium, but their absence does not protect neurons from the delayed effects of glutamate toxicity. Neurons die several hours after exposure to glutamate, and this irreversible injury is at least partially dependent on extracellular calcium triggering one of the toxic processes discussed

Ischaemia increases calcium influx into cells because depolarisation and transmitter release open voltage-gated calcium channels and agonist-gated calcium channels, and because energy failure prevents ATP-dependent calcium extrusion (Siesjo 1987). Loss of ATP combined with anoxia prevents the mitochondria from sequestering calcium and, in the absence of ATP, sequestration of calcium by the endoplasmic reticulum is also compromised. Since calcium influx enhances breakdown of proteins and lipids, cytoskeletal and membrane functions are damaged and catabolism and cell death result.

The influx of calcium through the voltage-gated calcium channels in the brain is a possible explanation of the selective neuronal necrosis occurring in ischaemia, hypoglycaemia and status epilepticus (Siesjo 1992 a and b). This hypothesis has been

challenged; in vitro, cells may die of anoxia without an increase in calcium (Cheung et al 1986). In addition, the beneficial effect of calcium channel blockers seems to be related more to an improvement in collateral circulation and reduced workload of ischaemic cells than to the prevention of calcium overload (Cheung et al 1986). Other in vitro results support the calcium hypothesis and suggest that the potentially adverse effect of calcium in the brain is exerted at neuronal sites containing a high density of ligand-gated calcium channels gated by excitatory amino acids (Choi 1987).

NMDA receptor activation, neuronal increases in calcium, or both can activate a series of enzymes including protein kinase C, phospholipases, proteases, protein phosphatases, and nitric oxide synthase (Choi 1988, Dawson et al 1992). After phospholipase $A_2$ is activated, arachidonic acid, its metabolites and platelet-activating factor are generated. Platelet activating factor increases neuronal calcium levels , apparently by stimulating the release of glutamate (Miller et al 1992). Arachidonic acid potentiates NMDA-evoked currents and inhibits reuptake of glutamate into astrocytes and neurons further exacerbating the situation (Volterra et al 1992) ; oxygen free radicals can be formed during arachidonic acid metabolism (Lafon-Cazal et al 1993) leading to further phospholipase $A_2$ activation which represents further feedback. These processes can cause the neuron to digest itself by protein breakdown, free radical formation, and lipid peroxidation. It is possible in cerebral ischaemia that tissue reperfusion increases this damage by providing additional free radicals in the form of superoxide anions.

Superoxide ions and nitric oxide

Superoxide ions can participate in reactions to form products that may be toxic to neurons (Lipton et al 1993). Such a reaction involves nitric oxide, formed in neurons by nitric oxide synthase, which is activated by calcium influx triggered by NMDA-receptor stimulation. When NMDA receptors are excessively stimulated, nitric oxide and superoxide may be produce in increased quantities. Under these conditions, nitric oxide and superoxide ions may react to form a toxic substance called peroxynitrite, resulting in neuronal death (Lipton et al 1993)

Depending on its chemical state the NO group can lead to the destruction or protection of neurons. When one electron is removed from the nitric oxide molecule it becomes a nitrosium ion (NO+) which binds to a regulatory site on the NMDA receptor. Such binding results in decreased activity of NMDA receptors affording protection from excessive stimulation (Lipton et al 1993). This has led to therapeutic approaches to decrease NMDA-receptor overactivity with the use of drugs resembling nitrosium, such as nitroglycerin (Lipton et al 1993).

Reperfusion injury

Further cellular damage occurs during reperfusion of ischaemic brain tissue and neurons which are still viable may be irredeemably damaged (Krause et al 1988). There are several possible causes of this. Under normal conditions endothelial cells release prostacyclin and thromboxane $A_2$. Lipid peroxides produced during ischaemia inhibit prostacyclin formation and allow the unopposed action of thromboxane $A_2$ (Raichle 1983); upon reoxygenation, oxygen dependent enzymes increase the production of thromboxane $A_2$ further (Messick and Milde 1987). This leads to thrombus formation and vascular contraction and possibly the post-ischaemia hypoperfusion syndrome (Stevens et al 1986). Reoxygenation restores ATP via oxidative phosphorylation, which may result in massive uptake of $Ca^{2+}$ into mitochondria resulting in the self destruction of mitochondria (Safar 1988). Increase in intracellular $Ca^{2+}$ also causes contraction of vascular smooth muscle and vasoconstriction (Siesjo 1984) which may cause hypoperfusion. Ischaemic and vasogenic oedema also contribute to hypoperfusion.

Free radicals are produced during reperfusion when there is a surge of $O_2$ supply to the tissues (McCord 1985, Messick and Milde 1987) these cause membrane and collagen breakdown and worsen microcirculatory failure. All these events occur during recirculation, but are the result of metabolic cascades triggered by agonist-receptor interactions, energy failure and/or calcium influx during the insult.

Neurons in different areas of the cerebral cortex vary in their response to hypoxia . Some of the neurons in vulnerable regions seem to survive the immediate damage of an hypoxic-ischaemic event only to die off more gradually over the following 72 hours, despite the restoration of the circulation and full oxygenation (Garcia 1988). Experimental animal studies show that the characteristic histological appearance of ischaemic neuronal damage becomes visible, and progresses at, different rates depending on the anatomic region affected (Pulsinelli et al 1982). This may be partly due to the reperfusion syndrome; other possibilities include subclinical fits, or the fact that the damaged neurons may already be dead and the apparent delay may be an histological artifact (Garcia 1988, Safar 1988). Delayed post-insult neuronal death may be seen clinically as postanoxic demyelination, and clinical deterioration at 36 to 72 hours after a cerebral infarct (Plum 1983). Clinical spectroscopy may be prove a useful tool with which to investigate this phenomenon, as there is evidence to suggest that spectroscopic changes precede anatomic changes seen with magnetic resonance imaging (Menon et al 1990 a).

Potential pharmacotherapy

Glutamate: there are several sites at which damage mediated by glutamate might be attenuated. The synthesis and release of glutamate could be reduced or its uptake increased. The effect of excessive concentrations of glutamate could be antagonized at the receptor level. Drugs could also be used to offset the intracellular and extracellular neurotoxic events set in motion by receptor overstimulation. All these approaches have met with some success in vitro, but the results are inconsistent (Xue al 1994, Pellegrini-Giampietro et al 1994) and many of the drugs have unacceptable clinical side effects (Choi 1988). Drugs used so far include the NMDA receptor antagonist MK-801 and another drug GYK152466 which seems only to be effective in certain regions of the central nervous system (Xue et al 1994).

The potentially neuroprotective effect of calcium channel blockers after ischaemic conditions has been known for many years. Mechanisms of calcium channel blockers include vasodilatation, blocking of further neuronal calcium load, and suppression of

chemical cascades producing noxious mediators (Safar 1993). Laboratory results with calcium channel blockers demonstrate some beneficial effects but again clinical results with drugs such as nimodipine (The European Study Group on Nimodipine in Severe Head Injury 1994) are generally disappointing.

The effect of NO, as explained above may be either beneficial or detrimental. The influential effect of NO on post-ischaemic CBF and cerebral metabolism appears to be very important to outcome (Faraciand 1994). NO synthase inhibitors (L-NAME) may help to improve the oxygen supply-to demand ratio (Wei et al 1994) in damaged brain, inhibition of NO synthesis may decrease infarct size after forebrain ischaemia (Nishikawa et al 1994).

Other substances that have been tested in regard to their influence on outcome after global ischaemic and cardiac arrest are the xanthine derivatives, the steroids, free radical scavengers of the superoxide dismutase type, pyrimidine derivatives and kappa-opioid agonists. All these drugs have one thing in common: they demonstrate only marginal if any, improvement on neuronal or functional outcome after global or focal ischaemia (Ebmeyer et al 1995).

Clinical spectroscopy, both animal and human, may help in the research to find the agent or agents that can ameliorate brain injury after hypoxia and or ischaemia.. It is the only technique at present that can potentially visualise lactate, glutamate, aspartate, GABA, ATP, PCr, Pi and measure intracellular pH; all of which are central to the pathological mechanisms of hypoxic and ischaemic injury. It is a noninvasive technique which offers a unique method of investigating the relationship between biochemical and structural changes as they occur in the damaged brain.

## MAGNETIC RESONANCE SPECTROSCOPY AND HYPOXIC-ISCHAEMIC DAMAGE TO THE HUMAN BRAIN

Magnetic resonance spectroscopy is a noninvasive way of studying the brain's metabolic response to hypoxia and ischaemia and it can therefore provide information about intracellular events which would be lost if the tissue was destroyed for chemical analysis. Since ionising radiation is not used, spectroscopy can be used repeatedly to observe changes with time in the metabolism of the damaged brain. In combination with magnetic resonance imaging, investigation is possible of the relationship between the biochemical and structural changes produced by hypoxic-ischaemic damage. As signal detection is not specific, resonances are observed from all the mobile components present in sufficiently high concentrations (greater than 0.2mM). Spectroscopy is not a very sensitive technique and to detect pathological changes consistently in a single patient, metabolite content will need to vary by about 20% or more from the baseline value. Fortunately, the changes that produce clinical signs in a patient after hypoxic-ischaemic injury are likely to be of this size.

### $^{31}$Phosphorus Magnetic Resonance Spectroscopy.

$^{31}$P MRS allows observation of the metabolites central to cellular energy status (adenosine triphosphate (ATP), phosphocreatine (PCr) and inorganic phosphate (Pi)) as well as intracellular pH, phosphomonoesters (PME) and phosphodiesters (PDE). The presence of PCr allows calculation of ADP concentration based on the reaction catalysed by creatine kinase

$$PCr + ADP \rightleftharpoons Cr + ATP + H^{+}.$$

The sum of Cr and PCr is relatively constant in the brain, which allows calculation of Cr from PCr. Chance et al (1985) showed that the Pi/PCr ratio behaves very similarly to the ADP concentration. Since the Pi/PCr is easy to measure from the phosphorus spectrum it provides a convenient measure of metabolic status. In hypoxia there is an

increase in Pi/PCr, and as lactate accumulates the intracellular pH declines.

In extreme cases the Pi/PCr ratio approaches infinity, reflecting major loss of ATP. Unless this situation is remedied within minutes, the cells will die. If reversed soon enough, the system tends to return to steady state, although at a speed which depends on the insult and the species studied.

The effects of hypoxia and ischaemia on the human phosphorus spectrum have been demonstrated in several clinical situations by a number of workers. The first studies of ischaemic injury in humans were those possible with the small bore magnets of the time. There were two types: studies of neonates who had suffered birth asphyxia; and spectroscopy of the ischaemic limbs of adults with peripheral vascular disease. All these early studies were with surface coils. Although gross metabolic changes were detected, there was no information about the metabolic heterogeneity that might result from acute or chronic hypoxia and ischaemia.

The work done in chronically ischaemic limbs showed that pH was higher in patients with severe claudication than a control group. The main spectral differences between patients and controls occurred after exercise, when there was a much greater decrease in PCr and corresponding increase in Pi in the ischaemic group. Recovery of the spectral abnormalities was slower in the ischaemic group (Hands et al 1986).

Cady and his colleagues in 1983 were the first to obtain phosphorus spectra from the brains of neonates. Spectroscopic changes appeared to precede structural damage and they modified the spectra by infusing mannitol, showing that the $^{31}P$ spectra were sensitive almost immediately to biochemical changes.

The following year (1984), Younkin and coworkers published a report of phosphorus spectra acquired from seven newborns, all with a history of birth asphyxia but no clinical signs at the time of examination. They suggested that the large phosphomonoester peak was not composed of sugar phosphates as proposed by Cady

et al (1983) but of phosphorylethanolamine and phosphorylcholine, precursors for membrane synthesis. This peak was not present in other newborn animals studied with the same methods. They calculated a PCr/Pi ratio of 1.3 +/- 0.7 for the human infants, lower than that found in newborn lambs.

Hope et al (1984) reported the first spectra from normal neonatal brain and compared these with the changes produced by birth asphyxia in ten abnormal infants. An exciting finding was that although there were no obvious differences between the spectra from the abnormal and normal infants on the first day of life, by the 2nd to 9th day a fall in the PCr to Pi ratio occurred in the abnormal group. The lowest PCr/Pi ratios occurred at a mean time of 5 days after birth (range 16 hours - 9 days). A PCr/Pi ratio of less than 0.8 was associated with a very poor prognosis for survival and neurological outcome. They suggested that the delay in spectral change in the first 24 hours of life may provide a time for effective therapy. They also found a raised intracellular pH in the asphyxiated infants and contrasted this finding with previous animal studies where acute cerebral ischaemia caused a large fall in PCr/Pi and a profound reduction in pHi. This was an important point, illustrating that human studies of asphyxia are made after restoration of oxygenation and circulation, not during the insult, and cannot therefore be compared directly with animal studies that last minutes and hours, not days and weeks.

This study was followed by a larger study from the same group (Hamilton et al 1986). Twenty seven infants with increased cerebral echodensities detected by cranial ultrasound and consistent with hypoxic-ischaemic injury were examined with $^{31}P$ MRS. The phosphorus spectra predicted outcome more accurately than the cranial ultrasound. Nine of 15 infants with low PCr/Pi values died and all the other six infants developed cerebral atrophy. Serial MRS on five of the survivors showed that the spectra always returned to normal as cerebral atrophy became established. All 12 infants with PCr/Pi ratios within the normal range survived. Intracellular pH was very low (less than 6.7) in two terminally ill infants; in the other infants it was raised. The infants were studied for a median of 12 weeks (up to a maximum of 36 weeks) after

birth. The PCr/Pi ratio from the spectra of the normal infants increased markedly with maturation of the brain.

Azzopardi and coworkers (1989b) extended this work and compared the PCr/Pi values obtained in the first days of life with neurodevelopmental outcome at one year in a group of infants suspected of hypoxic-ischaemic brain injury. The sensitivity of the PCr/Pi ratio, used to predict which infants would have multiple impairments, was high. Infants with increased echodensities, thought to be due to periventricular leukomalacia, often had normal PCr/Pi ratios but subsequent abnormal outcomes. This may have been due to the inability of the technique, at that time, to localize to deeper lesions.

Laptook and colleagues (1989) studied one severely abnormal infant until the age of 10 months, and one normal infant until 8.5 months. The abnormal infant had a persistently elevated Pi peak and an alkalotic pH. Five other infants with less severe birth asphyxia were also examined in their first fourteen days, as were seven normal term infants aged eight hours to two days. Their spectra were indistinguishable apart from intracellular pH, which was increased in the axphyxiated infants.

There have now been many phosphorus magnetic resonance studies of cerebrovascular injury in adults in the first few hours and up to several years after injury, for example Welch et al 1985, Bottomley et al 1986 and Levine et al 1988. Bottomley and colleagues (1986) found a reduction of up to 40% in total phosphorus signal from the infarct, months and years after the insult, compared with the total $^{31}P$ signal from the normal contralateral hemisphere. In another study (Levine et al 1988), there was a decrease in the PCr/Pi ratio from the infarcted regions but the changes all resolved within seven days after injury despite persisting clinical neurological deficits. There was an acid pH for the first 32 hours after the stroke, the pH then became alkaline and returned to normal by ten days .

Most phosphorus spectroscopy studies of injured human brain suggest that abnormal phosphate metabolism does not last long. Either the cells are so badly damaged that

they die, leaving only their metabolically normal counterparts, or mechanisms restore the PCr/Pi ratio to normal and excrete excess protons soon after injury.

Proton ($^1$H) Magnetic Resonance Spectroscopy.

Proton MRS can detect brain lactate, and therefore proton and phosphorus spectroscopy together, may enable the study of the inter-relationship of intracellular pH and lactate in normal and abnormal brain.

Clinical proton spectroscopy began in the late 1980's and the first reports of pathological changes in proton spectra were from patients with cerebral infarcts (Berkelbach van der Sprenkel et al 1988, Bruhn et al 1989). The main changes were an obvious lactate peak and a decline in the NAA/Cr and NAA/Cho ratios consistent with neuronal loss or damage. Recent work by Urenjak and coworkers (1993) has shown that oligodendrocyte-type 2 astrocyte (O-2A) progenitor cells also contain a large amount of NAA, raising the possibility that some brain disorders in infants may reflect abnormalities in the development of oligodendroglia or their precursors.

As the (Cr) peak is composed of both phosphocreatine and creatine, this peak should remain relatively stable during hypoxia and ischaemia. This resonance has been used as an internal reference in clinical proton spectroscopy. The "choline peak" (Cho) represents a complex mixture of choline-containing compounds. Choline itself is a precursor for the neurotransmitter acetylcholine and for the membrane constituent phosphotidylcholine. Choline may increase with ischaemia (Scremin and Jenden 1989).

Glutamate and aspartate can be identified at short echo times (e.g 20 ms at a field strength of 2.0T [Michaelis et al 1993]) , and it may be possible to monitor changes in the concentration of these excitotoxic amino acids. At such short TE's other signals including those of GABA, taurine, myo-inositols and the aspartyl group of NAA can also be seen. In normal brain there is very little signal from mobile lipids. It is possible that an increase may be seen in this peak after ischaemia, as both global

(Yoshida et al 1980, 1983) and regional levels of free fatty acids are known to increase after hypoxia and ischaemia (Bhakoo et al 1984).

A lactate peak can be detected in normal human brain at a concentration of less than 1mM (Hanstock et al 1988) and spectroscopy has shown changes in this peak due to visual stimulation within a normal physiological range (Prichard et al 1989). The brain lactate concentration increased in neurologically normal volunteers when they hyperventilated and phosphorus spectroscopy performed at the same time showed an increase in intracellular pH (van Rijen et al 1989). As lactate is the end product of glycolysis it rises in concentration when the glycolytic rate in the tissue exceeds the tissue's capacity to catabolize lactate or export it to the bloodstream. Proton spectroscopy offers a non-invasive method of following changes in lactate concentration in pathological states.

There is some evidence that the spectral changes produced by hypoxia and ischaemia precede imaging changes (Cady et al 1983, Brant-Zawadzki et al 1987, Menon et al 1990 a). Therefore spectroscopy may indicate when brain injury is reversible or amenable to therapy. To our knowledge our studies in infants were the first proton spectroscopic studies of the effects of hypoxic-ischaemic injury on the immature brain. Comparing spectroscopy with other more established means of observing brain injury such as clinical neurological examination and cranial ultrasound, as well as animal models and tissue biopsies, may increase our understanding of the biochemical lesions underlying clinical syndromes, and extend our knowledge of the clinical applications of magnetic resonance spectroscopy.

## SEDATION, ANAESTHESIA AND MONITORING OF INFANTS WITHIN MAGNETIC RESONANCE SYSTEMS

Care of any sick patient within a magnetic resonance system is difficult for a number of reasons:

(a). The presence of a high magnetic field. The attractive force of the magnet exerts a substantial pull on ferromagnetic objects, and when free these can move towards the magnet centre at great speed. All equipment taken into the magnet area must therefore be either non-ferromagnetic or firmly secured. Patients and personnel must be screened for ferromagnetic implants.

(b). Space is usually very limited around the magnet bore, and often there is no separate patient preparation or recovery area.

(c). Access to, and visualisation of, the patient is severely limited. Once infants are in the magnet bore they may not be visible at all.

(d). In common with other imaging sites radiology personnel may be unfamiliar with managing sick patients, and resuscitation equipment may not be immediately available.

(e). Monitoring equipment malfunctions in the presence of a high magnetic field, the rapidly changing gradient magnetic fields and radiofrequency currents.

(f). The presence of monitoring equipment can induce current and entrain stray radiofrequency currents resulting in degradation of magnetic resonance spectra and images.

In addition there are particular problems associated with monitoring, sedating and anaesthetizing sick infants within a magnetic resonance system:

(a). Transport to the MR unit must be considered; often the neonatal unit is far away from the MR unit and so a transport incubator will be required to move neonates.

(b). Maintenance of body temperature is critical in sick children but the MR environment is cold and air-conditioned to ensure optimal function of gradient coils and computer systems. Methods of keeping the children warm must be developed.

(c). If a ventilator is to be used, not only must it be valveless to ensure that no working parts can jam within the magnetic field, but it must also be compatible for use in the

smallest neonate.

(d). Children who have been heavily sedated or anaesthetized must be monitored to ensure adequate cardiovascular and respiratory function. All anaesthetized children will need to be intubated as the airway cannot be managed safely any other way when the child is in the magnet bore.

Placement of equipment

Monitoring and ventilation equipment can be kept outside the magnetic field strength at which ferromagnetic attraction is likely to occur (normally between 30 and 50 gauss). Long monitoring leads and ventilation tubing (which has a large compressible volume) are required. There is an increased risk of disconnection.

Alternatively the monitoring equipment and ventilator can be sited close to the magnet bore, in which case the majority of equipment components must be non-ferromagnetic. Ideally, an MRI compatible anaesthetic machine and ventilator should be purchased (e.g. Pneupac, UK) although this type of commercial system was not available at the time of these studies.

Monitoring problems

All children were monitored during these studies despite the problems involved (Shellock 1986; Roth et al 1985). The presence of monitoring equipment can result in degradation of image and spectral quality (Fig.29). As the NMR signals being studied are of very low intensity they can be interfered with by stray high frequency electromagnetic radiation or interference arising from electrical equipment and monitoring devices (Fig.30). It is common practice therefore to enclose the scanning area in a radiofrequency shield or Faraday cage which can be built into the walls of the imaging room or can immediately surround the magnet. Non conductive devices such as ventilator tubing can be safely passed through the shield (using specially constructed copper lined RF ports) but wires that transgress the Faraday cage act as aerials feeding in noise from the external environment. This problem can be overcome by filtering the wires using standard filters or filters gated on and off with signals from an ECG, or by

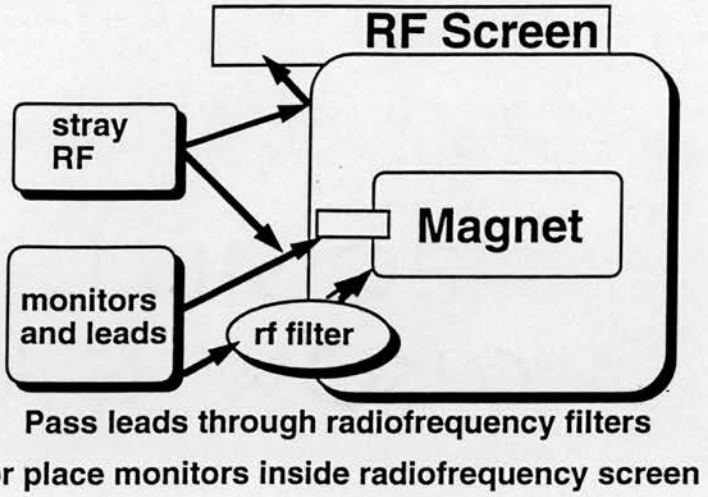



Fig. 29 Radiofrequency interference from external sources (BBC) and monitoring equipment is prevented from entering the imaging area by the radiofrequency (RF) shield. This shield is breached by monitoring cables that can pick up and carry interference into the scanner. The interposition of low pass filters in the circuit prevents this.

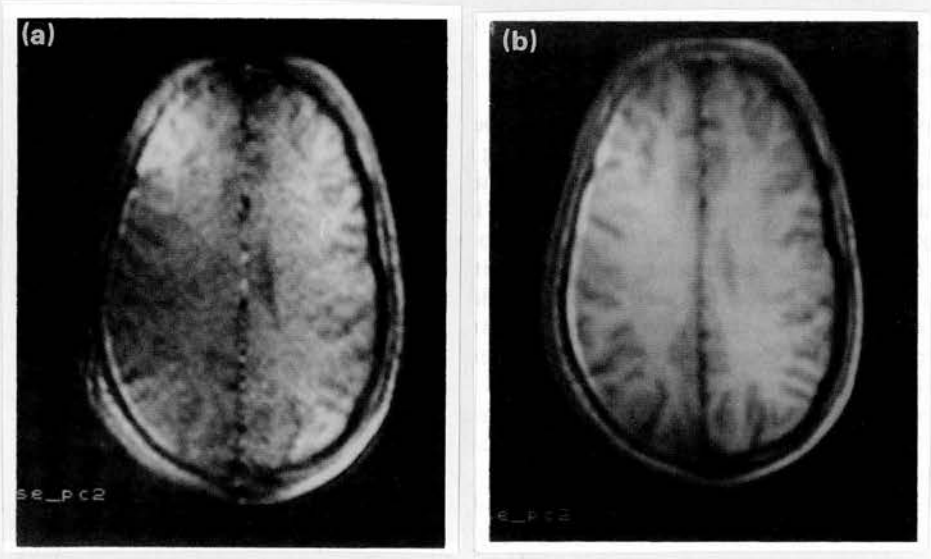



Fig. 30. Transverse $T_1$ weighted images of the brain of a normal volunteer demonstrating (a) the interference produced by an unfiltered pulse oximetry lead and (b) the improvement after filtering.

using an optical or radio link to isolate the area within the RF screen. If standard radiofrequency Pi ($\pi$) filters are used, care must be taken to match filters to specific monitors. Another method is to house the monitoring equipment within its own radiofrequency shield; such a system has been produced commercially by Bruker for a cost of about £33,000.

Mains power supplies can carry interference into the Faraday cage and so monitoring equipment should use an adequately filtered and isolated power source or be run by batteries. Batteries are strongly ferromagnetic, and any battery powered monitoring equipment must be very firmly secured within the magnetic field.

The ECG of a patient within a static magnetic field shows significant changes. According to Faraday's law, a voltage is induced across a column of conducting fluid (in this case blood). The changes are maximal when the fluid flow is at $90^{o}$ to the field, which occurs in the supine patient when blood flows through the transverse aorta; hence the changes are principally in leads I, II, $V_1$ and $V_2$. These superimposed potentials are greatest in the early T wave and late ST segments. The potentials increase with field strength. The rapidly changing magnetic fields of the imaging gradients also induce potential differences across the loops formed by the ECG leads, and the radiofrequency currents induce currents within the leads. These problems can be ameliorated by the use of shielded cables. Another solution is to transmit the ECG data by telemetry or a fibreoptic system. All electrodes and leads attached to the patient should be non-magnetic to avoid current induction. Careful placement of the ECG electrodes and leads can minimise ECG changes (Wendt et al 1988, Dimick et al 1987). The beam of a standard cathode ray oscilloscope ECG display will be pulled off centre by the powerful magnetic field.

Pulse oximetry is the single most useful piece of monitoring equipment for the observation of neonates and infants, however it has proved to be the most difficult monitor to use within magnetic resonance systems. Currents are induced in the cable

resulting in interference which is aggravated by poor signal, due to patient movement or to poor probe placement. All magnetic components must be removed from the probe. Patient injuries, especially burns, have resulted from currents and heating induced in monitoring probes and leads by the changing magnetic field gradients and rapidly switching radiofrequency currents. The occurrence of burns has been particularly associated with the use of pulse oximetry (Kanal and Shellock 1990).

The ways in which we modified commercially available equipment to overcome the problems listed above are discussed further in the methods and results sections.

## CLINICAL METHODS

Permission for these studies was obtained from the Research Ethics Committee of the Royal Postgraduate Medical School, Hammersmith Hospital. Informed consent was obtained from each patient or parent and documented in the case notes. All the children were referred from the neonatal unit (or follow up clinic) at either Hammersmith Hospital or Queen Charlotte's Hospital.

### Patients

Most of the children were selected for magnetic resonance spectroscopy examination because they had a history of birth asphyxia or clinical signs of hypoxic-ischaemic injury. Other children were studied because they had evidence of an ischaemic or haemorrhagic lesion on cranial ultrasound, computerized axial tomography (CT) or magnetic resonance imaging. A few children were referred for study because they had persistently abnormal tone, and an unclear clinical diagnosis.

All the children had full clinical neurological examinations and MRI. All the infants had repeated cranial ultrasound scans. When indicated clinically, 24 hour or standard electroencephalograms, evoked potentials (visual, auditory and somatosensory), Doppler blood flow studies and computerised axial tomography scans were done.

At follow up examinations from eighteen months onwards, all children had a structured neurological examination. Children were scored on the Griffiths developmental scale when possible but many children could not perform the tests adequately as they were so handicapped; therefore we have not included Griffiths scores in the clinical details (Appendices A and B). Because of the incomplete Griffiths scores developmental quotients (DQ) were not recorded by the paediatricians involved in this study. The main clinical diagnoses in the abnormal infants were perinatal ischaemic and haemorrhagic brain injury.

To obtain neurologically normal infants as controls, we approached mothers at antenatal

clinics and gave them information about our studies.

The abnormal children were divided into four outcome groups on the basis of clinical neurological examination at eighteen months or more:

Normal: infants who were normal at eighteen months or more, but who may have had transient abnormalities of tone before this;

Moderate: infants who had persisting mild abnormalities of tone e.g. hypotonia; minor movement disorders e.g clumsiness; speech delay; mild developmental delay; or mild sensory (visual/hearing) impairment;

Severe: infants with a central motor deficit i.e. hemiplegia, spastic diplegia, spastic quadriplegia, athetoid quadriplegia; severe hearing/visual impairment; severe developmental delay;

Other: infants who were lost to follow up before neurological assessment at eighteen months could be performed; infants who died before one year of age and did not have a post-mortem examination; infants in whom a subsequent diagnosis explained the abnormal clinical signs and in whom there was no other evidence of hypoxic, ischaemic or haemorrhagic brain injury e.g Hurler's syndrome.

The clinical details of the children who had proton spectroscopy examinations are given in Appendix A, and the clinical details of the children who had phosphorus spectroscopy examinations are given in Appendix B. The children who had both proton and phosphorus spectroscopy examinations are included in both appendices. Table 2 (next page) gives the clinical details of a sub-group of patients all of whom were born at 39-42 weeks PCA and who were examined with proton spectroscopy within the first month of life. The severity of hypoxic-ischaemic encephalopathy was graded according to Sarnat and Sarnat (1976).

Monitoring and Ventilation Equipment

Equipment modifications had to be investigated before we could safely study these sick neonates within the magnet bore, because of the problems of monitoring patients and using anaesthetic machines and ventilators within the magnetic field (see p. 73).

TABLE 2.

| CASE | GESTATIONAL AGE | APGAR SCORE | HIE SCORE | CLINICAL OUTCOME AT EIGHTEEN MONTHS |
|---|---|---|---|---|
| K.R | 42 | 0 , 0 | II | normal |
| S.B | 42 | 1 , 4 | I | normal |
| I.S | 40 | 7 , 8 | II | normal |
| G.B.S | 42 | 9 , 10 | II | normal |
| K.H | 40 | 9 , 10 | II | normal |
| M.B | 38 | 0 , 2 | III | spastic quadriplegia, fits, severe developmental delay |
| M.L | 40 | 3 , 9 | II | spastic quadriplegia |
| T.H | 40 | 0 , 5 | II | spastic quadriplegia, fits, severe developmental delay |
| J.M | 42 | 3 , 9 | II | microcephaly, fits, severe developmental delay |
| A.R | 39 | 3 , 4 | II | spastic quadriplegia, severe developmental delay. |

Table 2. Subgroup of infants who were born at 39 - 42 weeks postconceptional age (PCA) and who were examined with proton spectroscopy within the first month of life. HIE, hypoxic-ischaemic encephalopathy, graded according to Sarnat and Sarnat (1976).

Anaesthetic machine and ventilators

We sited the ferromagnetic anaesthetic machine and monitoring equipment between the 5 gauss and 30 gauss lines (8-9m from the infant in the magnet bore). We found that there was no significant magnetic attraction exerted on the equipment at this site, but all items were secured firmly. We used an unmodified Excel 210 anaesthetic machine (Ohmeda: Hatfield, UK) supplied by piped gases. We used either a Penlon Nuffield Series 200 ventilator with a Newton paediatric valve or a new CW 200 ventilator and tested them connected to 10m Bain and modified Ayre's T- piece breathing systems to measure maximum pressure generated at the mouth, and expiratory resistance. Both the ventilators are valveless, with no magnetic moving parts to 'stick' within the field.

Resuscitation equipment

A defibrillator (Lifepak 5, Physio-Control, Basingstoke) was modified by the manufacturer at our request. The leads to the paddles were lengthened by 2m with no decrease in power output, which enabled us to site the defibrillator safely at the edge of the magnetic field but still keep it within range of the patient. A plastic paediatric laryngoscope was made safe by removing the standard ferromagnetic batteries and replacing them with a single paper covered, nonmagnetic 3V lithium battery; a nonmagnetic aluminium spacer was required to hold the single battery in place (Fig.31). We used a Laerdal (Laerdal Medical Ltd, Orpington, Kent) paediatric resuscitator, a self-inflating valveless silicone bag with no magnetic working parts.

ECG

We used carbon fibre leads (NDM American Hospital Supply, Dayton, Ohio, USA) and "Red Dot" electrodes (3M Medical , St. Paul, Minnesota). The leads were braided and placed close together as near to the centre of the field as possible. A liquid crystal display was used (Marquette Inc., Bewdly, Worcs.) as that type of screen is not distorted by the magnetic field.

Pulse oximetry

Pulse oximetry had not been successfully used by any other UK department within an



Fig. 31 Plastic laryngoscope (Penlon) powered by a single paper covered, non-magnetic 3V lithium battery. A non-magnetic aluminium spacer is required to hold the single battery in place.

MR system at the time of this study. Some of the possible solutions to the problems discussed earlier (p.73) that we tried, included: careful selection of probe site and placement of the probe; screening the cable and minimising its length to reduce current induction; passing the lead through radiofrequency filters; amplifying the pulse oximeter signal, when possible, before passing through the radiofrequency filters; removing all magnetic components from the probe or using plastic/disposable probes.

We tested four pulse oximeters initially: the Nellcor 100, the Nellcor 200, the Datex OSP-200, and the Ohmeda Biox 3700. Later we tested the Nonin 8604, a pulse oximeter designed to be MR compatible. The pulse oximeters were evaluated on the basis of the image and spectral degradation produced and the adequacy of pulse oximeter information provided during all types of sequences. The probe site was examined for burns after use.

Capnography

We adapted a standard Ohmeda 5200 capnograph by extending the sampling tubing to 11m.

Noninvasive blood pressure

The ferrous connections were removed from a neonatal standard (Dinamap) blood pressure cuff and replaced with nylon connections; the tubing was lengthened.

Figure 32 shows all the monitoring equipment in place on the anaesthetic machine, the Nuffield Penlon 200 ventilator, and the incubator for transferring premature and ventilated infants to the MR unit.

Procedure

Most of the children were examined during natural sleep after a feed. Three neonates who were being ventilated on the neonatal unit were ventilated during the examination.

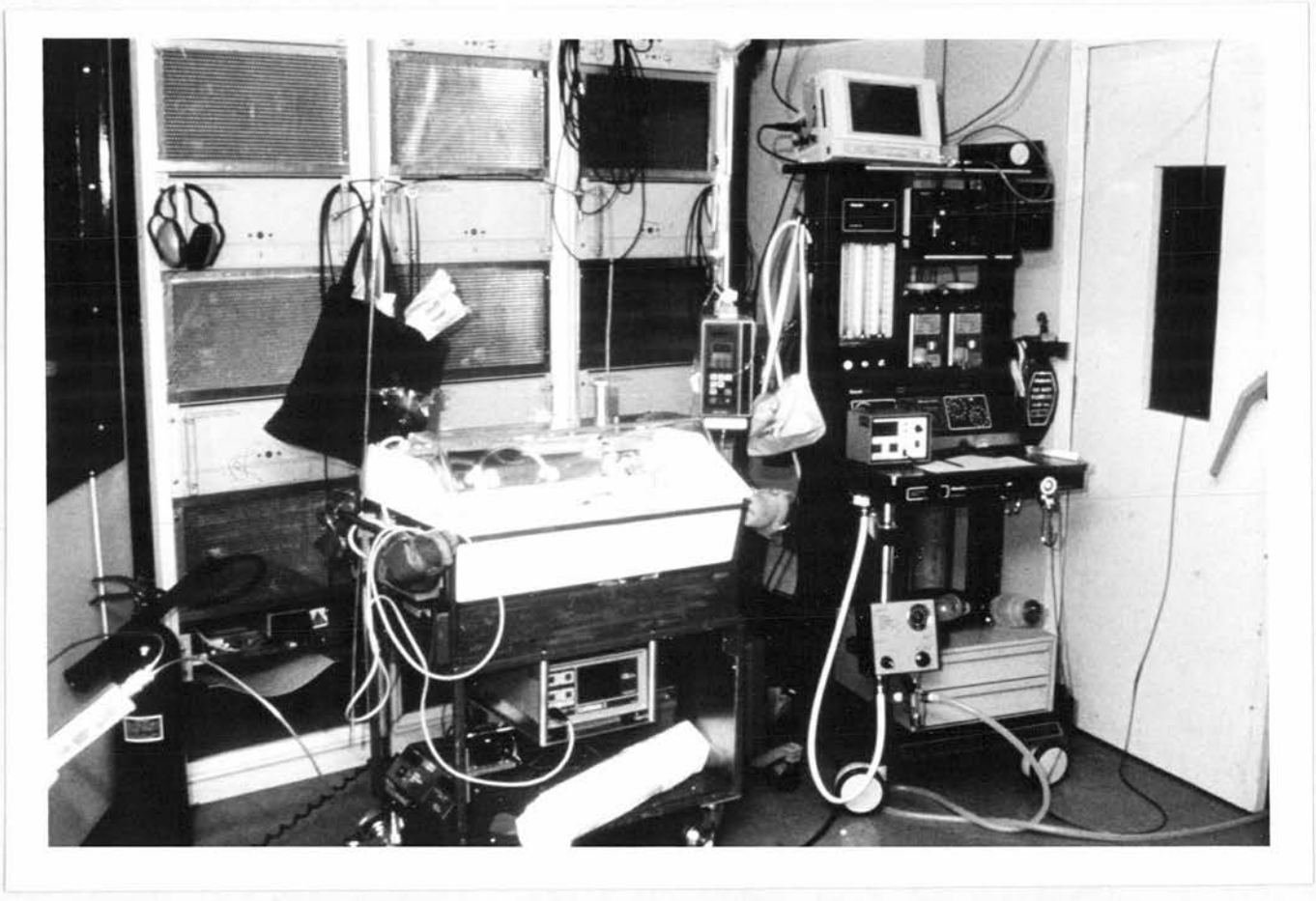


Fig. 32 Anaesthetic machine with a Penlon Nuffield series 200 ventilator plus Newton paediatric valve, and transport incubator are shown sited outside the radiofrequency screen doors while a neonate is ventilated within the magnet. All the adapted monitoring equipment is present on the anaesthetic machine.

Older children were examined during natural sleep when possible. If this was not possible, and if their clinical state allowed, oral chloral hydrate (80mg/kg) was given. This dose exceeds that recommended in the British National Formulary, but it has been used without untoward consequences since 1983 by paediatricians working with the MR unit to produce reliable sedation. Ethics committee permission was not given to study the children under general anaesthesia.

All the children were monitored with an electrocardiograph (ECG) (Marquette systems), an apnoea alarm (Graseby), and pulse oximetry (Nellcor N-200). On several occasions when supplementary oxygen was given by face mask, extended narrow bore sampling tubing from a capnograph was attached to the facemask and end tidal $CO_2$ (Datex 5200) was monitored.

The children were wrapped in warm blankets and placed prone or on their side. No child was examined supine. When necessary the head was held in position by standard X-ray positioning pads. A doctor was always present during the MR examination of a child and the child was removed from the magnet bore if there was any clinical concern; nasopharyngeal/oral suction was possible in the magnet area. If the children remained still or asleep from the start of the procedure, the total examination (imaging and spectroscopy) lasted between one hour and two and a half hours.

Certain assumptions had to be made about our clinical paediatric proton spectra because of time restraints and technical problems. To try to validate our paediatric spectra other proton spectra were obtained from eleven adults. These were patients in whom a contrast enhanced CT scan (third or fourth generation) displayed a low attenuation focal lesion with evidence of a mass effect, consistent with the presence of an intracranial tumour. These patients subsequently had the tumours resected and biopsies were frozen in liquid nitrogen within 30s of surgical removal. Spectroscopy was performed before surgery on the patients (5 men and 6 women; 30-72 years old ) and five normal volunteers (all men; 25-47 years old). The volunteers were neurologically normal.

Imaging was in at least two orthogonal planes, using a partial saturation sequence (TR 500/ TE17). We selected a cubic volume of interest (64 $cm^3$) to contain the bulk of the tumour and to avoid overlap with the skull and surrounding bone marrow. Proton spectra were collected as described (p. 32), except from one patient, when optimisation of the $1\bar{3}3\bar{1}$ pulse was for lactate.

In five patients, spectra were obtained from a radiologically normal region within the contralateral hemisphere as well as from the tumour volume. In the normal subjects the spectra were obtained from volumes of interest placed either in the temporoparietal region of one hemisphere or spanning the temporoparietal regions of both hemispheres.

The clinical spectra were analysed by four individuals who did not know the clinical diagnosis. The peak heights of the NAA, Cr and Cho peaks were compared with control spectra and were scored: no change; moderate change; or marked change. Any lactate and/or lipid peak was noted, as were any additional resonances. The changes in the clinical spectra were compared with the <u>in vitro</u> spectra from the tumour biopsies.

The biopsy samples weighed from 5mg to 2.6g. They were extracted into 12% perchloric acid, using standard procedures for extraction and neutralisation. Sodium

2,2,3,3-tetradeuteropropionate was added to the samples as a chemical shift and concentration standard. Spectroscopy was performed on lyophilised samples redissolved in deuterium oxide; comparison of spectra before and after lyophilisation showed that this procedure caused no significant loss of metabolites.

Histology was performed on all samples, including normal white matter. Immediate diagnosis was made on smear results and confirmed in sections of fixed and embedded material. The results were classified according to Kernohan's classification of central nervous system tumours.

Proton spectra of these biopsies were acquired at 360MHz on a Bruker spectrometer or at 500 MHz on a JEOL spectrometer. Concentrations were determined from relative peak areas in fully relaxed spectra (or after correction for saturation), taking into account the number of protons contributing to each signal (three for phosphocreatine and creatine (Cr) and NAA, nine for Cho and sodium 2,2,3,3-tetradeuteropropionateTSP). This permitted measurement of absolute concentrations in millimoles per kilogram wet weight of tissue. Data are presented as means +/- SEM and statistical significance was evaluated using a two tailed Student t-test.

# RESULTS

# RESULTS

The work in this thesis was carried out over a twenty month period; during that time we studied 42 children with proton spectroscopy (82 examinations, 60 successful) and 37 children with phosphorus spectroscopy (47 examinations, 46 successful). The children were aged between 33 weeks post-conceptual age (PCA) and 4 years and three months post natal age (PNA) at the time of their initial magnetic resonance spectroscopy examination. Fourteen of the children had proton and phosphorus spectra acquired during the same examination, allowing direct comparisons of age related changes, and changes due to brain injury, to be made between the two types of spectra.

## Technical limitations of this work

Proton spectroscopy is technically more demanding than phosphorus due to the need to suppress the 80M water signal, and the much narrower chemical shift range of the metabolites that can be observed; it is for these reasons that proton spectroscopy developed much later than phosphorus. Proton spectroscopy had not previously been reported in children at the time this work was done, and indeed clinical proton spectroscopy in adults was still a relatively new technique. As a result thte proton MRS studies described in this thesis were subject to a number of technical limitations.

The 1.6T magnet system used was a prototype system, with a full time team of physicists and engineers working on it. This meant in some areas we had greater technical ability than other groups e.g. the ability to do both proton and phosphorus spectroscopy, but it also meant that there were long periods when modifications were occurring when the system was not available for clinical studies.

Technical capabilities did evolve as these studies were done; in the earliest studies the smallest volume achievable with spectroscopy was 64$cm^3$, a very large volume with which to study the brain of a neonate. The achievable volume improved with time, and we modified the studies accordingly.

Because of the time involved in collecting a single spectrum it was very difficult to acquire repeated spectra to assess the reproducibility of the technique; when it was possible to collect more than one spectrum a different echo time was used in order to estimate $T_2$ effects. Although the examination was repeated on several occasions within one or two days, that was not soon enough to guarantee that the brain had not changed during that time.

The principal problems we faced were: a sloping base line due to difficulties with water suppression and difficulty in separating the signal intensity peaks resulting in poor spectral resolution. These problems were compounded by the fact that we were studying unanaesthetized children; movement caused further deterioration in the spectra, and the time required to collect good quality spectra was limited by the time these sick infants could spend in the cold magnet bore.

The problems encountered are apparent from the spectra presented here, resulting in problems with spectral analysis which was itself at the time very unsophisticated. When this work was done an easily usable programme was available to run on "Sun" workstations to smooth and process phosphorus spectra. Phosphorus spectroscopy was a well established technique at the Hammersmith Hospital and the technical quality of the spectra was high. There was no such programme available to process proton spectra i.e. there was no means of smoothing the data and achieving a flat baseline, and indeed there are limitations to what any data processing technique can achieve. Proton and phosphorus spectra are not directly comparable, and no attempt is made to compare the spectra themselves in this thesis although information is acquired by analysing the biochemical data provided by each type of spectrum from an individual patient.

The processing of the proton spectra was time consuming and done by hand. It was not possible, within a small team of workers, to truly "blind" the analyst. This may have introduced a degree of bias; however, the outcome groups were only allocated once the child was more than eighteen months old, and so the outcome group was rarely known at the time of analysis of the spectra. Problems of bias will be reduced

with automatic spectral processing.

Proton spectra are rapidly improving as technical breakthroughs are made, and a software package for producing areas from these processed smoothed spectra is now running at the Hammersmith (1996). The work performed in this thesis represents the earliest work in this field. Undoubtedly, for the reasons discussed above, the quantity and quality of our proton spectra were impaired and are not comparable with current state of the art spectra; however, similar studies have since been performed by other groups and our work has been validated.

Normal infants

Recruitment of normal infants for comparison of proton and phosphorus spectra was difficult, despite approaching mothers with information about the aims of the study in the ante-natal clinic. Most were unwilling or unable to participate, often because they were not in hospital long and did not live near the hospital. Four mothers brought their newborn infants for study and the magnet system was not working; one of these mothers came four times. The child of one of the paediatricians involved in the study was examined as a normal, twice. The spectra were not within the limits expected for a normal infant and sadly the child was diagnosed several months later as having developmental delay; no formal diagnosis has yet been made. In total, only four normal infants were studied with a total of six examinations. Two of these infants (RT, Nat T) were siblings of abnormal infants in the study.

Not all of our examinations produced analysable data; there were several reasons for this:

Withdrawals and failed studies (technical reasons)

The first two infants examined with proton spectroscopy were studied with sequences optimized for the detection of lactate but were excluded from analysis because all other sequences were optimized for N-acetylaspartate. For two of the examinations no spectra were obtained, perhaps because of equipment faults. Eddy currents from the unshielded gradients used were a persistent problem and are likely to have contributed

to the large number of proton spectra which were not suitable for analysis.

Good quality data (both proton and phosphorus) from one patient (SB) were lost during a computer disc back up. The spectra which had already been printed, were used for measurements by hand, but no computer analysis was performed.

During the twenty months of the study there were periods (up to two months at one time) when technical work and upgrading of the magnet system prevented studies. Some follow ups were missed because of this.

Withdrawals and failed studies (patient reasons)

One child (SAB) was re-examined aged one year. She was sedated for the examination with oral chloral hydrate by one of the paediatricians involved with the study. She became hypoxic during the examination, which was immediately stopped. She was admitted to the intensive care unit for overnight observation and made an uneventful recovery.

In ten cases the infant was restless and awoke, or moved persistently during the first stages of the examination. These children were removed from the magnet bore and successfully re-examined later the same day or the next day.

In all the other cases where the spectra were of unsatisfactory quality, the most likely reason was patient movement during the examination, although eddy currents may have contributed. In total the 82 proton examinations produced 60 sets of analysable proton spectra and the 47 phosphorus examinations produced 46 sets of analysable phosphorus spectra.

## MONITORING EQUIPMENT

Before we could study sick neonates and children we had to ensure that we could adequately monitor, oxygenate, and ventilate them as necessary, within the whole body magnet system. The modifications we made to monitoring and life-support have been described earlier (p.78).

The adapted monitoring equipment worked effectively, and often permitted an increase in examination time as we were reassured that the children were well, without having to remove them from the magnet bore.

### ECG

Some distortion of the ST segment and T waves was produced by the flow of blood through the magnetic field. The changing magnetic gradient fields caused artifacts on the ECG which could cause the heart rate to appear artificially elevated (Fig.33).

### Pulse oximetry

The Ohmeda Biox 3700 and Datex OSP-200 pulse oximeter did not function at all. Despite our precautions (see p.80) the radiofrequency field and magnetic gradients produced marked interference. The Nellcor 100 gave information when the magnetic field gradients were not in use. However, the ECG link present in the Nellcor 200 markedly improved reliability, although some interference still resulted from very rapid rates of gradient change. The most reliable pulse oximeter was the Nonin 8604, which became available only towards the end of our studies. This oximeter has been specifically designed for use within magnetic resonance systems. The information from the Nellcor 200 and the Nonin 8604 on adequacy of oxygenation and heart rate, was so useful, that we often used pulse oximetry alone for the examination of patients who were not seriously ill.

### Burns

There were no burns from any piece of monitoring equipment.

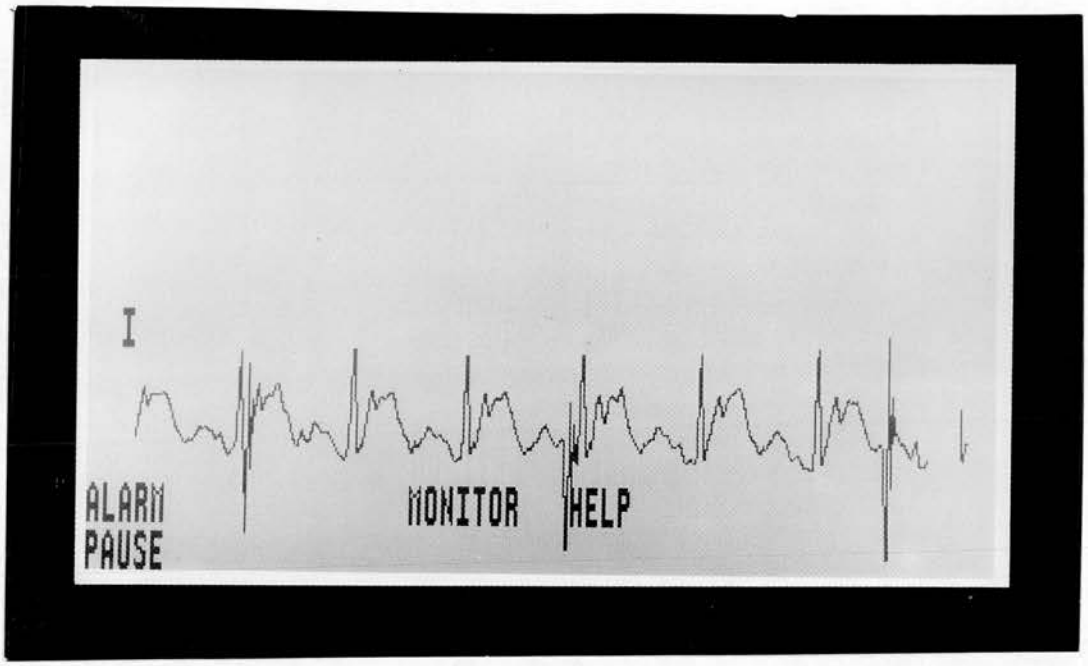



Fig. 33 ECG recorded from a healthy volunteer within the bore of the 1.6T magnet. The T wave and ST abnormalities, caused by the voltage induced by blood flow, are clearly shown. The changing magnetic fields of the imaging gradients have produced spike artifacts superimposed on the ECG.

## PROTON SPECTROSCOPY

Our methods for acquiring proton spectra were described on p.49. A proton spectrum from normal adult brain is shown in Fig.34(a) and resonances attributed to N-acetyl aspartate (NAA) at 2.0ppm; creatine and phosphocreatine (Cr) at 3.0 ppm, and choline containing compounds (Cho) at 3.2 ppm. In some normal adult spectra a peak at 1.3ppm due to lactate or fat can be seen (Lac/fat).

The most prominent resonances seen on all the paediatric spectra were also at 2.0 ppm, N-acetylaspartate (NAA), 3.0 ppm, creatine and phosphocreatine (Cr), and 3.2 ppm, choline-containing compounds (Cho), although the relative heights of these peaks varied in relation to the childrens age. Peaks were seen in the lactate/fat region and some of these peaks had the typical doublet shape of a lactate peak. However, we could not attribute any of these peaks definitively to lactate as the only way to do this with certainty is to see the doublet invert at the shorter echo time of 135 ms. Spectra acquired at this echo time were not analysable.

The absolute peak heights measured from all the proton spectra and the metabolite ratios calculated from them are shown in Table 3. The proton spectra are all scaled individually and so it is not possible to compare the peak heights among different examination or to perform data analysis on the peak heights alone.

Table 3 also shows the mean NAA/Cho, NAA/Cr and Cho/Cr ratios acquired from 22 adult volunteers with no neurological disease. The mean for NAA/Cho is 3.6 +/- 0.59 with a range of 2.9 - 4.8; the mean for NAA/Cr is 3.5 +/- 0.71 with a range of 2.4 - 4.8; the mean for Cho/Cr is 1.0 +/- 0.20 with a range of 0.7 - 1.3. The peak heights and metabolite ratios from all the adult spectra are shown in appendix C.

### Region studied

Our aim was to study the same region of brain in each child, namely the parieto-occipital region at mid-ventricular level. In the early examinations the smallest volume

of interest achievable was 64cm$^3$ and that volume completely filled the brain of children of < 38w PCA. In seven of the fifteen children of <38w PCA a central volume of 64cm$^3$ was studied, in the other eight (as technical capabilities improved) a 27cm$^3$ volume placed closer to the parieto-occipital region was studied. These volumes occupy large amounts of a child's brain, and therefore it was not possible to make any comments on regional spectral variability. Table 3A shows the region studied and the voxel size for each child.

Age related changes

Spectra acquired as described (p.49) were analysed using peak height ratios. Proton spectra from an infant with a normal outcome studied at 35 weeks (PCA) age and a normal infant at 40.5 weeks (PCA) are shown in Figs.35 and 36. When compared with the adult spectrum (Fig.34) the age-related changes are clear; the NAA/Cho and NAA/Cr ratios increase with age and the Cho/Cr ratio decreases with age. The Cho peak is dominant in the spectrum of the premature infant. The NAA peak is dominant in the adult spectrum and the Cr peak is larger than the Cho peak.

The NAA/Cho, NAA/Cr and Cho/Cr ratios are plotted against post-conceptional age for all the children, normal and abnormal in Figs 37, 38 and 39. The NAA/Cho and NAA/Cr ratios increase with age and the Cho/Cr ratios decrease within the first few months after birth.

Table 3B shows the metabolite ratios for the 14 children who had more than one proton examination. The values are shown in chronological order. Figures 3Bi, 3Bii and 3Biii show the same metabolite ratios plotted graphically.

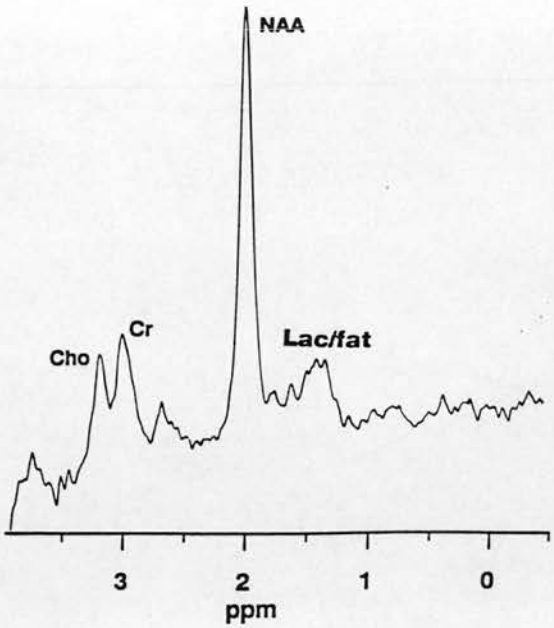
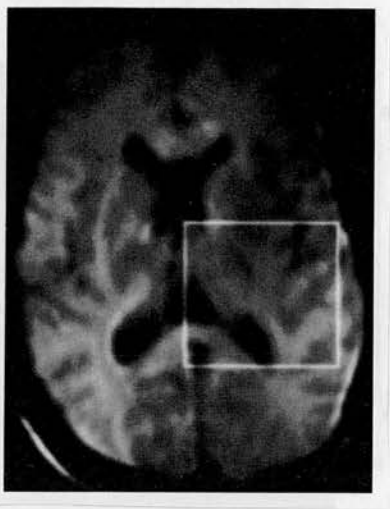



Fig. 34(a) Proton spectrum acquired from volume shown in (b). TR 2,000ms, TE 270ms, 128 data collects. For this and subsequent figures the proton spectra are not scaled vertically for comparison. The principal peaks seen in this spectrum are NAA, N-acetylaspartate; Cho, choline containing compounds; Cr, creatine and phosphocreatine; and a peak at 1.3ppm which could be due to lactate or fat (Lac/fat).



(b) Magnetic resonance image (SE 500/22) of the brain of a normal adult volunteer. The 64cm$^3$ volume of interest for proton spectroscopy is shown in the parieto-occipital region.

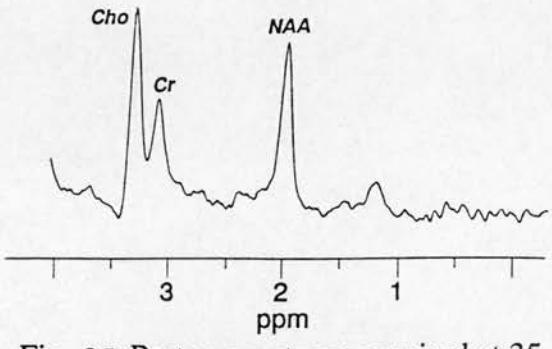



Fig. 35 Proton spectrum acquired at 35 weeks (PCA) from a 27cm$^3$ volume in the centre of the brain of DH an infant with little neurological abnormality in the neonatal period, who was thought to be normal at discharge, but was lost to further follow up. TR 2,000ms, TE 270ms, 128 data collects. The NAA/Cho ratio is 0.8, the NAA/Cr ratio is 1.6 and the Cho/Cr ratio is 2.0.




Fig. 36 Proton spectrum acquired from a 64cm$^3$ volume in the parieto-occipital region of the brain of a neurologically normal infant (RT) at 40 weeks PCA. The NAA/Cho ratio is 1.4, the NAA/Cr ratio is 1.5 and the Cho/Cr ratio is 1.1.

| | | | | | | | | | |
|---|---|---|---|---|---|---|---|---|---|
| 1 | 33.0 | severe | .5 | 1.6 | 3.0 | sab | 25 | 48 | 16 |
| 2 | 35.0 | other | .8 | 1.6 | 2.0 | dh | 30 | 38 | 19 |
| 3 | 35.0 | severe | 1.1 | 1.8 | 1.6 | lc | 49 | 45 | 28 |
| 4 | 82.0 | severe | 3.1 | 2.6 | .9 | lc | 53 | 17 | 20 |
| 5 | 35.0 | moderate | 1.1 | 2.1 | 1.8 | ae | 66 | 58 | 32 |
| 6 | 36.0 | severe | .8 | 1.4 | 1.8 | sg | 53 | 70 | 38 |
| 7 | 36.0 | control | .8 | 2.2 | 2.6 | mc | 56 | 65 | 25 |
| 8 | 80.0 | control | 2.2 | 2.2 | 1.1 | mc | 92 | 44 | 41 |
| 9 | 37.0 | normal | .8 | .9 | 1.1 | joh | 68 | 85 | 75 |
| 10 | 75.0 | normal | 2.7 | 2.8 | 1.0 | joh | 95 | 35 | 34 |
| 11 | 37.0 | other | .9 | 1.8 | 2.0 | zca | 60 | 71 | 35 |
| 12 | 37.0 | normal | .9 | 1.2 | 1.4 | jeh | 57 | 63 | 46 |
| 13 | 75.0 | normal | 2.1 | 2.5 | 1.2 | jeh | 57 | 27 | 23 |
| 14 | 37.0 | moderate | .7 | 1.3 | 1.9 | ac | 54 | 77 | 41 |
| 15 | 82.0 | moderate | 4.1 | 3.2 | .8 | ac | 145 | 35 | 45 |
| 16 | 38.0 | moderate | .5 | 1.0 | 2.0 | nw | 44 | 86 | 44 |
| 17 | 77.0 | moderate | 1.6 | 2.5 | 1.5 | nw | 136 | 83 | 55 |
| 18 | 38.0 | severe | .8 | .9 | 1.1 | eb | 42 | 54 | 48 |
| 19 | 38.0 | normal | 1.0 | 1.6 | 1.6 | vjn | 59 | 59 | 37 |
| 20 | 82.0 | normal | 2.9 | 3.3 | 1.1 | vjn | 132 | 46 | 40 |
| 21 | 38.0 | normal | .9 | 1.2 | 1.4 | jl | 73 | 82 | 60 |
| 22 | 38.0 | moderate | 1.2 | 1.6 | 1.3 | sc | 99 | 80 | 61 |
| 23 | 39.0 | control | 1.0 | 1.6 | 1.6 | natt | 42 | 42 | 26 |
| 24 | 39.0 | severe | .5 | 1.5 | 3.3 | ct | 28 | 62 | 19 |
| 25 | 40.0 | severe | .8 | 1.5 | 1.7 | ct | 37 | 44 | 25 |
| 26 | 45.0 | severe | .9 | 1.1 | 1.2 | ct | 43 | 46 | 40 |
| 27 | 49.0 | severe | 1.1 | 1.2 | 1.1 | ct | 47 | 42 | 40 |
| 28 | 40.0 | control | 1.4 | 1.5 | 1.1 | rt | 51 | 36 | 33 |
| 29 | 45.0 | control | 1.9 | 2.2 | 1.2 | rt | 75 | 40 | 34 |
| 30 | 40.0 | other | 1.4 | 1.8 | 1.3 | mw | 51 | 37 | 28 |
| 31 | 41.0 | normal | 1.1 | 1.6 | 1.5 | is | 40 | 38 | 26 |
| 32 | 41.0 | severe | .3 | 1.0 | 3.2 | ml | 15 | 48 | 15 |
| 33 | 42.0 | severe | .2 | .3 | 1.8 | mb | 13 | 71 | 39 |
| 34 | 42.0 | severe | .8 | 1.0 | 1.3 | ar | 30 | 39 | 30 |
| 35 | 42.0 | moderate | 1.4 | 2.1 | 1.5 | km | 42 | 30 | 20 |
| 36 | 43.0 | moderate | 1.3 | 2.0 | 1.5 | km | 40 | 30 | 20 |
| 37 | 42.0 | normal | 1.0 | 1.9 | 1.9 | kr | 51 | 51 | 27 |
| 38 | 42.0 | severe | .8 | 1.6 | 2.0 | jm | 52 | 63 | 32 |
| 39 | 42.5 | severe | .7 | .8 | 1.2 | jm | 53 | 76 | 63 |
| 40 | 43.0 | severe | 1.0 | 1.5 | 1.5 | jm | 40 | 40 | 27 |
| 41 | 44.0 | severe | .6 | .7 | 1.2 | jm | 39 | 69 | 60 |
| 42 | 42.0 | normal | 1.4 | 1.9 | 1.4 | kh | 46 | 34 | 24 |
| 43 | 42.0 | normal | 1.4 | 2.2 | 1.4 | gbs | 64 | 38 | 24 |
| 44 | 42.5 | other | 1.6 | 2.3 | 1.4 | mh | 46 | 28 | 20 |
| 45 | 43.0 | normal | 1.1 | 1.6 | 1.6 | sb | 69 | 65 | 42 |
| 46 | 43.0 | severe | .8 | 1.1 | 1.4 | th | 40 | 52 | 36 |
| 47 | 80.0 | severe | 1.7 | 1.5 | .9 | th | 74 | 44 | 48 |
| 48 | 44.0 | severe | 1.1 | 1.9 | 1.6 | kf | 40 | 35 | 21 |
| 49 | 45.0 | severe | 1.5 | 2.8 | 1.9 | aj | 53 | 36 | 19 |
| 50 | 46.0 | normal | 1.0 | 1.2 | 1.2 | ch | 55 | 55 | 46 |
| 51 | 46.0 | normal | 1.9 | 2.6 | 1.4 | thi | 73 | 39 | 28 |
| 52 | 48.0 | normal | 1.6 | 2.4 | 1.5 | me | 76 | 48 | 32 |
| 53 | 49.0 | normal | 1.5 | 3.0 | 2.0 | iv | 86 | 59 | 29 |
| 54 | 72.0 | normal | 1.8 | 2.1 | 1.2 | iv | 104 | 59 | 50 |
| 55 | 57.0 | severe | .9 | 1.0 | 1.1 | nt | 60 | 66 | 62 |
| 56 | 96.0 | severe | 1.0 | 1.0 | 1.1 | nt | 60 | 62 | 58 |
| 57 | 57.0 | severe | 1.1 | 1.3 | 1.2 | rs | 55 | 51 | 44 |
| 58 | 67.0 | severe | 2.5 | 1.8 | .7 | cm | 69 | 27 | 38 |
| 59 | 110.0 | severe | 1.7 | 1.5 | .9 | as | 47 | 25 | 31 |
| 60 | 124.0 | moderate | 2.7 | 3.4 | 1.3 | rh | 91 | 34 | 27 |
| 61 | 140.0 | control | 3.6 | 3.5 | 1.0 | adult | • | • | • |

Table 3. Peak heights and metabolite ratios from all the proton spectra (TR 2,000ms, TE 270ms) with postconceptional age (PCA) at the time of examination, and neurological outcome at two years or more. Note that each spectrum is scaled individually and so peak heights cannot be compared between spectra. The peak heights for individual adult spectra are to be found in Appendix C.

| | | | | | | | | |
|---|---|---|---|---|---|---|---|---|
| 1 | 33.0 | severe | .5 | 1.6 | 3.0 | sab | central | 64 |
| 2 | 35.0 | other | .8 | 1.6 | 2.0 | dh | parieto-occ. | 27 |
| 3 | 35.0 | severe | 1.1 | 1.8 | 1.6 | lc | central | 64 |
| 4 | 82.0 | severe | 3.1 | 2.6 | .9 | lc | parieto-occ. | 27 |
| 5 | 35.0 | moderate | 1.1 | 2.1 | 1.8 | ae | central | 64 |
| 6 | 36.0 | severe | .8 | 1.4 | 1.8 | sg | parieto-occ. | 27 |
| 7 | 36.0 | control | .8 | 2.2 | 2.6 | mc | central | 64 |
| 8 | 80.0 | control | 2.2 | 2.2 | 1.1 | mc | parieto-occ. | 64 |
| 9 | 37.0 | normal | .8 | .9 | 1.1 | joh | parieto-occ. | 27 |
| 10 | 75.0 | normal | 2.7 | 2.8 | 1.0 | joh | parieto-occ. | 27 |
| 11 | 37.0 | other | .9 | 1.7 | 2.0 | zca | parieto-occ. | 27 |
| 12 | 37.0 | normal | .9 | 1.2 | 1.4 | jeh | parieto-occ. | 27 |
| 13 | 75.0 | normal | 2.1 | 2.5 | 1.2 | jeh | parieto-occ. | 27 |
| 14 | 37.0 | moderate | .7 | 1.3 | 1.9 | ac | central | 64 |
| 15 | 82.0 | moderate | 4.1 | 3.2 | .8 | ac | parieto-occ. | 64 |
| 16 | 38.0 | moderate | .5 | 1.0 | 2.0 | nw | central | 64 |
| 17 | 77.0 | moderate | 1.6 | 2.5 | 1.5 | nw | parieto-occ. | 27 |
| 18 | 38.0 | severe | .8 | .9 | 1.1 | eb | parieto-occ. | 27 |
| 19 | 38.0 | normal | 1.0 | 1.6 | 1.6 | vjn | central | 64 |
| 20 | 82.0 | normal | 2.9 | 3.3 | 1.1 | vjn | parieto-occ. | 27 |
| 21 | 38.0 | normal | .9 | 1.2 | 1.4 | jl | parieto-occ. | 27 |
| 22 | 38.0 | moderate | 1.2 | 1.6 | 1.3 | sc | parieto-occ. | 27 |
| 23 | 39.0 | control | 1.0 | 1.6 | 1.6 | natt | parieto-occ. | 27 |
| 24 | 39.0 | severe | .5 | 1.5 | 3.3 | ct | parieto-occ. | 64 |
| 25 | 40.0 | severe | .8 | 1.5 | 1.7 | ct | parieto-occ. | 64 |
| 26 | 45.0 | severe | .9 | 1.1 | 1.2 | ct | parieto-occ. | 64 |
| 27 | 49.0 | severe | 1.1 | 1.2 | 1.1 | ct | parieto-occ. | 64 |
| 28 | 40.0 | control | 1.4 | 1.5 | 1.1 | rt | parieto-occ. | 64 |
| 29 | 45.0 | control | 1.9 | 2.2 | 1.2 | rt | parieto-occ. | 64 |
| 30 | 40.0 | other | 1.4 | 1.8 | 1.3 | mw | parieto-occ. | 64 |
| 31 | 41.0 | normal | 1.1 | 1.6 | 1.5 | is | parieto-occ. | 27 |
| 32 | 41.0 | severe | .3 | 1.0 | 3.2 | mi | parieto-occ. | 27 |
| 33 | 42.0 | severe | .2 | .3 | 1.8 | mb | parieto-occ. | 27 |
| 34 | 42.0 | severe | .8 | 1.0 | 1.3 | ar | parieto-occ. | 64 |
| 35 | 42.0 | moderate | 1.4 | 2.1 | 1.5 | km | parieto-occ. | 27 |
| 36 | 43.0 | moderate | 1.3 | 2.0 | 1.5 | km | parieto-occ. | 27 |
| 37 | 42.0 | normal | 1.0 | 1.9 | 1.9 | kr | parieto-occ. | 27 |
| 38 | 42.0 | severe | .8 | 1.6 | 2.0 | jm | parieto-occ. | 27 |
| 39 | 42.5 | severe | .7 | .8 | 1.2 | jm | parieto-occ. | 27 |
| 40 | 43.0 | severe | 1.0 | 1.5 | 1.5 | jm | parieto-occ. | 27 |
| 41 | 44.0 | severe | .6 | .7 | 1.2 | jm | parieto-occ. | 27 |
| 42 | 42.0 | normal | 1.4 | 1.9 | 1.4 | kh | parieto-occ. | 27 |
| 43 | 42.0 | normal | 1.7 | 2.7 | 1.6 | gbs | parieto-occ. | 27 |
| 44 | 42.5 | other | 1.6 | 2.3 | 1.4 | mh | parieto-occ. | 27 |
| 45 | 43.0 | normal | 1.1 | 1.6 | 1.6 | sb | parieto-occ. | 27 |
| 46 | 43.0 | severe | .8 | 1.1 | 1.4 | th | parieto-occ. | 64 |
| 47 | 80.0 | severe | 1.7 | 1.5 | .9 | th | parieto-occ. | 64 |
| 48 | 44.0 | severe | 1.1 | 1.9 | 1.6 | kf | parieto-occ. | 27 |
| 49 | 45.0 | severe | 1.5 | 2.8 | 1.9 | aj | parieto-occ. | 27 |
| 50 | 46.0 | normal | 1.0 | 1.2 | 1.2 | ch | parieto-occ. | 27 |
| 51 | 46.0 | normal | 1.9 | 2.6 | 1.4 | thi | parieto-occ. | 27 |
| 52 | 48.0 | normal | 1.6 | 2.4 | 1.5 | me | parieto-occ. | 27 |
| 53 | 49.0 | normal | 1.5 | 3.0 | 2.0 | iv | parieto-occ. | 27 |
| 54 | 72.0 | normal | 1.8 | 2.1 | 1.2 | iv | parieto-occ. | 27 |
| 55 | 57.0 | severe | .9 | 1.0 | 1.1 | nt | parieto-occ. | 64 |
| 56 | 96.0 | severe | 1.0 | 1.0 | 1.1 | nt | parieto-occ. | 64 |
| 57 | 57.0 | severe | 1.1 | 1.3 | 1.2 | rs | parieto-occ. | 27 |
| 58 | 67.0 | severe | 2.5 | 1.8 | .7 | cm | parieto-occ. | 27 |
| 59 | 110.0 | severe | 1.7 | 1.5 | .8 | as | parieto-occ. | 27 |
| 60 | 124.0 | moderate | 2.7 | 3.4 | 1.3 | rh | parieto-occ. | 27 |
| 61 | 140.0 | control | 3.6 | 3.5 | 1.0 | adult | parieto-occ. | 27 |

Table 3A. Data from all the children studied and mean metabolite values from 22 adult controls. The region of brain studied at mid-ventricular level is shown, as well as the voxel size from which the proton spectra were acquired.

| | PCA at exam | outcome | NAA/Cho | NAA/Cr | Cho/Cr | initials |
|---|---|---|---|---|---|---|
| 1 | 35.0 | severe | 1.1 | 1.8 | 1.6 | lc |
| 2 | 82.0 | severe | 3.1 | 2.6 | .9 | lc |
| 3 | 36.0 | control | .8 | 2.2 | 2.6 | mc |
| 4 | 80.0 | control | 2.2 | 2.2 | 1.1 | mc |
| 5 | 37.0 | normal | .8 | .9 | 1.1 | joh |
| 6 | 75.0 | normal | 2.7 | 2.8 | 1.0 | joh |
| 7 | 37.0 | normal | .9 | 1.2 | 1.4 | jeh |
| 8 | 75.0 | normal | 2.1 | 2.5 | 1.2 | jeh |
| 9 | 37.0 | moderate | .7 | 1.3 | 1.9 | ac |
| 10 | 82.0 | moderate | 4.1 | 3.2 | .8 | ac |
| 11 | 38.0 | moderate | .5 | 1.0 | 2.0 | nw |
| 12 | 77.0 | moderate | 1.6 | 2.5 | 1.5 | nw |
| 13 | 38.0 | normal | 1.0 | 1.6 | 1.6 | vjn |
| 14 | 82.0 | normal | 2.9 | 3.3 | 1.1 | vjn |
| 15 | 39.0 | severe | .5 | 1.5 | 3.3 | ct |
| 16 | 40.0 | severe | .8 | 1.5 | 1.7 | ct |
| 17 | 45.0 | severe | .9 | 1.1 | 1.2 | ct |
| 18 | 49.0 | severe | 1.1 | 1.2 | 1.1 | ct |
| 19 | 40.0 | control | 1.4 | 1.5 | 1.1 | rt |
| 20 | 45.0 | control | 1.9 | 2.2 | 1.2 | rt |
| 21 | 42.0 | moderate | 1.4 | 2.1 | 1.5 | km |
| 22 | 43.0 | moderate | 1.3 | 2.0 | 1.5 | km |
| 23 | 42.0 | severe | .8 | 1.6 | 2.0 | jm |
| 24 | 42.5 | severe | .7 | .8 | 1.2 | jm |
| 25 | 43.0 | severe | 1.0 | 1.5 | 1.5 | jm |
| 26 | 44.0 | severe | .6 | .7 | 1.2 | jm |
| 27 | 43.0 | severe | .8 | 1.1 | 1.4 | th |
| 28 | 80.0 | severe | 1.7 | 1.5 | .9 | th |
| 29 | 49.0 | normal | 1.5 | 3.0 | 2.0 | iv |
| 30 | 72.0 | normal | 1.8 | 2.1 | 1.2 | iv |
| 31 | 57.0 | severe | .9 | 1.0 | 1.1 | nt |
| 32 | 96.0 | severe | 1.0 | 1.0 | 1.1 | nt |
| 33 | 140.0 | control | 3.6 | 3.5 | 1.0 | adult |

Table 3B. Data presented chronologically from all the children who had more than one proton examination, as well as mean metabolite values from 22 adult controls.

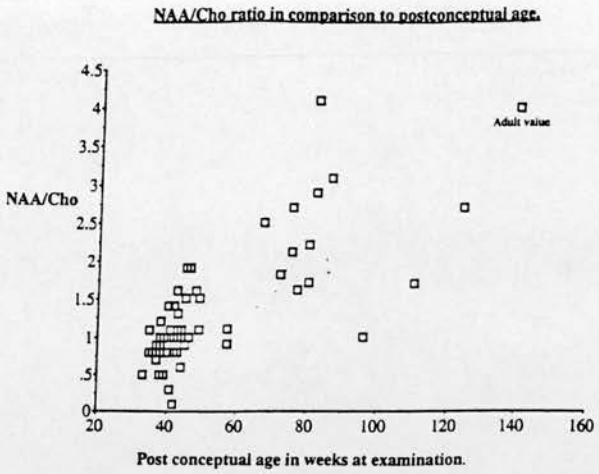



Fig. 37 Ratio of N-acetylaspartate (NAA) to choline containing compounds (Cho), in relation to postconceptional age at the time of examination, for all the children studied and an adult control.

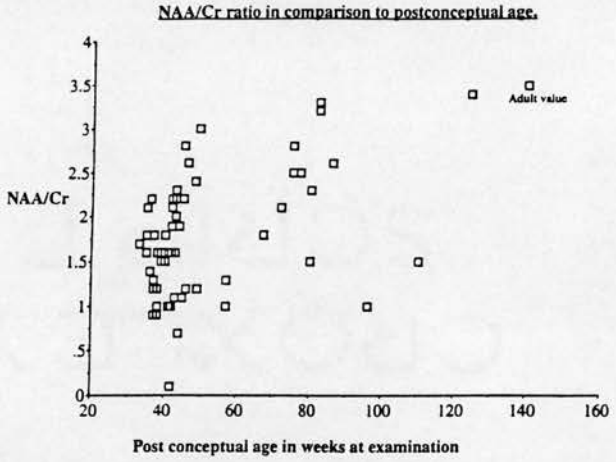



Fig. 38 Ratio of N-acetylaspartate (NAA) to creatine and phosphocreatine (Cr), in relation to postconceptional age at the time of examination, for all the children studied and an adult control.

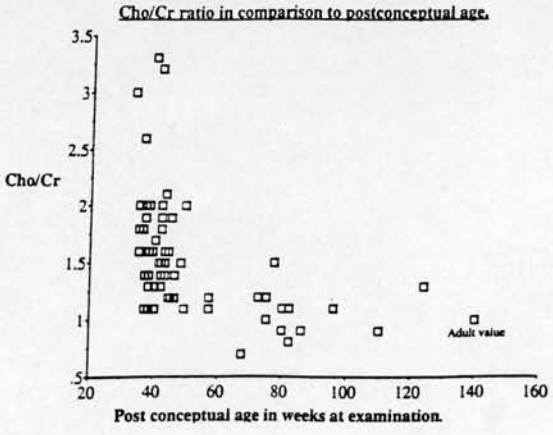



Fig. 39 Ratio of choline containing compounds (Cho) to creatine and phosphocreatine (Cr), in relation to postconceptional age at the time of examination, for all the children studied and an adult control.

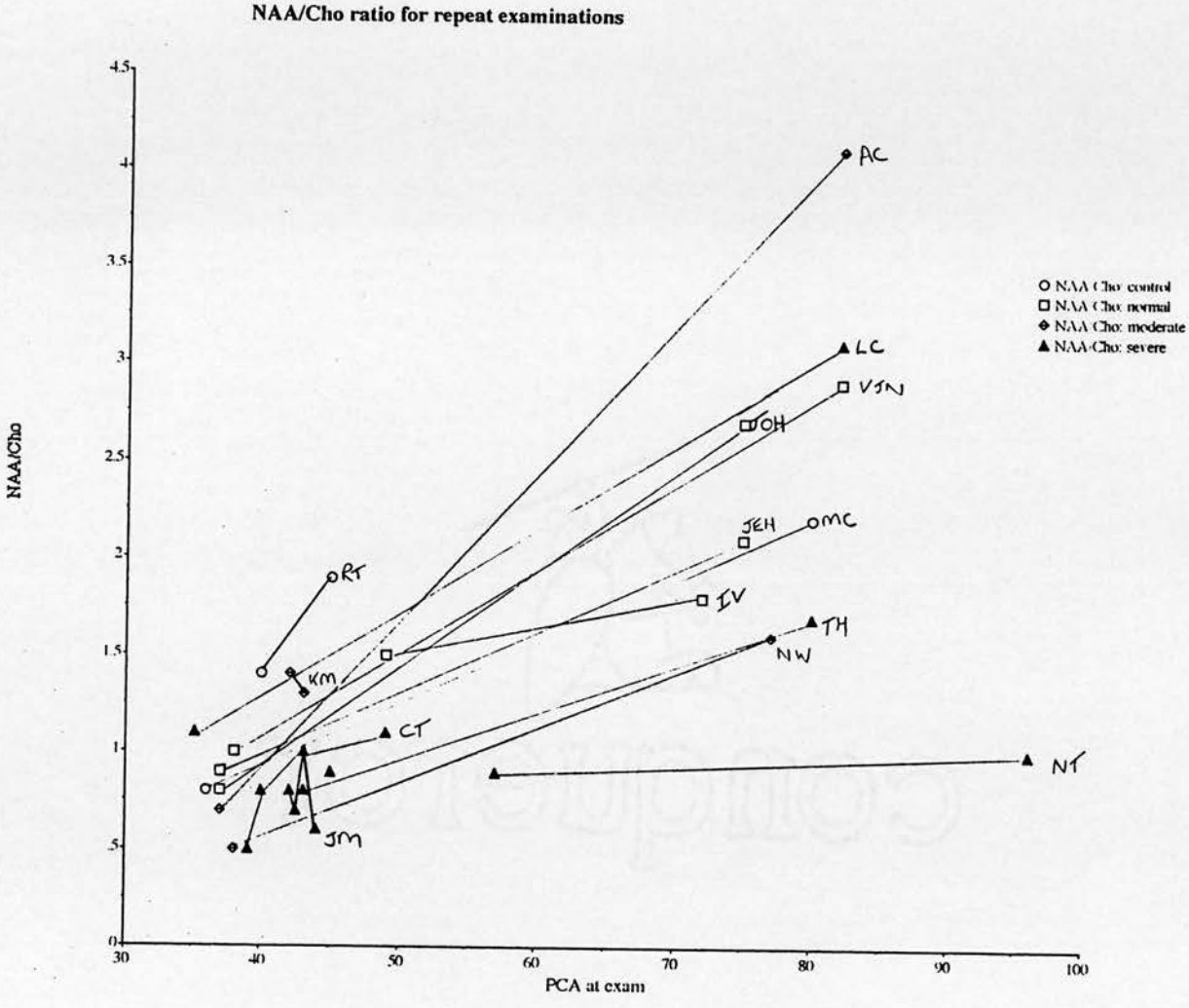



Fig. 3Bi
The NAA/Cho ratios are shown against age for the individual children who had more than one examination. The points are linked to demonstrate age related changes.

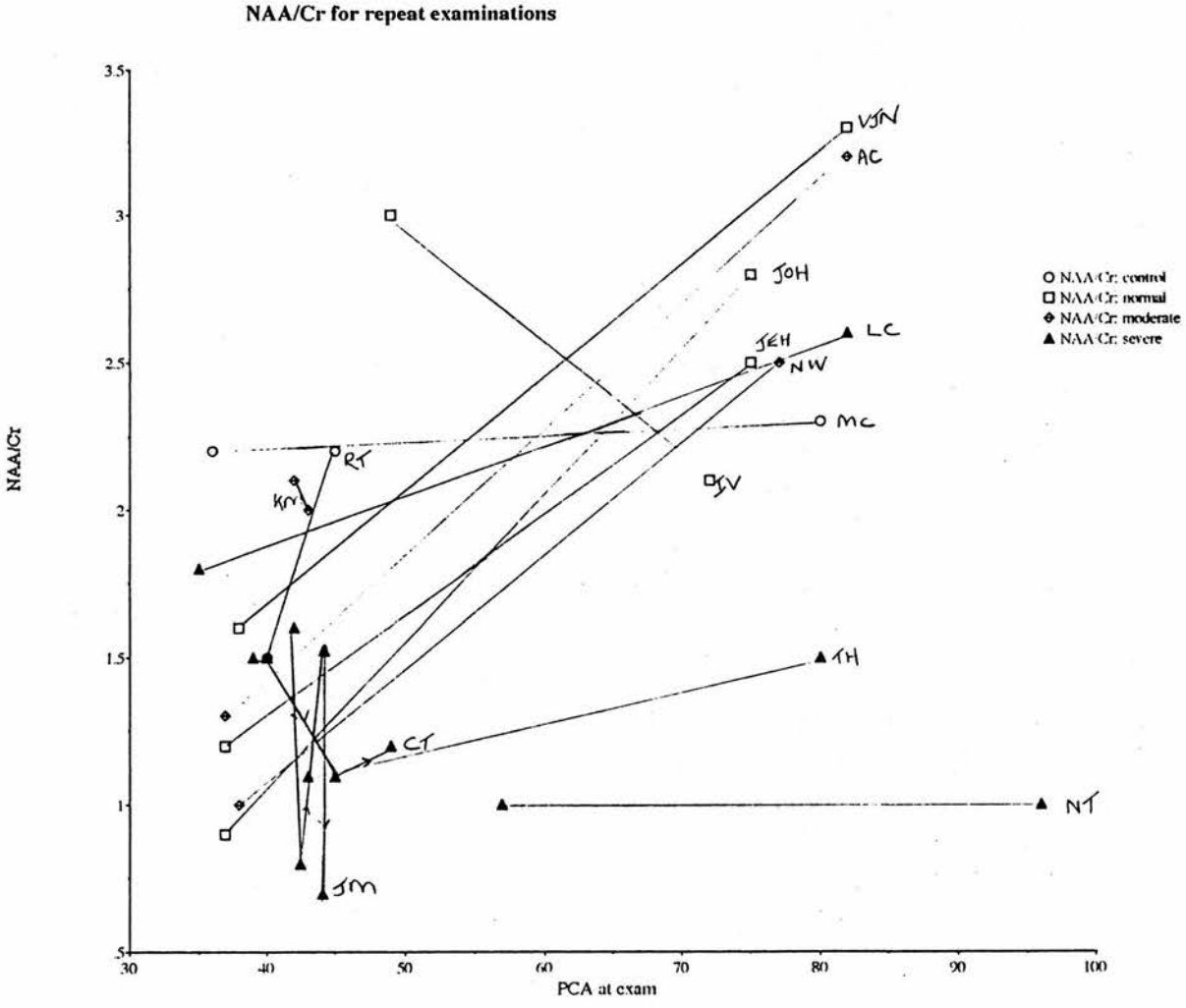



Fig. 3Bii
The NAA/Cr ratios are shown against age for the individual children who had more than one examination. The points are linked to demonstrate age related changes.

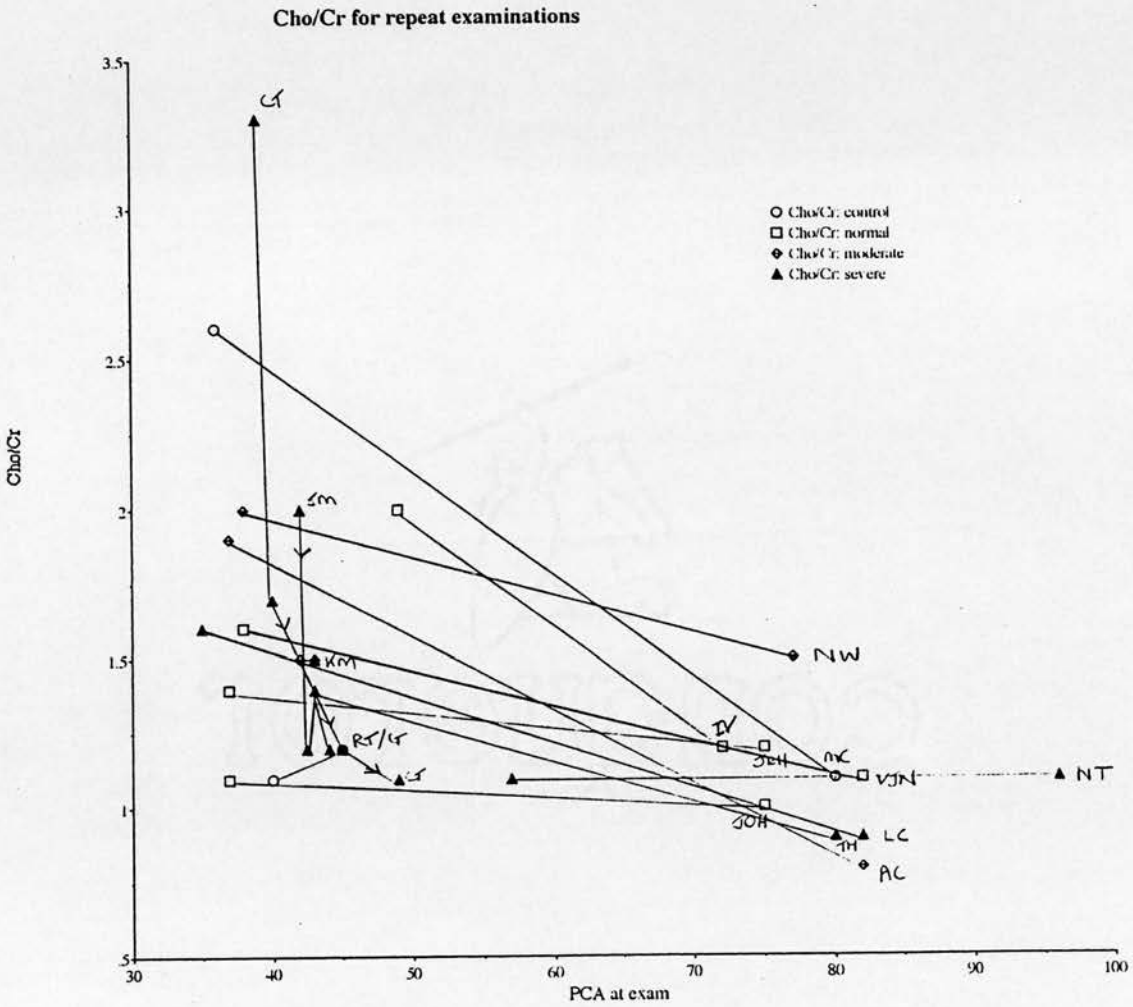



Fig. 3Biii
The Cho/Cr ratios are shown against age for the individual children who had more than one examination. The points are linked to demonstrate age related changes.

$T_1$ and $T_2$ effects.

The peak height ratios at 5,000 and 2,000 ms of three normal infants (MC, Nat T and RT) and 14 abnormal infants were used to assess the effects of saturation ($T_1$). These are shown in Table 4; there is little difference from adult values. Spectra were acquired at 135 ms as well as 270 ms to estimate T2 effects; however the spectra at 135 ms were poor quality and could not be analysed. This may have been due to eddy currents.

Changes related to hypoxic ischaemic injury

The NAA/Cho, NAA/Cr and Cho/Cr ratios for all the children studied are plotted in Figs. 40, 41, 42 in relation to neurological outcome, assessed by clinical neurological examination at eighteen months or more (see p.77). In all the figures which show spectral ratios against clinical outcome, the trend is that the NAA/Cho and NAA/Cr ratios are lower in children with moderate and severe hypoxic-ischaemic encephalopathy than in those who were neurologically normal at birth, or those who had a normal outcome at one year. The trend for the Cho/Cr ratios is less obvious, but this ratio may be slightly higher in the abnormal children, than in those who were normal at birth or those who had a normal outcome at one year.

A proton spectrum, acquired at four weeks after birth (42 weeks PCA) from a child (MB) with severe neurological abnormality, is shown in Fig.43 with the magnetic resonance image. This spectrum appears to be very abnormal with a NAA/Cho ratio of 0.2, an NAA/Cr ratio of 0.3 and a Cho/Cr ratio of 1.9. The image shows the voxel from which the spectra were acquired. There are large bilateral subdural fluid collections, the ventricles are dilated and there is extensive subcortical cystic change.

A proton spectrum also acquired at 42 weeks PCA, 18 days after birth from a term infant (KH) is shown in Fig.44 and appears relatively normal. This child had an hypoxic collapse one and a half hours after birth but was neurologically normal at one year.

The proton spectrum acquired on follow up at 9 months post natal age of a child with

Table 4. Signal height ratios for normal infants, abnormal infants and normal adults at repetition times (TR) of 5,000ms and 2,000ms, at an echo (TE) time of 270ms.

| Cases | No. of studies | NAA mean (range) | Cr mean (range) | Cho mean (range) |
|---|---|---|---|---|
| Normal infants (3) | 5 | 1.2 (1.0 - 1.3) | 1.5 (1.0 - 2.0) | 1.4 (1.0 - 1.8) |
| Abnormal infants (14) | 18 | 1.2 (1.0 - 1.6) | 1.2 (1.0 - 2.0) | 1.3 (1.0 -2.1) |
| Normal adults (6) | 6 | 1.3 (1.2 - 1.5) | 1.5 (1.0 - 1.7) | 1.5 (1.2 - 2.2) |

Fig. 40. N-Acetylaspartate (NAA) to choline containing compound ratios (Cho) against post conceptual age in weeks, classified according to neurological outcome at one year or more.

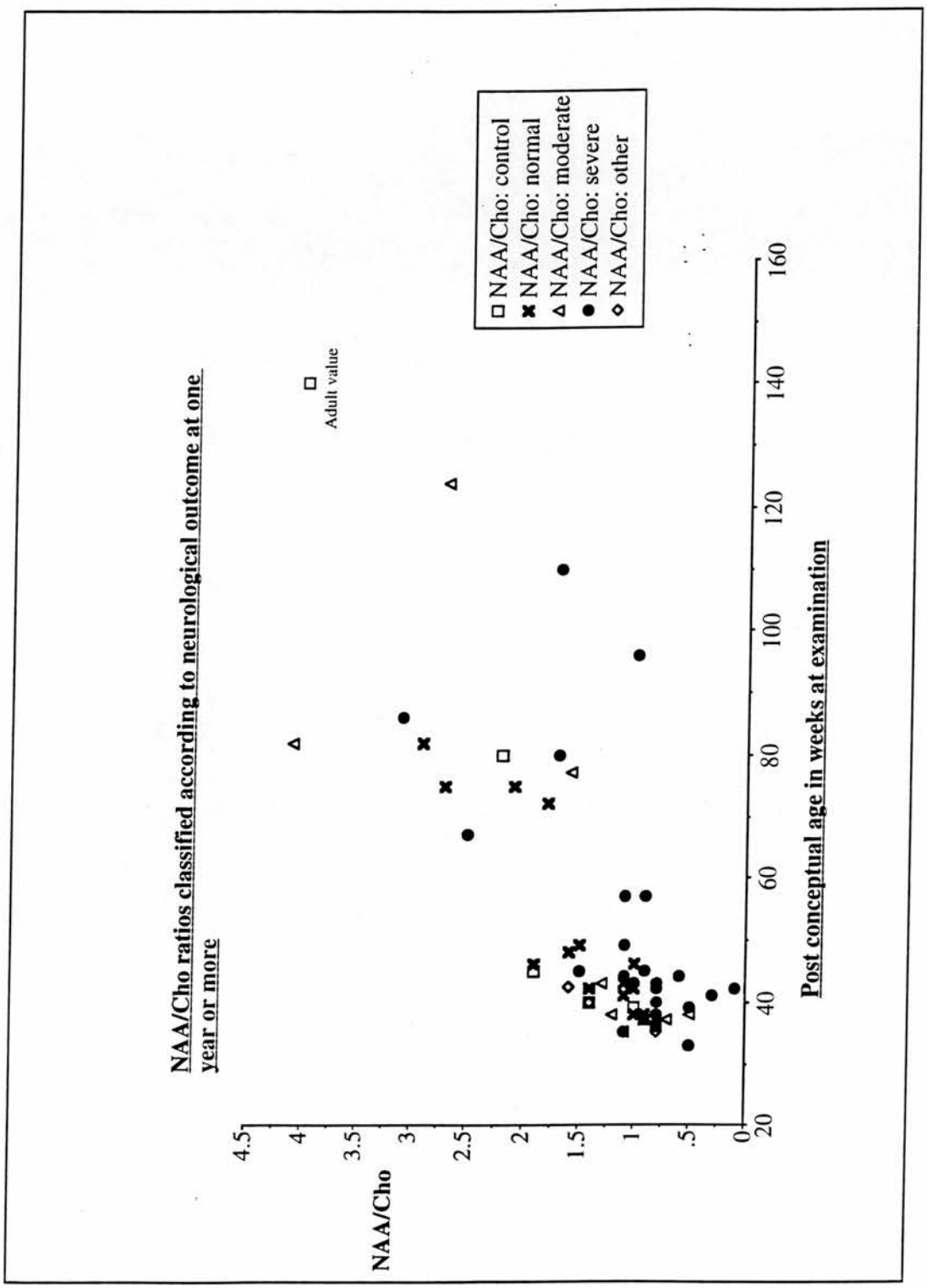


Fig. 41. N-Acetylaspartate (NAA) to creatine and phosphocreatine (Cr) ratios against post conceptual age in weeks, classified according to neurological outcome at one year or more.

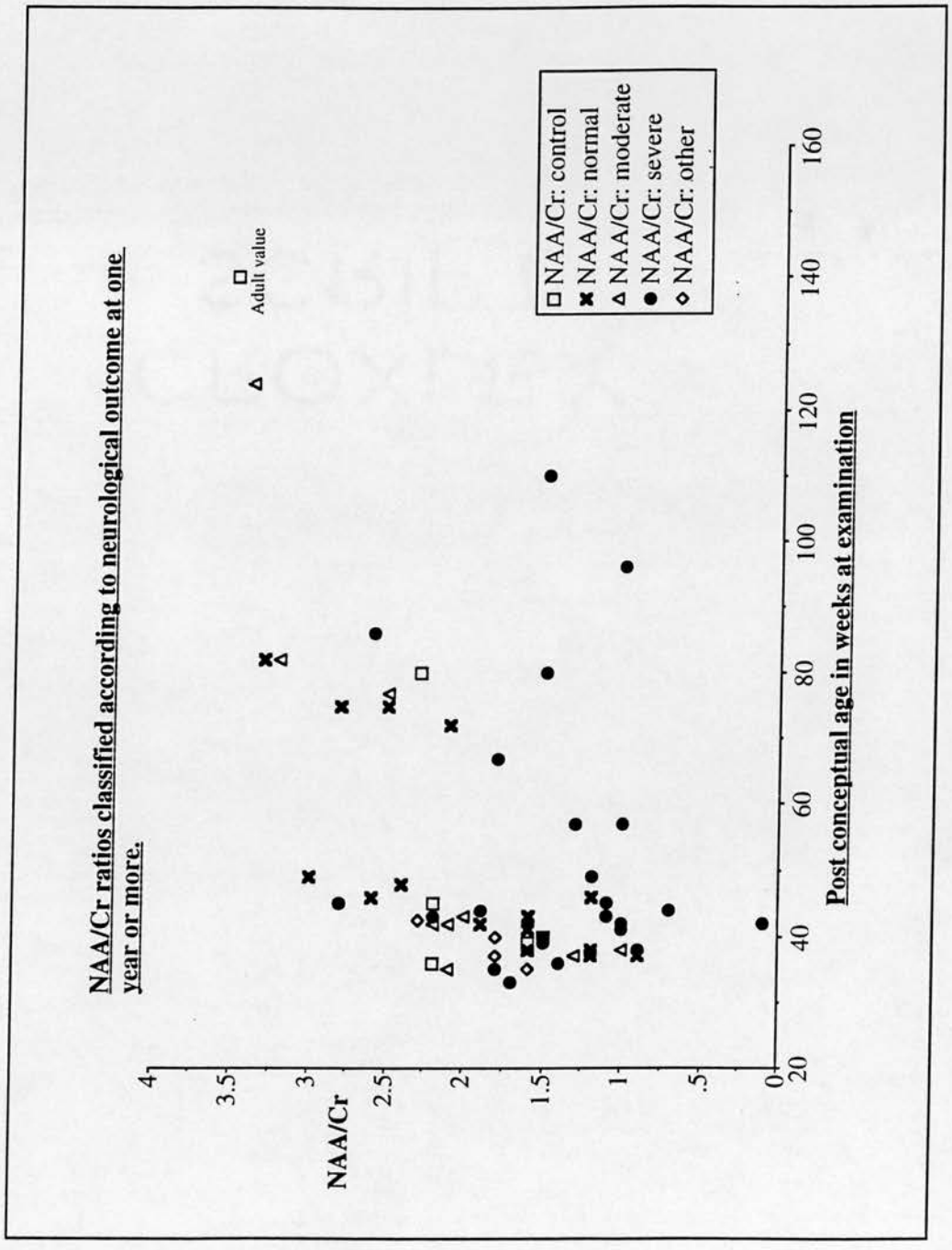
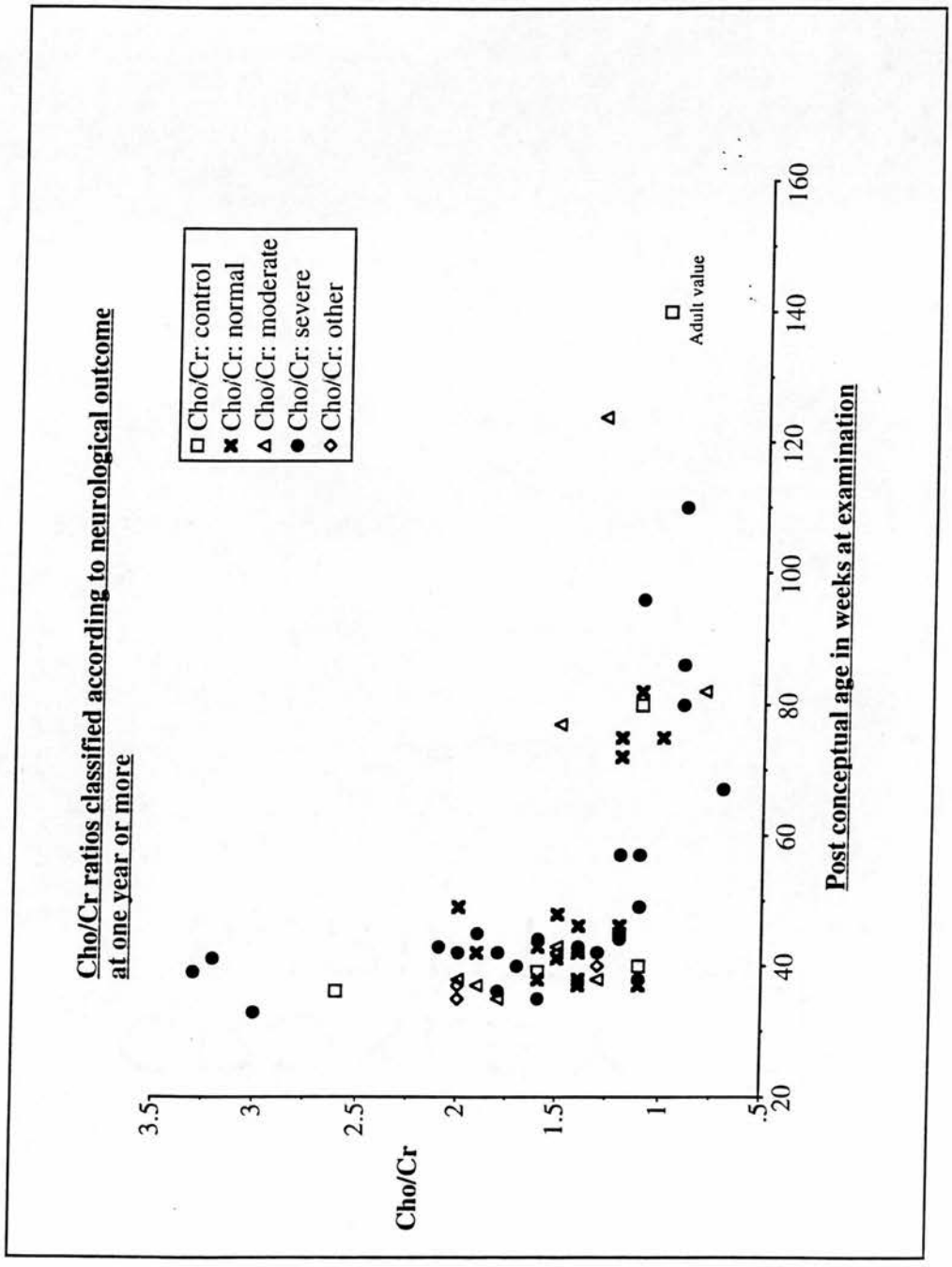
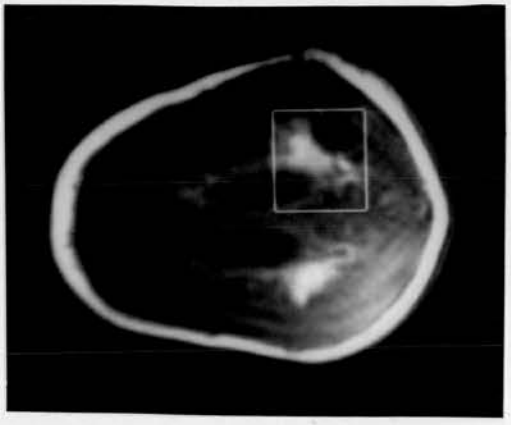


Fig. 42. Choline containing compounds (Cho) to creatine and phosphocreatine (Cr) ratios against post conceptual age in weeks, classified according to neurological outcome at one year or more.





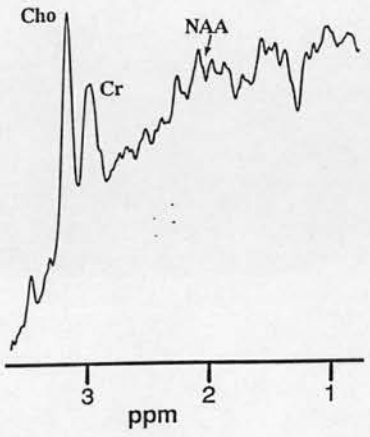



Fig. 43(a) Transverse $T_1$ weighted spin-echo image (TR 500ms, TE 22ms) showing the voxel from which spectra were acquired in the brain of MB, a child with hypoxic ischaemic encephalopathy and a severe outcome. There are large bilateral subdural fluid collections: the ventricles are dilated and there is extensive subcortical cystic change.

(b) Proton spectrum acquired with a TE of 270ms and a TR of 2,000ms, with 128 data collects from MB at 42 weeks PCA. The NAA/Cho ratio is very low at 0.2, the NAA/Cr ratio is 0.3 and the Cho/Cr ratio is 1.9.

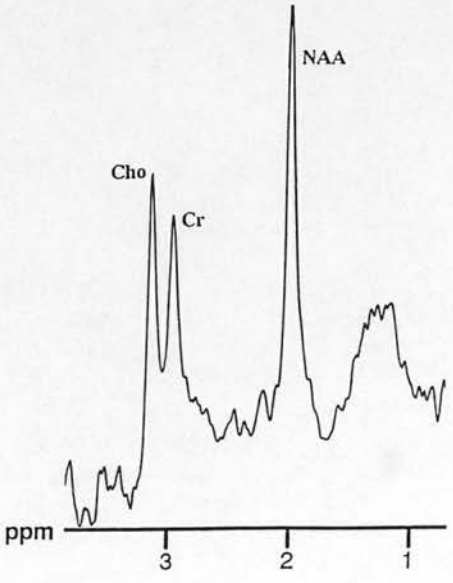



Fig. 44 Term infant (KH) also at 42w PCA, who had an hypoxic collapse one and a half hours after birth, but who was neurologically normal at one year. Proton spectrum acquired from a 64cm$^3$ volume, TR 2,000ms, TE 270ms, 128 data collects. The NAA/Cho ratio is 1.4, the NAA/Cr ratio is 1.9 and the Cho/Cr ratio is 1.4.

severe neurological abnormality (TH) (Fig.45) is compared with the follow-up proton spectrum of a child at 10 months post natal age with minor neurological problems (AC) (Fig.46). The first child's (TH) proton spectrum had an NAA/Cho ratio of 1.7, an NAA/Cr ratio of 1.5 and a Cho/Cr ratio of 0.9. In comparison the proton spectrum of AC had an NAA/Cho ratio of 4.1, an NAA/Cr ratio of 3.2 and a Cho/Cr ratio of 0.8 and appears similar to a spectrum from normal adult brain (see Fig.34).

Statistical analysis, as described on p 51A and B, was applied to the metabolite ratios, taking into account the effects of age, to see whether there was a statistical difference in the metabolite ratios between the different outcome groups. For the purposes of analysis the normal and control children were grouped together. The computer programme (SAS) was run to only select variables which had a significance of $P < 0.15$. The discriminant analysis did not show age to be a significant variable. The only metabolite ratio which showed a statistical significance in relation to outcome group was NAA/Cr ($P = 0.02$) with an $R^2$ value of 0.21, the observed trends for NAA/Cho and NAA/Cr were not significant.

As age was shown not to be a discriminant factor Chi squared tests with Yates' correction were performed on the normal/ control and severe outcome group data. For the NAA/Cho metabolite ratio the null hypothesis was that NAA/Cho of $\geq 1.0$ or $< 1.0$ was unrelated to neurological outcome. The $X^2_Y$ value was 2.3009 on 1 degree of freedom giving $P<0.1$. For the NAA/Cr metabolite ratio the null hypothesis was that NAA/Cr of $> 1.5$ or $\leqslant 1.5$ was unrelated to neurological outcome. The $X^2_Y$ value was 8.5468 on 1 degree of freedom giving $P<0.01$. For the Cho/Cr metabolite ratio the null hypothesis was that Cho/Cr of $\geqslant 1.5$ or $< 1.5$ was unrelated to neurological outcome. The $X^2_Y$ value was 0.4507 on 1 degree of freedom giving $P<0.2$. Therefore, the only significant finding was that a NAA/Cr metabolite ratio of $>1.5$ demonstrates a significant difference between the normal/control group and the severe outcome group ($P<0.01$).

The statistical analysis of the moderate outcome group data and the normal/control group data was performed using Fisher's exact test as there were small frequencies in the cells of the 2x2 tables. For the NAA/Cho metabolite ratio the null hypothesis was that NAA/Cho of $\geqslant$ 1.0 or < 1.0 was unrelated to neurological outcome;analysis gave P =0.01. For the NAA/Cr metabolite ratio the null hypothesis was that NAA/Cr of > 1.5 or $\leqslant$ 1.5 was unrelated to neurological outcome; analysis gave P=0.36. For the Cho/Cr metabolite ratio the null hypothesis was that Cho/Cr of $\geqslant$ 1.5 or < 1.5 was unrelated to neurological outcome; analysis gave P=0.09. Therefore, the only significant finding was that a NAA/Cho metabolite ratio of >1.0 demonstrates a significant difference between the normal/control group and the moderate outcome group (P=0.01).

Infants born at term and examined in the first month of life

To minimize spectral changes produced by age differences, and in order to see more clearly the changes due to hypoxic and ischaemic injury, the results for a subgroup of infants (see Table 2 p.79) born at term and post term (37 to 42 weeks) and one control infant (RT) studied within the first month of life are shown in Figs.47, 48, 49.

A study of spectral quality was also made on this well defined patient group, as the spectra varied in their signal to noise ratios. To assess the effects of this, spectra for this group of term infants were measured by four independent observers who had no knowledge of the infants outcome.

Table 4A shows the absolute peak heights measured by three of the observers (the other set of absolute peak heights was not recorded) and the ratios calculated from the peak heights by these three observers. If the actual peak heights are examined it can be seen that the ratios are much more consistent than the peak heights. This provides gratifying reassurance that despite the variable quality of the spectra the peak height method we adopted gave consistent results.

The metabolite ratios were compared in relation to outcome for this group of ten

patients and one control. The control and normal outcome patients were grouped together and compared with those children with a severe neurodevelopmental outcome. The mean (control/normal) for NAA/Cho was 1.38 +/- 0.38, the mean (severe) for NAA/Cho was 0.51 +/- 0.26. The mean (control/normal) for NAA/Cr was 1.96 +/- 0.44, the mean (severe) for NAA/Cr was 0.81 +/- 0.33. The mean (control/normal) for Cho/Cr was 1.50 +/- 2.04, the mean (severe) for Cho/Cr was 1.77 +/- 0.85. These results are statistically significant for NAA/Cho ($p=0.02$) and NAA/Cr ($p=0.01$), but not significant for Cho/Cr ($p=0.47$).

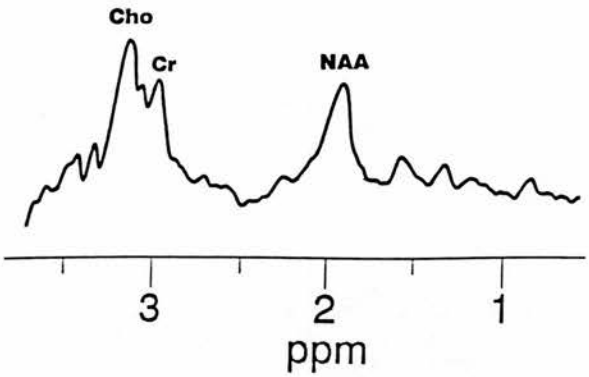



Fig. 45 Proton spectrum acquired at nine months PNA from a 64cm$^3$ volume in the brain of TH, a child with a severe neurological outcome. TE 270ms, TR 2, 000ms, 128 data collects. The NAA/Cho ratio is 1.7, the NAA/Cr ratio is 1.5 and the Cho/Cr ratio is 0.9.

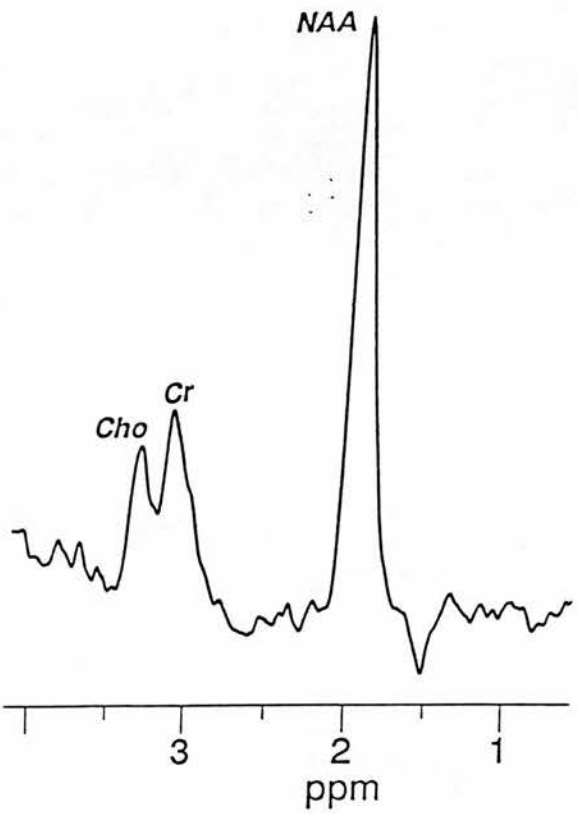



Fig. 46 Proton spectrum acquired at ten months PNA from a 64cm$^3$ volume in the brain of AC, a child with minor neurological problems. TE 270ms, TR 2, 000ms, 128 data collects. The NAA/Cho ratio is 4.1, the NAA/Cr ratio is 3.2 and the Cho/Cr ratio is 0.8.

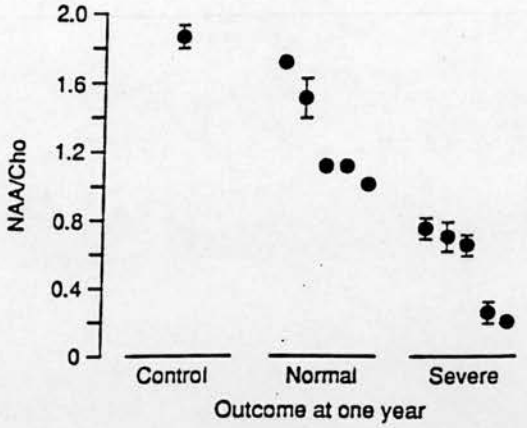



Fig. 47 Mean and one standard deviation (from four 'blind' observer measurements) of NAA/Cho ratios, from all the term infants who were examined within four weeks of birth. There were no infants in the 'moderate' outcome group.

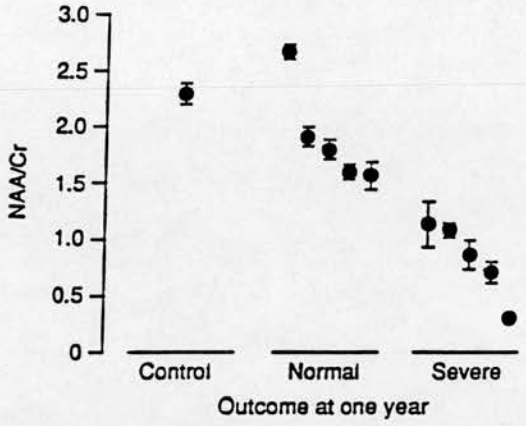



Fig. 48 Mean and one standard deviation (from four 'blind' observer measurements) of NAA/Cr ratios, from all the term infants who were examined within four weeks of birth. There were no infants in the 'moderate' outcome group.

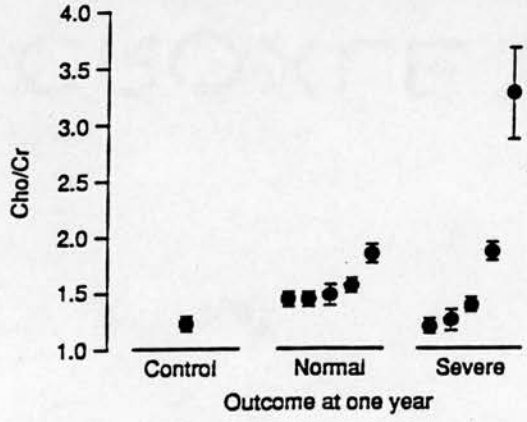



Fig. 49 Mean and one standard deviation (from four 'blind' observer measurements) of Cho/Cr ratios, from all the term infants who were examined within four weeks of birth. There were no infants in the 'moderate' outcome group.

# TABLE 4A

| | A | B | C | D | E | F | G | H | K | L | M |
|---|---|---|---|---|---|---|---|---|---|---|---|
| 1 | Spectrum AR | Peak height | | | Calculated ratio | | | | | | |
| 2 | | i | ii | iii | i | ii | iii | iv | mean of i-iv | std. dev. | 95% con.lim |
| 3 | NAA | 75 | 52 | 59 | | | | | | | |
| 4 | Cho | 110 | 71 | 77 | | | | | | | |
| 5 | Cr | 96 | 56 | 59 | | | | | | | |
| 6 | NAA/Cho | | | | 0.7 | 0.7 | 0.8 | 0.6 | 0.7 | 0.08 | 0.62 - 0.78 |
| 7 | NAA/Cr | | | | 0.8 | 0.7 | 1 | 0.9 | 0.85 | 0.13 | 0.72 - 0.98 |
| 8 | Cho/Cr | | | | 1.2 | 1.1 | 1.3 | 1.3 | 1.23 | 0.01 | 1.22 -1.24 |
| 9 | | | | | | | | | | | |
| 10 | Spectrum SB | Peak height | | | Calculated ratio | | | | | | |
| 11 | | i | ii | iii | i | ii | iii | iv | mean of i-iv | std. dev. | 95% con.lim |
| 12 | NAA | 77 | 70 | 69 | | | | | | | |
| 13 | Cho | 62 | 62 | 64 | | | | | | | |
| 14 | Cr | 42 | 43 | 42 | | | | | | | |
| 15 | NAA/Cho | | | | 1.1 | 1.1 | 11 | 1.1 | 1.1 | 0 | 1.1-1.1 |
| 16 | NAA/Cr | | | | 1.6 | 1.5 | 1.6 | 1.6 | 1.58 | 0.05 | 1.53 -1.63 |
| 17 | Cho/Cr | | | | 1.4 | 1.5 | 1.6 | 1.4 | 1.45 | 0.06 | 1.39 -1.51 |
| 18 | | | | | | | | | | | |
| 19 | Spectrum TH | Peak height | | | Calculated ratio | | | | | | |
| 20 | | i | ii | iii | i | ii | iii | iv | mean of i-iv | std. dev. | 95% con.lim |
| 21 | NAA | 20 | 20 | 20 | | | | | | | |
| 22 | Cho | 28 | 26 | 26 | | | | | | | |
| 23 | Cr | 21 | 18 | 18 | | | | | | | |
| 24 | NAA/Cho | | | | 0.7 | 0.8 | 0.8 | 0.7 | 0.75 | 0.06 | 0.69 - 0.81 |
| 25 | NAA/Cr | | | | 1 | 1.1 | 1.1 | 1.1 | 1.08 | 0.05 | 1.03 - 1.13 |
| 26 | Cho/Cr | | | | 1.4 | 1.3 | 1.4 | 1.4 | 1.38 | 0.05 | 1.33 - 1.43 |
| 27 | | | | | | | | | | | |
| 28 | Spectrum IS | Peak height | | | Calculated ratio | | | | | | |
| 29 | | i | ii | iii | i | ii | iii | iv | mean of i-iv | std. dev. | 95% con.lim |
| 30 | NAA | 20 | 20 | 21 | | | | | | | |
| 31 | Cho | 20 | 18 | 20 | | | | | | | |
| 32 | Cr | 14 | 13 | 13 | | | | | | | |
| 33 | NAA/Cho | | | | 1 | 1.1 | 1.1 | 1.1 | 1.1 | 0 | 1.1 |
| 34 | NAA/Cr | | | | 1.4 | 1.7 | 1.6 | 1.5 | 1.55 | 0.13 | 1.42 - 1.68 |
| 35 | Cho/Cr | | | | 1.6 | 1.4 | 1.5 | 1.4 | 1.48 | 0.1 | 1.38 - 1.58 |
| 36 | | | | | | | | | | | |
| 37 | Spectrum KR | Peak height | | | Calculated ratio | | | | | | |
| 38 | | i | ii | iii | i | ii | iii | iv | mean of i-iv | std. dev. | 95% con.lim |
| 39 | NAA | 51 | 52 | 51 | | | | | | | |
| 40 | Cho | 52 | 53 | 51 | | | | | | | |
| 41 | Cr | 27 | 30 | 27 | | | | | | | |
| 42 | NAA/Cho | | | | 1 | 1 | 1 | 1 | 1 | 0 | 1 |
| 43 | NAA/Cr | | | | 1.4 | 1.8 | 1.9 | 1.7 | 1.77 | 0.1 | 1.67 - 1.87 |
| 44 | Cho/Cr | | | | 1.8 | 1.9 | 1.9 | 1.8 | 1.85 | 0.06 | 1.79 - 1.91 |
| 45 | | | | | | | | | | | |
| 46 | Spectrum RT | Peak height | | | Calculated ratio | | | | | | |
| 47 | | i | ii | iii | i | ii | iii | iv | mean of i-iv | std. dev. | 95% con.lim |
| 48 | NAA | 95 | 94 | 75 | | | | | | | |
| 49 | Cho | 51 | 52 | 40 | | | | | | | |
| 50 | Cr | 41 | 39 | 34 | | | | | | | |
| 51 | NAA/Cho | | | | 1.9 | 1.8 | 1.9 | 1.8 | 1.85 | 0.06 | 1.79 - 1.91 |
| 52 | NAA/Cr | | | | 2.3 | 2.2 | 2.2 | 2.4 | 2.27 | 0.1 | 2.17 - 2.37 |
| 53 | Cho/Cr | | | | 1.2 | 1.2 | 1.2 | 1.3 | 1.22 | 0.05 | 1.17 - 1.27 |
| 54 | | | | | | | | | | | |
| 55 | | | | | | | | | | | |
| 56 | | | | | | | | | | | |
| 57 | Spectrum GBS | Peak height | | | Calculated ratio | | | | | | |
| 58 | | i | ii | iii | i | ii | iii | iv | mean of i-iv | std. dev. | 95% con.lim |
| 59 | NAA | 64 | 64 | 64 | | | | | | | |

Table 4A. Spectra from ten term infants and one normal control infant (RT) were analysed by me and three other observers. The absolute peak heights are given as measured by three observers (columns B,C,D); the measured metabolite ratios are given, columns E,F,G,H; the means of the measured metabolite ratios are given in column K, with the standard deviation (column L) and 95% confidence limits (M).

# TABLE 4A

| | A | B | C | D | E | F | G | H | K | L | M |
|---|---|---|---|---|---|---|---|---|---|---|---|
| 60 | Cho | 38 | 37 | 38 | | | | | | | |
| 61 | Cr | 24 | 24 | 24 | | | | | | | |
| 62 | NAA/Cho | | | | 1.7 | 1.7 | 1.7 | 1.7 | 1.7 | 0 | 1.7 |
| 63 | NAA/Cr | | | | 2.7 | 2.6 | 2.7 | 2.6 | 2.67 | 0.05 | 2.62 - 2.72 |
| 64 | Cho/Cr | | | | 1.6 | 1.6 | 1.6 | 1.6 | 1.55 | 0.06 | 1.49 - 1.61 |
| 65 | | | | | | | | | | | |
| 66 | Spectrum MB | Peak height | | | Calculated ratio | | | | | | |
| 67 | | i | ii | iii | i | ii | iii | iv | mean of i-iv | std. dev. | 95% con.lim |
| 68 | NAA | 12 | 12 | 12 | | | | | | | |
| 69 | Cho | 71 | 72 | 71 | | | | | | | |
| 70 | Cr | 38 | 38 | 38 | | | | | | | |
| 71 | NAA/Cho | | | | 0.2 | 0.2 | 0.2 | 0.2 | 0.2 | 0 | 0.2 |
| 72 | NAA/Cr | | | | 0.3 | 0.3 | 0.3 | 0.3 | 0.3 | 0 | 0.3 |
| 73 | Cho/Cr | | | | 1.8 | 1.9 | 1.6 | 1.9 | 1.85 | 0.06 | 1.79 - 1.91 |
| 74 | | | | | | | | | | | |
| 75 | Spectrum ML | Peak height | | | Calculated ratio | | | | | | |
| 76 | | i | ii | iii | i | ii | iii | iv | mean of i-iv | std. dev. | 95% con.lim |
| 77 | NAA | 17 | 12 | 15 | | | | | | | |
| 78 | Cho | 56 | 52 | 48 | | | | | | | |
| 79 | Cr | 16 | 17 | 15 | | | | | | | |
| 80 | NAA/Cho | | | | 0.2 | 0.2 | 0.3 | 0.3 | 0.25 | 0.06 | 0.19 - 0.31 |
| 81 | NAA/Cr | | | | 1.3 | 1.3 | 1 | 0.9 | 1.12 | 0.21 | 0.91 - 1.33 |
| 82 | Cho/Cr | | | | 3.8 | 2.9 | 3.2 | 3 | 3.22 | 0.4 | 2.83 - 3.61 |
| 83 | | | | | | | | | | | |
| 84 | Spectrum JM2 | Peak height | | | Calculated ratio | | | | | | |
| 85 | | i | ii | iii | i | ii | iii | iv | mean of i-iv | std. dev. | 95% con.lim |
| 86 | NAA | 39 | 46 | 48 | | | | | | | |
| 87 | Cho | 69 | 70 | 71 | | | | | | | |
| 88 | Cr | 60 | 62 | 62 | | | | | | | |
| 89 | NAA/Cho | | | | 0.7 | 0.7 | 0.6 | 0.6 | 0.65 | 0.06 | 0.59 - 0.71 |
| 90 | NAA/Cr | | | | 0.8 | 0.6 | 0.7 | 0.7 | 0.7 | 0.08 | 0.62 - 0.78 |
| 91 | Cho/Cr | | | | 1.2 | 1.2 | 1.2 | 1.1 | 1.17 | 0.05 | 1.12 - 1.22 |
| 92 | | | | | | | | | | | |
| 93 | Spectrum KHo | Peak height | | | Calculated ratio | | | | | | |
| 94 | | i | ii | iii | i | ii | iii | iv | mean of i-iv | std. dev. | 95% con.lim |
| 95 | NAA | 23 | 23 | 22 | | | | | | | |
| 96 | Cho | 17 | 17 | 16 | | | | | | | |
| 97 | Cr | 11 | 12 | 11 | | | | | | | |
| 98 | NAA/Cho | | | | | 1.4 | 1.4 | 1.8 | 1.5 | 0.12 | 1.38 - 1.62 |
| 99 | NAA/Cr | | | | | 1.8 | 1.9 | 2 | 1.9 | 0.08 | 1.82 - 1.98 |
| 100 | Cho/Cr | | | | 1.4 | 1.4 | 1.6 | 1.5 | 1.45 | 0.06 | 1.39 - 1.51 |

Table 4A. Spectra from ten term infants and one normal control infant (RT) were analysed by me and three other observers. The absolute peak heights are given as measured by three observers (columns B,C,D); the measured metabolite ratios are given, columns E,F,G,H; the means of the measured metabolite ratios are given in column K, with the standard deviation (column L) and 95% confidence limits (M).

When we started these studies clinical proton spectroscopy was a relatively new technique, there were no published proton spectra from infants, and no proton spectroscopy examinations had been performed in our 1.6T prototype magnet. As a means of validating our proton spectroscopy methods, and as an aid to analysis of the proton spectrum from human brain, we acquired proton spectra from tumours and from a region of normal brain in adults about to have surgery for an intracerebral tumour. At surgery we obtained biopsies from the tumour and from adjacent normal brain and performed proton spectroscopy on these.

The proton spectrum shown in Fig.34 is typical of those obtained from neurologically normal adults. The dominant peak at 2.0ppm is from NAA, and signals from Cr (3.0 ppm) and Cho (3.2ppm) are also observed. The peak ratios are influenced by the water suppression technique used (1331 optimized for NAA), which explains, partly, why the ratios of NAA/Cho and NAA/Cr are higher in vivo than in parallel studies of biopsy specimens.

Eleven patients were studied in vivo. The spectra obtained from the radiologically normal volume of the patients' brain were similar to those of control subjects, and were used to assess the spectra from the tumours. The combined results of tumour histology, in vitro MRS analysis of the tumour biopsies and analysis of the in vivo spectra are shown in Table 5 (reproduced from Gill et al 1990). We chose to use a qualitative scale rather than quantitative measures as this was very early work. After considerable discussion by the group, which included basic scientists as well as physicians, it was felt that the data were not of a standard where quantitative analysis would provide additional information. We chose to use a qualitative scale which we performed by ranking the spectra.

Some of the results from the in vivo and in vitro spectra were consistent, and when unexpected peaks such as alanine were present on the in vitro spectrum (see patient B

TABLE 5.

| PATIENT | AGE | SEX | DIAGNOSIS | IN VITRO | | IN VIVO | | |
|---|---|---|---|---|---|---|---|---|
| | | | | Cho/Cr | NAA/Cr | Cho/Cr | NAA/Cr | Lac/Cr |
| A | 68 | M | Astrocytoma III | 1 | -2 | 0 | -2 | 0 |
| B | 41 | F | Meningioma | 2 | x | 2 | 0 | x |
| C | 48 | M | Recurrent astrocytoma IV post radio-therapy | x | x | 2 | -1 | 2 |
| D | 44 | F | Astrocytoma II | 2 | -2 | 2 | -2 | 0 |
| E | 72 | M | Secondary adenocarcinoma | 2 | -2 | x | x | 2 |
| F | 57 | F | Necrotic astrocytoma III | x/0 | x/-1 | 0 | 0 | 2 |
| G | 50 | M | Astrocytoma I/II | 0 | -2 | 0 | 0 | 1 |
| H | 71 | F | Astrocytoma IV | x | x | x | -1 | 0 |
| I | 30 | M | Infiltrative astrocytoma I/II | 0 | 0 | 0 | -2 | 0 |

Table 5. The in vivo spectra were ranked by four observers 'blinded' to the histological results. The tumours were graded I to IV by standard histological methods, with grade IV being highly malignant. Cho, choline containing compounds; Cr, creatine and phosphocreatine; NAA, N-acetylaspartate; Lac, lactate; (+2), definite increase; (+1), moderate increase; (0), within normal limits; (-1), moderate decrease; (-2), definite decrease; (x), no comment could be made.

below) they were also detected with our in vivo technique.

Data from two of the patients are discussed below to illustrate the relationship between the in vivo and in vitro results

Patient A: the in vitro spectrum from one of five serial stereotactic biopsies is shown in Fig.50a. The extracts showed a moderate increase in the Cho/Cr ratio within the tumour and no detectable NAA. The main feature of the in vivo spectrum (Fig.50b) was a marked reduction in the NAA/Cho and NAA/Cr ratios. The Cho/Cr ratio was ranked within normal limits, but is consistent with a moderate increase. The residual NAA signal observed in vivo may be from normal tissue, or from other N-acetyl containing compounds.

The signal at 1.3ppm, containing contributions from lactate and fat, was ranked as normal. Considering the low level of total creatine (measured from the biopsies to be 1.3mmol/kg wet wt.), there was no evidence for an elevation of lactate within this tumour.

Patient B: the in vitro spectrum (Fig.51a) shows a peak attributable to alanine and no NAA, the characteristic features of a meningioma; the in vivo spectrum (Fig.51b) also showed a peak at 1.5ppm that can be assigned to alanine, and an elevated ratio of Cho/Cr. The in vivo spectrum has an NAA signal which is not present in the in vitro spectrum. This residual signal is likely to be from adjacent normal tissue within the volume studied or may be from other compounds. One of the major problems of in vivo proton spectroscopy is dilution of change produced by the contribution of signal from non-tumour tissue within the volume of study. Our early voxel size ($64cm^3$) is very likely to contain normal brain as well as tumour.

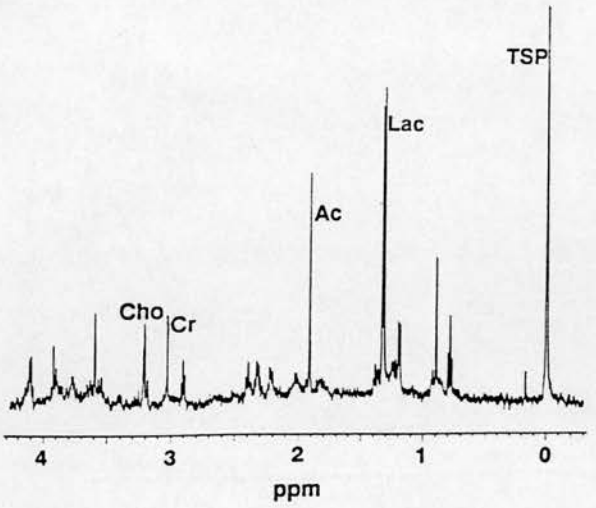
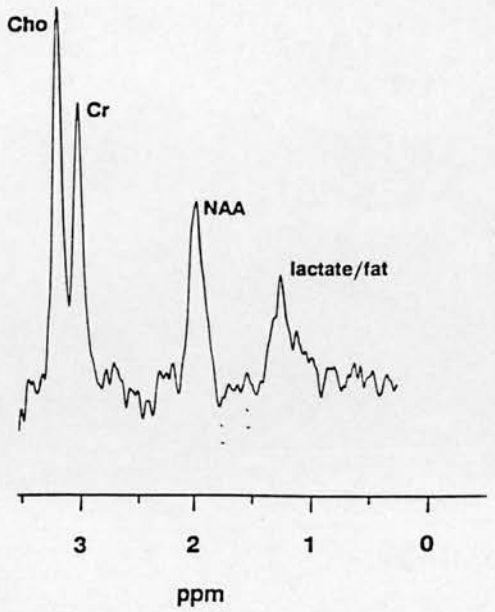



Fig. 50 (a) In vitro spectrum obtained from a stereotactic biopsy of tumour tissue, from a 68 year old man with a grade III astrocytoma. (Ac, acetate an impurity which enters during extraction and storage; Lac, lactate; TSP, sodium 3-(trimethylsilyl) 2,2,3,3-tetradeuteropropionate, a chemical shift and concentration standard.




(b) Proton spectrum from a 64cm$^3$ volume containing mainly tumour. The NAA/Cho ratio is reduced in comparison with that from normal adult brain.

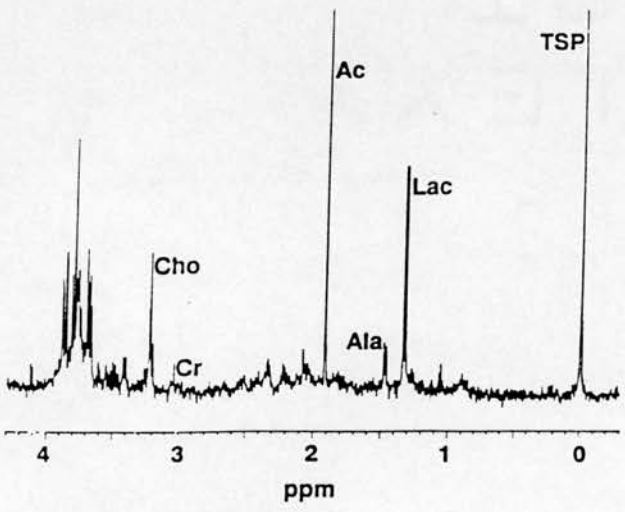
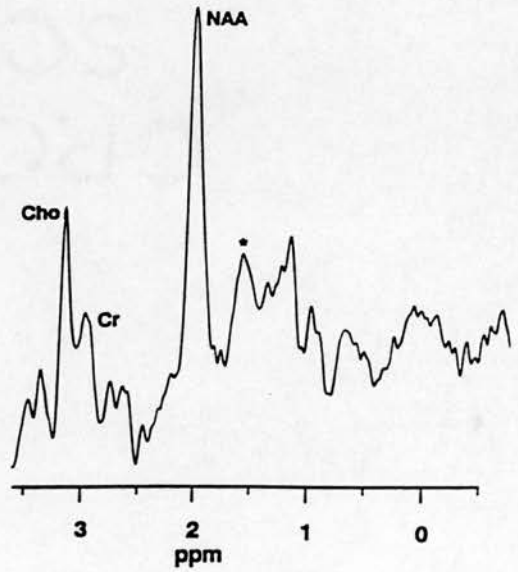



Fig. 51 (a) In vitro proton spectrum from a biopsy extract of a meningioma from a 48 year old woman. (Ala, alanine).




(b). Proton spectrum from a 64cm$^3$ volume containing mainly tumour. A peak due to alanine can be seen (*).

## PHOSPHORUS SPECTROSCOPY

Thirty nine children completed phosphorus spectroscopy examinations. Four children were examined twice with phosphorus MRS and two children had three $^{31}P$ MRS examinations. The details of the 45 analysable examinations are given in Table 6.

Our methods for acquiring phosphorus spectra were described on p.45. A phosphorus spectrum from normal adult brain is shown in Fig.52 and resonances attributed to phosphocreatine (PCr), inorganic phosphate (Pi), phosphomonoesters (PME), phosphodiesters (PDE) and the three peaks ($\alpha$, $\beta$, $\gamma$) of adenosine triphosphate (ATP) are clearly seen.

### Data analysis

Our phosphorus spectra were analysed using peak areas derived by two different methods, as described on p.47, to demonstrate problems with spectral analysis. The results of the analysis of all the 5s unlocalized phosphorus spectra by method one (see Fig. 24a) are shown in Table 7, it is the metabolite ratios obtained by this method that are used throughout this thesis (nine children did not have analysable unlocalized 5s spectra). The two different methods of analysis produced markedly different numerical results, see Table 8, although the trends in metabolic ratios (e.g PME/PDE against age) are similar (Fig.53a and b and Fig.54a and b).

### Changes related to age

The PCr/Pi ratios and the PME/PDE ratios for all the children examined are shown in Figs.53 and 54. These show that PCr/Pi increases with increasing age and PME/PDE decreases with increasing age. PME decreases rapidly within the first few months of life and PDE increases correspondingly. A phosphorus spectrum from a child with a normal neurological outcome (RhD), examined at 43.5 weeks PCA is shown in Fig. 55, and can be compared with the phosphorus spectrum from a neurologically normal adult shown in Fig.52.

| Patient details | | Repetition times (TR) | | | | | Chemical shift imaging | |
|---|---|---|---|---|---|---|---|---|
| Name | PCA at exam | 0.5s | 1s | 5s | 20s | other | 2DCSI | 4DCSI |
| MG | | | x | x | | | Y,2cm (1s;8x64) | |
| NT(1) | 37.5 | x | x | x | x | 10s | Y,1cm | |
| AC | 37.5 | x | x | x | x | | Y,2cm | |
| MT | 38 | x | x | x | | | Y,2cm (1s; 8x16) | |
| TF | 38 | x | x | x | x | | Y,2cm (1s; 8x64: 5s 8x16) | |
| Nat T | 39 | | | x | x | | | |
| JM(1) | 41 | | | x | | | | |
| WG | 41 | | x | | | | | |
| ML(1) | 41 | x | x | x | | | | |
| CW(1) | 41 | | x | x | | | | |
| GBS | 41.5 | | x | x | x | | Y,2cm (1s;8x128: 5s; 8x 64) | |
| JM(2) | 41.5 | | x | x | | | | |
| MD | 42 | x | x | x | x | | Y,2cm (1s;8x128) | |
| CK | 42 | | x | x | | | Y,2cm (0.5s; 8x64) 1s; 8x32: 5s; 8x32) | |
| AR | 42 | x | x | x | x | | Y,1cm (1s;16x64) Y,1.5 cm (1s;8x64) | |
| KR | 42 | | x | x | | | Y,2cm (1s;8x128) | |
| ST | 42 | | | x | | | | |
| JM(3) | 42 | | | x | | | | |
| TH | 42.5 | x | x | x | x | | Y,1.5cm (8x64) | |
| SB | 43 | | x | x | | | | |
| ML(2) | 43 | x | x | x | | | | |
| CW(2) | 43 | | x | x | | | Y,1cm | 4cm |
| KR(1) | 43 | | | x | | | | |
| CO'K | 43 | x | x | x | x | | X,2cm (1s; 8x64) | |
| RD | 43.5 | x | x | x | x | | Y,2cm (1s;8x64) | |
| KR(2) | 44 | | x | x | | | | |
| JMcG | 44 | x | x | x | x | | Y,2cm (1s; 8x32) | |
| JW | 44 | x | x | x | x | | | |
| CH | 44 | | x | | x | | | |
| AS | 44 | | x | | | | Y, 2cm (1s;8x32): X ,1cm(1s;16x32) | 4cm |
| IV | 46 | | x | | x | | Y,1.5cm (1s; 8x32) | |
| AA | 47 | x | x | x | x | | | 3cm |
| RM | 50 | | x | | | | | |
| LO'N | 51 | x | x | x | | 10s | Y,1cm (1s; 16x 32) | |
| RS | 60 | | x | x | | | | |
| NT(2) | 73 | x | x | x | x | | | |
| TMcL | 76 | x | x | x | x | | | 3cm |
| PP | 77 | x | x | x | | 0.2,2,30s | Y,2cm | 4cm |
| RV | 78 | x | x | x | x | 2s | | |
| TH(2) | 79 | x | x | x | x | | | |
| NT(3) | 96 | | | x | | | | |
| RB | 177 | x | x | x | x | | | 3cm |
| SJ | 202 | | x | x | | | Z,2cm;Y,2cm | 4cm |
| TB | 218 | x | x | x | x | | | 3cm |
| RDe | 261 | x | x | x | x | | | 3cm |

Table 6. Details of all the phosphorus spectroscopy examinations performed showing which repetition times were used for unlocalized phosphorus spectra; the plane examined, the repetition time used, the number of lines and number of repetitions for each line for two dimensional (2D) chemical shift imaging (CSI); and the volume of each voxel for four dimensional (4D) chemical shift imaging. PCA, post conceptional age; s, seconds; Y, Y axis of the magnet; X, X axis of the magnet; 8x32, 8 lines by 32 repetitions.

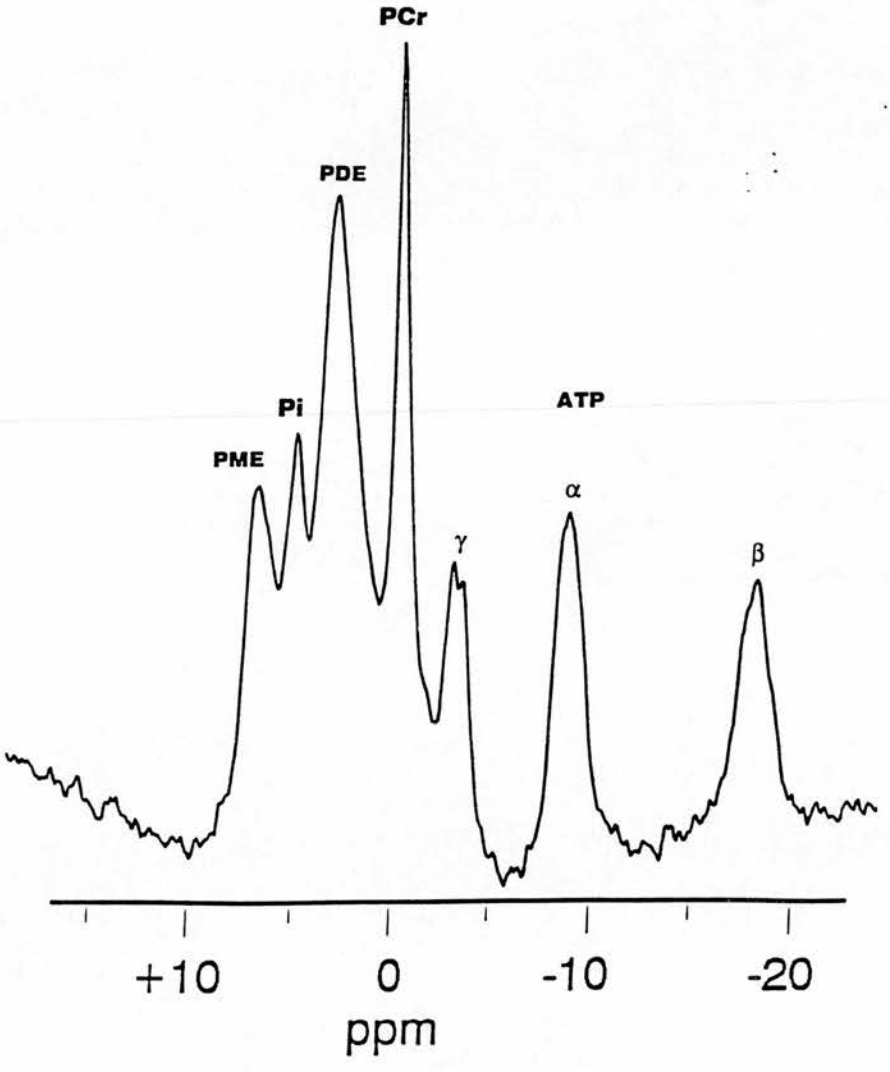



Fig. 52 Unlocalized phosphorus spectrum from the brain of a neurologically normal adult at a TR of 5s with 64 data collections. For this and subsequent phosphorus spectra: PCr, phosphocreatine; Pi, inorganic phosphate; PME, phosphomonoesters; PDE, phosphodiesters; ATP, adenosine triphosphate. The phosphorus spectra are not scaled vertically for comparison. The PCr/Pi ratio is 2.5, the PCr/βATP ratio is 2.5 and the PME/PDE ratio is 0.4. The pH is 6.95.

| | Outcome | PCA at exam | PNA at exam | PCR/Pi | PME/PDE | pH | PCr/ATP | Initials |
|---|---|---|---|---|---|---|---|---|
| 1 | Normal | 42.0 | .2 | 1.4 | 1.1 | 7.05 | 1.1 | kr |
| 2 | Control | 39.0 | .2 | 1.4 | 1.2 | 7.05 | 1.4 | natt |
| 3 | Severe | 41.0 | .2 | .7 | 1.3 | 7.12 | 1.1 | jm1 |
| 4 | Severe | 41.5 | .5 | .5 | 1.1 | 7.33 | 1.2 | jm2 |
| 5 | Normal | 38.0 | 1.0 | 1.3 | 1.2 | 7.05 | 1.0 | dt |
| 6 | Severe | 43.0 | 1.0 | 1.0 | .8 | 7.20 | 1.3 | kf1 |
| 7 | Severe | 42.0 | 1.0 | .8 | 1.0 | 7.22 | 1.1 | jm3 |
| 8 | Severe | 41.0 | 1.0 | .2 | .9 | 7.20 | .7 | ml1 |
| 9 | Severe | 42.0 | 1.0 | 1.3 | 1.1 | 7.09 | 1.1 | cw1 |
| 10 | Normal | 42.0 | 1.0 | 1.3 | 1.4 | 7.05 | 1.7 | ck |
| 11 | Normal | 41.5 | 1.5 | 1.4 | 1.2 | 7.05 | 1.2 | gbs |
| 12 | Normal | 43.5 | 1.5 | 1.1 | .9 | 7.05 | 1.3 | rhd |
| 13 | Severe | 44.0 | 2.0 | 1.2 | 1.1 | 7.28 | 1.4 | kf2 |
| 14 | Severe | 43.0 | 2.0 | 1.3 | 1.0 | 7.05 | 1.8 | cw2 |
| 15 | Severe | 42.0 | 2.0 | .8 | 1.4 | 7.22 | 1.0 | ar |
| 16 | Moderate | 38.0 | 2.0 | 1.3 | 1.3 | 7.05 | .9 | tf |
| 17 | Severe | 42.5 | 2.5 | 1.1 | 1.0 | 7.05 | 1.2 | th1 |
| 18 | Severe | 38.0 | 3.0 | 1.3 | 1.1 | 7.22 | 1.1 | nt1 |
| 19 | Severe | 43.0 | 3.0 | .7 | 1.0 | 7.35 | 1.2 | ml2 |
| 20 | Other | 42.0 | 3.0 | 1.4 | 1.2 | 7.05 | 1.1 | md |
| 21 | Moderate | 38.0 | 3.0 | 1.3 | 1.3 | 7.09 | 1.4 | ac |
| 22 | Severe | 44.0 | 3.0 | .9 | .9 | 7.43 | 1.3 | jmcg |
| 23 | Moderate | 44.0 | 4.0 | 1.6 | .8 | 7.05 | 1.5 | jw |
| 24 | Moderate | 43.0 | 6.0 | 1.5 | 1.0 | 7.16 | 1.5 | cok |
| 25 | Other | 47.0 | 7.0 | 1.4 | .8 | 7.05 | 1.4 | aa |
| 26 | Other | 47.0 | 9.0 | 1.4 | 1.0 | 6.92 | • | mg |
| 27 | Moderate | 51.0 | 13.0 | 1.5 | .8 | 6.95 | 1.5 | lon |
| 28 | Severe | 73.0 | 38.0 | 1.4 | .7 | 7.09 | 1.5 | nt2 |
| 29 | Severe | 79.0 | 39.0 | 2.1 | .6 | 7.05 | 1.6 | th2 |
| 30 | Severe | 76.0 | 39.0 | 1.9 | .6 | 6.95 | 2.1 | tmcl |
| 31 | Severe | 78.0 | 39.0 | 1.6 | .5 | 7.05 | 1.8 | rv |
| 32 | Severe | 77.0 | 40.0 | 1.9 | .4 | 7.05 | 2.0 | pp |
| 33 | Severe | 96.0 | 61.0 | 2.5 | .7 | 7.05 | 2.0 | nt3 |
| 34 | Severe | 177.0 | 139.0 | 1.4 | .4 | 6.95 | 1.7 | rb |
| 35 | Severe | 218.0 | 182.0 | 1.3 | .5 | 6.95 | 1.8 | tb |
| 36 | Severe | 261.0 | 221.0 | 1.6 | .4 | 6.95 | 2.4 | rd |
| 37 | Control | 280.0 | 240.0 | 2.0 | .4 | 6.92 | 2.3 | adult |
| 38 | Control | 280.0 | 240.0 | 2.4 | .3 | 7.05 | 2.5 | adult |
| 39 | Control | 280.0 | 240.0 | 2.2 | .5 | 6.92 | 2.3 | adult |
| 40 | Control | 280.0 | 240.0 | 2.1 | .4 | 7.05 | 2.4 | adult |
| 41 | Control | 280.0 | 240.0 | 2.2 | .4 | 6.95 | 2.5 | adult |
| 42 | Control | 280.0 | 240.0 | 2.5 | .4 | 6.95 | 2.5 | adult |

Table 7. Metabolite ratios and pH, derived from unlocalized 5s phosphorus spectra, with outcome, post conceptional age (PCA) and postnatal age (PNA) at the time of examination for 36 children and six adult controls. Nine children did not have 5s unlocalized phosphorus spectra acquired, or the spectra were not of adequate quality for analysis (WC, SB, CH, AS, IV, RM, RS, SJ, ST).

| | Initials | PCr/Pi(1) | PCr/Pi(2) | PME/PDE(1) | PME/PDE(2) | PCA at exam |
|---|---|---|---|---|---|---|
| 1 | ac | 1.3 | 2.3 | 1.3 | 3.0 | 38.0 |
| 2 | nt1 | 1.3 | 2.2 | 1.1 | 2.2 | 38.0 |
| 3 | natt | 1.4 | 5.0 | 1.2 | 2.7 | 39.0 |
| 4 | jm1 | .7 | 1.1 | 1.3 | 2.3 | 41.0 |
| 5 | jm2 | .5 | 1.0 | 1.1 | 1.1 | 41.5 |
| 6 | md | 1.4 | 2.8 | 1.2 | 1.9 | 42.0 |
| 7 | ar | .8 | .9 | 1.4 | 2.1 | 42.0 |
| 8 | ck | 1.3 | 2.8 | 1.4 | 2.2 | 42.0 |
| 9 | kr | 1.4 | 4.7 | 1.1 | 1.9 | 42.0 |
| 10 | jm3 | .8 | 1.3 | 1.0 | 1.4 | 42.0 |
| 11 | cw1 | 1.3 | 3.2 | 1.1 | 1.9 | 42.0 |
| 12 | th1 | 1.1 | 2.6 | 1.0 | 1.3 | 42.5 |
| 13 | cok | 1.5 | 1.5 | 1.0 | 1.6 | 43.0 |
| 14 | kf1 | 1.0 | 2.0 | .8 | 1.5 | 43.0 |
| 15 | cw2 | 1.3 | 3.1 | 1.0 | 2.6 | 43.0 |
| 16 | jw | 1.6 | 3.1 | .8 | 1.6 | 44.0 |
| 17 | kf2 | 1.2 | 2.4 | 1.1 | 1.8 | 44.0 |
| 18 | jmcg | .9 | 1.9 | .9 | 1.7 | 44.0 |
| 19 | aa | 1.4 | 1.4 | .8 | 1.5 | 47.0 |
| 20 | lon | 1.5 | 4.0 | .8 | 1.4 | 51.0 |
| 21 | nt2 | 1.4 | 3.5 | .7 | .7 | 73.0 |
| 22 | tmcl | 1.9 | 5.0 | .6 | 1.0 | 76.0 |
| 23 | pp | 1.9 | 4.8 | .4 | .7 | 77.0 |
| 24 | rv | 1.6 | 3.4 | .5 | .8 | 78.0 |
| 25 | th2 | 2.1 | 6.9 | .6 | .8 | 79.0 |
| 26 | nt3 | 2.5 | 9.1 | .7 | 1.1 | 96.0 |
| 27 | rb | 1.4 | 2.8 | .4 | .7 | 177.0 |
| 28 | tb | 1.3 | 3.0 | .5 | .7 | 218.0 |
| 29 | rd | 1.6 | 4.6 | .4 | .5 | 261.0 |
| 30 | adult | 2.1 | 6.0 | .4 | .5 | 280.0 |
| 31 | adult | 2.2 | 5.0 | .4 | .4 | 280.0 |
| 32 | adult | 2.5 | 8.8 | .4 | .5 | 280.0 |
| 33 | adult | 2.0 | 5.5 | .4 | .4 | 280.0 |
| 34 | adult | 2.4 | 8.0 | .3 | .4 | 280.0 |
| 35 | adult | 2.2 | 2.3 | .5 | .4 | 280.0 |

Table 8. Results from 5s unlocalized phosphorus spectra analysed in two different ways, see Fig. 25. Method 1; the method used for all the results presented in this thesis unless otherwise stated (Fig 25 a), the peak areas were defined by perpendiculars dropped to a baseline common to the full spectrum. Method 2; (Fig 25b), peak areas were defined by a line drawn across the minimum points of the peak. The two methods produced markedly different results.

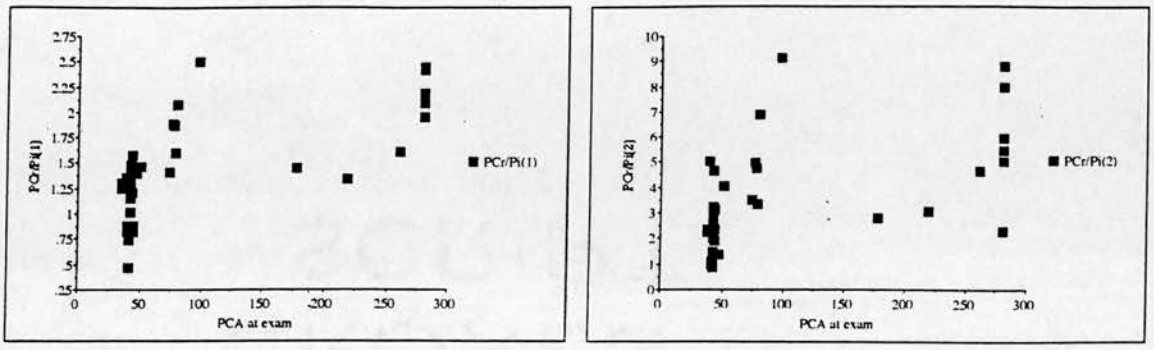



Fig. 53.
(a). Phosphocreatine (PCr) to inorganic phosphate ratios derived from 5s unlocalized spectra analysed using method 1 (see Fig. 25 page 48), plotted against postconceptional age (PCA).
(b). Phosphocreatine (PCr) to inorganic phosphate (Pi) ratios derived from 5s unlocalized spectra analysed using method 2 (see Fig. 25 page 48), plotted against postconceptional age (PCA).

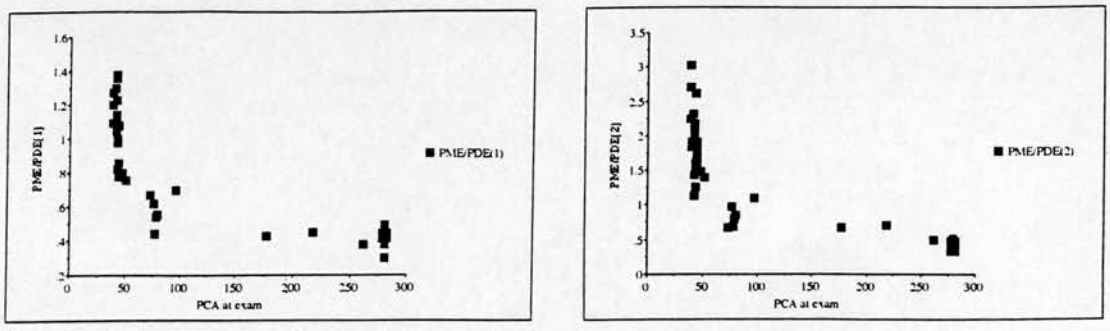



Fig. 54.
(a). Phosphomonoester (PME) to phosphodiester (PDE) ratios derived from 5s unlocalized spectra analysed using method 1 (see Fig. 25 page 48), plotted against postconceptional age (PCA).
(b). Phosphomonoester (PME) to phosphodiester (PDE) ratios derived from 5s unlocalized spectra analysed using method 2 (see Fig. 25 page 48), plotted against postconceptional age (PCA).

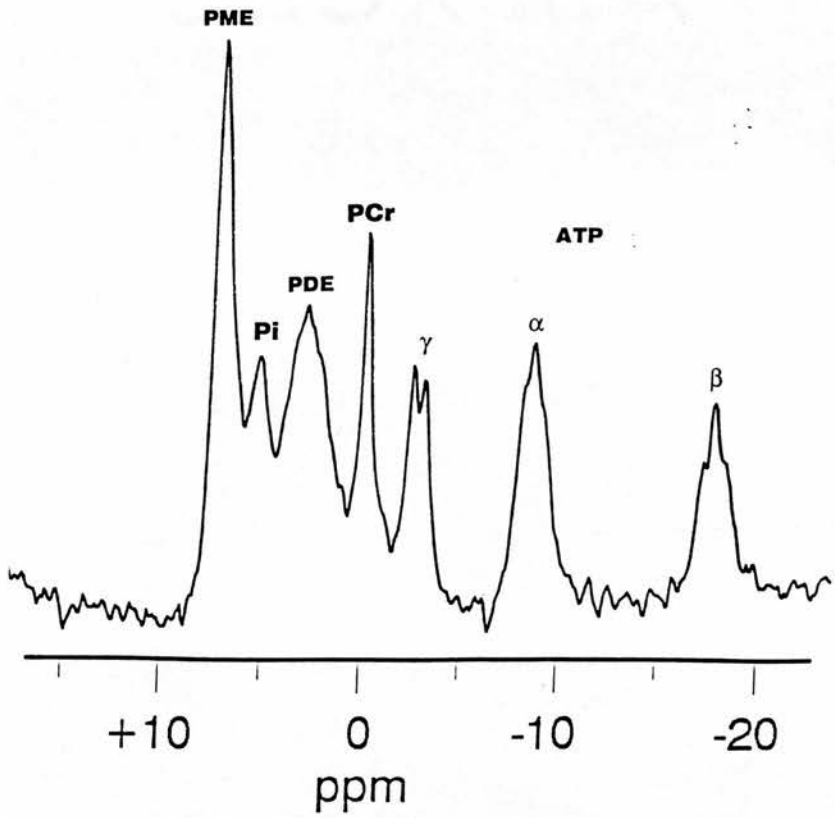



Fig. 55. Unlocalized phosphorus spectrum acquired at 43.5 weeks PCA, 1.5 weeks PNA from RhD, a child with a normal neurological outcome at one year. PCr/Pi 1.1, PME/PDE 0.9, PCr/βATP 1.3. Age related changes in the PME/PDE and PCr/βATP ratios are clearly seen if this spectrum is compared with that from a neurologically adult (Fig 52).

Changes due to hypoxic-ischaemic injury

The PCr/Pi ratios from all the children studied up to one year of age are shown in Fig.56 in relation to their PNA at the time of examination and their neurological outcome at one year or greater. Within approximately the first month of life (i.e up to 44 weeks PCA) PCr/Pi was related to outcome: infants with a poor neurological outcome had a lower PCr/Pi ratio. After the first four weeks there was no obvious relationship between PCr/Pi and neurological outcome.

The PME/PDE ratios within the first month of life showed no relationship with subsequent neurological outcome (Fig.57).

After hypoxic-ischaemic injury the intracellular pH increased. This change was very marked in the infants with a severe neurogical outcome. pH eventually returned to normal, and after the first month of life did not appear to be related to the degree of brain injury (Fig.58a and b).

Two spectra from an infant (ML) with severe hypoxic-ischaemic encephalopathy at seven and 21 days after birth are shown in Fig 59a and b. Although the second spectrum (b) remains abnormal there is some recovery in the PCr/Pi ratio (0.24:0.65) and the PCr/βATP ratio (0.7:1.2). The pH values are 7.20 and 7.35. Cranial ultrasounds acquired at ten days show extensive cystic changes (Fig. 59c).

A phosphorus spectrum from an infant (R D) aged four years three months, with a very poor outcome, is shown in Fig.60 with a magnetic resonance image acquired at the same age. The MR image shows a very abnormal brain, but there are no abnormalities in the metabolite ratios and the pH is within normal limits (6.95).

$T_1$ effects.

Various repetition times were used to study the effects of hypoxic-ischaemic injury on relaxation time. The saturation factors for PCr, Pi, PME, PDE and β–ATP derived from the 19 data sets obtained at 1s and 20s, as well as adult control values at 1s and

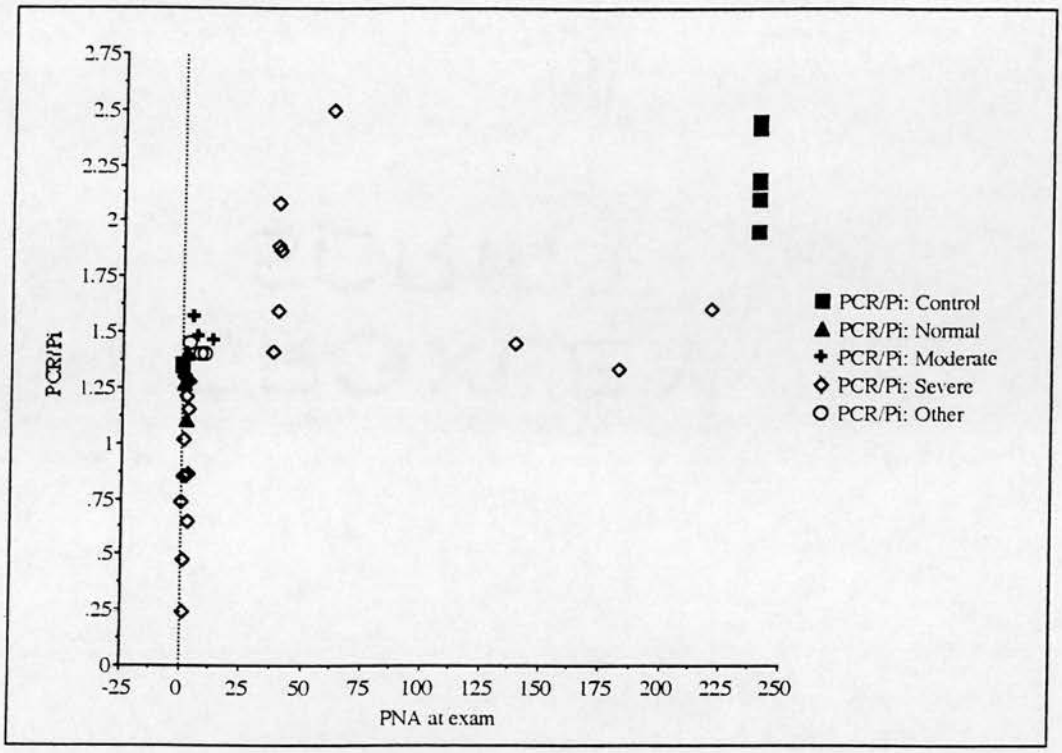



Fig. 56. Phosphocreatine (PCr) to inorganic phosphate (Pi) ratios plotted against postnatal age (PNA) at the time of the examination for all the children examined and six adult controls (two points overlap). Neurological outcome at one year of age or more is also shown.

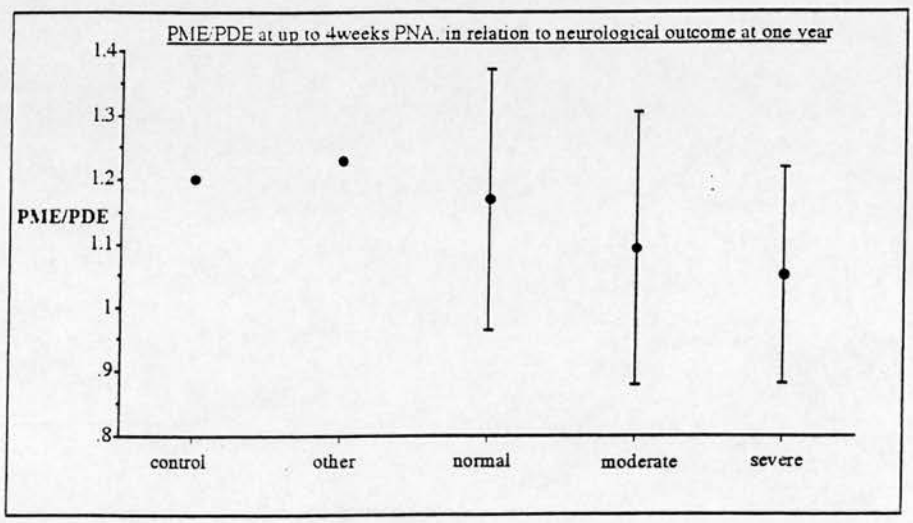



Fig. 57. Phosphomonoester (PME) to phosphodiester (PDE) ratios (mean +/- one standard deviation) at up to four weeks postnatal age (PNA) in relation to neurological outcome at one year. (Control, n=1; other n=1; normal, n=4, mean 1.17 +/- 0.02; moderate, n=5, mean 1.09 +/- 0.21; severe, n=11, mean 1.05 +/- 0.17).

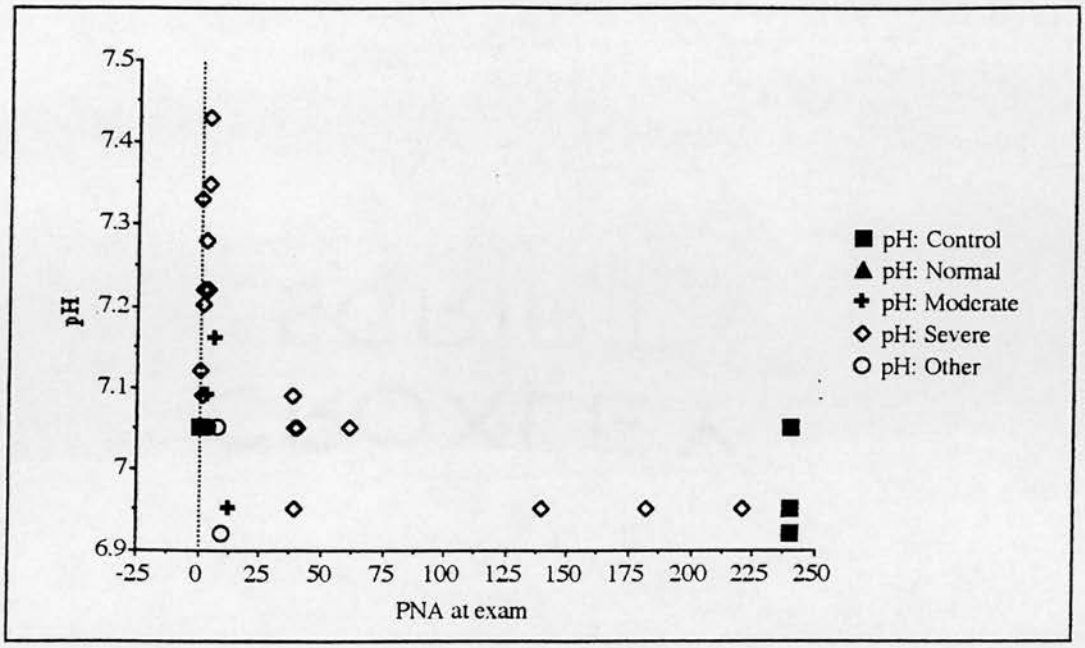
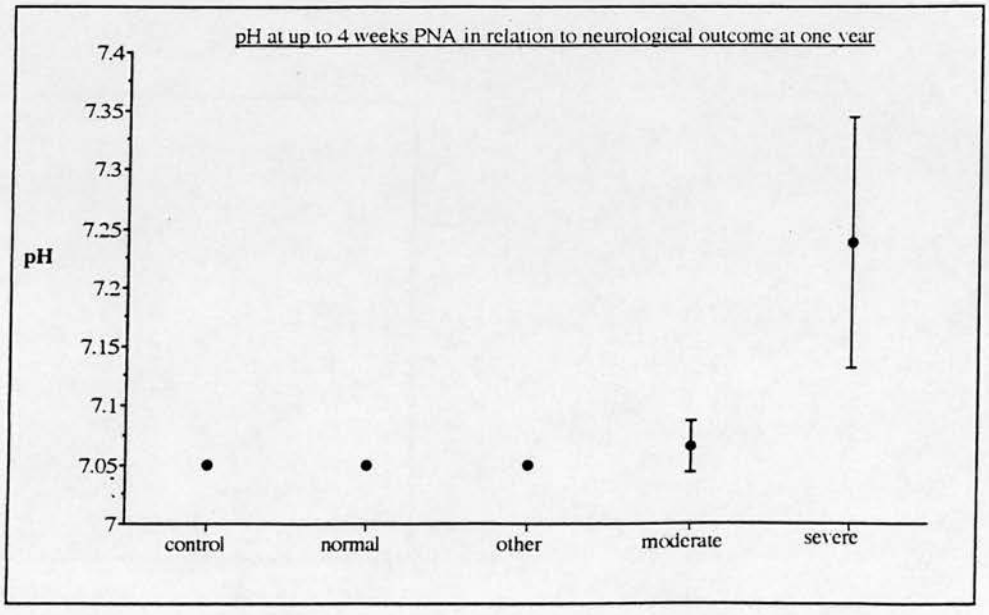



Fig. 58
(a) Intracellular pH in relation to postnatal age (PNA) at the time of examination and neurological outcome at one year or more.




(b). Mean +/- one standard deviation for all the pH values in each outcome group up to four weeks postnatal age (PNA). (Control, n=1; normal, n=4, mean 7.05 +/- 0; other, n=1; moderate, n=5, mean= 7.066 +/- 0.022; severe, n=11, mean=7.238 +/- 0.106).

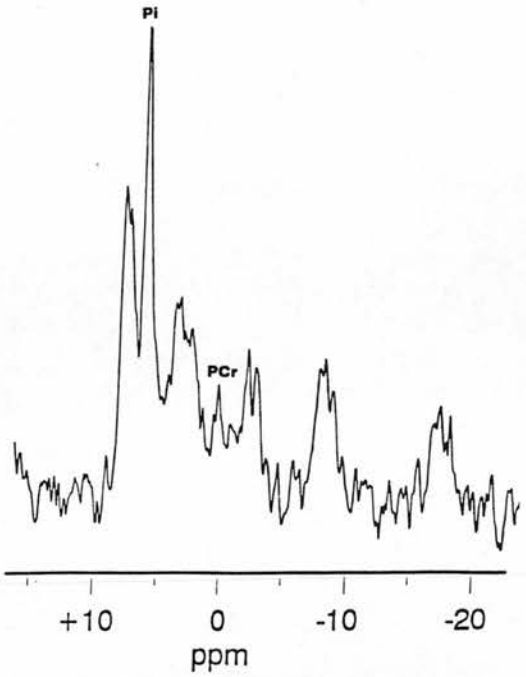
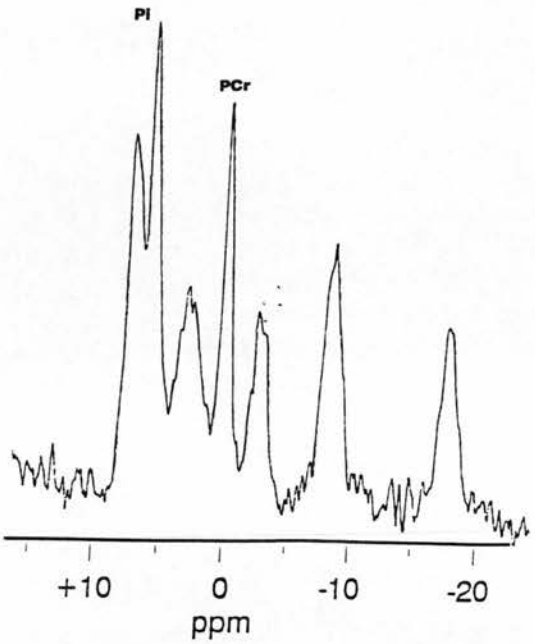



Fig. 59 (a) Unlocalized phosphorus spectrum acquired at 41weeks PCA, one week PNA, from the brain of ML an infant with a severe outcome. TR 5s, 64 data collects. The pH is 7.20, the PCr/Pi is very abnormal at 0.2 with virtually no PCr present, PME/PDE is 0.9 and the PCr/βATP is 0.7.




(b) Unlocalized phosphorus spectrum acquired at 43 weeks PCA, three weeks PNA from the brain of ML an infant with a severe outcome. TR 5s, 64 data collects. The pH is very alkaline at 7.35, the PCr/Pi is 0.7, PME/PDE is 1.0 and the PCr/βATP is 1.2. Although the Pi peak is still very abnormal, PCr has shown some recovery.



(c) Ultrasound at ten days from ML showing extensive cortical and subcortical cysts.

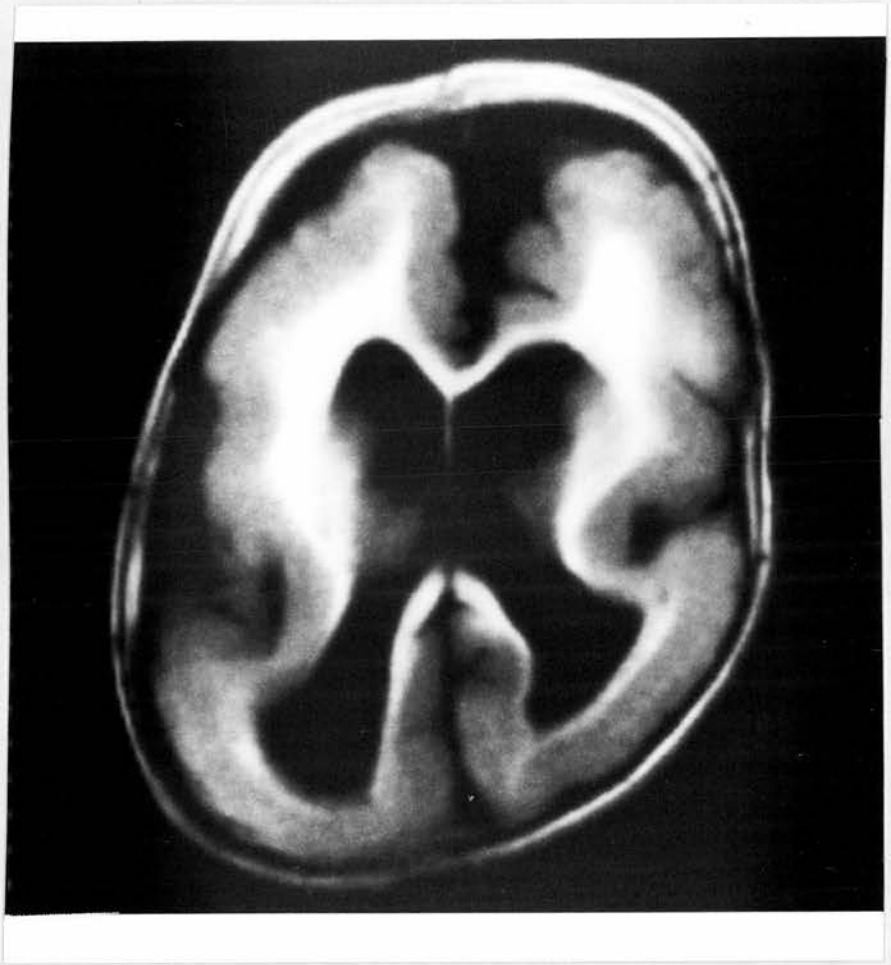
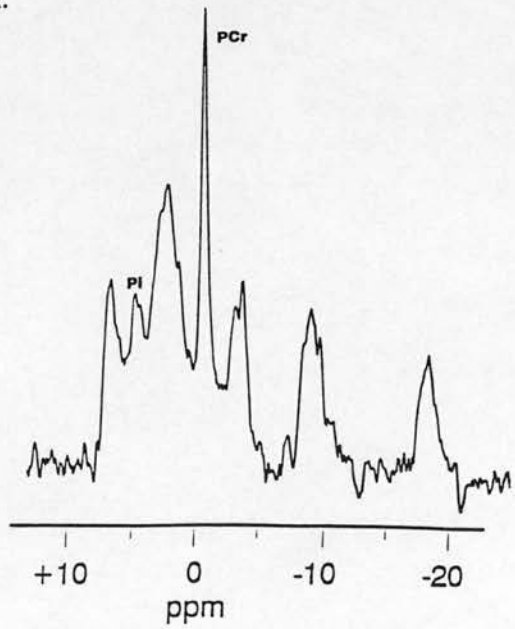


Fig. 60 (a) A magnetic resonance image (SE 500/22) from the brain of RD, a child with severe outcome, aged 4 years and 5 months. The image shows a very abnormal brain with gross ventricular dilatation.




(b) Unlocalized phosphorus spectrum acquired at 4 years and 5 months from the brain of RD (TR 5s, 64 data collects). The pH is 6.95, the PCr/Pi is 1.6, PME/PDE is 0.4 and the PCr/βATP is 2.4.

20s, are shown in Table 9 with clinical outcome at one year or more. The 0.5s data sets were not used for numerical analysis as the signal to noise ratio was much lower with such a short signal acquisition time, although 0.5s data sets are used in Figs.62 and 63 for illustrative purposes.

The saturation factor of Pi is noticeably prolonged in the children with severe outcome within the first four weeks of life (Fig.61). These changes are illustrated by the spectra shown in Fig. 62 and Fig. 63. Figure 62 shows spectra at different repetition times from an infant (Rh D) at 43.5 PCA who was neurologically normal at two years. The spectra in Fig.63 are from an infant (AR) at 42 weeks PCA who suffered severe birth asphyxia and who had a very poor outcome. Both sets of spectra were acquired under the same conditions but the saturation factor for Pi at the longer repetition time is very different in the two cases; markedly prolonged in the infant with a severe outcomc.

The differences in the saturation factor of Pi are most apparent if the data are compared up to 44 weeks PCA. In the older children there is no obvious relationship between outcome and saturation factors; for example, see Fig.64 two sets of spectra acquired from the brain of the same child (NT), the first (a) at 3 weeks PNA and the second (b) at 9 months PNA. Despite the fact that this child has residual serious neurological injury there is no prolongation of the saturation factor of Pi at nine months of age.

| | PCA at exam | PNA at exam | PME | Pi | PDE | PCr | ATP | outcome | initials |
|---|---|---|---|---|---|---|---|---|---|
| 1 | 43.5 | 1.5 | 3.1 | 1.4 | 1.8 | 2.1 | 1.3 | normal | rhd |
| 2 | 38.0 | 2.0 | 2.8 | 1.9 | 1.9 | 2.0 | 1.3 | moderate | tf |
| 3 | 42.0 | 2.0 | 3.6 | 3.5 | 1.5 | 2.6 | 1.5 | severe | ar |
| 4 | 37.5 | 2.5 | 3.5 | 2.3 | 1.3 | 2.9 | 1.6 | severe | ntl |
| 5 | 42.5 | 2.5 | 3.2 | 2.3 | 2.4 | 2.2 | 1.3 | severe | thl |
| 6 | 42.0 | 3.0 | 3.2 | 1.8 | 1.7 | 2.5 | 1.3 | other | md |
| 7 | 38.0 | 3.0 | 3.3 | 1.7 | 1.8 | 2.0 | 1.6 | moderate | ac |
| 8 | 44.0 | 3.0 | 2.4 | 2.1 | 1.5 | 1.8 | 1.1 | severe | jmcg |
| 9 | 44.0 | 4.0 | 2.7 | 1.6 | 1.8 | 2.0 | 1.6 | moderate | jw |
| 10 | 44.0 | 4.0 | 3.0 | 1.6 | 1.7 | 2.0 | 1.5 | normal | ch |
| 11 | 43.0 | 6.0 | 3.6 | 1.3 | 1.5 | 2.1 | 1.1 | moderate | cok |
| 12 | 46.0 | 6.0 | 2.0 | 1.9 | 2.2 | 2.4 | 1.3 | normal | iv |
| 13 | 47.0 | 7.0 | 1.8 | 1.3 | 1.3 | 1.6 | 1.4 | other | aa |
| 14 | 51.0 | 13.0 | 2.9 | 1.8 | 2.0 | 1.5 | 1.6 | moderate | lon |
| 15 | 76.0 | 39.0 | 3.3 | 2.0 | 1.4 | 1.8 | 1.4 | severe | tmcl |
| 16 | 78.0 | 39.0 | 2.6 | 1.8 | 1.6 | 2.2 | 1.8 | severe | rv |
| 17 | 79.0 | 39.0 | 2.1 | 1.5 | 1.7 | 1.8 | 1.4 | severe | th2 |
| 18 | 218.0 | 182.0 | 2.8 | 1.9 | 1.9 | 1.9 | 1.5 | severe | tb |
| 19 | 261.0 | 221.0 | 2.3 | 1.7 | 1.3 | 2.1 | 1.3 | severe | rd |
| 20 | 280.0 | 240.0 | 2.3 | 1.6 | 2.2 | 2.1 | 1.5 | control | adult |
| 21 | 280.0 | 240.0 | 2.8 | 1.5 | 2.3 | 2.2 | 1.4 | control | adult |
| 22 | 280.0 | 240.0 | 2.6 | 1.2 | 1.6 | 1.8 | 1.5 | control | adult |
| 23 | 280.0 | 240.0 | 2.4 | 1.4 | 1.8 | 2.1 | 1.4 | control | adult |

Table 9. Saturation factors derived from unlocalized phosphorus spectra collected at repetition times of 1s and 20s are shown for 19 children and four adults. Outcome category, postconceptional age (PCA) and postnatal age (PNA) at the time of examination are also shown.

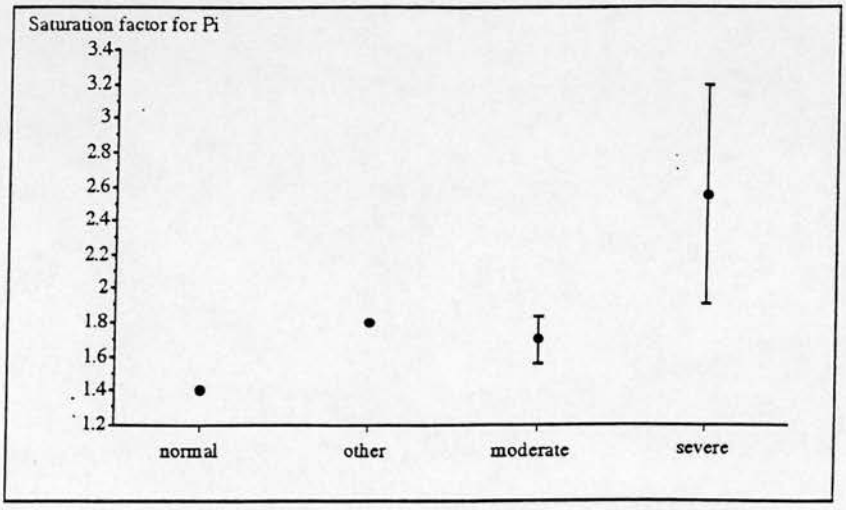



Fig. 61 Saturation factor for inorganic phosphate derived from unlocalized spectra at repetition times (TR's) of 1s and 20s, within the first four weeks of life. The mean +/- one standard deviation for each clinical outcome group is shown. ( There was no control infant in this group; normal, n=1; other n=1; moderate, n=4, mean=1.7 +/- 0.14; severe, n=4, mean= 2.55 +/- 0.64)

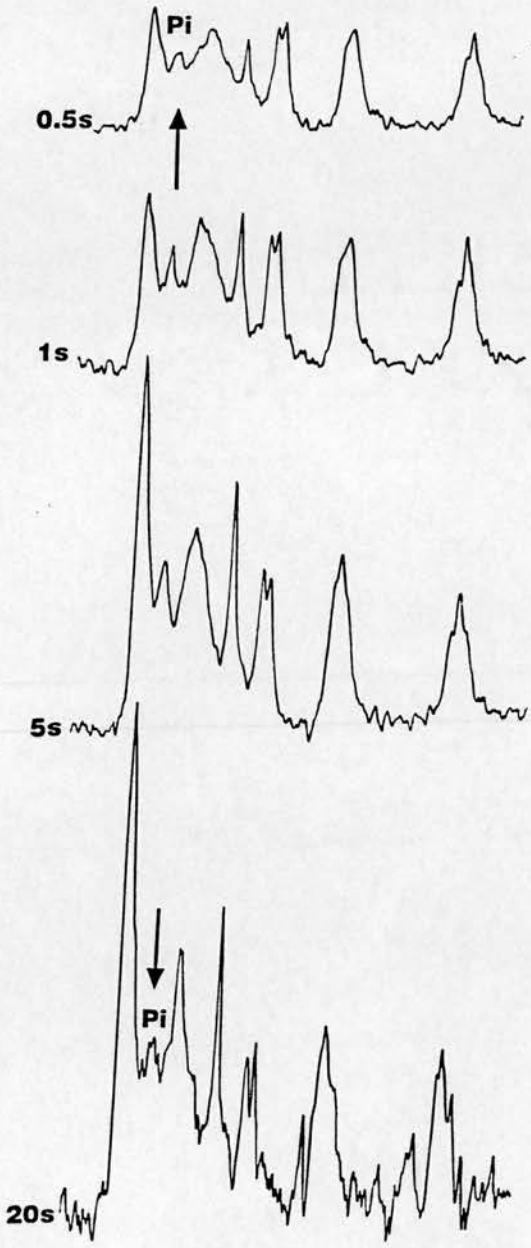



Fig. 62 Unlocalized phosphorus spectra acquired at different TR's from the brain of Rh D, a child with a normal outcome, at 43.5 weeks PCA, 1.5 weeks PNA. TR 0.5s, 256 data collects; TR 1s, 128 data collects; TR 5s, 64 data collects; TR 20s, 16 data collects.

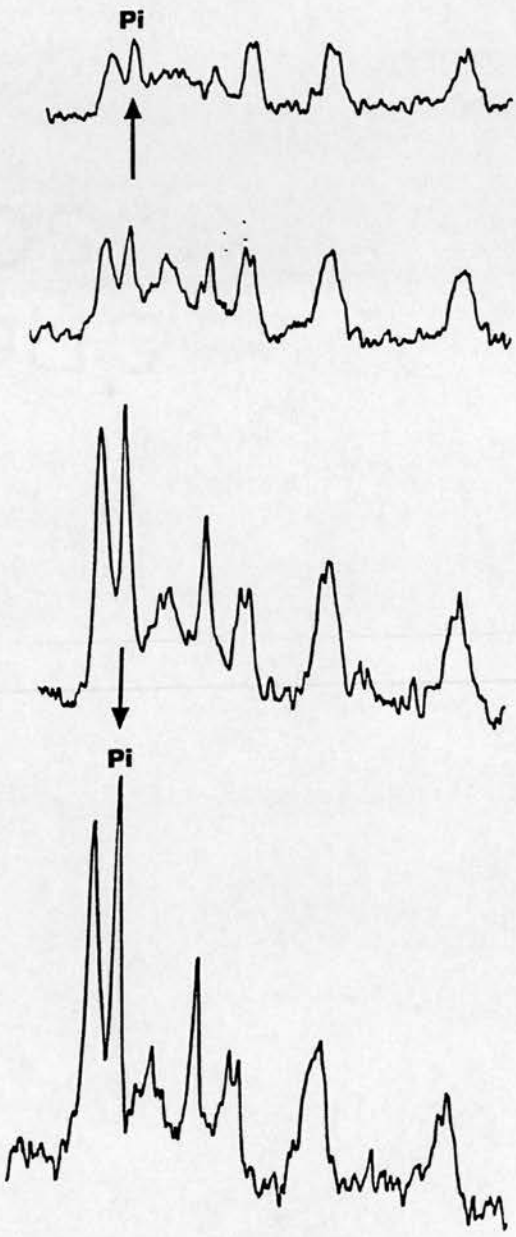



Fig. 63 Unlocalized phosphorus spectra acquired at different TR's from the brain of AR, a child with a severe outcome, at 42 weeks PCA, 2 weeks PNA. TR 0.5s, 256 data collects; TR 1s, 128 data collects; TR 5s, 64 data collects; TR 20s, 16 data collects.

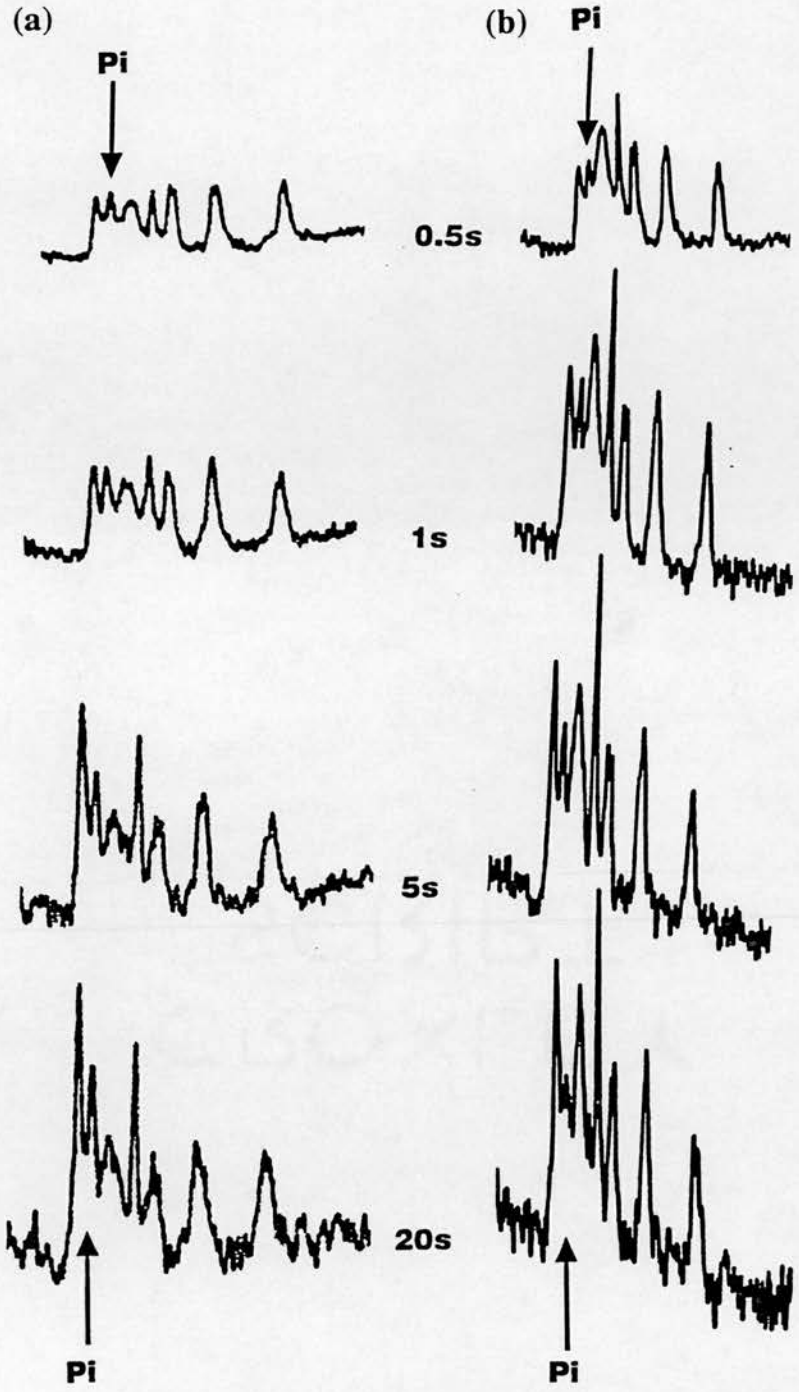



Fig. 64 (a) Unlocalized phosphorus spectra acquired at different TR's from the brain of NT, a child with a severe outcome, at 38 weeks PCA, 3 weeks PNA.
TR 0.5s, 256 data collects; TR 1s, 128 data collects; TR 5s, 64 data collects; TR 20s, 16 data collects.

(b) Unlocalized phosphorus spectra acquired at different TR's from the brain of NT at nine months PNA.
TR 0.5s, 256 data collects; TR 1s, 128 data collects; TR 5s, 64 data collects; TR 20s, 16 data collects. The saturation factor of Pi is not as prolonged in these later spectra campared with those shown opposite.

## LOCALIZED PHOSPHORUS SPECTRA

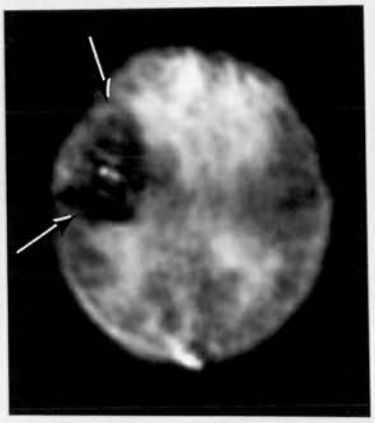
Twenty one children were studied with 2D chemical shift imaging (CSI); one child was examined on two occasions. Only nine of these children (ten examinations) had evidence of a focal ischaemic or haemorrhagic intracerebral lesion on cranial ultrasound, CT or MRI. The children who had no focal intracerebral lesion showed no localized changes with 2D CSI. Two children who did have focal lesions, but in whom no localized spectra were obtained, showed no abnormalities in either PME/PDE or the PCr/Pi ratios on their unlocalized phosphorus spectra.

Two children (JMcG and CK), with known focal lesions, shown in Fig.65 and Fig.66 had unlocalized phosphorus spectra and 2D CSI data sets acquired. JMcG had a poor neurological outcome and an abnormal PCr/Pi ratio on analysis of a 5s unlocalized spectrum; CK had a normal neurological outcome and a normal 5s unlocalized spectrum. Both children showed changes in their localized phosphorus spectra corresponding to the region of abnormality shown on MRI. There was a spatial variation in the PCr/Pi ratio, the lowest PCr/Pi ratio corresponding to the region of abnormality shown on imaging.

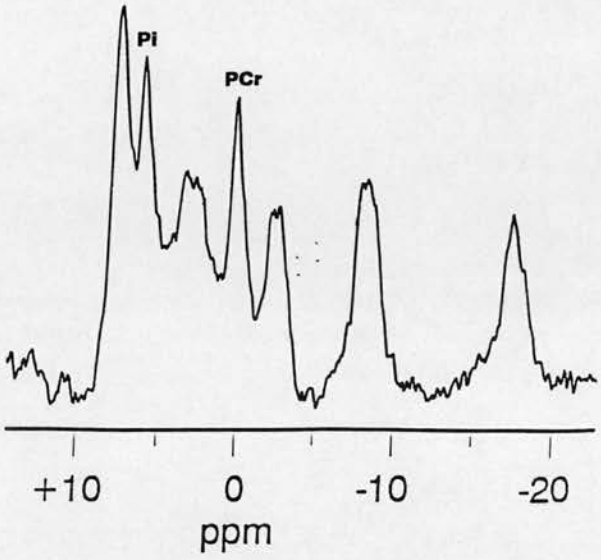
Another child (AC) with a moderate neurological outcome, who had localized cysts, showed no spatial variation on 2D CSI (with a resolution of 2 cm). The whole volume spectrum was also normal.

Nine children were examined on ten occasions with 4D CSI. Two of these children (CW and TMcL) had an intracerebral focal lesion. No changes related to hypoxic or ischaemic injury were detectable in any voxel. CW also had 2D CSI performed twice; there were no changes detectable on any of the 2D CSI spectra. There were no changes in any of the spectra obtained from the children without focal lesions. An unlocalized phosphorus spectrum and spectra obtained with 4D CSI from AA are shown in Fig.67 and show the quality of spectra that can be obtained with chemical shift imaging.

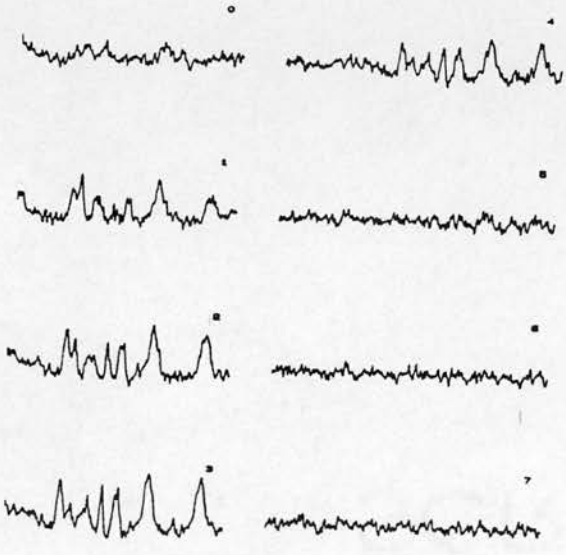
Fig. 65 (a) Magnetic resonance image (partial saturation sequence) of J McG at 44 weeks PCA, 3 weeks PNA showing a large left middle cerebral artery infarct with extensive involvement of left frontal and parietal lobes. (The images are reversed). Clinically, the child has a residual dense right hemiplegia.



(b) Unlocalized phosphorus spectrum from the brain of J McG (TR 5s, 64 data collects). The pH is extremely abnormal at 7.43. The PCr/Pi is 0.9, PME/PDE is 0.9 and PCr/βATP is 1.3.




(c) Set of 2D spectra from 2cm planes along the Y axis from left to right from the brain of J McG. Planes 0, 5, 6 and 7 show very low metabolite concentrations as they are partly composed of scalp and bone and may have no brain tissue within them.



(d) Planes 1 and 3 from (c) enlarged.
Plane 1 : pH 7.43; PCr/Pi 0.3
Plane 3 : pH 7.09; PCr/Pi 1.8.
Plane 1 is taken from the infarcted region of brain, plane 3 from more normal brain.

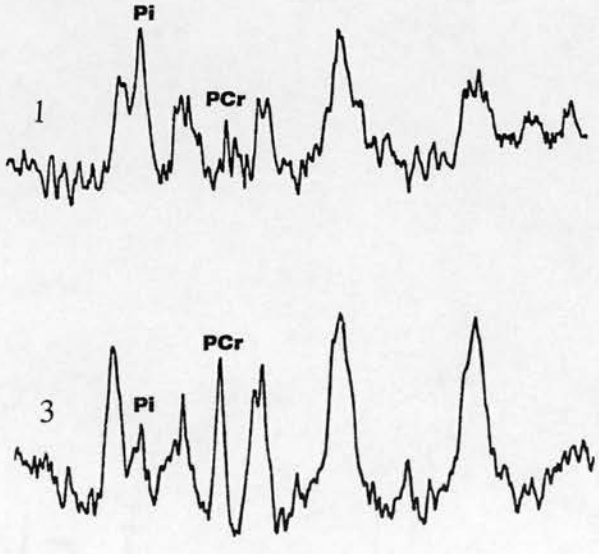
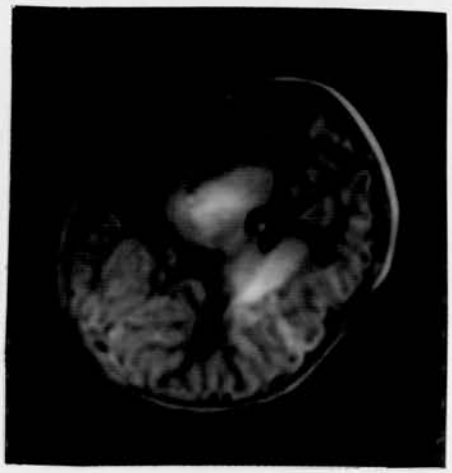
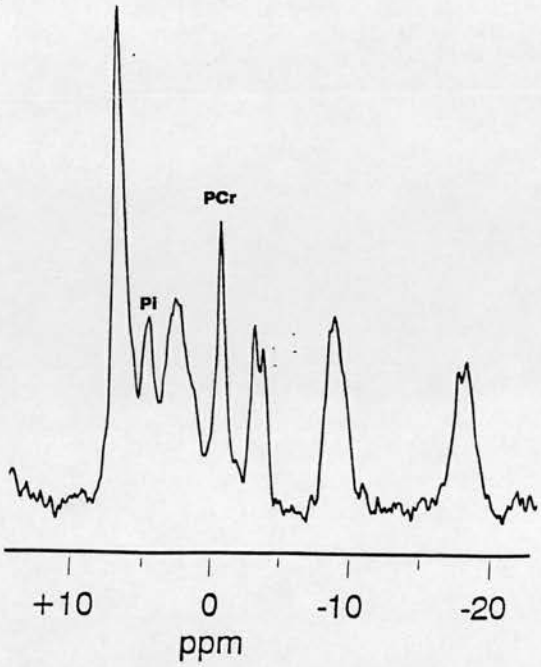


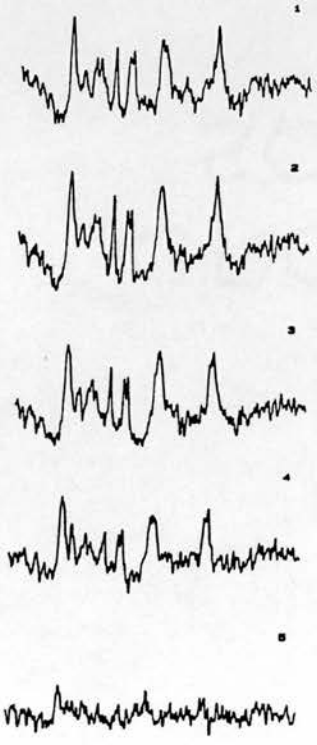
Fig. 66 (a) Magnetic resonance image of CK at 42 weeks PCA, 1 week PNA. The image shows changes suggestive of haemorrhage into the basal ganglia, periventricular areas, cortex, subarachnoid and possibly subdural spaces.



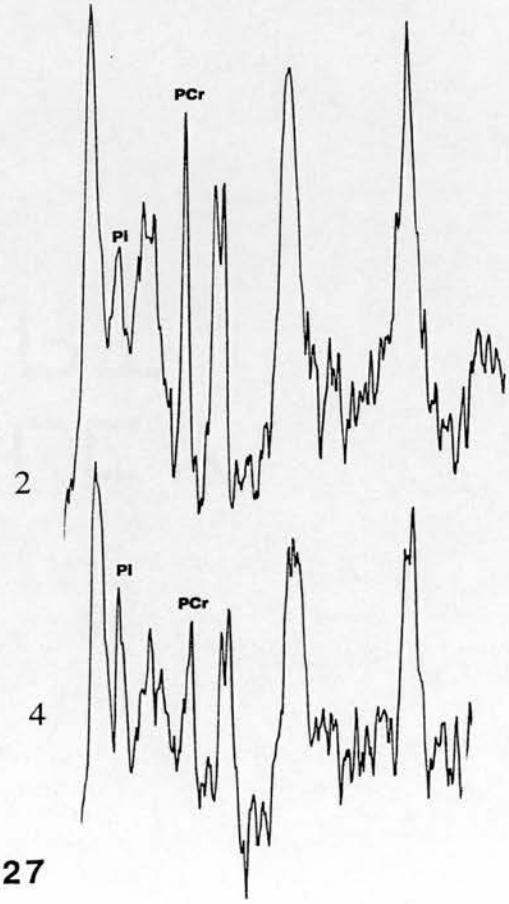
(b) Unlocalized phosphorus spectrum of the brain (TR 5s, 64 data collects). The pH is 7.05, PCr/Pi is 1.3, PME/PDE is 1.4 and PCr/βATP is 1.7.




(c) Set of 2D spectra from 2cm planes in the X axis from the brain of CK. Planes 0 and 5 show very low metabolite concentrations as they are partly composed of scalp and bone and may only have a very small component of brain within them.



(d) Planes 2 and 4 from (c) enlarged.
Plane 2: pH 6.85, PCr/Pi 1.2.
Plane 4: pH 7.28, PCr/Pi 0.8.



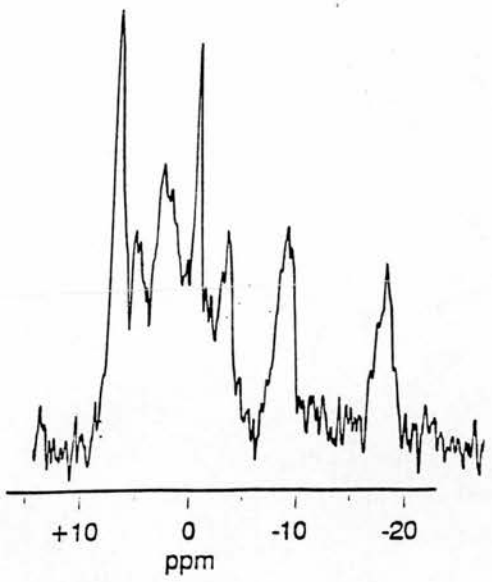
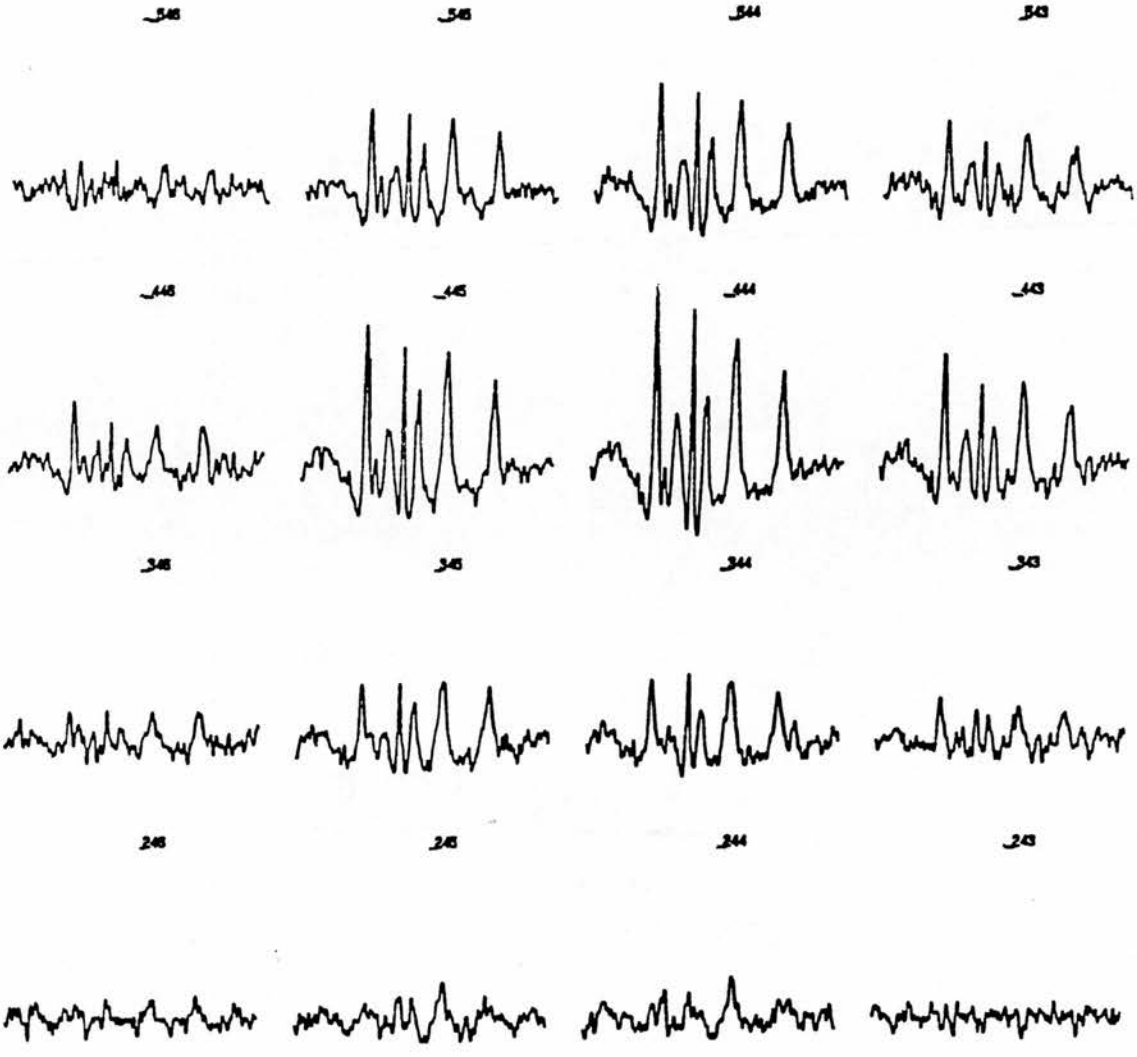



Fig. 67 (a) Unlocalized phosphorus spectrum from AA at 47 weeks PCA and 7 weeks PNA. TR 5s, 64 data collects. The pH is 7.05,the PCr//Pi is 1.4 and the PME/PDE is 0.8.



(b) Set of spectra obtained from AA with 4 dimensional chemical shift imaging, illustrating the quality of spectra obtained.

## PROTON AND PHOSPHORUS SPECTROSCOPY

Thirteen children were studied with both proton and phosphorus spectroscopy (16 examinations). Phosphorus and proton spectra were acquired during the same examination in fourteen cases, allowing direct comparisons to be made between the two types of spectra.

Proton and phosphorus spectra obtained 48 hours after birth from a neurologically normal infant (Nat T) (Fig.68a and b) are shown alongside those from (JM) an infant with moderate birth asphyxia and hypoglycaemia (Fig.69a and b), also examined at 48 hours after birth. The ratios from Nat T's proton spectrum are 0.9 (NAA/Cho), 1.6 (NAA/Cr) and 1.6 (Cho/Cr); those from JM's proton spectrum are 0.8 (NAA/Cho), 1.6 (NAA/Cr) and 2.0 (Cho/Cr). There is little difference between these two spectra.

Comparing the phosphorus spectrum from Nat T (68b) with the phosphorus spectrum of JM (69b), the difference between the spectra are more obvious. The spectrum from JM is abnormal with a PCr/Pi ratio of 0.7 and a pH of 7.12. A phosphorus spectrum acquired 24 hours later from JM was even more abnormal (PCr/Pi 0.5; pH 7.33) showing that, in this case, the abnormalities in the phosphorus spectrum were evolving at 48-72 hours. This may refelect further cellular damage due for example to reperfusion injury.

A later proton spectrum from JM is shown in Fig.70c; it was acquired two weeks after birth (NAA/Cho 0.7, NAA/Cr 0.8, Cho/Cr 1.2), the NAA/Cr and Cho/Cr ratios have decreased compared to those in Fig. 69a. Two cranial ultrasounds from the same child are shown (Fig.70a and Fig.70d): the first, acquired at the same time as spectrum 69a shows a featureless brain with slit-like ventricles; the second, acquired at the same time as 70c, shows subcortical cysts. A further phosphorus spectrum acquired at 1 week PNA is also shown (70b), the acute phosphorus changes are resolving although the pH remains abnormal (PCr/Pi 0.8; pH 7.22).

Fig.68 (a) A proton spectrum acquired at 48 hours after birth from a 64cm$^3$ volume in the brain of NaT T, neurologically normal at birth (39 weeks PCA). TR 2,000ms, TE 270ms, 128 data collects. The NAA/Cho ratio is 0.9, the NAA/Cr ratio is 1.6 and the Cho/Cr ratio is 1.6.

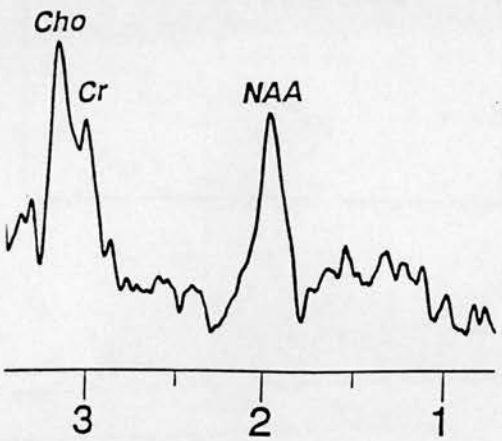



Fig. 69 (a) A proton spectrum acquired at 48 hours after birth from a 64cm$^3$ volume in the brain of JM, an infant who was neurologically abnormal at birth (41 weeks PCA) and who had a subsequent severe neurological outcome. TR 2,000ms, TE 270ms, 128 data collects. The NAA/Cho ratio is 0.8, the NAA/Cr ratio is 1.6 and the Cho/Cr ratio is 2.0.

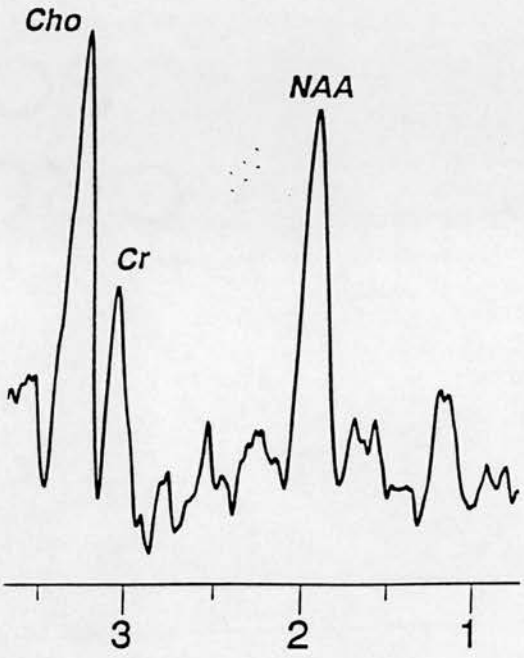



Fig. 68 (b) Unlocalized phosphorus spectrum acquired from the brain of NatT at 48 hours after birth (TR 5s, 64 data collects). The pH is 7.05, the PCr/Pi is 1.4, the PME/PDE is 1.2 and the PCr/βATP is 1.4.

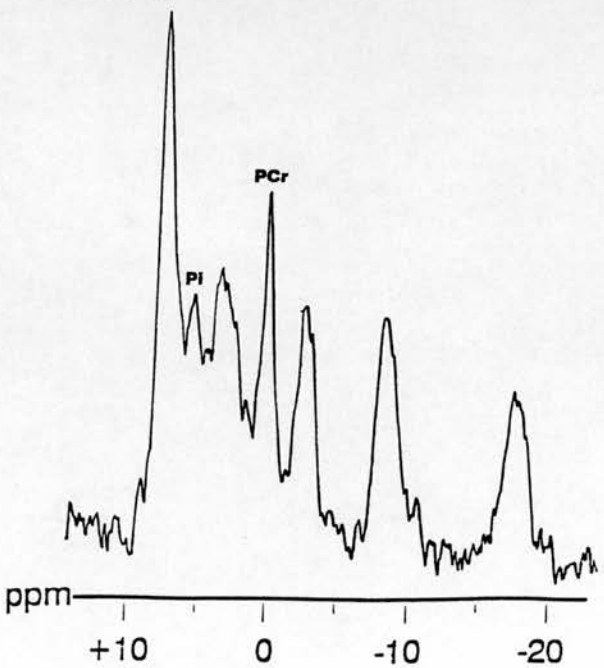



Fig. 69 (b) Unlocalized phosphorus spectrum acquired from the brain of JM at 48 hours after birth (TR 5s, 64 data collects). The pH is 7.12, the PCr/Pi is 0.7, the PME/PDE is 1.3 and the PCr/βATP is 1.1.

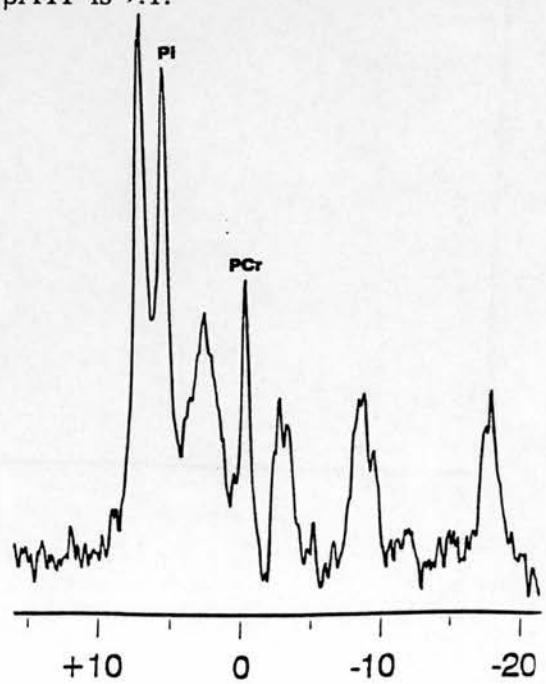
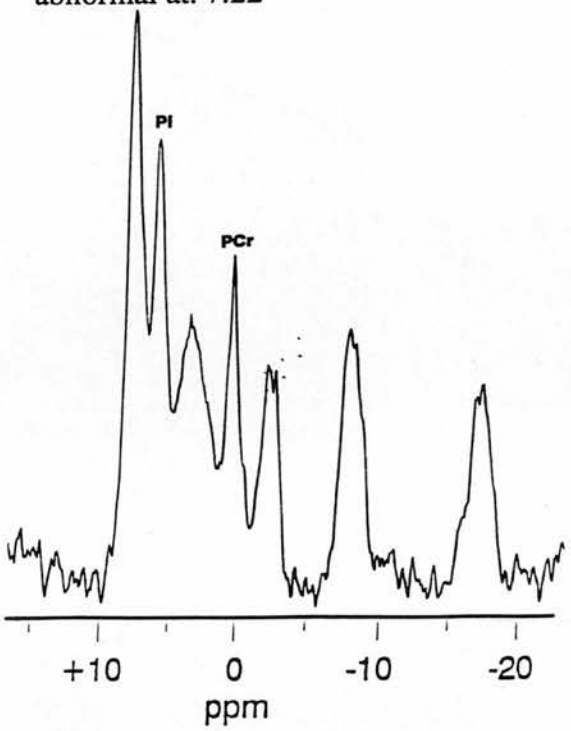


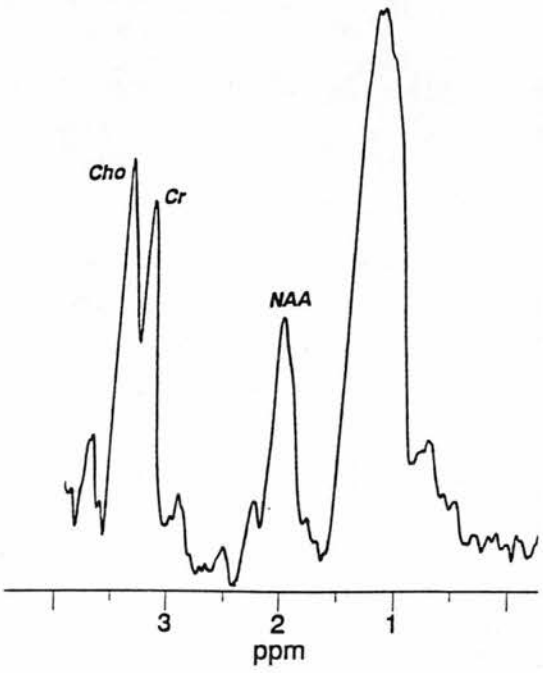
Fig. 70 (a). Cranial ultrasound acquired from JM at 48 hours after birth just before spectra 69(a) and (b) were acquired. It shows a featureless brain with slit like ventricles.



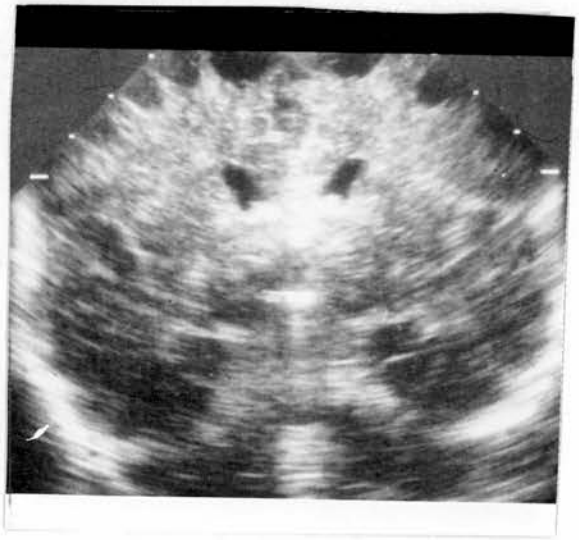
(b)Phosphorus spectrum acquired one week after birth from JM. The changes in PCr and Pi are now resolving (PCr/Pi 0.8) although the pH remains abnormal at. 7.22




(c) Proton spectrum acquired from JM two weeks after birth when cystic changes had developed in the brain. NAA/Cho is 0.7, NAA/Cr is 0.8 and Cho/Cr is 1.2. The NAA/Cr and Cho/Cr ratios have decreased compared to those in spectrum 69(a).




(d) Cranial ultrasound from JM at two weeks after birth, just before the spectrum in (c) was acquired, subcortical cysts have developed.

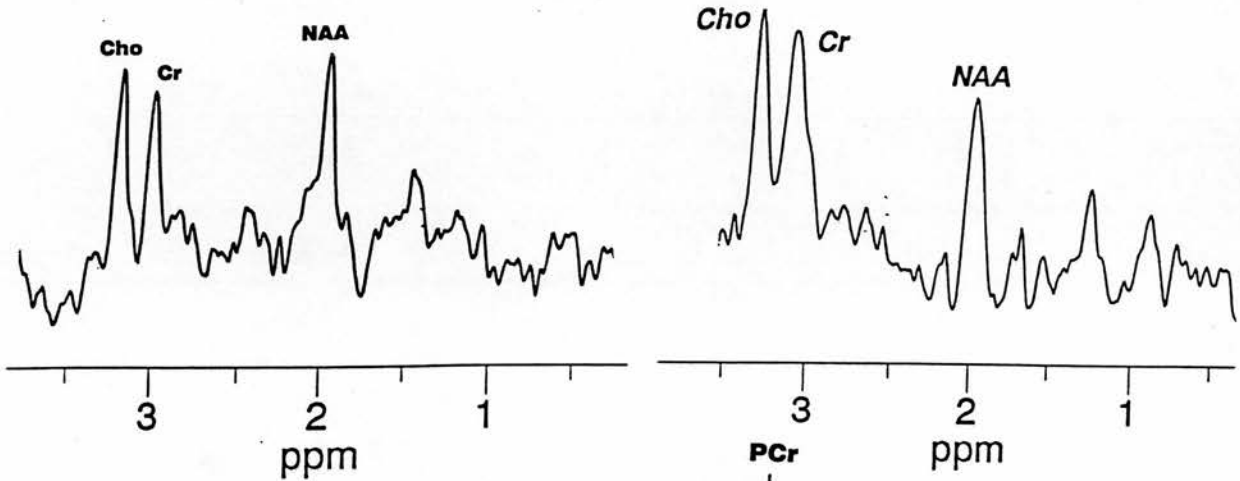


Two proton spectra acquired at five and 14 months from NT who developed extensive subcortical cysts, cerebral atrophy, microcephaly, and hypsarrhythmia, are shown in Fig.71a and b. A phosphorus spectrum, acquired at 14 months, is also shown (Fig.71c). The proton spectrum at five months (Fig.71a) has ratios of 0.9 (NAA/Cho), 1.0 (NAA/Cr) and 1.1(Cho/Cr); these ratios are similar in the spectrum nine months later (Fig.74b), (1.0, 1.1 and 1.1). The phosphorus spectrum, also obtained at 14 months, gives a pH of 7.12 and a PCr/Pi ratio of 2.5, within normal limits.

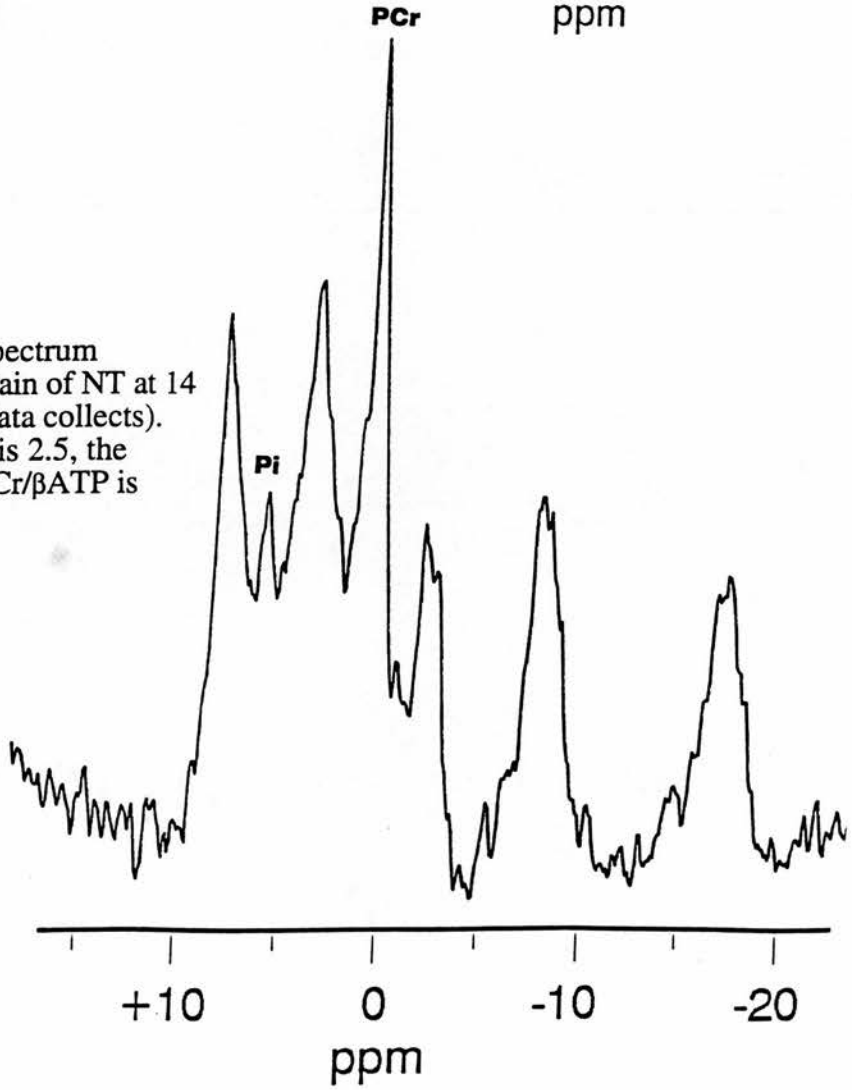
These examples suggest that phosphorus spectra eventually return to normal after hypoxic-ischaemic injury, but abnormalities persist in the proton spectra.

Fig. 71 (a) Proton spectrum acquired at five months PNA from NT a child with a severe neurological outcome (TR 2,000ms, TE 270ms 128 data collects). The NAA/Cho ratio is 0.9, the NAA/Cr ratio is 1.0, the Cho/Cr ratio is 1.1.

(b) Proton spectrum acquired at fourteen months PNA from NT (TR 2,000ms. TE 270ms, 128 data collects).
The NAA/Cho ratio is 1.0, the NAA/Cr ratio is 1.1, the Cho/Cr ratio is 1.1.




(c). Phosphorus spectrum acquired from the whole brain of NT at 14 months PNA (TR 5s, 64 data collects). The pH is 7.05 the PCr/Pi is 2.5, the PME/PDE is 0.7 and the PCr/βATP is 2.0.



# DISCUSSION

Magnetic resonance spectroscopy (MRS) is a rapidly moving technology where applications are still being sought. The work presented in this thesis uses spectroscopy as a non-invasive method to investigate changes in the biochemistry of the brain after hypoxic-ischaemic injury in neonates; an area of current clinical concern.

Successes with these studies

We adapted monitoring equipment and commercially available life support equipment to monitor, and when necessary ventilate, sick infants and children within the magnetic resonance (MR) system. Studying sick neonates and infants in MR systems is not an easy undertaking; a particular problem relating to neonates is that the surroundings are air conditioned and cold. In general, despite these difficulties, our adapted monitoring and ventilation equipment worked well and the children were cared for to the same standard as in the neonatal unit. By using this equipment routinely we improved safety for all patients in the MR unit.

To our knowledge, the work reported in this thesis generated the first published data of abnormal proton brain spectra from infants, and the first reported proton spectra from any child less than one month of age. In addition, we used phosphorus spectroscopy to study the brains of older, neurologically abnormal children; used localization techniques not previously reported in paediatric phosphorus spectroscopy; and observed changes in the saturation factor of Pi after injury. We studied some infants with both proton and phosphorus spectroscopy, which allowed us to compare the two techniques at different stages of development of the brain, and to gain additional biochemical information not available from either technique alone.

Clinical problems with these studies.

A major problem with this thesis is the lack of neurologically normal infants as controls. Some of the reasons for the small number of normal infants studied are given in the Results section.

No group has found it easy to recruit normal infants even though MR studies are non-

invasive. We were very strict in describing infants as controls, they had to be absolutely normal. Other groups have been more generous e.g. "results were age matched and compared with MR spectroscopy findings in 12 other children... with circumscribed cerebral or spinal disease in whom MR imaging revealed no evidence of delayed or disturbed myelination" (Grodd et al. 1991) or " Group A consisted of 12 examinations of either healthy children or patients who were expected to have undisturbed spectra for amnestic and clinical reasons (Boesch et al. 1989). We did not classify children who had other illnesses, but no hypoxic-ischaemic injury, as normal. In addition, we did not have ethical permission to sedate or anaesthetize normal infants.

Another clinical problem we encountered was the distance from the neonatal unit to the NMR unit: the two departments are located in different buildings within the hospital. This meant that sick neonates had to be transferred long distances for us to perform a study. The time required to move the infants reduced our total study time. Because of these problems our earliest study was at forty hours after birth. Earlier and more frequent studies may be easier in other units.

Technical problems

Our magnet system was a prototype, and at the time of these studies many improvements were being made. "Shielded" gradients have subsequently been installed, with an improvement in spectral quality. Other restrictions, such as the size of the volume of interest, which at the time of these studies was 64-27$cm^3$ for proton spectra, are improving all the time. All the data analysis and quantification of spectra were done "by hand", using computers only to calculate the area of a peak defined manually for the phosphorus spectra. No automatic spectral data analysis programmes were available.

Some of the effects that influence spectral lines and can cause inaccuracy in data analysis, were discussed in the introduction and results sections. The commonest of these are $T_1$ and $T_2$ differences, the spatial localization technique used, and for proton spectroscopy, the technique used for water suppression. The effect of observer

variation on the measurement of proton spectra has been included in the results section (p. 104), and we have shown how different methods of analysis of phosphorus spectra produce widely differing results (p. 113, 114). These problems are common to all spectroscopy studies (Bottomley 1991) and must be improved before data from different centres can be compared properly and multicentre studies undertaken. It is unlikely that the full potential of clinical spectroscopy will be realised until these problems are resolved.

Quantification

In these studies the results presented use metabolite ratios calculated from spectral peak heights and peak areas. Quantification of clinical spectra has provoked much discussion (Bottomley 1991). Several studies indicate the importance of measuring absolute as well as relative concentrations; for example, in necrosis absolute concentrations decline while relative concentrations remain unchanged (Bottomley et al 1986). However, determining absolute concentrations is not straightforward in in vivo spectroscopy, especially when no data on $T_1$ or $T_2$ values or even the types of metabolites that might be visualized are available, as was the case when we started these studies. It is only recently that in vivo proton spectroscopy studies using absolute concentrations from a large number of examinations have appeared in the literature; these illustrate the problems involved (Michaelis et al 1993).

Relative concentrations can be determined from the relative areas of signals, provided that the appropriate calculations are made for several factors; these include signal loss through $T_1$ and $T_2$ effects, frequency dependence of radiofrequency pulses and the combined effects of $B_1$ inhomogeneity and metabolic heterogeneity. As all techniques that are used to acquire proton spectra involve spin-echo formation, all signals are attenuated by $T_2$ as well as $T_1$ and relaxation effects. Knowledge of these effects under normal and pathological conditions is required to measure the absolute quantities. Secondly, even for spectra having very high signal to noise ratios the problem of measuring the intensity of the signal is far from trivial. In vivo spectra at moderate field strengths contain many overlapping signals and spectral patterns that may be heavily

influenced by *J*-modulation or *J* splitting (p20) effects (Luyten et al 1991). The effect of *J* modulation is not a problem with our proton spectra as the three main metabolites of interest are not *J* coupled.

When these factors have been taken into account the measurement of absolute concentrations (e.g. in mmol/kg wet wt) then requires the additional use of a concentration standard. In principle, this can be internal or external to the region of interest. Possibilities include: water from the region of interest; a standard metabolite whose concentration is not thought to change; metabolites from a normal region; or an external reference compound. For example, Toft et al (1992) used the fully relaxed water signal suppressed by a STEAM sequence as an internal standard and corrected the signal intensities for $T_1$ and $T_2$ attenuation to calculate absolute concentrations from the proton brain spectra of four neonates and eight adolescents. In our studies the 1331 water suppression pulse possesses frequency response characteristics which can cause significant spectral distortion; in our spectra this pulse was optimized for NAA, thus increasing the ratio of NAA to other metabolites.

The use of other internal endogenous markers is also problematic. For example, NAA has been used as a concentration standard for experimental ischaemia as its concentration does not appear to change in acute animal experiments (Crockard et al 1987, Hope et al 1987, Petroff et al 1988). However, our results and those of others show that NAA concentration does change in hypoxic-ischaemic regions of brain observed over a longer time span.

When using reference compounds that are outside the region of interest the main problem is of the spatial dependence of signal intensities. Another problem is contamination of spectra from signals whose sources lie outside a declared voxel. If the voxel is defined only by the amplitude of a sensitivity profile, it can easily be swamped by the integrated signal from the bulk of the sample, even if the amplitude of the signal at any point outside the voxel is tiny. Motion, for example, which is likely in unanaesthetized children, is a potentially large source of contamination (Tofts and Wray

1988).

An accurate accounting of the voxel volume contributing to the spectrum being quantified, the transmitter and receiver radio-frequency field homogeneity, signal loss or distortion through partial saturation, $T_2$ relaxation, *J* modulation or *J* splitting (as explained on p20), water suppression and any Overhauser effect must all be included in any measurements of absolute concentration (Bottomley 1991). Small systematic errors in each calculation required to derive an absolute concentration can accumulate to produce a significant error.

We used area and peak height ratios in these studies, as they can be can be applied easily to all spectra and provide an adequate basis for spectral interpretation. Errors will occur if the concentration of the reference, e.g. βATP or Cho, is assumed to remain constant but in fact changes. This possibility is discussed in the relevant sections of this thesis.

The purpose of these studies was to establish the changes that occur in spectra from the brain of children, with increasing age and with injury, and then to observe trends both within individuals with increasing age and between individuals after varying degrees of brain injury. The use of absolute concentrations will undoubtedly increase knowledge in this field, but was not practical within the time limits and the technical constraints that existed at the time of these studies.

## PROTON SPECTROSCOPY

### Main conclusions

Metabolite peaks attributable to N-acetylaspartate (NAA), choline-containing compounds (Cho) and to creatine plus phosphocreatine (Cr) are visible in spectra from paediatric brain. The relative intensities of these metabolite peaks change with age. The ratios of N-acetylaspartate (NAA) to choline-containing compounds (Cho) and to creatine plus phosphocreatine (Cr) also change after significant brain injury. We found that there was a statistically significant difference in the NAA/Cr metabolite ratios of children with a normal outcome compared with those with a severe outcome, at any age studied (P=0.02). Statistical significance increased when a Chi squared test with Yates' correction was applied to examine outcome in children with an NAA/Cr ratio > than 1.5 or < than 1.5. Children with a severe neurological outcome were statistically likely to have an NAA/Cr ratio < 1.5 (P=0.01). When a Chi squared test with Yates' correction was applied to examine outcome in children with an NAA/Cho ratio > 1.0 or < 1.0, children with a moderate neurological outcome were statistically likely to have an NAA/Cho ratio < 1 (P=0.01); there was no statistical difference between the NAA/Cho ratios for the normal/control and severe outcome groups. When a smaller and more highly selected group of infants born at term or post-term, and examined within the first month of life were compared, then both the NAA/Cr and the NAA/Cho ratios were significantly different between the normal and severe outcome groups (there were no moderate outcome children in this sub-group). The changes in the proton spectrum induced by severe brain injury may persist with age, but spectral changes are more difficult to interpret in children than adults, as normal age-related changes must be taken into account.

### Age related changes

We found increasing NAA/Cho and NAA/Cr ratios, and decreasing Cho/Cr ratios with age, in both the normal and abnormal infant brain. The age related changes in proton spectra have been reported by others (van der Knaap et al 1990, Grodd et al 1991 and Huppi et al 1991). Van der Knaap and coworkers examined 41 normal children aged between 1 month and 16 years; NAA/Cr and NAA/Cho increased with age and Cho/Cr

decreased with age. The most marked changes were within the first year of life. Huppi et al (1991) recorded spectra from the cerebellum in 12 premature infants (mean PCA 35 weeks) and eight infants at a mean PCA of 41 weeks (five of the twenty infants were neurologically abnormal). They estimated in vivo concentrations of metabolites by using total Cr concentrations from human cerebellum as an internal endogenous marker. NAA increased from 1.8mM in the preterm infant to 3.1mM in the term infant and to 6.5mM in adults. The Cho concentrations were the same in the two infant groups and were slightly lower than in adults.

N-Acetylaspartate

Our spectra and those of the other workers show that the main change in the proton spectrum with age is the increase in NAA, and this increase is rapid within the first few months of life. This finding is supported by animal work (Tallan et al 1957, Bates et al 1989). The reasons for the change in NAA concentration are unclear as little is known about its function, although there is much evidence to suggest it is predominately located within neurons (Nadler and Cooper 1972; Koller et al 1984; Bruhn et al 1989). Most neurons are formed before birth, but their development is incomplete until after birth when there is an increase in the number and size of dendrites and in the number and complexity of axonal and dendritic connections. The rapid increase in NAA concentration in the developing brain may be related to neuronal function.

The increase in NAA concentration with increasing age could also be related to myelination (D'Adamo and Yatsu 1966), which mainly occurs after birth (Barkovich et al 1988, Valk and van der Knaap 1989). NAA has been found in a higher concentration than in neurons, in O-2A progenitor cells in neonatal rats (Urenjak et al 1992). O-2A progenitors are cells which are functionally different from neurons but have some similarities; they contain similar gangliosides and can express a protein which may be central to neurite outgrowth. As these progenitors differentiate into oligodendrocytes the level of NAA within them decreases dramatically. In developing brain there may be two pools of NAA; one in O-2A progenitor cells which may be used

to facilitate myelination ; the other in neurons. Abnormalities in NAA concentration in neonatal brain may therefore reflect abnormalities in the development of oligodendroglia or their precursors.

NAA may act as a donor of acetyl groups for lipid synthesis especially for myelination (D'Adamo and Yatsu 1966; Burri et al 1991). The acetyl group of NAA is incorporated into brain lipids more effectively than acetate alone with a maximal rate of incorporation just before, or at the beginning of myelination (D'Adamo and Yatsu 1966). Shigematsu et al (1983) showed that NAA is a component of a heat stable factor essential for the conversion of lignoceric acid to ceramide which is incorporated into cerebroside, the major lipid component of myelin. The incorporation of carbons from pyruvate into lipids may involve NAA in a transport mechanism (Patel and Clark 1979,1980).

Other studies in the developing rat brain show that NAA is synthesized in the mitochondria from aspartate and acetyl-coA; after transport across the mitochondrial membrane it is cleaved by aspartoacylase into aspartate and acetate in the cytosol and the resulting acetyl groups are incorporated into brain lipid (D'Adamo and Yatsu 1966). Therefore, NAA may have a role as a transporter of acetyl groups across the mitochondrial membrane for lipogenesis during development. Any relationship between NAA and myelination is likely to be complex, as NAA concentrations in hypomyelinated mouse mutants ultimately reach the same concentration as in normally myelinated mice, although they take longer to do so (Small et al 1990).

Nakada et al (1989) did not detect any NAA in the brains of rat fetuses, but found high concentrations of taurine. Huppi et al (1991) showed that taurine increased from 1.1mM in preterm infants to 2.3mM in term infants; there was no further increase in concentration in the adult brain. Taurine and NAA levels show inversely related concentrations, taurine decreasing and NAA increasing, from zero to 35 days of age in rat brain (Nakada 1991). After a series of experiments Nakada proposed that NAA replaces taurine in the maturing brain as the main amino acid anion, when the buffering

system in the cytosol changes from fetal to adult type. He suggested that NAA speeds the passive diffusion of ATP in the cytosol. ATP consumption by the $Na^+$-$K^+$ pump is faster in mature brain (Nakada 1991).

The actual concentration of NAA is thought to be 30-40% less than that suggested by the size of the NAA peak in the proton spectrum (Hanstock et al 1989). N-acetyl-aspartyl-glutamic acid (NAAG) and other compounds contribute to the NAA peak (Frahm et al 1989) and the concentration of these other compounds may also change with age. In one-day-old rats, 25% of the NAA peak is NAAG; in the adult rat brain, the NAAG contribution has decreased to 10%.

Choline-containing compounds

Our spectra and those of others (van der Knaap et al 1990, Grodd et al 1991) suggest a decrease in choline-containing compounds with increasing age, although the decrease in absolute concentration may not be very great (Huppi and colleagues 1991). There is a slight decrease in choline-containing compounds with increasing age in developing rat brain (Bates et al 1989).

The choline peak contains major contributions from a number of choline containing compounds including phosphorylcholine and glycerophosphorylcholine, as well as free choline (Bates et al 1989, Gill et al 1989). In vitro studies of rabbit brain (Tunggal et al 1990) found the following concentrations of compounds; choline plasmogen, 0.6mmol/kg, glycerophosphorylcholine 0.4mmol/kg, phosphorylcholine 0.4mmol/kg, cytidinediphosphate-choline 0.05mmol/kg, acetylcholine 0.03mmol/kg and choline 0.002mmol/kg. Accordingly, the total Cho pool is approximately 1.5mmol/kg, an amount in good agreement with the in vivo concentrations in grey and white matter derived from adult human spectroscopic studies (Soher et al 1996, Kreis et al 1993). A biochemical study of normal elderly human brains (obtained postmortem) also found similar levels of "total" Cho (Nitsch et al 1992).

A decrease in the Cho signal with age may be analogous to the reduction in

phosphorylethanolamine, a constituent of the phosphomonoester peak that is seen with phosphorus MRS in the developing brain (Brenton et al 1985). Phosphorylethanolamine is an anabolic precursor to phosphatidylethanolamine and a catabolic product of sphingomyelin. Similarly phosphorylcholine is an anabolic precursor to phosphatidylcholine and sphingomyelin, as well as a catabolic product of sphingomyelin (Pettegrew et al 1987). These compounds are therefore involved in brain phospholipid metabolism and a relative elevation in developing brain may be consistent with increased membrane phospholipid synthesis.

Creatine and phosphocreatine (Cr)

The Cr peak is thought to be the most stable metabolite peak in the proton spectrum, and is often used as an internal reference. Huppi et al (1991) used Cr concentrations from autopsy specimens of human brains to "calibrate" the Cr peaks in their proton spectra; they then used the Cr peak as an internal reference. The Cr concentration in the brain tissue was 3.78mM in preterm brain, 4.69 mM in term brain and 6.22mM in adult brain. Bates and colleagues (1989) recorded an increase in Cr concentration from approximately 2μmol/g wet weight at one day to 5μmol/g wet weight at 21 days in neonatal rat brain.

The creatine peak is composed of creatine and phosphocreatine. It is known from phosphorus spectroscopy that phosphocreatine increases with age; the changes are clearly demonstrated in the spectra shown in Fig 14 p. 24 and Fig 52 p. 111. Buchli et al 1991 derived absolute metabolite concentrations from phosphorus spectra, and found the phosphocreatine concentration to change from 2.4 mmol/l in newborns to 3.2 mmol/l in adults.

All the studies discussed above, therefore support our findings that the most obvious change in metabolite ratio in the growing brain is in NAA/Cho, as NAA increases with age and Cho decreases slightly. The NAA/Cr ratio also increases, but less markedly, and the Cho/Cr ratio decreases.

$T_1$ and $T_2$ changes with age

The changes in signal intensities are unlikely to arise from $T_1$ differences as there was little difference in saturation factors between adults, and normal and abnormal children. The changes could possibly arise from $T_2$ differences. Our examination time was limited, and our early attempts to acquire spectra at TE's shorter than 270 ms did not produce analysable spectra. Until our technical capabilities improved, using TE's less than 270ms was a waste of valuable examination time. At a TE of 270 ms some signal loss inevitably occurs.

Grodd et al (1991) evaluated the peak intensities of NAA, Cho and Cr in occipital white matter in a control group of children aged between one month and nine years, at TE's of 135 ms and 270ms. The trends with age in all peak intensities were the same at both echo times: a marked rise in NAA, little change in Cr and a decrease in Cho; small changes in Cr were less apparent at 270ms. Toft et al (1992) found that the $T_2$ of choline-containing compounds decreased slightly with age. At the long echo times used in our studies this would cause a further apparent increase in NAA/Cho ratios with increasing age. Toft et al (1992) found no other significant differences in the $T_2$ values of NAA, Cho and Cr between neonates (n=4) and adolescents (n=8). Extensive data on $T_1$ and $T_2$ changes occurring with age in the normal human brain are not yet available.

Lactate/lipid

No obvious lactate peaks were seen in any of the spectra that we obtained from either normal or abnormal infants; the peaks occasionally seen in the region 1.0 - 1.5 ppm were attributed to fat. Even when we did see peaks in this region with the typical doublet appearance of lactate we could not attribute them to lactate as we did not invert the peak with a 135 ms pulse.

Regional variation

There is some regional variation within the brain in the concentration of metabolites and

their relaxation times, as detected with proton spectroscopy. Frahm et al (1989b) reported that the concentration of NAA was greater in grey matter than white matter. This is in agreement with in vitro studies (Tallan et al 1957, Koller et al 1984). Tallan suggests that "roughly twice as much NAA per gram is present in grey matter as in white matter". That paper however refers to work performed on cat brain using a simple ion-exchange chromatography technique, which is now recognised to not be as accurate as HPLC or proton spectroscopy (Birken and Oldendorf 1989). Tallan in a later experiment found that the concentration of NAA increased six-fold from the time of birth to the age of twenty days in rats when levels peaked and then fell to a slightly lower adult concentration work which supports our findings of age related changes. (Tallan 1957b.) The regional distribution of total creatine did not vary. The concentration of choline-containing compounds was slightly higher in grey matter than white matter.

A recent paper which quantitated multislice proton MR spectroscopic images using a phantom replacement technique (Soher et al 1996) found the whole brain NAA concentration to be in good agreement with previously determined metabolite levels using other methods of quantification. However, this group found cortical grey matter to have a lower NAA concentration than white matter. They postulated that this could be due to a longer $T_2$ of NAA in white matter (as yet unproven) or to an increased contribution from NAAG which is present in higher concentration in white matter than in grey matter (Michaelis et al 1993).

Frahm et al (1989b) found no significant regional variation in $T_1$ values of the major metabolites, but did report an increase in the $T_2$ relaxation time of NAA in white matter, particularly in the occipital region, compared with other areas of the brain. This suggests a higher mobility of NAA in white matter, which may be related to its neuronal function. No significant regional variations in the $T_2$ of Cho or Cr were found.

A recent report by Knufman et al (1992) suggests that at the echo time (270ms) and

repetition time (2000ms) we used, the NAA peak is higher in white matter than in grey matter because of signal loss at these times. This suggestion requires further investigation, as we did not have time or small enough voxel sizes to examine normal regional variations.

As regional variation of metabolite concentration is a difficult issue which has yet to be completely resolved by groups performing the most complex spectral analysis, no attempt has been made to discuss regional variation in this thesis. Regional variability was minimised by studying children with diffuse brain injury from hypoxic-ischaemic encephalopathy, and when possible, by studying the same region in each child. As discussed previously, in our early spectra the smallest volume achievable was 64$cm^3$. In infants of less than 38w PCA we could therefore make no attempt to localise to any particular area and the volume filled much of the brain. Voxel size was reduced to 27$cm^3$ as the studies progressed; but these voxels were still large, partial volume effects were substantial and we were not able to make any statements about the amount of grey matter versus white matter in the regions studied.

conqueror

Changes in the proton spectrum due to hypoxic-ischaemic injury

We have demonstrated changes in the proton spectrum associated with hypoxic-ischaemic encephalopathy. NAA/Cr metabolite ratios from all children who subsequently had a moderate or severe neurological outcome, at eighteen months or more, were significantly lower than the metabolite ratios from the normal/control group; this was independent of the age at which the child was studied. NAA/Cho ratios decreased in some children, but this was only significant for the moderate outcome group in whom an NAA/Cho ratio of< 1.0 showed a significant difference from the control group. The Cho/Cr ratios showed no significant differences for any of the outcome groups. In the group of term infants all studied within four weeks of birth, there was a statistical difference in both the NAA/Cho and NAA/Cr values between the control and normal outcome group, and those infants with a severe outcome. Again, the Cho/Cr ratios showed no statistical difference. Some of the infants who had severe neurological abnormality, who were followed up and re-studied with proton spectroscopy, had NAA/Cho and NAA/Cr ratios that remained abnormal when compared with expected values for their age; however, this was not statistically significant.

Although our results do not show age to be a significant factor when abnormal metabolite ratios are examined this is perhaps surprising, as premature brain has relatively little NAA (Nakada et al 1989), and therefore there may be very little difference in NAA/Cho and NAA/Cr ratios between normal and abnormal brains in very small infants. As NAA is located in neurons, the reduced NAA/Cho and NAA/Cr ratios in abnormal infants could be due to loss of neurons, or delayed or abnormal neuronal development or function, all of which are likely to become more apparent with increasing age.

Inconsistencies in our data

The changing trends in metabolite ratios we have reported are clear from the majority of the data. However, in these early studies there are some inconsistencies, some of

which are difficult to explain. Table 3B (p92B) provides data from all the children who had more than one proton examination. Child MC shows an increase in NAA/Cho over a 44w period, but the NAA/Cr ratio (which was high for his age on the first examination) remains unchanged. This is difficult to explain. Child CT had 3 proton exams, the third shows a decrease in the NAA/Cr ratio at 45w compared to 39 and 40w PCA. This could be explained by a rise in creatine and phosphocreatine, perhaps due to recovery from acute hypoxia. The data from the four examinations from child JM are consistent with the hypothesis that NAA/Cho and NAA/Cr decrease after hypoxic-ischaemic injury, apart from the 3rd examination. This spectrum was of very poor quality and was included to demonstrate the fact that poor quality spectra make data interpretation very difficult. Child IV showed a small increase in NAA/Cho over a 23 week period but a decrease in NAA/Cr, again this is difficult to explain. The data from the other ten examinations are consistent with increasing NAA/Cho and NAA/Cr ratios with age and decreasing Cho/Cr.

Time course of metabolite changes

There is uncertainty in the literature about the timing of the changes that take place with hypoxic-ischaemic injury. In earlier live animal experiments lasting several hours (Crockard et al 1987, Hope et al 1987) and in post mortem studies (Petroff et al 1988, Tews et al 1963), the concentration of NAA was so constant during hypoxia and ischaemia that it was used as an internal reference for analysis of proton spectra (Crockard et al 1987, Hope et al 1987, Petroff et al 1988). More recent experiments show different results. Van Rijen and colleagues (1991) showed a significant decrease in the NAA/Cr ratio from rat brain at 5 and 15 minutes of ischaemia, which failed to recover during reperfusion. They attributed this to a decrease in the concentration of NAA, as they assumed no large changes in the total Cr pool. Espanol and colleagues (1992) showed an acute decrease in NAA concentration in rat brain after occlusion of two vessels. These changes resolved after reperfusion in normoglycaemic rats but not in hyperglycaemic rats. Rosenberg and coworkers (1991) suggested that since NAA was shown to be stable in earlier biochemical studies of hypoxia (Crockard et al 1987, Hope et al 1987, Petroff et al 1988, Tews et al 1963), it is the other compounds making

up this peak that are decreasing. Another component of the NAA peak, N-acetylaspartyl glutamate, can be cleaved enzymatically to NAA and glutamate. Glutamate persists in ischaemic regions where NAA has decreased (Higuchi et al 1991).

Proton spectroscopy studies of human brain to date have shown the effects of hypoxia and ischaemia on the brain, in localized regions in adults who have had cerebrovascular accidents (Berkelbach van der Sprenkel et al 1988, Bruhn et al 1989, Duijn et al 1992, Fenstermacher et al 1990, Sappey-Marinier et al 1992a). There was a persistent decrease in the NAA peak of these proton spectra but they were not acquired until several days after the stroke. In our study the most abnormal spectra, with little or no NAA peak, were acquired one to four weeks after birth. To establish the time course of the decrease in NAA, sequential studies starting within hours of birth are required.

The changes in the NAA /Cho and NAA/Cr ratios after hypoxic-ischaemic encephalopathy may be caused by increases in Cho and Cr as well as a decrease in NAA. Some workers assume that the total brain creatine pool remains stable during hypoxia (Lewis et al 1974; Petroff et al 1988); others show a decrease in Cr in states such as focal ischaemia (Higuchi et al 1991). An increase in the choline peak is consistent with the findings of Scremin and Jenden (1989), who have shown an increase in free brain choline after ischaemia. This may explain the slight increase in the Cho/Cr ratio in those infants with a poor outcome. Other authors report no change (Fenstermacher et al 1989), or a fall in Cho (Higuchi et al 1991) in infarcted regions. The wide distribution of Cho/Cr values acquired between 96 hours and four weeks after birth in our severe outcome group, may indicate that the Cho concentration alters with time after injury, perhaps rising acutely in the first few hours and then falling to normal or low levels. Again, sequential studies are needed.

It seems likely that there can be some recovery in NAA/Cho and NAA/Cr ratios after injury. We reported this in a child who had Herpes simplex encephalitis (Menon et al 1990 c). The recovery in metabolite ratios coincided with the resolution of oedema in

the magnetic resonance images. Arnold (1992) also reported some improvment in NAA/Cr after acute central nervous system damage, although there was no return to normal values. He suggested that this represented reversible neuronal damage or limited neuronal regeneration. An improvement in NAA/Cr or NAA/Cho after injury is more readily interpretable in adult spectra than in infant spectra, as changes after injury are difficult to separate from changes due to ageing in the latter group.

Correlation between in vivo proton spectra from brain and in vitro spectra from brain biopsies

Spectroscopy of the tumour biopsies was performed over many hours using a very high magnetic field, yielding spectra that are much better resolved than those obtained in vivo. In addition, the in vitro spectra were obtained from small samples of tumour tissue taken under direct vision at the time of surgery, while the in vivo spectra were acquired from large volumes of interest placed to encompass the tumour, but which inevitably contained adjacent normal brain.

Our in vitro data from normal white matter biopsies agree well with typical metabolite levels and concentration ratios measured in mammalian brain using MR and more conventional biochemical techniques. Proton spectra from adult human brain have an NAA/Cr ratio of between 3.5 (our spectra) or lower depending on the region of brain studied(Frahm et al 1989b) and on the sequences used to acquire the spectra. These ratios are all greater than those measured in our biopsies of normal human brain, which may be due to contributions to the "NAA" signal from other acetyl-containing compounds such as N-acetyl neuraminic acid and N-acetyl galactosamine (Hanstock et al 1988, Vanier et al 1971). (These compounds are not extractable by perchloric acid.)

In the spectra from tumours, both in vitro and in vivo, total creatine was decreased. Our tumour data was in agreement with that from other groups; NAA is very low or absent in astrocytomas. We saw some NAA signal from astrocytomas in vivo, which is likely to be due to the contamination of the spectra by adjacent normal tissue, which is impossible to exclude from the large volume of study ($64cm^3$) used in these

experiments. As volumes of study become smaller with technical improvements then the in vivo spectra will more accurately reflect the in vitro spectra.
Our in vivo spectra detected the presence of an unexpected peak, the alanine in the meningioma. Very little NAA was present in both the in vitro and in vivo spectra, reflecting the fact that meningeal tissue does not contain neurons.

The amount of lactate in vitro is not an accurate reflection of the value in vivo, because of the unavoidable accumulation of lactate in the period between surgical removal of the biopsy and freezing of the tissue. Tumours that were later found to contain large necrotic areas had high lactate or lipid concentrations both in vivo and in vitro. Necrotic tissue may contain low concentrations of phosphorus-containing metabolites, and proton spectroscopy may be more useful to study this type of tissue.

Ideally, we would have evaluated our neonatal proton spectra using biopsies from neonatal brain. Obviously this was not possible, and brain tissue from normal adult brain was the only alternative. The correlation between the in vivo and in vitro spectra was encouraging; we detected the presence of the unexpected alanine peak in the meningioma, and most of the discrepancies between the in vivo and in vitro spectra could be explained by the fact that abnormal regions of study inevitably contained normal brain tissue. Most neonates studied with proton spectroscopy had global brain injury and so the problems of contamination of the volume under study do not apply. This problem is relevant however, to the localized phosphorus spectra and is discussed again in that section.

## PHOSPHORUS SPECTROSCOPY

### Age related changes

Changes in the phosphorus spectrum with age have been described by other authors (Azzopardi et al 1989a, Boesch et al 1989, Tofts and Wray 1985, van der Knaap et al 1990) and our results agree with their findings; there is an increase in PDE/ATP and PCr /ATP and a decrease in PME/ATP. The main components of the PME peak are phosphorylethanolamine, phosphorylcholine and glycerol-3-phosphate; minor components are phosphorylserine and phosphoinositol. All the PME components are involved in phospholipid anabolism which may explain the high concentration in neonatal brain. Phosphorylcholine is a precursor of phosphatidylcholine and sphingomyelin (van der Knaap et al 1990). Phosphorylethanolamine is a precursor of phosphatidylethanolamine; glycerol-3-phosphate is a precursor of phosphatidylethanolamine, phosphatidylcholine and plasmalogens (van der Knaap et al 1990). Some of these compounds are involved in the catabolism of others: phosphorylcholine and phosphorylethanolamine with sphingomyelin and glycerol-3-phosphate with phosphatidylethanolamine, phosphatidylcholine and plasmalogens (van der Knaap et al 1990). The precise composition of the phosphomonoester peak and the reasons for the dramatic change with age are still under investigation .

The phosphodiesters are phospholipid breakdown products. Major PDE components are glycerophosphorylyethanolamine and glycerophosphorylcholine; minor components are glycerophosphorylserine and glycerophosphoinositol. These compounds are present in the catabolic pathways of phospatidylcholine, phosphatidylethanolamine, phosphatidylserine, phosphatidylinositol and plasmalogens (van der Knaap et al 1990). Pi/ATP does not change with age.

### pH

Kato et al (1992) suggested that intracellular brain pH is elevated in the normal neonate with a mean value of 7.20 which declines to 7.03 in children over four years of age. The Pi peak was bifid in the neonates, and they proposed that this was due to

contamination from extracellular Pi. They took their pH measurement from the larger Pi peak. It is not clear from their abstract whether or not the neonates studied had suffered any form of birth injury, although they were classed as normal on the basis of later outcome. Our spectra and those from other workers in phosphorus spectroscopy find normal neonatal intracellular pH to be between 7.04 and 7.24 (Hope et al 1984, Azzopardi et al 1989a).

$T_1$ changes of phosphorus metabolites with age

A recent report from Hida et al (1992) showed that while the ratios of PME/ATP and PCr/ATP clearly decreased with age in the developing rat brain, the $T_1$ values of PME, PCr and ATP did not show any relation to age. In contrast, Buchli et al (1992) after studies of the human brain suggested that the $T_1$ of PME does decrease with age. The $T_1$ of the other metabolites showed no significant change We do not have enough data to show clear trends.

Changes in the phosphorus spectrum after hypoxic-ischaemic injury

Phosphorus spectra from birth injured infants are abnormal in the first few weeks of life (Hamilton et al 1989) and these changes correlate with subsequent neurodevelopmental outcome (Roth et al 1992). Few studies have been done in these children when they are older. We have shown that despite marked clinical neurological abnormalities and imaging abnormalities detected with MRI in older children, the phosphorus spectrum appears normal in metabolite ratios and $T_1$ measurements.

Bottomley and coworkers (1986) reported that the ratios of the high energy phosphorus metabolites and Pi, as well as pH were within normal limits in spectra from adults with chronic cerebral infarction, but there was a decrease of up to 40% in the total phosphorus signal from infarcted tissue, consistent with a reduction in the total number of metabolically active cells or a decrease in cellular function after infarction. Bottomley concluded that phosphorus metabolite ratios are not a sensitive indicator of abnormal energy reserve in chronic brain infarction in adults.

Our results also suggest that phosphorus metabolite ratios are not useful in chronic brain injury in infants or children, appearing normal when magnetic resonance imaging identifies an anatomical lesion. The extremely abnormal MR image shown on p120 was used to illustrate the fact that such grossly abnormal brain can produce a normal phosphorus spectrum. CSF has no detectable phosphorus signal, and therefore only the brain tissue present in the area of study contributes to the spectrum. The only effect that occurs is that the signal to noise ratio of the spectrum is decreased. The decrease in measured tissue would be significant if we were deriving absolute values, but we are not.

Sappey-Marinier and colleagues (1992b) found that phosphorus metabolite concentrations were reduced in regions of chronic infarction in adult brain although, in contrast to our studies and those of Bottomley et al (1986), they found the reduction in some metabolites to be greater than others, resulting in changes in metabolite ratios. PDE/PME and PCr/ATP were increased while PME/PCr and PDE/PCr were decreased.

The pH of the infarcted region was alkaline. They suggested that the decrease in PME and PDE may reflect particularly a loss of white matter rich in phospholipid, and the increase in PME/PDE may be due to an increase in phospholipid mobility that occurs in ischaemic tissue (Yoshida et al 1980).

Kato et al (1991) used $^{31}P$ MRS to study the brains of adults and children who met the clinical criteria for brain death, for up to 40 weeks after the diagnosis of brain death.

The phosphorus spectra did not improve in any of the patients, and the main finding was a single, high inorganic phosphate peak with no other phosphorus metabolites present. Martin et al (1991) also described a brain dead patient who only had an inorganic phosphate peak on his spectrum; this patient did not survive. Our studies support the finding that brain injury must be extremely severe to result in phosphorus spectra that do not improve with time; our patients all survived and even those with severe brain injury and very poor initial phosphorus spectra had phosphorus spectroscopy that were normal or returning to normal on follow up.

<u>$T_1$ changes of phosphorus metabolites after hypoxic-ischaemic injury</u>

Previous studies have suggested that the only significant effect of applying saturation factors is an increment in the PME peak relative to other peaks (Hope et al 1984). We found that the saturation factor for Pi was prolonged in the first few weeks of life in many of the children with a subsequent poor neurological outcome. To our knowledge there have been no other reports of an alteration in the saturation factor of Pi after injury, which has important implications for the analysis of phosphorus spectra from hypoxic tissue. The change in the saturation factor of inorganic phosphate could be due to a change in its position, from intracellular to extracellular, as the affected cells break down and die. The change in the saturation factor for Pi was not apparent after 44 weeks' post-conceptional age; this might be because the severely injured cells die and those that survive have normal phosphorus metabolism. Englander et al (1992) suggested from preliminary results, that the $T_1$ of Pi may change with the pH. This is another possible explanation of our findings, as the pH was alkaline and most abnormal

in the brains of the infants with the prolonged saturation factors and the poorest neurogical outcome. We may be observing extracellular inorganic phosphate, at a pH of 7.4, which may also have a prolonged $T_1$ due to greater mobility.

2D and 4D CSI

The use of 2D and 4D CSI to study focal lesions produced good quality data within reasonable examination times. Changes in phosphorus spectra due to a known focal lesion occurred on only two occasions out of a total of thirteen examinations, in children with focal lesions detected by MRI or CT. If it is accepted that focal changes will be detected only in the first month after injury (except with a severe, fatal lesion, which is not applicable here) then changes were detected in two focal lesions out of eight. Both the infants in whom the focal lesions were detected with phosphorus spectroscopy were studied with 2D CSI with a nominal plane width of 2cm. In the other cases, the plane or volume was probably not small enough to detect focal changes within the infant brain. Because of the low sensitivity of the phosphorus nucleus it is not possible to reduce the 4D CSI voxel size below $27cm^3$. This volume is a large amount of the infant brain; we feel that 4D CSI is of limited use in paediatric phosphorus spectroscopy. A problem with CSI is "bleed" of signal from adjacent voxels, which may dilute abnormal signal from an abnormal region of brain (Bottomley et al 1989b). However, the results from 2D CSI, although lacking in sensitivity, did allow us to compare changes in opposite hemispheres of the brain in two of the infants, without needing to reposition a surface coil half way through the examination. This may provide a method of studying the effect of therapies on the injured and normal brain simultaneously.

Moorcraft and colleagues (1991) used phase-modulated rotating frame imaging to study the brains of neonates after birth asphyxia. With this localization technique they showed that metabolic derangement was less in superficial than in deeper brain tissue. They suggested that the sensitivity of phosphorus spectroscopy for identifying neonates with a poor short term outcome was increased by using the Pi/ATP ratio from subcortical regions, as it is this area of the brain in a full term neonate that is most

vulnerable to asphyxia. We did not observe changes due to increasing depth in the infant brain. However, superficial planes containing scalp muscle and bone were excluded from analysis. In addition, we did not use our localization technique to obtain metabolite ratios from all the children studied, but to observe the changes produced in different regions of the brain by focal abnormalities.

Very few, if any, other groups have compared proton and phosphorus spectra in the abnormal human paediatric brain.

pH and Lactate:

We hoped to study the relationship between pH and lactate in the living brain using both proton and phosphorus spectroscopy . However, no obvious lactate peaks were seen in any of the spectra that we obtained from either normal or abnormal infants (the peaks occasionally seen in the region 1.0 - 1.5 ppm were attributed to fat). With subsequent technical developments by our group, after the work done in this thesis was completed, lactate has been seen in the brain of some birth asphyxiated infants. Therefore, it is possible there was an increase in lactate in some of the abnormal infants. However, it is likely that the amounts of lactate present, would be less than that seen in animal models of hypoxia and ischaemia. The earliest study of a birth asphyxiated baby was at 40 hours PNA, which in comparison with animal studies is a long time from the insult. In addition, the immature brain can utilize lactate rapidly, and lactate can pass easily across the immature blood-brain barrier (Johanson 1989). A study of hypoxic-ischaemic brain damage in the immature rat showed that lactate levels declined rapidly in the first hour of recovery to only just above control values (Palmer et al 1990). The immature brain also has less capacity to produce lactate than mature brain: in a study of neural activity and high energy phosphate in adult and immature rat brain, Kawai et al (1989), showed that lactate production in response to injury was much less in a 4-day old rat than in an adult rat.

Alkaline pH

Our spectra do show that while lactate may or may not be present, the pH values derived from many of the abnormal phosphorus brain spectra are alkaline. An alkaline pH has been reported by other groups (Laptook et al 1989), and it has been suggested that the greater the degree of alkalinity after hypoxic-ischaemic injury the worse the prognosis. Our results support that hypothesis. Martin et al (1991) in a study of

human brain after cardiac resuscitation suggested that the pH shift to alkalosis may represent irreversible injury, given the complex mechanisms that exist to maintain cerebral acid-base homeostasis.

Other methods of investigation, such as positron emission tomography (PET) (Syrota et al 1983), have shown that pH is abnormally high in infarcted regions. Post-ischaemic alkalosis is a well established phenomenon (Mabe et al 1983), the reasons for which are as yet unknown. Glia which replace neurons in injured brain may have a higher pH; this is a possibility noted in other studies (Hubesch et al 1990), and our findings that NAA/Cho and NAA/Cr ratios were decreased in infants with alkaline pH support the hypothesis that neurons may have been replaced by glia. Alternatively, metabolism in the damaged region may remain abnormal, altering the factors that control pH. There may be decreased carbon dioxide and other acid metabolites produced, which may be removed by local perfusion in excess of metabolic needs (Syrota et al 1983). Another explanation is that that $Na^+/H^+$ antiporter and other cell buffering mechanisms are increased, resulting in intracellular alkalosis. A final possibility is that the dominant inorganic phosphate species present in the region of study has become extracellular phosphorus when the pH is 7.4.

Phosphorus spectroscopy and analysis of proton spectra

When the proton studies presented here were performed we did not know what they would show as there was no information available on proton spectroscopy of the infant brain; it had not been done before. Phosphorus spectroscopy, however was well established and the changes caused by hypoxia and ischaemia are well recognised (Azzopardi 1989 b). Therefore the information available from phosphorus spectroscopy performed at the same examination aided our interpretation and analysis of the proton spectral changes, as shown for example on p.129.

Time course of changes in proton and phosphorus spectra

The phosphorus spectra are most abnormal in the first week after injury. The proton spectra are also abnormal, but in very young infants the differences between normal

and abnormal proton spectra are much less clear. Over the next few weeks the changes in the phosphorus spectra resolve and at one month only those infants whose prognosis is extremely poor have phosphorus spectra which are still abnormal. This is consistent with other clinical neonatal studies (Hope et al 1984; Azzopardi et al 1989b). In most cases the changes in the phosphorus spectra, no matter how severe, resolve.

Although there may be some resolution of the changes seen in the proton spectra (Menon et al 1990 c; Arnold 1992) where brain injury has been severe enough to cause neuronal loss or abnormal development of the brain, it seems that the proton spectra are unlikely to return completely to normal. The decrease in NAA/Cho and NAA/Cr ratios reflect a relative loss of NAA, which could be associated with failure of neurons to develop normally or with areas of neuronal loss and gliosis resulting from hypoxic-ischaemic damage. A change in the relative populations of the different cell types would have little effect on the $^{31}P$ spectra, if, as studies of cell cultures have suggested, neurons and glia have similar phosphorus metabolite ratios (Gill et al 1989).

The acute and subacute effects that are observed by phosphorus MRS are characteristic of energy failure. Presumably the subsequent return to normal of the phosphorus metabolite ratios is because severely damaged cells are lost completely and the remaining viable cells have normal metabolite ratios.

Proton spectroscopy can therefore show abnormal biochemistry, even when infants are referred for neurological assessment, weeks or months after birth. Another potential advantage of proton spectroscopy over phosphorus spectroscopy, is that it may be possible to perform proton spectroscopy with additional software only, on the rapidly increasing number of commercial imaging systems operating at 1.0 Tesla or more. Phosphorus spectroscopy requires additional hardware and is likely to remain confined to a small number of research centres.

Future potential studies

We need more data from both proton and phosphorus spectra from normal children. It

would be informative to observe sequential proton spectra from the first few hours after birth, at frequent intervals. Many questions need to be answered. Do choline-containing compounds increase acutely after injury? When does NAA start to fall? Is lactate visible in the first few hours after injury and what are the corresponding pH changes detected with phosphorus spectroscopy? Can we change proton spectra from the damaged brain of a neonate by therapeutic interventions ? There is potential to observe the efficacy of established modes of treatment and of new therapeutic agents. Some of this work will be in animals, but other problems such as the effect of sedative agents on the injured brain may need to be studied in humans.

# CONCLUSIONS

Hypoxic-ischaemic injury produces observable changes in proton spectra of the neonatal brain. Some of these changes correlate with clinical neurological outcome at eighteen months or more. Phosphorus spectroscopy measures changes in the phosphorus spectrum of the birth injured neonate, but in the majority of cases these changes resolve within a few weeks.

Proton spectroscopy, like phosphorus spectroscopy, may not only become useful in prognosis, but may lead to a better understanding of those changes that cause permanent neurological damage, or those that aid recovery, following hypoxic-ischaemic events in infants. A question central to the use of proton spectroscopy in human brain is; what does NAA do ? Further work to clarify the role of metabolites and the changes in their concentration, as observed with proton spectroscopy, may lead to a better understanding of the biochemical changes caused by hypoxia, and provide in future a more widely available magnetic resonance spectroscopy technique for the non-invasive assessment of therapy.

# REFERENCES

Ackerman JJH, Grove TH, Wong GG, Gadian DG, Radda GK. Mapping of metabolites in whole animals by $^{31}P$ NMR using surface coils. *Nature* 1980;**283**:167-170.

Amiel-Tison C, Ellison P. Birth asphyxia in the fullterm newborn; early assesment and outcome. *Developmental Medicine and Child Neurology* 1986;**28**:671-682.

Arnold DL. Reversible reduction of N-acetylaspartate after acute central nervous system damage. *Society of Magnetic Resonance in Medicine , Berlin Meeting* 1992: Book of Abstracts; p 643.

Aue WP. Localization methods for in vivo NMR spectroscopy. *Reviews of Magnetic Resonance in Medicine*. 1986;**1**:21-72.

Austin SJ, Connelly A, Gadian DG, Benton JS, Brett EM. Localized $^{1}H$ NMR spectroscopy in Canavan's disease:a report of two cases. *Magnetic Resonance in Medicine* 1991;**19**:439-445.

Azzopardi D, Wyatt JS, Cady EB, Delpy DT, Baudin J, Stewart AL, Hope PL, Reynolds EOR. Prognosis of newborn infants with hypoxic-ischemic brain injury assessed by phopsphorus magnetic resonance spectroscopy. *Pediatric Research* 1989;**25**:445-451. (b)

Azzopardi D, Wyatt JS, Hamilton PA, Cady EB, Delpy DT, Hope PL, Reynolds EOR. Phosphorus metabolites and intracellular pH in the brains of normal and small for gestational age infants investigated by magnetic resonance spectroscopy. *Pediatric Research* 1989;**25**:440-444. (a)

Babcock DS, Ball W. Post asphyxial encephalopahy in full-term infants: ultrasound diagnosis. *Radiology* 1983:**148**:417-423.

Bada HS, Hajjar W, Chua C, Sumner DS. Non-invasive diagnosis of neonatal asphyxia and intraventricular haemorrhage by Doppler ultrasound. *Journal of Pediatrics* 1979;**95**:775-779.

Bailes DR, Bryant DJ, Case HA, Collins AG, Cox IJ, Hall AS, Harman RR, Khenia S, McArthur P, Ross BD, Young IR. In vivo implementation of three-dimensional phase encoded spectroscopy with a correction for field inhomogeneity. *Journal of Magnetic Resonance* 1987;**77**:460-470.

Banker BQ, Larroche JC. Periventricular leukomalacia of infancy: a form of neonatal hypoxic encephalopathy. *Arch Neurol* 1962;**7**:386-410.

Barkovich AJ, Kjos BO, Jackson DE, Norman D. Normal maturation of the neonatal and infant brain: MR imaging at 1.5T. *Radiology* 1988;**166**:173-180.

Barkovich AJ, Truwit CL. Brain damage from perinatal asphyxia: correlation of MR findings with gestational age. *American Journal of Neuroradiology* 1989;**11**:1087-1096.

Barkovich AJ, Westmark K, Partridge C, Sola A, Ferriero DM. Perinatal asphyxia: MR findings in the first 10 days. *American Journal of Neuroradiology* 1995;**16**(3):427-438.

Barkovich AJ. MR and CT evaluation of profound neonatal and infantile asphyxia. *American Journal of Neuroradiology* 1992;**13**:959-972.

Bates TE, Williams SR, Gadian DG, Bell JD, Small RK, Iles RA. $^{1}H$ NMR study of cerebral development in the rat. *NMR in Biomedicine* 1989;**2**:225-229

Behar KL, den Hollander JA, Stromski ME, Ogino T, Shulman RG, Petroff OAC, Prichard JW. High resolution $^{1}H$ nuclear magnetic resonance study of cerebral hypoxia in vivo. *Proceedings of the National Academy of Science USA* 1983:**80**;4945-4948.

Berkelbach van der Sprenkel JW, Luyten PR, van Rijen PC, Tulleken CAF, den Hollander JA. Cerebral lactate detected by regional proton magnetic resonance spectroscopy in a patient with cerebral infarction. *Stroke* 1988;**19**:1556-1560.

Bhakoo KK, Crockard HA, Lascelles PT. Regional studies of changes in brain fatty acids following experimental ischaemia and reperfusion in the gerbil. *Journal of Neurochemistry* 1984;**43**:1025-1031.

Birken DL, Oldendorf WH. N-Acetyl-L-Aspartic acid: a literature review of a compound prominent in $^{1}H$ NMR spectroscopic studies of brain. *Neuroscience and Biobehavioural Reviews* 1989;**13**:23-31.

Blair AW. Sensory examinations using electrically induced somatosensory potentials. *Developmental Medicine and Child Neurology* 1971;**13**:447-455.

Blennow M, Hagberg H, Ingvar M, Zeman J, Wang Y, Lagercrantz H. Neurochemical and biophysical assessment of neonatal hypoxic-ischemic encephalopathy. *Seminars in Perinatology* 1994;**18**:30 -35.

Bloch F, Hansen WW, Packard M. Nuclear induction. *Physics Review* 1946;**69**:127.

Boesch C, Gruetter R, Martin E, Duc G, Wuthrich K. Variations in the in vivo P-31 MR spectra of the developing human brain during postnatal life. *Radiology* 1989;**172**:197-199.

Bottomley PA, Drayer BP, Smith LS. Chronic adult cerebral infarction studied by phosphorus NMR spectroscopy. *Radiology* 1986;**160**:763-766.

Bottomley PA, Edelstein WA, Foster TH, Adams WA. In vivo solvent suppressed localized hydrogen nuclear magnetic resonance spectroscopy: a window to metabolism? *Proceedings of the National Academy of Sciences USA* 1985:**82**:2148-2152.

Bottomley PA, Foster TH, Darrow RD. Depth resolved surface coil spectroscopy (DRESS) for in vivo $^{1}H$, $^{31}P$ and $^{13}C$ NMR. *Journal of Magnetic Resonance* 1984;**59**:338-341.

Bottomley PA, Hardy CJ, Roemer PB, Weiss RG. Problems and expediencies in human $^{31}P$ spectroscopy: the definition of localized volumes, dealing with saturation and the technique-dependence of quantification. *NMR in Biomedicine* 1989;**2**:284 - 289. (b)

Bottomley PA, Hardy CJ. Progress in efficient 3D spatially localized in vivo $^{31}P$ NMR spectroscopy using multidimensional spatially selective (P) pulses. *Journal of Magnetic Resonance* 1987;**74:**550-556. (b)

Bottomley PA, Hart HR, Edelstein WA, Schenck JF, Smith LS, Leue WM, Mueller OM, Redington RW. NMR imaging/spectroscopy system to study both anatomy and metabolism. *Lancet* 1983;**ii**:273-274.

Bottomley PA, Herflens RJ, Smith LS, Bashore TM. Altered phosphate metabolism in myocardial infarction: P-31 MR spectroscopy. *Radiology* 1987;**165**:703-707. (a)

Bottomley PA. Human in vivo NMR spectroscopy in diagnostic medicine: clinical tool or research probe? *Radiology* 1989;**170**:1-115. (a)

Bottomley PA. Spatial localization in NMR spectroscopy in vivo. *Annals of New York Academy of Sciences* 1987;**508**:333-348. (c)

Bottomley PA. The trouble with spectroscopy papers. *Radiology* 1991;**181**:334-350.

Brant-Zawadzki M, Weinstein P, Bartkowski H, Moseley M. MR Imaging and spectroscopy in clinical and experimental cerebral ischaemia: A review. *American Journal of Roentgenology* 1987;**148**:579-588.

Brenton DP, Garrow PJ, Krywawych S, Reynolds EOR, Bachelard HS, Cox DW, Morris PG. Phosphoethanolamine is a major constituent of the phosphomonoester peak detected by $^{31}P$ NMR in newborn brain. *Lancet* 1985;**i**:115.

Brown JK, Purvis RJ, Forfar JO, Cockburn F. Neurological aspects of perinatal asphyxia. *Developmental Medicine and Child Neurology* 1974;**16**:567.

Brown TR, Kincaid BM, Ugurbil K. NMR chemical shift imaging in three dimensions. *Proceedings of the National Academy of Sciences* 1982;**79**:3523-3526.

Bruhn H, Frahm J, Gyngell ML, Merboldt KD, Hanicke W, Sauter R. Cerebral metabolism in man after acute stroke: new observations using localized proton NMR spectroscopy. *Magnetic Resonance in Medicine.* 1989;**9**:126-131.

Buchli R, Rumpel H, Martin E, Baenziger O, Burger C, Meier D, Boesiger P. $T_1$ - times of $^{31}P$ metabolites in the brain of human neonates and adults. *Society of Magnetic Resonance in Medicine* 1992; Book of Abstracts: p1903.

Buchli R, Rumpel H, Martin E, Baenzinger O, Burger C, Meier D, Boesiger P. Molar concentrations of $^{31}P$ metabolites in the brain of healthy human neonates, children and adults. *Society of Magnetic Resonance in Medicine* 1991; Book of Abstracts p1902.

Burri R, Steffen C, Herschokowitz N. N-acetyl-L aspartate is a major source of acetate groups for lipid synthesis during rat brain development. *Developmental Neuroscience* 1991;**13**:403-411.

Busby SJW, Gadian DG, Radda GK, Richards RE and Seeley PJ. Phosphorus Nuclear -Magnetic - Resonance studies of compartmentation in muscle. *Biochemistry Journal* 1978;**170**:103-114.

Cady EB, Costello AM de L, Dawson MJ, Delpy DT, Hope PL, Reynolds EOR, Tofts PS, Wilkie DR. Non-invasive investigation of cerebral metabolism in newborn infants by phosphorus nuclear magnetic resonance spectroscopy. *Lancet* 1983; **i:**1059-1062

Chance B, Leigh JS Jr, Clark BJ, Maris J, Kent J, Nioka S, Smith B. Control of oxidative metabolism and oxygen delivery in human skeletal muscle: a steady state analysis of the work/energy cost transfer function. *Proceedings of the National Academy of Sciences USA* 1985;**82**:8384

Chance B, Nakase Y, Bond M, Leigh JS Jr, McDonald G. Detection of $^{31}P$ nuclear magnetic resonance signals in brain by in vivo and freeze trapped assays. *Proceedings of the National Academy of SciencesUSA* 1978;**75**:4925-4929.

Cheung JY, Bonventre JV, Malis CD, Leaf A. Calcium and ischemic injury. *New England Journal of Medicine* 1986;**314**:1670-1676.

Choi DW Ionic dependence of glutamate neurotoxicity. *Journal of Neuroscience* 1987:**7**:369.

Choi DW, Maulucci Gedde M, Krigstein AR. Glutamate toxicity in neuronal cell culture. *Journal of Neuroscience* 1987;**7**:369-379.

Choi DW. Glutamate neurotoxicity and diseases of the nervous system. *Neuron* 1988;**1**:623-634.

Choi DW. Glutamate neurotoxicity in cortical cell culture is calcium dependent. *Neurosci Lett* 1985;**58**:293-297.

Choi DW. Ionic dependence of glutamate neurotoxicity. *Journal of Neuroscience* 1987;7:369-379.

Coulter DL. Neurologic uncertainty in newborn intensive care. *New England Journal of Medicine* 1987;**316**:840-844.

Coutts GA, Bryant DJ, Collins AG, Cox IJ, Sargentoni J, Gadian DG. $^{31}P$ magnetic resonance spectroscopy of the normal human brain: approaches using four dimensional chemical shift imaging and phase mapping techniques. *NMR in Biomedicine* 1989; **1**: 190-197.

Cox SJ, Styles P. Towards biochemical imaging. *Journal of Magnetic Resonance* 1980;**40**:209-212.

Coyle JT, Bird SJ, Evans RH, Gulley RL, Nadler JV, Nicklas WJ, Olney JW. Excitatory amino acid neurotoxins; selectivity, specificity, and mechanisms of action. *Neurosciences Research Program Bulletin* 1981;**19**:1-427.

Crockard HA, Gadian DG, Frackowiack RSJ, Proctor E, Allen K, Williams SR, Ross Russell RW. Acute cerebral ischaemia: concurrent changes in cerebral blood flow, energy metabolites, pH, and lactate measured with hydrogen clearance and $^{31}P$ and $^{1}H$ nuclear magnetic resonance spectroscopy. II: Changes during ischaemia. *Journal of Cerebral Blood Flow and Metabolism* 1987;**7**:394-402.

D'Adamo AF, Yatsu FM. Acetate metabolism in the nervous sytem. N-acetyl-L-aspartic acid and the biosynthesis of brain lipids. *Journal of Neurochemistry* 1966;**13**:961-965.

Dawson TM, Dawson VL, Synder SH. A novel neuronal messenger molecule in brain: the free radical, nitric oxide. *Annals of Neurol ogy* 1992;**32**:297-311.

De Vries LS, Dubowitz LMS, Dubowitz V, Kaiser A, Lary S, Silverman M, Whitelaw A, Wigglesworth JS. Predictive value of cranial ultrasound in the newborn baby: a reappraisal. *Lancet* 1985;**ii**:137-140.

DeVries LS, Wigglesworth JS, Regev R, Dubowitz LMS. Evolution of periventricular leukomalacia during the neonatal period and infancy: correlation of imaging and postmortem findings. *Early Human Development* 1988;**17**:205-219.

Dimick RN, Hedlund LW, Herfkens RJ, Fram EK, Utz J. Optimizing electrocardiograph electrode placement for cardiac-gated magnetic resonance imaging. *Investigative Radiology* 1987;**22**:17-22.

Duijn JH, Matson GB, Maudsley AA, Hugg JW, Weiner MW. Human brain infarction: proton spectroscopy. *Radiology* 1992;**183**:711-718.

Ebmeyer U, Abramson NS, Katz LM. Current research directions in cerebral resucitation after cardiac arrest. *Current Opinion in Critical Care* 1995;**1**:182-188.

Edwards RHT, Wilkie DR, Dawson MJ, Gordon RE, Shaw D. Clinical use of nuclear magnetic resonance in the investigation of myopathy. *Lancet* 1982;**i**:725-731.

Ekholm A, Asplund B, Siesjo BK. Perturbation of cellular energy state in complete ischemia: relationship to dissapative ion fluxes. *Experimental Brain Research* 1992;**90**:47-53.

Englander SA, Bolinger L, Leigh JS. Changes in in-vivo $^{31}P$ $T_1$. *Society of Magnetic Resonance in Medicine, Berlin Meeting* 1992; Book of Abstracts: p773.

Espanol MT, Yang G, Shimizu H, Xu Y, Chang L, Weinstein P, Litt L, James TL. Does N-acetyl aspartate (NAA) predict outcome of transient global cerebral ischaemia in rat brain? *Society of Magnetic Resonance in Medicine, Berlin Meeting* 1992: Book of Abstracts; p 2148.

Eyre JA, Oozeer RC, Wilkinson AR. Diagnosis of neonatal seizure by continuous recording and rapid analysis of the electroencephalogram. *Archives of Disease in Childhood* 1983;58:785-790.

Eyre JA. Neurophysiological assessment of the immature central nervous sytem. *British Medical Bulletin* 1988;**44**:1076-1092.

Fan T, W-M, Higashi RM, Lane AN, Jardetsky O. Combined use of $^{1}H$-NMR and GC-MS for metabolite monitoring and in-vivo $^{1}H$-NMR assignments. *Biochimica et Biophysica Acta* 1986;**882**:154-167.

Faraci FM, Brian JE. Nitric oxide and the cerebral circulation. *Stroke* 1994;**25**:692-703.

Fenichel GM. Asphyxia. In: Fenichel GM, ed. *Neonatal Neurology*. New York: Churchill Livingstone, 1990.

Fenstermacher MJ, Narayana AA. Serial proton magnetic resonance spectroscopy of ischemic brain injury in humans. *Investigative Radiology* 1990;**25**:1034-1039.

Finer NN, Robertson CM, Richards RT, Pinnell LE, Peters KE. Hypoxic-ischemic encephalopathy in term neonates : Perinatal factors and outcome. *Journal of Pediatrics* 1981;**98**:112-117.

Frahm J, Bruhn H, Gyngell ML, Merboldt KD, Hanicke W, Sauter R. Localized high-resolution proton NMR spectroscopy using stimulated echoes: initial applications to human brain in vivo. *Magnetic Resonance in Medicine* 1989;**9**:79-93. (a)

Frahm J, Bruhn H, Gyngell ML, Merboldt KD, Hanicke W, Sauter R. Localized proton NMR spectroscopy in different regions of the human brain in vivo, relaxation times and concentrations of cerebral metabolites. *Magnetic Resonance in Medicine* 1989; **11**:47-63. (b)

Frahm J, Merboldt K, Gyngell ML, Hanicke W, Villringer A. Localized proton spectroscopy of brain and muscle in vivo. *Radiology* 1987;**165**:345

Gadian DG, Proctor E, Williams SR, Cady EB, Gardiner RM. Neurometabolic effects of an inborn error of amino acid metabolism demonstrated in vivo by $^{1}H$ NMR *Magnetic Resonance in Medicine* 1986;**3**:150-156.

Gadian DG. Nuclear Magnetic Resonance and its applications to living systems. New York: Oxford University Press, 1982.

Garcia J. Morphology of global cerebral ischaemia.
*Critical Care Medicine* 1988;**16**:979.

Gill SS, Porteous R, Small RK, Thomas DGT , Patel P, Van Bruggen N, Gadian DG, Kauppinen RA. Brain metabolites as $^{1}H$ markers of neuronal and glial disorders. *NMR in Biomedicine* 1989;**2**:196-200.

Gill SS, Thomas DGT, van Bruggen N, Gadian DG, Peden CJ, Bell JD, Cox IJ, Menon DK, Iles RA, Bryant DJ, Coutts GA. Proton MR spectroscopy of intracranial tumours: in vitro and in vivo studies. *Journal of Computer Assisted Tomography*1990;**14**:407-504.

Gluckman PD, Williams CE. When and why do brain cells die? Annotation. *Developmental Medicine and Child Neurology* 1992;**11**:1010-1014.

Gordon RE, Hanley PE, Shaw D, Gadian DG, Radda GK, Styles P, Bore PJ, Chan L. Localization of metabolites in animals using $^{31}P$ topical magnetic resonance. *Nature* 1980; **287**:736-738.

Gorke W. Somatosensory evoked cortical potentials indicating impaired motor development in infancy. *Developmental Medicine and Child Neurology* 1986;**28**:633-641.

Griffiths JR, Cady E, Edwards RHT, McCready VR, Wilkie DR, Wiltshaw E. $^{31}P$ NMR studies of a human tumour in situ. *Lancet* 1983;**i**:1435- 1436.

Grodd W, Krageloh-Mann I, Klose U, Sauter R. Metabolic and destructive brain disorders in children: findings with localized proton MR spectroscopy. *Radiology* 1991;**181**:173-181.

Grunnet ML, Curless RG, Bray PF, Jung AL. Brain changes in newborns from an intensive care unit. *Developmental Medicine and Child Neurology.* 1974:**16**;320-328.

Hall LD, Rajanayagam V, Sukumar S. Chemical shift-resolved tomography using four-dimensional FT imaging. *Journal of Magnetic Resonance.* 1985;**61**:188-191.

Hamilton PA, Hope PL, Cady EB, Delpy DT, Wyatt JS, Reynolds EOR. Impaired energy metabolism in brains of newborn infants with increased cerebral echodensities. *Lancet* 1986; **i** :1242-1246.

Hamilton PA, Hope PL, Cady EB, Delpy DT, Wyatt JS, Reynolds EOR. Prognosis of newborn infants with hypoxic ischemic brain injury assessed by phosphorus magnetic resonance spectroscopy. *Pediatric Research* 1989:**25**;5;445-451.

Hands LJ, Bore PJ, Galloway G, Morris PJ, Radda GK. Muscle metabolism in patients with peripheral vascular disease investigated by $^{31}P$ nuclear magnetic resonance spectroscopy *Clinical Science* 1986;**71**:283-290.

Hanstock CC, Rothman DL, Howseman A et al. In vivo determination of NAA concentration in the human brain using the proton aspartyl resonance. *Society of Magnetic Resonance in Medicine, Amsterdam Meeting* 1989;Book of Abstracts:p442.

Hanstock CC, Rothman DL, Prichard JW, Jue T, Shulman RG. Spatially localised $^{1}H$ NMR spectra of metabolites in the human brain. *Proceedings National Academy of Sciences USA* 1988;**85**:1821-1825.

Hawes DR, Mishkin FS. Brain scans in watershed infarction and laminar cortical necrosis. *Radiology* 1972;**103**:131-134.

Hellstrom Westas L, Rosen I, Svenningsen NW. The prognostic value of early CFM tracings after severe birth asphyxia in full term infants: a retrospective analysis. *Biol Neonate* 1992;**64**:306.

Hida K, Kwee IL, Nakada T. $T_1$ values of phophomonoester and phosphocreatine of brain show no significant change during development. *Magnetic Resonance in Medicine* 1992;**27**:179-182.

Higuchi T, Fernandez EJ, Shimizu H, Weinstein PR, Maudsley AA, Weiner MW. Effect of focal brain ischemia on N-Acetyl aspartate and glutamate. *Society of Magnetic Resonance in Medicine, San Francisco Meeting* 1991;Book of Abstracts:p145.

Hill A. Current concepts of hypoxc-ischemic injury in the term newborn. *Pediatric Neurology* 1991;**7**:317-325.

Hope PL, Cady EB, Chu A, Delpy DT, Gardner RM, Reynolds EOR. Brain metabolism and intracellular pH during ischaemia and hypoxia: an in vivo $^{31}P$ and $^{1}H$ nuclear magnetic resonance study in the lamb. *Journal of Neurochemistry* 1987;**49**:75-82.

Hope PL, Costello AM de L, Cady EB, Delpy DT, Tofts PS, Chu A, Hamilton PA, Reynolds EOR, Wilkie DR. Cerebral energy metabolism studied with phosphorus NMR spectroscopy in normal and birth-asphyxiated infants. *Lancet* 1984;**ii**:366-370.

Hore PJ. Solvent Suppression in Fourier transform nuclear magnetic resonance *Journal of Magnetic Resonance* 1983;**55**:283-300.

Hoult DI, Richards RE. The signal to noise ratio of the nuclear magnetic resonance experiment. *Journal of Magnetic Resonance* 1976;**24**:71.

Hoult DI, Busby SJW, Gadian DG, Radda GK, Richards RE, Seeley PJ. Observation of tissue metabolites using $^{31}P$ nuclear magnetic resonance. *Nature* 1974;**252**:285-287

Hoult DI, Richards RE. Critical factors in the design of sensitive high resolution nuclear magnetic resonance spectrometers. *Proceedings Royal Society London* 1975; **344**: 311-340.

Hubesch B, Sappy-Marinier D, Roth K, Meyerhoff DJ, Matson GB, Weiner MW. 31P NMR spectroscopy of normal human brain and brain tumours. *Radiology* 1990;**174**:401-409.

Huppi PS, Posse S, Lazeyras F, Burri R, Bossi E, Herschkowitz N. Magnetic Resonance in preterm and term newborns: $^{1}H$-spectroscopy in developing human brain. *Pediatric Research* 1991;**30**:574-578.

Ikonomidou C, Price M, Mosinger J et al. Hypobaric-ischemic conditions produce glutamate-like cytopathology in infant rat brain. *J Neurosci.* 1989;**9**:1693-1700.

Johanson CE. Ontogeny and phylogeny of the blood brain barrier. In: Neuwelt EA, ed. *Implications of the blood brain barrier and its manipulation*, vol 1. New York: Plenum, 1989:157-98.

Johnson MA, Pennock JM, Bydder GM, Dubowitz LM, Thomas DJ, Young IR. Serial MR imaging in neonatal cerebral injury. *American Journal of Neuroradiology* 1987;**8**:83-92.

Kanal E, Shellock FG. Burns associated with clinical MR examinations. *Radiology* 1990;**175**:585.

Kato T, Mikami I, Kouchirou N, Takashima S, Okuyama K. Intracellular pH, alkalosis and human brain development. *Society of Magnetic Resonance in Medicine, Berlin Meeting* 1992; Book of Abstracts: p 2007.

Kato T, Tokumaru A, O'uchi T, Mikami I, Umeda M, Nose K, Eguchi T, Hasegawa M, Okuyama K. Assessment of brain death in children by means of P-31 MR spectroscopy: preliminary note. *Radiology* 1991;**179**:95-99.

Kawai S, Yonetani M, Nakamura H, Okada Y. Effects of deprivation of oxygen and glucose on the neural activity and the level of high energy phosphates in the hippocampal slices of immature and adult rat. *Developmental Brain Research* 1989;**48**:11-8.

Keeney S, Adcock E, McArdle C. Prospective observations of 100 high-risk neonates by high field (1.5Tesla) magnetic resonance imaging of the central nervous system. II. Lesions associated with hypoxic-ischaemia encephalopathy. *Pediatrics* 1991;**87**:431-438.

Knufman NMJ, Berkelbach van der Sprenkel JW, Tulleken CAF. N-acetyl-aspartate differences between gray and white matter as observed by proton spectroscopic imaging in normal subjects. *Society of Magnetic Resonance in Medicine Berlin Meeting* 1992; Book of Abstracts:p1905.

Koller KJ, Zaczek R, Coyle JT. N-Acetyl- aspartyl glutamate: regional levels in rat brain and the effects of brain lesions in rat brain as determined by a new HPLC method. *Journal of Neurochemistry* 1984;**43**:1136-1142.

Krause GS, White BC, Aust SD, Nayini NR, Kumar K. Brain cell death following ischaemia and reperfusion: A proposed biochemical sequence. *Critical Care Medicine* 1988;**16**:714 -26.

Kreis R, Ernst T, Ross BD. Absolute quantitation of water and metabolites in the human brain. II Metabolite concentrations. *Magnetic Resonance in Medicine* 1993;**102**:9-19.

Kreussner L, Schmidt RE, Shackleford GD, Volpe JJ. Value of ultrasound for identification of acute haemorrhagic necrosis of thalamus and basal ganglia in an asphyxiated term infant. *Annals of Neurology* 1984;**16**:361-363.

Lafon-Cazal M, Pietri S, Culcasi M, Bockaert J. NMDA-dependent superoxide production and neurotoxicity. *Nature* 1993;**364**:535-537.

Lampman D, Hurst G, Mcnally J, Paley M. Volume selective $^{1}H$ NMR spectroscopy with solvent suppression. *Magnetic Resonance Imaging* 1986;**4**:115.

Laptook AR, Corbett RJT, Uauy R, Mize C, Mendelsohn D, Nunnally RL. Use of $^{31}P$ magnetic resonance spectroscopy to characterize evolving brain damage after perinatal asphyxia. *Neurology* 1989;**39**:709-712.

Larroche JCL. *Developmental pathology of the neonate.* Amsterdam: Elsevier, North Holland, 1977.

Lauterbur PC. Image formation by induced local interactions: examples employing nuclear magnetic resonance. *Nature* 1973;**242**:190-191.

Levene MI, Kornberg J, Williams THC. The incidence and severity of post asphyxial encephalopathy in full-term infants. *Early Human Development* 1985;**11**:21-28.

Levene MI, Wigglesworth JS, Dubowitz V. Hemorrhagic periventricular leukomalacia in the neonate: a real time ultrasound study. *Pediatrics* 1983:**71**;794-797.

Levene MI. *Neonatal Neurology*. Edinburgh: Churchill Livingstone, 1987.

Levine SR, Welch KMA, Helpern JA, Chopp M, Bruce R, Selwa J, Smith MB. Prolonged deterioration of ischemic brain energy and acidosis associated with hyperglycaemia: human cerebral infarction studied by serial $^{31}$P NMR spectroscopy. *Annals of Neurology* 1988;**23**:416-418.

Lewis LD, Ljunggren B, Ratcheson RA, Siesjo BK. Cerebral energy state in insulin-induced hypoglycaemia,related to blood glucose and to EEG. *Journal of Neurochemistry* 1974;23:673-679.

Lipton SA Choi Y-B, Pan Z-H, et al. A redox-based mechanism for the neuroprotective and neurodestructive effects of nitric oxide and related nitroso-compounds. *Nature* 1993;**364**:626-632.

Lipton SA, Rosenberg PA. Excitatory amino acids as a final common pathway for neurologic disorders. *New England Journal of Medicine*; 1994;**330**:613-622.

Ljunggren B, Norberg K, Siesjo BK. Influence of tissue acidosis upon restitution of brain energy metabolism following total ischaemia. *Brain Research* 1974;**77**:173.

Luyten PR, Berkelbach van der Sprenkel JW, van Rijen PC, Tulleken AF, den Hollander JA. H-1 MR spectroscopy detection of cerebral lactate in patients with cerebral infarction. *Radiology* 1987;**165**:166.

Luyten PR, den Hollander JA. Observation of metabolites in the human brain by MR spectroscopy. *Radiology* 1986;**161**:795-798. (b)

Luyten PR, Marien AJH, den Hollander JAH. Acquisition and quantitation in proton spectroscopy. *NMR in Biomedicine* 1991;**4**:64-69.

Luyten PR, Marien AJH, Sutsma B, den Hollander J A. Solvent suppressed spatially resolved spectroscopy : an approach to high resolution NMR on a whole-body MR system. *Journal of Magnetic Resonance* 1986;**67**:148-155. (a)

Mabe H, Blonqvist P, Siejso BK. Intracellular pH in the brain following transient ischaemia. *Journal of Cerebral Blood Flow and Metabolism* 1983;**3**:109-114.

Madden A, Leach MO, Collins DJ, Easton D. A quantitative analysis of the accuracy of in vivo pH measurements with $^{31}P$ NMR spectroscopy: assessment of pH measurement methodology. *NMR in Biomedicine* 1991;**4**:1-11.

Martin GB, Paradis NA, Helpern JA, Nowak RM, Welch KMA. Nuclear magnetic resonance spectroscopy study of human brain after cardiac resuscitation. *Stroke* 1991;**22**:462-468.

Matson GB, Weiner MW. Spectroscopy. In: DD Stark and WG Bradley, eds. *Magnetic Resonance Imaging*;. St Louis, Mosby Year Book, 1992:438-478.

McArdle CB, Richardson CJ, Hayden CK, Nicholas DA, Amparo EG. Abnormalities of the neonatal brain: MR imaging II: Hypoxic -ischaemic brain injury. *Radiology* 1987;163:395-403.

McCord JM. Oxygen-derived free radicals in postischaemic tissue injury. *New England Journal of Medicine* 1985;**312**:159-163.

Menon DK, Baudoin CJ, Cox IJ, Sargentoni J, Peden CJ, Bell JD. Abnormal proton magnetic resonance spectroscopy in patients with AIDS in the presence of normal imaging. *Radiology* 1990:**177**(SS);231. (a)

Menon DK, Lockwood GG, Peden CJ, Cox IJ, Bell JD, Bryant DJ, Sargentoni J, Whitwam JG. 19- fluorine magnetic resonance spectroscopy studies of brain in humans. *British Journal of Radiology* 1990;**64**:79.(b)

Menon DK, Sargentoni J, Peden CJ, Bell JD, Cox IJ, Coutts GA, Baudoin C, Newman CGH. Proton MR spectroscopy in herpes simplex encephalitis:assessment of neuronal loss. *Journal of Computer Assisted Tomography* 1990;**14**:449-452.(c)

Messer J, Haddad J, Casanova R. Transcranial Doppler evaluation of cerebral infarction in the neonate. *Neuropediatrics* 1991;**22**:147-151.

Messick JM Jr, Milde LM. Brain protection. *Advances in Anethesiology* 1987;**4**:47-88

Meyer RA, Fisher MJ, Nelson SJ, Brown TR. Evaluation of manual methods for integration of in vivo phosphorus NMR spectra. *NMR in Biomedicine* 1988;**3**:131-135.

Michaelis T, Merboldt K-D, Bruhn H, Hanicke W, Math D, Frahm J. Absolute quantification of metabolites in the adult human brain in vivo: quantification of localized proton MR spectra. *Radiology* 1993;**187**:219-227.

Miller B, Sarantis M, Traynelis SF, Attwell D. Potentiation of NMDA recpetor currents by arachidonic acid. *Nature* 1992;**355**:722-725.

Moon RB, Richards JH. Determination of intracellular pH by $^{31}P$ magnetic resonance. *Journal of Biological Chemistry* 1973;**248**:7276-7278.

Moorcraft J, Bolas NM, Ives NK, Sutton P, Blackledge MJ, Rajagopalan B, Hope PL, Radda GK. Spatially localized magnetic resonance spectroscopy of the brains of normal and asphyxiated newborns. *Pediatrics* 1991;**87**:273-282.

Morris GA, Smith KL, Waterton JC. Pulse sequences for solvent suppression with minimal spectral distortion. *Journal of Magnetic Resonance* 1986:**2**;526-532

Murdoch J, Hall R. Brain protection: physiological and pharmacological considerations. Part I: the physiology of brain injury. *Canadian Journal of Anaesthesia* 1990;**37**:663-71.

Nadler JV, Cooper JR. N-acetyl-L-aspartic acid content of human neural tumours and bovine peripheral nervous tissues. *Journal of Neurochemistry* 1972;**19**:313-319.

Nakada T, Kwee IL, Suzuki N, Houkin K. Intrauterine fetal brain NMR spectroscopy: $^{1}H$ and $^{31}P$ studies in rats. *Magnetic Resonance in Medicine.* 1989;**12**:172-80.

Nakada T. Brain maturation and acid base control: taurine/N-acetyl Aspartate replacement hypothesis. In: Niimi H, Hori M, Naritomi H, eds. *Microcirculatory disorders in the heart and brain* . New York: Gordon and Breach Science Publishers 1991:175-190.

Narayana PA, Fotedar LK, Jackson EF, Bohan TP, Butler IJ, Wolinsky JS. Regional in vivo proton magnetic resonance spectroscopy of brain. *Journal of Magnetic Resonance* 1989;**83**:44-52.

Nishikawa T, Kirsch JR, Koehler RC, Miyabe M, Traystman RJ. Nitric oxide synthase inhibition reduces caudate injury following transient ischaemia in cats. *Stroke* 1994;**25**:877-885.

Nitsch RM, Blusztajn JK, Pittas AG, Slack BE, Growdon JH, Wurtman RJ. Evidence for a membrane defect in Alzheimer disease brain. *Proc Natl Acad Sci* 1992;**89**:1671-1675.

Nordstrom CH and Siesjo BK. Effects of pentobarbital in cerebral ischaemia. Part I: cerebral energy metabolism during pronounced incomplete ischaemia. *Stroke* 1978:**9**:327.

Norman MG. Perinatal brain damage. *Perspectives in Pediatric Pathology* 1978;**4**:41.

Norwood WI, Norwood CR, Ingwall JS, Castaneda AR, Fossel ET. Hypothermic circulatory arrest. 31-Phosphorus nuclear magnetic resonance of isolated perfused neonatal rat brain. *Journal of Thoracic and Cardiovascascular Surgery* 1979:**78**;823

O'Brien MJ, Ash JM, Gilday DL. Radionuclide brain-scanning in perinatal hypoxia/ischemia. *Developmental Medicine and Child Neurology*. 1979;**21**:161-173.

Oberhaensli RD, Galloway GJ, Hilton-Jones D, Bore PJ, Styles P, Rajagopalan B, Taylor DJ, Radda GK. The study of human organs by phosphorus -31 topical magnetic resonance spectroscopy. *British Journal of Radiology* 1987;**60**:367-373.

Odeblad E, Bhar BN, Lindstrom G. Proton magnetic resonance of human red blood cells in heavy-water exchange experiments. *Archives of Biochemistry and Biophysics* 1956;**63**:221-225.

Ogawa S, Shulman RG, Glynn P, Yamane T, Navon G. On the measurement of pH in Escheria Coli by $^{31}$P Nuclear Magnetic Resonance. *Biochimica et Biophysica Acta* 1978;**502**:45-50.

Ordidge RJ, Connelly A, Lohman JAB. Image-selected <u>in vivo</u> spectroscopy (ISIS). A new technique for spatially selective NMR spectroscopy. *Journal of Magnetic Resonance* 1986;**66**:283-294.

Palmer C, Brucklacher RM, Christensen MA, Vannucci RC. Carbohydrate and energy metabolism during the evolution of hypoxic-ischaemic brain damage in the immature rat. *Journal of Cerebral Blood Flow and Metabolism* 1990;**10**:227-35.

Patel TB, Clark JB. Lipogenesis in the brain of suckling rats. *Biochemistry Journal* 1980;**188**:163-168.

Patel TB, Clark JB. Synthesis of N-acetyl-L aspartate by rat brain mitochondria and its involvement in mitochondrial/cytosolic carbon transport. *Biochemistry Journal* 1979;**184**:539-546.

Pellegrini-Giampietro DE, Pulsinelli WA, Zukin RS. NMDA and non-NMDA receptor gene expression following global brain ischaemia in rats: effect of NMDA and non-NMDA receptor antagonists. *Journal of Neurochemistry* 1994;**62**:1067-1073.

Petroff OAC, Ogino T, Alger JR. High resolution proton magnetic resonance spectroscopy of Rabbit brain: Regional metabolite levels and post-mortem changes. *Journal of Neurochemistry* 1988;**51**:163-171.

Petroff OAC, Prichard JW, Behar KL, Alger JR, den Hollander JA, Shulman RG. Cerebral intracellular pH by $^{31}P$ magnetic resonance spectroscopy. *Neurology* 1985;**35**:781-8

Pettegrew JW, Kopp SJ, Minshew NJ, Glonek T, Feliksik JM, Tow JP, Cohen MM. $^{31}P$ Nuclear magnetic resonance studies of phosphoglyceride metabolism in developing brain: preliminary observations. *Journal of Neuropathology and Experimental Neurology* 1987;**46**:419-430.

Pharaoh POD, Cooke T, Rosenbloom I, Cooke RWI. Trends in birth prevalence of cerebral palsy. *Archives of Disease in Childhood* 1987; **62**:379-384.

Plum F. What causes infarction in ischaemic brain? The Robert Wartenberg lecture. *Neurology* 1983;**33**:222-33.

Pourcelot L. Diagnostic ultrasound for cerebrovascular disease . In: Donald I, Levi S (eds). Present and future in diagnostic ultrasound. Kooker, Rotterdam 1976; p 141.

Prichard JW, Rothman DL, Novotny EJ, Petroff OAC, Avison MJ, Howseman A, Hanstock CC, Shulman RG. Photic stimulation raises lactate in human visual cortex. *Society of Magnetic Resonance in Medicine Amsterdam Meeting* 1989; Book of Abstracts:p 1071.

Pulsinelli WA, Brierley JB, Plum F. Temporal profile of neuronal damage in a model of transient forebrain ischaemia. *Ann Neurol* 1982;**11**:499-509.

Purcell EM, Torrey HC, Pound RV. Resonance absorption by nuclear magnetic moments in a solid. *Physics Review* 1946;**69**:37.

Radda GK, Rajagopalan R, Taylor DJ. Biochemistry in vivo: an appraisal of clinical magnetic resonance spectroscopy. *Magnetic Resonance Quarterly* 1989;**5**:122-151.

Raichle ME. The pathophysiology of brain ischaemia. *Annals of Neurology* 1983;**13**:2-10.

Robertson C, Finer N. Term infants with hypoxic-ischemic encephalopathy: outcome at 3.5 years. *Developmental Medicine and Child Neurology* 1985;**27**:473-484.

Rosenberg GA, White J, Gasparovic C, Crisotomo EA, Griffey RH. Effect of hypoxia on cerebral metabolites measured by proton nuclear magnetic resonance in rats. *Stroke* 1991;**22**:73-79.

Ross BD, Radda GK, Gadian DG, Rocker G, Esiri M, Falconer-Smith J. Examination of a case of suspected McArdle's syndrome by $^{31}P$ nuclear magnetic resonance. *New England Journal of Medicine* 1981;**304** :1388-1342

Roth JL, Nugent M, Gray JE, Julsrud PR, Berquist TH, Sill JC, Kispbert DB. Patient monitoring during magnetic resonance imaging. *Anesthesiology* 1985;**62**:80-83.

Roth SC, Azzopardi D, Edwards DA, Baudin J, Cady EB, Townsend J, Delpy DT, Stewart AL, Wyatt JS, Reynolds EOR. Relation between cerebral oxidative metabolism following birth asphyxia, and neurodevelopmental outcome and brain growth at one year. *Developmental Medicine and Child Neurology* 1992:**34**;285-295.

Rothman S. Synaptic release of excitatory amino acid neurotransmitter mediates anoxic neuronal death. *Journal of Neuroscience* 1984;**4**:1884.

Rothman SM, Olney JW. Glutamate and the pathophysiology of hypoxic-ischaemic brain damage. *Annals of Neurology* 1986;**19**:105.

Rutherford MA, Pennock JM, Dubowitz LMS. Cranial ultrasound and magnetic resonance imaging in hypoxic-ischamic encephalopathy: a comparison with outcome. *Developmental Medicine and Child Neurology* 1994;**36**:813-825.

Safar P. Cerebral resuscitation after cardiac arrest: research initiatives and future directions. *Annals of Emergency Medicine* 1993;**22**:324-349.

Safar P. Resuscitation from clinical death: pathophysiologic limits and therapeutic potentials. *Critical Care Medicine* 1988;**16**:923-941.

Sappey-Marinier D, Calabrese G, Hetherington HP, Fisher SNG, Deicken R, Van Dyke C, Fein G, Weiner MW. Proton magnetic resonance spectroscopy of human brain: Applications to normal white matter, chronic infarction, and MRI white matter signal intensities. *Magnetic Resonance in Medicine* 1992;**26**:313-327.(a)

Sappey-Marinier D, Hubesch B, Matson GB, Weiner MW. Decreased phosphorus metabolite concentrations and alkalosis in chronic cerebral infarction. *Radiology* 1992;**182**:29-34.(b)

Sargentoni J, Bell JD, Bryant DJ, Coutts GA, Cox IJ, Hamid SK, Cowan FM, Rutherford MA. Proton 3D CSI of infants presenting with hypoxic-ischaemic encephalopathy. *Society of Magnetic Resonance in Medicine Berlin Meeting*; 1992 Book of Abstracts:p2010.

Sarnat HB, Sarnat MS. Neonatal encephalopathy following fetal distress. *Archives of Neurology* 1976:**33**;696-705.

Scher MS, Belfar H, Martin J, Painter MJ. Destructive brain lesion of presumed fetal onset: antepartum courses of cerebral palsy. *Pediatrics* 1991; **88**:898-906.

Scremin OU, Jenden DJ. Focal ischaemia enhances choline output and decreases acetylcholine output from rat cerebral cortex. *Stroke* 1989;**20**:92-95.

Shellock FG. Monitoring during MRI. An evaluation of the effect of high-field MRI on various patient monitors. *Medical Electronics* 1986;**17**:93-97.

Shigematsu H, Okamura N, Shimeno H, Kishimoto Y, Kan L, Feneslau C. Purification and characterization of the heat-stable factors essential for the conversion of lignoceric acid to cerebronic acid and glutamic acid: identification of N-acetyl-L aspartic acid. *Journal of Neurochemistry* 1983:**40**:814-820.

Shulman GI, Rothman DL, Jue T, Stein P, De Fronzo RA, Shulman RG. Quantitation of muscle glycogen synthesis in normal subjects and subjects with non-insulin dependent diabetes by $^{13}C$ nuclear magnetic resonance spectroscopy. *New England Journal of Medicine* 1990;**322**:262-263.

Shulman RG, Brown TR, Ugurbil K, Ogawa S, Cohen SM, den Hollander JA. Cellular applications of $^{31}P$ and $^{13}C$ NMR. *Science* 1979;**205**:160-166.

Siesjo BK. Cerebral circulation and metabolism. *J ournal of Neurosurgery* 1984;**60**:883-908.

Siesjo BK. Historical overview. Calcium, ischaemia and death of brain cells. *Annals of the New York Academy of Sciences*. 1987;**507**;133-140.

Siesjo BK. Mechanisms of ischemic brain damage. *Critical Care Medicine* 1988; **16**:954-963.

Siesjo BK. Pathophysiology and treatment of focal cerebral ischaemia. Part II: Mechanisms of damage and treatment. *Journal of Neurosurgery* 1992;**77**:337-354. (b)

Siesjo BK. Pathophysiology and treatment of focal cerebral ischemia. Part I: Pathophysiology. *Journal of Neurosurgery* 1992;**77**:169-84. (a)

Singer JR. Blood flow rates by nuclear magnetic resonance measurements. *Science* 1959;**130**:1652-1653.

Small RK, Bates TE, Urenjak J, Bell JD, Williams SR, Riley K, Watkins B, Gadian DG. N-Acetylaspartate: a neuronal marker that can predict abnormal brain development. *Society of Magnetic Resonance in Medicine, New York Meeting* 1990; Book of Abstracts: p72.

Smith ML, von Hanwehr R, Siesjo BK. Changes in extra and intracellular pH in the brain during and following ischaemia in hyperglycaemic and in moderately hypoglycaemic rats. *Journal of Cerebral Blood Flow and Metabolism* 1987;**7**:76.

Soher BJ, Peter CM, van Zijl PCM, Duyn JH, Barker PB. Quantitative proton MR spectroscopic imaging of the human brain. *Magnetic Resonance in Medicine* 1996;**35**:356-363.

Stark DD, Bradley WG. Magnetic Resonance Imaging. Mosby Year Book 1992; St Louis, Missouri.

Stevens MK, Yaksh TL, Hansen RB II et al. Effect of preischaemia cyclooxygenase inhibition by zomepirac sodium on reflow, cerebral autoregulation, and EEG recovery in the cat after global ischaemia. *J Cereb Blood Flow Metab.* 1986;**6**:691-702.

Stockard JE, Stockard JJ, Kleinberg F, Estmoreland BF. Prognostic value of brainstem auditory evoked potentials in neonates.
*Arch Neurol* 1983;**40**:360-365.

Syrota A, Castaing M, Rougemont D, Berridge M, Baron JC, Bousser MG, Pocidalo JJ. Tissue acid-base balance and oxygen metabolism in human cerebral infarction studied with positron emision tomography. *Annals of Neurology* 1983;**14**:419-428.

Takashima S, Tanaka K. Development of cerebrovascular architecture and its relationship to periventricular leukomalacia. *Arch Neurol* 1978;**35**:11-16.

Tallan HH, Moore S, Stein WH. N-Acetyl -L-Aspartic acid in brain.
*Journal of Biological Chemistry* 1957;**219**:257-264

Tallan HH. Studies on the distribution of N-acetyl-L-aspartic acid in brain.
*Journal of Biological Chemistry* 1957;**224**:41-45.

Taylor DJ, Bore PJ, Styles P, Gadian DG, Radda GK. Bioenergetics of intact human muscle; a 31P nuclear magnetic resonance study. *Mol ecular Biol ogy in Medicine* 1983;**1**:77-94 .

Tews JK, Carter SH, Roa PD, Stone WE. Free amino acids and related compounds in dog brain: post mortem and anoxic changes, effects of ammonium chloride infusion, and levels during seizures induced by picrotoxin and pentylenetrazol.
*Journal of Neurochemistry* 1963;**10**:641-653.

The European Study Group on Nimodipine in Severe Head Injury 1994. A multicenter trial of the efficacy of nimodipine on outcome after sevbere head injury.
*Journal of Neurochemistry* 1994;**80**:797-804.

Toft PB, Christiansen P, Pryds O, Lou H, Larsson HBW, Stubgard M, Henriksen O. Absolute concentrations of brain metabolites in childhood measured by $^{1}$H- magnetic resonance spectroscopy. *Society of Magnetic Resonance in Medicine, Berlin Meeting* 1992; *Book of Abstracts*: p 2001.

van Rijen PC, Luyten PR, Berkelbach van der Sprenkel JW, Kraaier V, van Huffelen AC, Tulleken CAF, den Hollander JA. $^{1}H$ and $^{31}P$ NMR measurement of cerebral lactate, high-energy phosphate levels, and pH in humans during voluntary hyperventilation: associated EEG, capnographic and Doppler findings. *Magnetic Resonance in Medicine* 1989;**10**:182-193.

van Rijen PC, Verheul HB, van Echteld CJA, Balazs R, Lewis P, Nasim MM, Tulleken CAF. Effects of dextromethorphan on rat brain during ischaemia and reperfusion assessed by magnetic resonance spectroscopy. *Stroke* 1991;**22**:343-350.

Vanier MT, Holm M, Ohman R, Svennerholm L. Developmental profiles of gangliosides in human and rat brain. *Journal of Neurochemistry*. 1971;**18**:581-592.

Vannucci RC. Experimental biology of cerebral hypoxia-ischaemia: relation to perinatal brain damage. *Pediatric Research* 1990; **27**:317-326.

Volpe JJ, Pasternak JF. Parasaggital cerebral injury in neonatal hypoxic-ischemic encephalopathy: Clinical and neuroradiologic features. *Journal of Pediatrics* 1977; **91**:472-476.

Volpe JJ. Current concepts of brain injury in the premature infant. *AJR* 1989;**153**:243-251.

Volpe JJ. *Neurology of the Newborn*. Philadelphia: WB Saunders 1987.

Volterra A, Trotti D, Cassutti P et al. High sensitivity of glutamate uptake to extracellular free arachidonic acid levels in rat cortical synaptosomes and astrocytes. J *Neurochem* 1992;**59**:600-606.

Watanabe K, Miyazaki S, Hara K, Hakamada S. Behavioural state cycles, background EEGs and prognosis of newborn infants with perinatal asphyxia. *Electroencephalogr Clin Neurophysiol* 1980; **49**:618-625.

Wei HM, Chi OZ, Liu X, Sinha AK, Weiss HR. Nitric oxide synthase inhibition alters cerebral blood flow and oxygen balance in focal cerebral ischaemia in rats. *Stroke* 1994;**25**:445-450.

Welch KMA, Helpern JA, Robertson WM, Ewing JR. 31-P topical magnetic resonance measurement of high energy phosphates in normal and infarcted human brain (Abstract). *Stroke* 1985;**16**:151.

Welsh FA, O'Connor MJ, Marcy VR, Sparacco AJ, Johns RL. Factors limiting regeneration of ATP following temporary ischaemia in cat brain. *Stroke* 1982;**13**:234-42.

Wendt RE, Rokey R, Vick GW, Johnston DL. Electrocardiographic gating and monitoring in NMR imaging. *Magnetic Resonance Imaging* 1988:**6**;89-95.

Xue D, Huang Z-G, Barnes K, Lesiuk HJ, Smith KE, Buchan AM. Delayed treatment with AMPA, but not NMDA, antagonists reduces neocortical infarction. *J Cereb Blood Flow Metab* 1994;**14**:251-261.

Yoshida S, Inoh S, Asano T , Sano K, Kubota M, Shimazaki H, Ueta N. Effect of transient ischaemia on free fatty acids and phospholipids in the gerbil brain. Lipid peroxidation as a possible cause of postischaemic injury. *Journal of Neurosurgery* 1980;**53**:323-331.

Yoshida S, Inoh S, Asano T, Sano K, Shimazaki H, Ueta N. Brain free fatty acids, edema and mortality in gerbils subjected to transient, bilateral ischemia and effects of barbiturate anaesthesia. *Journal of Neurochemistry* 1983;**40**:1278-1286.

Younkin DP, Delivoria-Papadopoulos M, Leonard JC, Subramanian VH, Eleff S, Leigh JS, Chance B. Unique aspects of human newborn cerebral metabolism: evaluation with phosphorus nuclear magnetic resonance spectroscopy. *Annals of Neurology* 1984;**16**:581-586.

# APPENDIX A, B and C

| Patient | PCA at birth(w)<br>PNA at exam<br>PCA at exam(w) | Birth wt(g) | Apgars/<br>delivery details | Clinical and Imaging findings | Outcome (age)<br><br>Outcome category |
|---|---|---|---|---|---|
| SAB | 29<br><br>24d,<br>9m (failed)<br><br>33 | 1410 | 1(1), 8(5).<br>Emergency LSCS.<br>Maternal infection with β haemolytic strep.<br>Prolonged rupture of membranes.<br>Intubated and ventilated. | Birth asphyxia, HIE II.<br>US; extensive cystic periventricular leukomalacia no evidence of infection. | Severe spastic quadriplegia (6y).<br><br>Severe |
| LC | 25<br><br>10w,14m<br><br>35, 86 | 820 | 5(1), 8(5).<br>APH at 6-8w,<br>? infected liquor.<br>Intubated at resus. | Collapse day 3, multiple apnoeic and bradycardic episodes.<br>Bronchopulmonary dysplasia.<br>Left facial palsy.<br>US; periventricular leukomalacia, left thalamic haemorrhage, right intraventricular haemorrhage.<br>Later US; cystic area posterior to right ventricle.<br>MRI confirmed later US findings. | Near miss cot -death.<br>Left facial palsy, spastic quadriplegia, severely intellectually handicapped. (3y).<br><br>Severe |
| AE | 32<br><br>23d<br><br>35 | 2160 | 8(1),10(5).<br>Forceps delivery. | Respiratory distress, ventilated for 6 days. | Mild delay in speech, otherwise normal (2y 6m).<br><br>Moderate |

Appendix A. Clinical details of the children who had proton spectroscopy d, days: w, weeks: m, months y, years: LSCS, lower segment Caesarian section: VD, vaginal delivery: HIE, hypoxic ischaemic encephalopathy: US, ultrasound: MRI, magnetic resonance imaging: CT computed tomography: EEG, electroencephalography.

| Patient | PCA at birth(w)<br>PNA at exam<br>PCA at exam(w) | Birth wt(g) | Apgars/<br>delivery details | Clinical and Imaging findings | Outcome (age)<br><br>Outcome category |
|---|---|---|---|---|---|
| DH | 32<br>19d<br>35 | 2230 | 0(1), 5(5), 9(10).<br>Emergency LSCS for placental abruption and fetal tachycardia. | Ventilated for respiratory distress syndrome.<br>Only neurological abnormality; Moro mainly extensor at 2/52.<br>US; normal. | Lost to follow up. Felt to be neurologically normal at hospital discharge. (24d).<br><br>Other |
| SG | 32<br>4w<br>36 | 1722 | 5(1), 8(5).<br>Footling breech delivery. | US; extensive periventricular leucomalacia. | Severely impaired, increased tone, not sitting. Spastic quadriplegia. Comprehension reasonable. (4y).<br><br>Severe |
| MC | 34<br>16d, 9m<br>36, 80 | 2000 | 9(1), 10(5)<br>Emergency LSCS for fetal distress.<br>No resuscitation needed. | Hyperbilirubinaemia.<br>Neurologically normal. Cranial US normal. | Normal (2y).<br><br>Control |

Appendix A. Clinical details of the children who had proton spectroscopy d, days: w, weeks: m, months y, years: LSCS, lower segment Caesarian section: VD, vaginal delivery: HIE, hypoxic ischaemic encephalopathy: US, ultrasound: MRI, magnetic resonance imaging: CT computed tomography: EEG, electroencephalography.

| Patient | PCA at birth(w)<br>PNA at exam<br>PCA at exam(w) | Birth wt(g) | Apgars/<br>delivery details | Clinical and Imaging findings | Outcome (age)<br><br>Outcome category |
|---|---|---|---|---|---|
| JeH | 35<br>10d, 8m<br>37, 75 | 2530 | 4(1), 7(5).<br>Elective LSCS<br>for twins. | Birth asphyxia, HIE I. Polycythaemia.<br>US; left thalamic haemorrhage,<br>porencephalic dilatation of left ventricle.<br>At 40w slightly increased tone. | Mild motor delay, slight<br>hypotonia (1y).<br>Normal (3y).<br><br>Normal |
| ZCA | 35<br>15d<br>37 | 2300 | 7(1), 10(5).<br>Emergency LSCS for<br>fetal distress. | Hypotonic with brisk reflexes.<br>Unable to feed - tube fed for 5 months. Not HIE. | ? Diagnosis.<br>Global delay, poor<br>vision, hypotonia. (9m).<br>Lost to further follow up.<br><br>Other |
| AC | 35<br>2w,11m<br>37, 82 | 1570 | 8(1), 9(10).<br>VD, type II dips.<br>No resuscitation. | Truncal hypotonia.<br>US; left intraventricular haemorrhage,<br>marked periventricular densities,<br>possible venous infarction.<br>Later US; unilateral left parietal infarction. | Moderately good; speech<br>delay; sensorineural<br>deafness. (2y 4m).<br><br>Moderate |

Appendix A. Clinical details of the children who had proton spectroscopy d, days: w, weeks: m, months y, years: LSCS, lower segment Caesarian section: VD, vaginal delivery: HIE, hypoxic ischaemic encephalopathy: US, ultrasound: MRI, magnetic resonance imaging: CT computed tomography: EEG, electroencephalography.

| Patient | PCA at birth(w)<br>PNA at exam<br>PCA at exam(w) | Birth wt(g) | Apgars/<br>delivery details | Clinical and Imaging findings | Outcome (age)<br><br>Outcome category |
|---|---|---|---|---|---|
| JoH | 35<br>10d, 8m<br>37, 75 | 1860 | 3(1), 9(5).<br>Elective LSCS<br>for twins. | Birth asphyxia, HIE I. Anaemia.<br>US; bilateral germinal layer haemorrhage. | Mild increased tone (1y).<br>Normal (3y).<br><br>Normal |
| SC | 28<br>10w<br>38 | 1180 | 5(10),10(5).<br>Emergency LSCS for<br>pre-eclampsia. | Prematurity, respiratory distress syndrome causing hypoxia, anaemia, jaundice.<br>US; normal.<br>Developed convulsions at 59 days ? cause. | Mild delay. Clumsy with apparent perceptual problems.<br>Hearing abnormal.<br>Squint requiring repair. (2y).<br><br>Moderate |
| EB | 35w<br>3w, (9m failed)<br>38 | Not known | Difficult VD. | Hypotonia.<br>Respiratory difficulties from birth. Dysmorphic.<br>US; density in right parenchyma.<br>CT; right parenchymal bleed.<br>MRI; (9w) haemorhage resolved, mild dilatation of ventricles, myelination delayed.<br>MRI; (9m), marked dilatation of lateral and third ventricles. | Severe developmental delay and severe sensorineural deafness. (4y).<br><br>Severe |

Appendix A. Clinical details of the children who had proton spectroscopy d, days: w, weeks: m, months y, years: LSCS, lower segment Caesarian section: VD, vaginal delivery: HIE, hypoxic ischaemic encephalopathy: US, ultrasound: MRI, magnetic resonance imaging: CT computed tomography: EEG, electroencephalography.

| Patient | PCA at birth(w)<br>PNA at exam<br>PCA at exam(w) | Birth wt(g) | Apgars/<br>delivery details | Clinical and Imaging findings | Outcome (age)<br><br>Outcome category |
|---|---|---|---|---|---|
| VJN | 35<br><br>25d, 11m<br><br>38, 82 | 3064 | 3(1), 8(5).<br>Maternal intestinal obstruction requiring laparotomy,<br>then emergency LSCS for fetal bradycardia.<br>pH 7.23. | ? NEC. Persistent hypotonia.<br>US; persistent parenchymal echodensities, mild ventricular dilatation. | Normal (4y)<br><br>Normal |
| JL | 35<br><br>20d<br><br>38 | 2140 | 5(1), 10(5).<br>Elective LSCS for placenta praevia. | Poor feeding. Hypotonia.<br>US; mild ventricular dilatation.<br>MRI; basal ganglia densities, high signal in both thalami compatible with haemorrhagic lesions (3w). | Normal development (5y).<br><br>Normal |
| NW | 34<br><br>4w, 10m<br><br>38, 77 | 2880 | 1(1), 1 (10).<br>Emergency LSCS for severe bradycardia during exchange transfusion.<br>Resus. with adrenaline required at birth.<br>pH 6.74 (30 mins). | Rhesus haemolytic disease. HIE grade II.<br>US; bilateral thalamic densities confirmed on MRI.<br>Marked increase in tone. | Mild global developmental delay and ataxia (18m).<br>Lost to further follow up.<br><br>Moderate |

Appendix A. Clinical details of the children who had proton spectroscopy d, days: w, weeks: m, months y, years: LSCS, lower segment Caesarian section: VD, vaginal delivery: HIE, hypoxic ischaemic encephalopathy: US, ultrasound: MRI, magnetic resonance imaging: CT computed tomography: EEG, electroencephalography.

| Patient | PCA at birth(w)<br>PNA at exam<br>PCA at exam(w) | Birth wt(g) | Apgars/<br>delivery details | Clinical and Imaging findings | Outcome (age)<br><br>Outcome category |
|---|---|---|---|---|---|
| CT | 37<br><br>18d, 24d,<br>8w,12w<br><br>39, 40, 45, 49 | 2100 | 3(1), 4(5).<br>VD.<br>Ist twin,<br>delay in delivery, feet<br>around other twins neck. | Birth asphyxia, HIE grade II.<br>US; thalamic densities. | Severe developmental delay (4m), died (6m). PM, brain showed cystic changes consistent with severe HIE.<br><br>Severe |
| NatT | 39<br><br>2d<br><br>39 | 2410 | 6(1), 9(5).<br>VD. | Small for dates. Neurologically normal.<br>US; normal. | Normal (4y).<br><br>Control |
| MW | 40<br><br>2d<br><br>40 | 3950 | 6(1), 9(5),10(10).<br>Spontaneous VD. | Abnormal facies. | Hurler syndrome<br><br>Other |

Appendix A. Clinical details of the children who had proton spectroscopy d, days: w, weeks: m, months y, years: LSCS, lower segment Caesarian section: VD, vaginal delivery: HIE, hypoxic ischaemic encephalopathy: US, ultrasound: MRI, magnetic resonance imaging: CT computed tomography: EEG, electroencephalography.

| Patient | PCA at birth(w)<br>PNA at exam<br>PCA at exam(w) | Birth wt(g) | Apgars/<br>delivery details | Clinical and Imaging findings | Outcome (age)<br><br>Outcome category |
|---|---|---|---|---|---|
| CH | 42<br>4w<br>46 | 4000 | 6(1), 7(5), 7(10).<br>VD, prolonged rupture of membranes. | HIE grade I, although initial signs may have been due to other problems. Congenital CMV. Myelofibrosis, mild neurological abnormalities. | No obvious developmental problems Normal (4y).<br><br>Normal |
| RT | 37<br>24d, 8w<br>40, 45 | 3500 | VD. | Normal twin.<br>US; normal. | Normal (2y)<br><br>Control |
| ML | 40<br>7d<br>41 | 3805 | 3(1), 9(5).<br>VD; 32h labour, pethidine 100mg x 3<br>Floppy at birth, needed resuscitation. | Birth asphyxia HIE II. Jittery, convulsions.<br>US; widespread diffuse parenchymal densities which became cysts by 10d.<br>CT; gross ischaemic changes involving whole cortex.<br>EEG; excessively discontinuous, low amplitude, and seizures.<br>MRI; extensive subcortical cysts in both hemispheres, bilateral haemorrhagic lesions in thalami and basal ganglia. | Spastic quadriplegia, fits, severe developmental delay (4y).<br><br>Severe |

Appendix A. Clinical details of the children who had proton spectroscopy d, days: w, weeks: m, months y, years: LSCS, lower segment Caesarian section: VD, vaginal delivery: HIE, hypoxic ischaemic encephalopathy: US, ultrasound: MRI, magnetic resonance imaging: CT computed tomography: EEG, electroencephalography.

| Patient | PCA at birth(w)<br>PNA at exam<br>PCA at exam(w) | Birth wt(g) | Apgars/<br>delivery details | Clinical and Imaging findings | Outcome (age)<br><br>Outcome category |
|---|---|---|---|---|---|
| IS | 40<br><br>3d (failed), 9d, 6w (failed).<br><br>41 | 2285 | 7(1), 8(5).<br>NVD. | Fetal distress, HIE grade II. Severe asphyxia post delivery due to subglottic stenosis. Tracheostomy at 6 hours. Convulsions.<br>US; IVH.<br>MRI; (1w), bilateral basal ganglia haemorrhage and subarachnoid haemorrhage.<br>EEG; sharp waves and transient low amplitude activity. | Normal. Tracheostomy: speach delay secondary to tracheostomy (3y)<br><br>Normal |
| KM | 40<br><br>12d,19d<br><br>42, 43 | 3950 | Normal.<br>NVD. | Hypoglycaemia. Otherwise normal. | Developmental and speech delay, abnormal tone and ataxic (5y).<br><br>Moderate |
| GBS | 40<br><br>10d<br><br>42 | 3450 | 9(1),10(5).<br>Forceps. | Birth asphyxia, HIE grade II. Neonatal convulsions.<br>US; right parietal density.<br>CT; right parietal infarct and bilateral occipital ischaemic areas consistent with parasaggital injury.<br>MRI; (9m), myelination slightly less on right.<br>Low signal lesion on right on inversion recovery. | Normal (5y).<br><br>Normal |

Appendix A. Clinical details of the children who had proton spectroscopy d, days: w, weeks: m, months y, years: LSCS, lower segment Caesarian section: VD, vaginal delivery: HIE, hypoxic ischaemic encephalopathy: US, ultrasound: MRI, magnetic resonance imaging: CT computed tomography: EEG, electroencephalography.

| Patient | PCA at birth(w)<br>PNA at exam<br>PCA at exam(w) | Birth wt(g) | Apgars/<br>delivery details | Clinical and Imaging findings | Outcome (age)<br><br>Outcome category |
|---|---|---|---|---|---|
| KR | 42<br>2d<br>42 | 3530 | 0(1),0(5).<br>Emergency LSCS. | Birth asphyxia, HIE II.<br>EEG; fits, normal background.<br>MRI; (8m), normal. | Good, normal (5y).<br><br>Normal |
| JM | 42<br>2d, 4d, 1w, 2w<br>42, 42.5, 43, 44 | 3240 | 3(1),9(5).<br>VD. | Birth asphyxia, HIE grade II. Hypoglycaemia.<br>US; initially featureless. At 2w cortical and subcortical cysts.<br>EEG; seizures on a good background.<br>MRI; (9m), cysts in frontal lobes, bilateral basal ganglia lesions. | Severe developmental delay, dystonic, fits, microcephalic, quadriplegic (5y).<br><br>Severe |
| AR | 40<br>18d<br>42 | 3010 | 3(1),4(5).<br>Forceps. | Birth asphyxia, HIE grade II.<br>US; cortical/subcortical cysts, cerebral atrophy. | Spastic quadriplegia, microcephaly, convulsions.<br>(2y 3m).<br><br>Severe |

Appendix A. Clinical details of the children who had proton spectroscopy d, days: w, weeks: m, months y, years: LSCS, lower segment Caesarian section: VD, vaginal delivery: HIE, hypoxic ischaemic encephalopathy: US, ultrasound: MRI, magnetic resonance imaging: CT computed tomography: EEG, electroencephalography.

| Patient | PCA at birth(w)<br>PNA at exam<br>PCA at exam(w) | Birth wt(g) | Apgars/<br>delivery details | Clinical and Imaging findings | Outcome (age)<br><br>Outcome category |
|---|---|---|---|---|---|
| MB | 38<br>4w<br>42 | Not known | 0(1), 2(5).<br>Emergency LSCS. | Group B streptococcal septicaemia. HIE grade III.<br>US; (4w) ventricular dilatation, cerebral atrophy, multiple parenchymal cysts.<br>Isoelectric EEG.<br>Early CT; cerebral oedema.<br>MRI; (4w), marked cystic changes, subdural fluid.<br>MRI; (8m) very dilated ventricles, thin rim of brain tissue. | Spastic quadriplegia, fits, severe developmental delay (5y).<br><br>Severe |
| KH | 40<br>18d<br>42 | 3500 | 9(1),10(5).<br>VD. | Post delivery hypoxia 2º to persistent fetal circulation, HIE grade II.<br>US normal.<br>EEG normal (3w).<br>MRI; (3m), old bilateral thalamic lesions. | Normal (2y).<br><br>Normal |
| MH | 39<br>24d<br>42.5 | 2480 | 8(1), 10(10).<br>Spontaneous vaginal delivery. | Mildly abnormal facies. Poor feeding.<br>? Fetal alcohol syndrome. | Failure to thrive. Poor feeding, won't take solids. Developmentally normal (2y).<br><br>Other |

Appendix A. Clinical details of the children who had proton spectroscopy d, days: w, weeks: m, months y, years: LSCS, lower segment Caesarian section: VD, vaginal delivery: HIE, hypoxic ischaemic encephalopathy: US, ultrasound: MRI, magnetic resonance imaging: CT computed tomography: EEG, electroencephalography.

| Patient | PCA at birth(w)<br>PNA at exam<br>PCA at exam(w) | Birth wt(g) | Apgars/<br>delivery details | Clinical and Imaging findings | Outcome (age)<br><br>Outcome category |
|---|---|---|---|---|---|
| TH | 40<br>20d,9m<br>43, 80 | 3590 | 0(1), 4(5), 8(10).<br>Emergency LSCS after 20 minutes of attempted forceps, severe fetal bradycardia.<br>Cord pH 6.75. | Birth asphyxia, HIE grade II.<br>Early US; normal.<br>Later US; thalamic densities, cortical atrophy.<br>EEG; discontinuous, no frank seizures. | Spastic quadriplegia, fits, severe developmental delay, microcephaly (5y)<br><br>Severe |
| SB | 42<br>1w<br>43 | 3090 | 1(1), 4(5), 7(10),10(15).<br>Forceps. | Bilateral pneumothoraces. Birth asphyxia, HIE grade I.<br>US normal.<br>EEG normal. | Normal (3y)<br><br>Normal |
| KF | 42<br>2w<br>44 | 4120 | 1(1), 1(5), 3(10), 4(15).<br>Emergency LSCS for fetal bradycardia <60/minute.<br>Heavy MSL.<br>Cord pH 6.75. | Birth asphyxia, HIE grade II.<br>Convulsions. Hypoglycaemia.<br>US; initially featureless, then developed subcortical flares and later atrophy.<br>EEG; seizures and poor background.<br>MRI; (3w), bilateral basal ganglia lesions and subarachnoid haemorrhage. | Spastic quadriplegia, poor vision, global retardation, fits. (5y).<br><br>Severe |

Appendix A. Clinical details of the children who had proton spectroscopy d, days: w, weeks: m, months y, years: LSCS, lower segment Caesarian section: VD, vaginal delivery: HIE, hypoxic ischaemic encephalopathy: US, ultrasound: MRI, magnetic resonance imaging: CT computed tomography: EEG, electroencephalography.

| Patient | PCA at birth(w)<br>PNA at exam<br>PCA at exam(w) | Birth wt(g) | Apgars/<br>delivery details | Clinical and Imaging findings | Outcome (age)<br><br>Outcome category |
|---|---|---|---|---|---|
| AJ | 43<br>14d<br>45 | 3146 | 7(1), 9(5).<br>Normal VD. | Transient tachypnoea and hypotonia. Frequent vomiting.<br>MRI; normal. | Congenital ocular apraxia, severe hypotonia.<br>Severe global developmental delay<br>? Also metabolic disorder (3y)<br>Severe |
| TruH | 42<br>4w<br>46 | 2650 | 8(1), 9(5).<br>VD.<br>Meconium aspiration. | Persistent fetal circulation.<br>HIE I.<br>US; partial agenesis of the corpus callosum.<br>MRI; basal ganglia lesions. | Normal (2y).<br><br>Normal |
| ME | 38<br>10w<br>48 | Not known | 9(1), 10(5).<br>Elective LSCS.<br>No fetal distress. | Respiratory distress syndrome ventilated for 18hr.<br>Persistent fetal circulation. Renal failure.<br>Abnormal movements and seizures.<br>US; normal (3w).<br>MRI; low signal lesions in thalamus and basal ganglia on right, consistent with previous haemorrhage (1m). | Normal (2y).<br><br>Normal |

Appendix A. Clinical details of the children who had proton spectroscopy d, days: w, weeks: m, months y, years: LSCS, lower segment Caesarian section: VD, vaginal delivery: HIE, hypoxic ischaemic encephalopathy: US, ultrasound: MRI, magnetic resonance imaging: CT computed tomography: EEG, electroencephalography.

| Patient | PCA at birth(w)<br>PNA at exam<br>PCA at exam(w) | Birth wt(g) | Apgars/<br>delivery details | Clinical and Imaging findings | Outcome (age)<br><br>Outcome category |
|---|---|---|---|---|---|
| IV | 39<br><br>10w, 8m<br><br>49, 72 | 2760 | 7(1), 9(5).<br>VD, type II dips. | Birth asphyxia, HIE grade II. Poor feeding, irritable odd movements.<br>US; mild irregular ventricular dilatation.<br>MRI; ? subarachnoid and thalamic haemorrhage on left.<br>EEG normal. | Relative acquired microcephaly. Normal development (5y).<br><br>Normal |
| RS | 40<br><br>4m<br><br>57 | 3278 | 3(1), 4(5), 7(10).<br>Forceps for heavy MSL and fetal tachycardia.<br>Cord pH 7.08. | Birth asphyxia, HIE grade II.<br>US; (48h), gross cerebral oedema, no intraventricular haemorrhage.<br>CT; cerebral oedema (1w). EEG; burst suppression.<br>MRI; (4m), high signal in both basal ganglia suggestive of haemorrhage. Dilated ventricles, prominent sulci suggestive of atrophy. | Severe microcephaly, spastic quadriplegia, fits (2y).<br><br>Severe |
| NT | 35<br><br>5m, 14m<br><br>57, 96 | 2180 | 8(1), 10(5).<br>VD.<br>Mother severe asthmatic, with significant attacks during pregnancy.<br>No fetal distress. | Abnormal myoclonic movements from birth.<br>Hypoglycaemia.<br>US; early thalamic densities, cerebral atrophy, subcortical cysts.<br>EEG; no fits. | Spastic quadriplegia, severe global retardation, hypsarrythmia (5y).<br><br>Severe |

Appendix A. Clinical details of the children who had proton spectroscopy d, days: w, weeks: m, months y, years: LSCS, lower segment Caesarian section: VD, vaginal delivery: HIE, hypoxic ischaemic encephalopathy: US, ultrasound: MRI, magnetic resonance imaging: CT computed tomography: EEG, electroencephalography.

| Patient | PCA at birth(w)<br>PNA at exam<br>PCA at exam(w) | Birth wt(g) | Apgars/<br>delivery details | Clinical and Imaging findings | Outcome (age)<br><br>Outcome category |
|---|---|---|---|---|---|
| CM | 42<br>15m<br>67 | 3860 | Forceps delivery. | Floppy at birth, ?birth asphyxia, ? HIE I, infantile spasms.<br>Gross motor intellectual delay.<br>? metabolic problem.<br>MRI; (11m) poor myelination, some atrophy. All other investigations negative. | Cortically blind, spastic quadriplegia, severe mental handicap, fits (2y).<br><br>Severe |
| AS | 42<br>25m<br>110 | 3250 | 3(1),7(5),8(10).<br>Emergency LSCS.<br>HR<60 for 40 mins. | Birth asphyxia, HIE II.<br>US; thalamic densities.<br>CT; generalised white matter low attenuation, consistent with asphyxia.<br>EEG; no fits, discontinuous low amplitude. | Athetoid quadriplegia with some spasticity.<br>Severe epilepsy (5y).<br><br>Severe |
| RH | 41<br>28m<br>124 | 2950 | 7(1),10(5).<br>VD.<br>Mother taking disopyramide, 9th pregnancy, 4th live birth. | Developmental delay.<br>US and EEG normal.<br>Chromosomes normal.<br>MRI; (2y) normal myelination, some high signal in lentiform nuclei compatible with basal ganglia lesions. | Developmental delay, hypotonia, dysmorphic features (4y).<br><br>Moderate |

Appendix A. Clinical details of the children who had proton spectroscopy d, days: w, weeks: m, months y, years: LSCS, lower segment Caesarian section: VD, vaginal delivery: HIE, hypoxic ischaemic encephalopathy: US, ultrasound: MRI, magnetic resonance imaging: CT computed tomography: EEG, electroencephalography.

| Patient | PCA at birth (w)<br>PNA at exam<br>PCA at exam (w) | Birth wt.(g) | Apgars/delivery details. | Clinical and imaging findings | Outcome (age)<br>Outcome category |
|---|---|---|---|---|---|
| N T | 35<br>19d, 8m, 14m<br>38, 73, 96 | 2180 | 8(1), 10(5).<br>VD, type II dips.<br>No fetal distress.<br>No resuscitation.<br>Mother asthmatic, severe attacks during pregnancy. | Poor feeding and abnormal myoclonic movements from birth. Hypoglycaemia.<br>US; early thalamic densities, cerebral atrophy, subcortical cysts.<br>Early EEG; no convulsions.<br>US; (2m), ventricular dilatation and cerebral atrophy. | Severe global retardation, spastic quadriplegia, hypsarrythmia (5y).<br>Severe |
| A C | 35<br>21d<br>38 | 1570 | 8(1), 9(10).<br>VD, type II dips.<br>No resuscitation. | Truncal hypotonia.<br>US; left intraventricular haemmorhage, marked periventricular densities, possible venous infarction.<br>Later US; cystic breakdown. | Speech delay.<br>Sensorineural deafness.<br>(2y 4m).<br>Moderate |

Appendix B. Clinical details of the children who had phosphorus spectroscopy d, days: w, weeks: m, months: LSCS, lower segment Caesarian section: VD, vaginal delivery : HIE, hypoxic ischaemic encephalopathy: US, ultrasound: MRI, magnetic resonance imaging: CT computed tomography: EEG, electroencephalography: MSL, meconium stained liquor.

| Patient | PCA at birth (w)<br>PNA at exam<br>PCA at exam (w) | Birth wt.(g) | Apgars/delivery details. | Clinical and imaging findings | Outcome (age)<br>Outcome category |
|---|---|---|---|---|---|
| T F | 36<br>15d<br>38 | 3200 | 5(1), 6(5).<br>VD.<br>Resuscitation.<br>Cord pH 7.1. | Major feeding difficulties.<br>Hypotonia, convulsions ? cause.<br>US; right occipital echogenicity.<br>CT; (6m), right subarachnoid haemorrhage and thalamic cysts. | Developmental delay (5-6m at 8m). Hypotonia. Delayed (2y), diagnosis unknown.<br>? arterio-hepatic dysplasia.<br>Moderate |
| DT | 37<br>5d<br>38 | 3100 | 9(1), 10(5).<br>Kiellands forceps.<br>No fetal distress. | Poor feeding, neonatal convulsions.<br>Lumbar puncture - blood suggestive of subarachnoid haemorrhage.<br>US; ? left IVH.<br>CT; normal.<br>MRI; normal.<br>24hr EEG; normal. | Good, normal (2y).<br>Normal |

Appendix B. Clinical details of the children who had phosphorus spectroscopy d, days: w, weeks: m, months: LSCS, lower segment Caesarian section: VD, vaginal delivery : HIE, hypoxic ischaemic encephalopathy: US, ultrasound: MRI, magnetic resonance imaging: CT computed tomography: EEG, electroencephalography: MSL, meconium stained liquor.

| Patient | PCA at birth (w)<br>PNA at exam<br>PCA at exam (w) | Birth wt.(g) | Apgars/delivery details. | Clinical and imaging findings | Outcome (age)<br>Outcome category |
|---|---|---|---|---|---|
| NatT | 39<br>2d<br>39 | 2410 | 6(1), 9 (5).<br>NVD. | Small for dates, neurologically normal.<br>US; normal. | Normal (4y).<br>Control |
| WC | 40<br>6d<br>41 | 3200 | 7(1), 8(5).<br>Emergency LSCS for fetal distress, meconium staining. Cord/fetal scalp pH within normal limits. | Feeding difficulties.<br>US; normal.<br>MRI; left thalamic haemmorhage.<br>EEG normal. | Normal (3y)<br>Normal |

Appendix B. Clinical details of the children who had phosphorus spectroscopy d, days: w, weeks: m, months: LSCS, lower segment Caesarian section: VD, vaginal delivery : HIE, hypoxic ischaemic encephalopathy: US, ultrasound: MRI, magnetic resonance imaging: CT computed tomography: EEG, electroencephalography: MSL, meconium stained liquor.

| Patient | PCA at birth (w)<br>PNA at exam<br>PCA at exam (w) | Birth wt.(g) | Apgars/delivery details. | Clinical and imaging findings | Outcome (age)<br>Outcome category |
|---|---|---|---|---|---|
| ML | 40<br>7d, 21d<br>41, 43 | 3805 | 3(1) 9(5)<br>VD; 32h labour, pethidine 100mg x 3. Floppy at birth, resuscitation needed. | Birth asphyxia, HIE II. Jittery, convulsions.<br>US; widespread diffuse parenchymal densities which became cysts by 10d.<br>CT; gross ischaemic changes involving whole cortex.<br>EEG; extremely discontinuous, low amplitude and seizures. MRI; extensive subcortical cysts in both hemispheres, bilateral haemorrhagic lesions in thalami and basal ganglia. | Spastic quadriplegia, fits, severe developmental delay (4y).<br>Severe |
| JM | 41<br>2d, 4d, 7d<br>41, 41.5, 42 | 3240 | 3(1),6(5)<br>Type II dips. NVD. | Birth asphyxia, HIE grade II. Hypoglycaemia.<br>US; initially featureless.<br>At 2w cortical and subcortical cysts.<br>MRI; (9m), cysts in frontal lobes, bilateral basal ganglia lesions. | Severe developmental delay, dystonic, fits, microcephalic,quadriplegic (5y).<br>Severe |

Appendix B. Clinical details of the children who had phosphorus spectroscopy d, days: w, weeks: m, months: LSCS, lower segment Caesarian section: VD, vaginal delivery : HIE, hypoxic ischaemic encephalopathy: US, ultrasound: MRI, magnetic resonance imaging: CT computed tomography: EEG, electroencephalography: MSL, meconium stained liquor.

| Patient | PCA at birth (w)<br>PNA at exam<br>PCA at exam (w) | Birth wt.(g) | Apgars/delivery details. | Clinical and imaging findings | Outcome (age)<br>Outcome category |
|---|---|---|---|---|---|
| GBS | 40<br>10d<br>41.5 | 3450 | 9(1),10(5).<br>Forceps | Birth asphyxia, HIE grade II. Neonatal convulsions.<br>US; right parietal density. CT; right parietal infarct and bilateral occipital ischaemic areas consistent with parasaggital injury.<br>MRI (3w) right frontoparietal bleed and bilateral occipital infarcts consistent with parasaggital injury.<br>MRI (9m), myelination slightly less on right.<br>Low signal lesion on right on inversion recovery. | Normal. (5y).<br>Normal |
| ST | 41<br>5d<br>42 | 2975 | Apgars N/K.<br>No birth information. | Congenital Cytomegalovirus | Deaf, mild developmental delay (3y 4m).<br>Moderate |

Appendix B. Clinical details of the children who had phosphorus spectroscopy d, days: w, weeks: m, months: LSCS, lower segment Caesarian section: VD, vaginal delivery : HIE, hypoxic ischaemic encephalopathy: US, ultrasound: MRI, magnetic resonance imaging: CT computed tomography: EEG, electroencephalography: MSL, meconium stained liquor.

| Patient | PCA at birth (w)<br>PNA at exam<br>PCA at exam (w) | Birth wt.(g) | Apgars/delivery details. | Clinical and imaging findings | Outcome (age)<br>Outcome category |
|---|---|---|---|---|---|
| CLW | 41<br>8d, 13d<br>42, 43 | 3650 | 6(1) 10(5)<br>Forceps for delay in 2nd stage. Type II dips. | Neonatal convulsions.<br>US; large left thalamic haemmorhage centred on basal ganglia.<br>MRI; (2m), bilateral thalamic haemmorhage, left greater than right.<br>MRI; (1y), normal myelination on right, delayed on left in area of infarct. | Right hemiplegia. (3y 4m).<br>Severe |
| MD | 39<br>21d<br>42 | 3200 | 8(1), 9(5).<br>Normal birth. | Congenital Cytomegalovirus<br>MRI; (1m), left IVH not shown on CT. | Died at 3m, portal hypertension, massive splenic enlargement (brain normal at PM).<br>Other |

Appendix B. Clinical details of the children who had phosphorus spectroscopy d, days: w, weeks: m, months: LSCS, lower segment Caesarian section: VD, vaginal delivery : HIE, hypoxic ischaemic encephalopathy: US, ultrasound: MRI, magnetic resonance imaging: CT computed tomography: EEG, electroencephalography: MSL, meconium stained liquor.

| Patient | PCA at birth (w)<br>PNA at exam<br>PCA at exam (w) | Birth wt.(g) | Apgars/delivery details. | Clinical and imaging findings | Outcome (age)<br>Outcome category |
|---|---|---|---|---|---|
| AR | 40<br>13d<br>42 | 3010 | 3(1), 4(5).<br>Emergency LSCS after 4h of type II dips.<br>Cord pH 6.95 | Birth asphyxia, HIE grade II.<br>Early US; fuzzy, loss of definition.<br>Late US; cortical/subcortical cysts, cerebral atrophy.<br>EEG; isoelectric, some sharp waves at vertex. | Spastic quadriplegia, microcephaly, convulsions (2y 3m).<br>Severe |
| CK | 41<br>6d<br>42 | 3490 | 5(1) 6(5) 6(10):<br>Failed ventouse.<br>Forceps for lift out and MSL.<br>Cord pH 6.93 | Birth asphyxia, HIE I. Shocked due to subaponeurotic haemorrhage. Hypotonia.<br>US; small left thalamic lesion.<br>MRI; (2w) high signal suggestive of basal gangia haemorrhage, subarachnoid and subdural haemorrhage<br>MRI; (3m)reduction of previous changes, myelination normal. | Normal (2y).<br>Normal |

Appendix B. Clinical details of the children who had phosphorus spectroscopy d, days: w, weeks: m, months: LSCS, lower segment Caesarian section: VD, vaginal delivery : HIE, hypoxic ischaemic encephalopathy: US, ultrasound: MRI, magnetic resonance imaging: CT computed tomography: EEG, electroencephalography: MSL, meconium stained liquor.

| Patient | PCA at birth (w)<br>PNA at exam<br>PCA at exam (w) | Birth wt.(g) | Apgars/delivery details. | Clinical and imaging findings | Outcome (age)<br>Outcome category |
|---|---|---|---|---|---|
| KR | 42<br>2d<br>42 | 3530 | 0(1),0(5)<br>Emergency LSCS for fetal distress.<br>Type II dips.<br>Resuscitation. | Birth asphyxia, HIE II.<br>EEG; fits, normal background.<br>MRI; (8m), normal. | Good, normal (5y).<br>Normal |
| TH | 40<br>18d, 9m<br>42.5, 79 | 3590 | 0(1), 4(5), 8(10).<br>Emergency LSCS after 20 minutes of attempted forceps, severe fetal bradycardia.<br>Cord pH 6.75 | Birth asphyxia, HIE II.<br>Early US; normal<br>Later US; thalamic densities, cortical atrophy.<br>EEG; discontinuous, no frank seizures. | Spastic quadriplegia, fits, severe developmental delay, microcephaly (5y).<br>Severe |

Appendix B. Clinical details of the children who had phosphorus spectroscopy d, days: w, weeks: m, months: LSCS, lower segment Caesarian section: VD, vaginal delivery : HIE, hypoxic ischaemic encephalopathy: US, ultrasound: MRI, magnetic resonance imaging: CT computed tomography: EEG, electroencephalography: MSL, meconium stained liquor.

| Patient | PCA at birth (w)<br>PNA at exam<br>PCA at exam (w) | Birth wt.(g) | Apgars/delivery details. | Clinical and imaging findings | Outcome (age)<br>Outcome category |
|---|---|---|---|---|---|
| CO'K | 37<br>6w<br>43 | 2700 | 5(1) 9(5)<br>VD. | Swallowing difficulty, hypotonia, probable congenital abnormality.<br>US normal.<br>EEG normal.<br>MRI normal. | Mild delay (3y).<br>Moderate |
| KF | 42<br>5d, 14d<br>43, 44 | 4120 | 1(1), 1(5), 3(10), 4(15).<br>Emergency LSCS for fetal bradycardia < 60/minute.<br>Heavy MSL.<br>Cord pH 6.75. | Birth asphyxia, HIE grade II.<br>Convulsions. Hypoglycaemia.<br>US: initially featureless, then developed subcortical flares and later atrophy.<br>MRI; (3w), bilateral basal ganglia haemorrhage and subarachnoid haemorrhage.<br>EEG; seizures and poor background. | Spastic quadriplegia, poor vision,<br>global retardation, fits (5y).<br>Severe |

Appendix B. Clinical details of the children who had phosphorus spectroscopy d, days: w, weeks: m, months: LSCS, lower segment Caesarian section: VD, vaginal delivery : HIE, hypoxic ischaemic encephalopathy: US, ultrasound: MRI, magnetic resonance imaging: CT computed tomography: EEG, electroencephalography: MSL, meconium stained liquor.

| Patient | PCA at birth (w)<br>PNA at exam<br>PCA at exam (w) | Birth wt.(g) | Apgars/delivery details. | Clinical and imaging findings | Outcome (age)<br>Outcome category |
|---|---|---|---|---|---|
| SB | 42<br>6d<br>43 | 3090 | 1(1), 4(5), 7(10), 10(15). Grade II MSL and fetal tachycardia, type II dips in 2nd stage. Emergency LSCS. Resuscitation. | Birth asphyxia, HIE grade I. Bilateral pneumothoraces. Abnormal movements. No convulsions. US; bright thalami. EEG; normal. | Good, normal (3y).<br>Normal |
| RhD | 42<br>11d<br>43.5 | 3700 | 9(1), 10(5). VD. No fetal distress. | Neonatal convulsions, ? cause. US; normal. CT; normal. EEG; normal. | Good, normal (2y).<br>Normal |

Appendix B. Clinical details of the children who had phosphorus spectroscopy d, days: w, weeks: m, months: LSCS, lower segment Caesarian section: VD, vaginal delivery : HIE, hypoxic ischaemic encephalopathy: US, ultrasound: MRI, magnetic resonance imaging: CT computed tomography: EEG, electroencephalography: MSL, meconium stained liquor.

| Patient | PCA at birth (w)<br>PNA at exam<br>PCA at exam (w) | Birth wt.(g) | Apgars/delivery details. | Clinical and imaging findings | Outcome (age)<br><br>Outcome category |
|---|---|---|---|---|---|
| JW | 40<br><br>28d<br><br>44 | 3120 | 7(1), 10(5).<br>Low forceps for maternal exhaustion. | Poor feeding at 2w. Reflux oesophagitis.<br>US; normal.<br>EEG normal. | Riley-Day syndrome.<br>Nissen's and gastrostomy.<br>Developmental delay (4y).<br><br>Moderate |
| CH | 41<br><br>21d<br><br>44 | 4000 | 6(1), 7(5), 7(10).<br>VD, prolonged rupture of membranes.<br>No fetal distress. | Birth asphyxia, HIE grade I, although initial signs could have been due to other problems.<br>Congenital CMV. Myelofibrosis, mild neurological abnormalities.<br>US; some thalamic streaks.<br>EEG; normal. | Normal (4y).<br><br>Normal |

Appendix B. Clinical details of the children who had phosphorus spectroscopy d, days: w, weeks: m, months: LSCS, lower segment Caesarian section: VD, vaginal delivery : HIE, hypoxic ischaemic encephalopathy: US, ultrasound: MRI, magnetic resonance imaging: CT computed tomography: EEG, electroencephalography: MSL, meconium stained liquor.

| Patient | PCA at birth (w)<br>PNA at exam<br>PCA at exam (w) | Birth wt.(g) | Apgars/delivery details. | Clinical and imaging findings | Outcome (age)<br><br>Outcome category |
|---|---|---|---|---|---|
| JMcG | 41<br>21d<br>44 | 3400 | 4(1), 8(5), 10(7).<br>Forceps for fetal distress and MSL. | Neonatal convulsions.<br>US; midline shift and large left echodensity.<br>MRI; large left middle cerebral artery infarct with extensive involvement of left frontal and parietal lobes.<br>EEG; assymetrical with poor background on left. | Dense right hemiplegia (2y 8m).<br><br>Severe |
| AS | 42<br>13d<br>44 | 3250 | 3(1), 7(5), 8(10), 8(20).<br>Failed Kiellands and ventouse. Emergency LSCS for fetal heart rate <60 for 40 minutes. | Birth asphyxia, HIE grade II.<br>US; thalamic densities.<br>CT; generalised white matter low attenuation consistent with asphyxia.<br>EEG; no seizures, discontinuous low amplitude. | Spastic quadriplegia, severe epilepsy, microcephalic, athetoid cerebral palsy (3y 3m).<br><br>Severe |

Appendix B. Clinical details of the children who had phosphorus spectroscopy d, days: w, weeks: m, months: LSCS, lower segment Caesarian section: VD, vaginal delivery : HIE, hypoxic ischaemic encephalopathy: US, ultrasound: MRI, magnetic resonance imaging: CT computed tomography: EEG, electroencephalography: MSL, meconium stained liquor.

| Patient | PCA at birth (w)<br>PNA at exam<br>PCA at exam (w) | Birth wt.(g) | Apgars/delivery details. | Clinical and imaging findings | Outcome (age)<br>Outcome category |
|---|---|---|---|---|---|
| MG | 38<br>7.5w, 9w<br>45.5, 47 | 2500 | 3(1), 3(5), 5(10).<br>VD.<br>Required intubation at birth. | Ventilator dependent. Hypotonia.<br>All investigations negative. | Died at 10w.<br>Other |
| IV | 39<br>7w<br>46 | 2760 | 7(1),9(5).<br>VD. Type II dips. | Poor feeding, irritable odd movements.<br>Birth asphyxia, HIE grade I/II ?<br>US; mild irregular venticular dilatation.<br>MRI; ? subarachnoid and thalamic haemorrhage on left.<br>EEG; normal. | Relative acquired microcephaly.<br>Normal development (5y).<br>Normal |

Appendix B. Clinical details of the children who had phosphorus spectroscopy d, days: w, weeks: m, months: LSCS, lower segment Caesarian section: VD, vaginal delivery : HIE, hypoxic ischaemic encephalopathy: US, ultrasound: MRI, magnetic resonance imaging: CT computed tomography: EEG, electroencephalography: MSL, meconium stained liquor.

| Patient | PCA at birth (w)<br>PNA at exam<br>PCA at exam (w) | Birth wt.(g) | Apgars/delivery details. | Clinical and imaging findings | Outcome (age)<br><br>Outcome category |
|---|---|---|---|---|---|
| AA | 40<br>7w<br>47 | 2060 | 9(1), 10(5).<br>Emergency LSCS for failure to progress. | Poor feeding, intractable fitting, pneumonia.<br>?cranio-oculo-facial syndrome.<br>US; basically normal but ? simple gyral pattern.<br>EEG; focal abnormal epileptic discharges. | Died (10m).<br>No post- mortem.<br><br>Other |
| RM | 41<br>2m<br>50 | 4370 | Apgars N/K.<br>Forceps for fetal bradycardia. | Left sided convulsion.<br>US; left middle cerebral artery infarct involving left thalamus.<br>MRI; (1y), extensive left middle cerebral artery infarction with Wallerian degeneration.<br>EEG; fast waves in left central and parietal regions, normal on right. | Dense right hemiplegia, hypotonia (2y 8m).<br><br>Severe |

Appendix B. Clinical details of the children who had phosphorus spectroscopy d, days: w, weeks: m, months: LSCS, lower segment Caesarian section: VD, vaginal delivery : HIE, hypoxic ischaemic encephalopathy: US, ultrasound: MRI, magnetic resonance imaging: CT computed tomography: EEG, electroencephalography: MSL, meconium stained liquor.

| Patient | PCA at birth (w)<br>PNA at exam<br>PCA at exam (w) | Birth wt.(g) | Apgars/delivery details. | Clinical and imaging findings | Outcome (age)<br>Outcome category |
|---|---|---|---|---|---|
| LO'N | 38<br>3m<br>51 | 2430 | 9(1), 9(5).<br>Elective LSCS(breech)<br>No fetal distress.<br>No resuscitation. | Persistent fetal circulation. Hypotonia, mild dysmorphism, no diagnosis.<br>Serial US normal.<br>EEG normal. | Moderate global delay (2y 8m).<br>Moderate |
| RS | 42<br>18w<br>60 | 3278 | 3(1), 4(5), 7(10):<br>Forceps for heavy MSL and fetal tachycardia.<br>Cord pH 7.08. | Severe birth asphyxia, HIE grade II.<br>US; (48h), gross cerebral oedema, no intraventricular haemorrhage.<br>CT; cerebral oedema.<br>EEG; abnormal burst suppression. | Severe microcephaly, spastic quadriplegia, fits (2y).<br>Severe |

Appendix B. Clinical details of the children who had phosphorus spectroscopy d, days: w, weeks: m, months: LSCS, lower segment Caesarian section: VD, vaginal delivery : HIE, hypoxic ischaemic encephalopathy: US, ultrasound: MRI, magnetic resonance imaging: CT computed tomography: EEG, electroencephalography: MSL, meconium stained liquor.

| Patient | PCA at birth (w)<br>PNA at exam<br>PCA at exam (w) | Birth wt.(g) | Apgars/delivery details. | Clinical and imaging findings | Outcome (age)<br>Outcome category |
|---|---|---|---|---|---|
| TMcL | 37<br>9m<br>76 | 1650 | 6(1), 7(10).<br>Precipitate VD.<br>Meconium.<br>Resuscitation with oxygen and suction. | Intrauterine growth retardation. Hypotonia.<br>US; (6d), intraventricular haemmorhage, periventricular leukomalacia, ventricular dilatation.<br>US; (1m), bilateral and 3rd ventricular dilatations, extensive left sided cortical and subcortical cysts. | Spastic quadriplegia, cerebral palsy, epilepsy, severe motor delay, visual loss (4y).<br>Severe |
| PP | 38<br>9m<br>77 | Not known | 9(1), 10(5).<br>VD. | Cardiorespiratory arrest at 9m due to electrocution, about 30 minutes without effective cardiac output. Fitting for 24 hours.<br>CT; (1 y), prominent sulci and dilated ventricles. | Moderate delay. Athetoid cerebral palsy (4y).<br>Severe |

Appendix B. Clinical details of the children who had phosphorus spectroscopy d, days: w, weeks: m, months: LSCS, lower segment Caesarian section: VD, vaginal delivery : HIE, hypoxic ischaemic encephalopathy: US, ultrasound: MRI, magnetic resonance imaging: CT computed tomography: EEG, electroencephalography: MSL, meconium stained liquor.

| Patient | PCA at birth (w)<br>PNA at exam<br>PCA at exam (w) | Birth wt.(g) | Apgars/delivery details. | Clinical and imaging findings | Outcome (age)<br>Outcome category |
|---|---|---|---|---|---|
| RV | 39<br>9m<br>78 | 2200 | 2(1), 8(5).<br>Emergency LSCS for sinusoidal CTG. | Intrauterine growth retardation. Floppy, irritable.<br>Hypoglycaemia.<br>US; ventricular diameter irregular.<br>MRI and CT at 3m; dilated ventricles, PVL and loss of cerebellar substance. | Hypotonic, feeding difficulties, quadriplegic.<br>Died post operatively (Nissen's), from unexplained cardiorespiratory arrest.<br>Severe |
| RB | 38<br>31m<br>177 | 3005 | Elective LSCS.<br>No resuscitation. | Hypotonia at 5m, diagnosis unknown.<br>US; normal.<br>EEG; normal.<br>Muscle biopsy normal, nerve conduction normal, chromosomes normal,<br>MRI; normal. | Poor (6.5y).<br>Severe |

Appendix B. Clinical details of the children who had phosphorus spectroscopy d, days: w, weeks: m, months: LSCS, lower segment Caesarian section: VD, vaginal delivery : HIE, hypoxic ischaemic encephalopathy: US, ultrasound: MRI, magnetic resonance imaging: CT computed tomography: EEG, electroencephalography: MSL, meconium stained liquor.

| Patient | PCA at birth (w)<br>PNA at exam<br>PCA at exam (w) | Birth wt.(g) | Apgars/delivery details. | Clinical and imaging findings | Outcome (age)<br>Outcome category |
|---|---|---|---|---|---|
| SJ | 33<br>3y 3m<br>202 | Not known | No birth details known. | Prematurity. Necrotizing enterocolitis, cardiorespiratory arrest in NNU.<br>US; subcortical cysts and periventricular leukomalacia, after arrest. | Spastic quadriplegia, microcephaly, low IQ. (6y 6m).<br>Severe |
| TB | 36<br>3y 6m<br>218 | 3600 | VD - breech. | Birth asphyxia, cerebellar hyoplasia. | Intellectually normal, cannot stand or walk (6y).<br>Severe |

Appendix B. Clinical details of the children who had phosphorus spectroscopy d, days: w, weeks: m, months: LSCS, lower segment Caesarian section: VD, vaginal delivery : HIE, hypoxic ischaemic encephalopathy: US, ultrasound: MRI, magnetic resonance imaging: CT computed tomography: EEG, electroencephalography: MSL, meconium stained liquor.

| Patient | PCA at birth (w)<br>PNA at exam<br>PCA at exam (w) | Birth wt.(g) | Apgars/delivery details. | Clinical and imaging findings | Outcome (age)<br>Outcome category |
|---|---|---|---|---|---|
| RD | 40<br>4y 3m<br>261 | 4120 | Ventouse for malpresentation.<br>Bleeding in second trimester | Severe convulsions.<br>US; dilatation of ventricles, cerebral atrophy.<br>EEG; hypsarrhythmia.<br>CT; cerebral atrophy. | Very poor, microcephalic, spastic quadriplegia (7y).<br>Severe |

Appendix B. Clinical details of the children who had phosphorus spectroscopy d, days: w, weeks: m, months: LSCS, lower segment Caesarian section: VD, vaginal delivery : HIE, hypoxic ischaemic encephalopathy: US, ultrasound: MRI, magnetic resonance imaging: CT computed tomography: EEG, electroencephalography: MSL, meconium stained liquor.

# APPENDIX C

Table showing absolute peak height measurements and calculated peak height ratios from 22 adult volunteers (6 female, 16 male) with no known neurological abnormalities. The spectra were acquired under the same conditions and from the same region of brain as described for the paediatric spectra. The mean for NAA/Cho is 3.6+/-0.59 (range 2.9 - 4.8); the mean for NAA/Cr is 3.5+/-0.71 (range 2.4 - 4.8); the mean for Cho/Cr is 1.0 +/- 0.20 (range 0.7 - 1.3).

| | NAA | Cho | Cr | NAA/Cho | NAA/Cr | Cho/Cr |
|---|---|---|---|---|---|---|
| 1 | 143.0 | 30.0 | 44.0 | 4.8 | 3.2 | .7 |
| 2 | 105.0 | 30.0 | 43.0 | 3.5 | 2.4 | .7 |
| 3 | 116.0 | 33.0 | 26.0 | 3.5 | 4.5 | 1.3 |
| 4 | 131.0 | 32.0 | 37.0 | 4.1 | 3.5 | .9 |
| 5 | 122.0 | 40.0 | 31.0 | 3.0 | 4.0 | 1.3 |
| 6 | 123.0 | 40.0 | 34.0 | 3.0 | 4.0 | 1.3 |
| 7 | 122.0 | 40.0 | 39.0 | 3.0 | 3.1 | 1.0 |
| 8 | 122.0 | 41.0 | 40.0 | 3.0 | 3.0 | 1.0 |
| 9 | 97.0 | 34.0 | 32.0 | 2.9 | 3.0 | 1.0 |
| 10 | 132.0 | 28.0 | 29.0 | 4.7 | 4.6 | 1.0 |
| 11 | 144.0 | 40.0 | 30.0 | 3.6 | 4.8 | 1.3 |
| 12 | 112.0 | 36.0 | 46.0 | 3.1 | 2.4 | .8 |
| 13 | 122.0 | 37.0 | 32.0 | 3.3 | 3.8 | 1.2 |
| 14 | 125.0 | 35.0 | 31.0 | 3.6 | 4.0 | 1.1 |
| 15 | 140.0 | 32.0 | 42.0 | 4.4 | 3.3 | .8 |
| 16 | 116.0 | 37.0 | 47.0 | 3.1 | 2.5 | .8 |
| 17 | 129.0 | 33.0 | 38.0 | 3.9 | 3.4 | .9 |
| 18 | 122.0 | 35.0 | 39.0 | 3.5 | 3.1 | .9 |
| 19 | 124.0 | 39.0 | 32.0 | 3.2 | 3.9 | 1.2 |
| 20 | 107.0 | 35.0 | 41.0 | 3.1 | 2.6 | .9 |
| 21 | 141.0 | 35.0 | 42.0 | 4.0 | 3.4 | .8 |
| 22 | 130.0 | 30.0 | 31.0 | 4.3 | 4.2 | 1.0 |

*Journal of Computer Assisted Tomography*
14(6):886–894, November/December
© 1990 Raven Press, Ltd., New York

# Proton MR Spectroscopy of the Brain in Infants

Carol J. Peden, Frances M. Cowan, David J. Bryant, Janet Sargentoni, I. Jane Cox, David K. Menon, David G. Gadian, Jimmy D. Bell, and Lilly M. Dubowitz

**Abstract:** Proton magnetic resonance spectroscopy (MRS) was used to study the brain of 2 normal and 15 abnormal infants aged from 33 weeks postmenstrual age (PMA) to 14 months postnatal age. Eleven of the infants were examined on at least two occasions. The principal clinical diagnoses in the abnormal infants were perinatal ischemic and hemorrhagic brain injury. All proton spectra demonstrated peaks that were assigned to *N*-acetylaspartate (NAA), choline containing compounds (Cho), and creatine plus phosphocreatine (Cr). The NAA/Cho and NAA/Cr ratios increased with age, while the Cho/Cr ratio decreased with age in the majority of infants. The NAA/Cho ratio was generally lower in abnormal infants, but the difference was not apparent before 40 weeks (PMA). This ratio was lowest in infants with the severest degree of neurological abnormality. Proton and phosphorus MRS was compared in seven infants. In those with severe brain lesions, early phosphorus spectra were abnormal. On follow-up the phosphorus spectra became normal, but the proton spectra showed persistently low NAA/Cho and NAA/Cr ratios. Proton MRS provides new information that may be complementary to phosphorus MRS in the diagnosis and monitoring of brain development in normal and neurologically damaged infants. **Index Terms:** Magnetic resonance imaging, techniques—Infants—Brain.

Although phosphorus-31 magnetic resonance spectroscopy (MRS) of the brain is established as a valuable prognostic indicator in neonates who have suffered cerebral hypoxic-ischemic damage (1,2), clinical pediatric studies with proton MRS have only recently started.

Promising results with proton MRS have been published in adult studies of the brain where resonances from *N*-acetylaspartate (NAA), choline containing compounds (Cho), creatine and phosphocreatine (Cr), as well as lactate can be identified (3–6). In adult cerebral tumors the NAA/Cho and NAA/Cr ratios are often decreased, while Cho/Cr is frequently increased (3). Elevated lactate is also seen in some tumors (4,5) and in cerebral infarction (6).

The aim of this preliminary study was to acquire proton brain spectra in normal and abnormal infants with neurological abnormalities due principally to perinatal ischemic and hemorrhagic brain injury, to design clinical studies and ascertain possible clinical applications for this technique.

From the Departments of Diagnostic Radiology (C. J. Peden, J. Sargentoni, I. J. Cox, D. K. Menon, D. G. Gadian, and J. D. Bell) and Pediatrics (F. M. Cowan and L. M. Dubowitz), Royal Postgraduate Medical School, Hammersmith Hospital, London, and Picker International, Wembley (D. J. Bryant), England. Address correspondence and reprint requests to Dr. C. J. Peden at NMR Unit, Department of Diagnostic Radiology, Royal Postgraduate Medical School, Hammersmith Hospital, Du Cane Road, London W12 OHS, England.

## MATERIALS AND METHODS

Permission for this study was obtained from the Research Ethics Committee of the Royal Postgraduate Medical School, Hammersmith Hospital. Informed consent was obtained from a parent in each case.

Seventeen infants were examined with proton MRS on 30 occasions. All were referred from the neonatal unit (or follow-up clinic) at either Hammersmith or Queen Charlotte's Hospital. The infants were aged between 33 weeks postmenstrual age (PMA) and 7 months postnatal age (PNA) at the time of their first proton MRS examination.

Full clinical neurological examinations and cranial ultrasound scans were performed repeatedly on all infants. All infants had MR imaging examinations and 11 of the abnormal infants were monitored

with 24 h or standard EEGs. Evoked potentials (visual, auditory, and somatosensory) were done when clinically indicated. Children at follow-up also had Griffith assessments of developmental quotient. The clinical details, current clinical diagnoses, and follow-up dates are listed in Table 1.

Two infants were classified as neurologically normal. The first of these children (Case l) was born at 34 weeks PMA and examined at 16 days and 9 months PNA. He had received four exchange transfusions and phototherapy for hyperbilirubinemia secondary to Rhesus incompatibility. He was neurologically normal on clinical and ultrasound examinations and remained so at follow-up 9 months later. The other infant (Case 2) was born at 37 weeks PMA and examined at 24 days and 8 weeks PNA. He was the twin of a patient (Case 9) in the abnormal group but had no detectable clinical abnormality.

In 14 of the abnormal infants the principal diagnoses were varying degrees of birth asphyxia with or without ultrasound evidence of cortical/subcortical cystic brain injury (7,8). The birth asphyxia was severe in Cases 3–5 and mild/moderate in Cases 8–13. Ultrasound evidence of subcortical/cortical brain injury was severe in Cases 4, 6, 7, and 8 and mild/moderate in Cases 3, 5, 9, 10, 12–16. Six infants also had thalamic densities [unilateral (Cases 10 and 14), bilateral (Cases 3, 5, 7, and 9)], two infants had unilateral intraventricular hemor-

**TABLE 1.** *Clinical details of infants examined with proton and phosphorus MRS*

| Case no. | Birth weight (g) | Post-menstrual age at birth (wks) | Nucleus studied | Postnatal age at examination | | | | Clinical and ultrasound diagnosis | Outcome to date (age) |
|---|---|---|---|---|---|---|---|---|---|
| Neurologically normals | | | | | | | | | |
| 1 | 2,000 | 34 | $^1H$ | 16 days | 9 mos | | | Hyperbilirubinemia | Normal (9 mos) |
| 2 | 3,500 | 37 | $^1H$ | 24 days | 8 wks | | | Normal twin | Normal (12 mos) |
| Group A: severe birth asphyxia and/or extensive parenchymal disease on ultrasound scan | | | | | | | | | |
| 3 | 2,820 | 34 | $^1H$ | 39 days | | | | Severe birth asphyxia, bilateral thalamic hemorrhage | Developmental delay (7 mos) |
| 4 | 3,010 | 40 | $^{31}P$<br>$^1H$ | 13 days<br>18 days | | | | Severe birth asphyxia, cortical/subcortical cysts, cerebral atrophy | Spastic quadriplegia, microcephaly, convulsions (12 mos) |
| 5 | 3,590 | 40 | $^1H/^{31}P$ | 20 days | 9 mos | | | Severe birth asphyxia, thalamic densities, cortical atrophy | Spastic quadriplegia, microcephaly, infantile spasms (9 mos) |
| 6 | 1,410 | 29 | $^1H$ | 24 days | | | | Extensive cystic periventricular leukomalacia | Spastic quadriplegia (12 mos) |
| 7 | 2,180 | 35 | $^{31}P$<br>$^1H$ | 14 days | <br>5 mos | 8 mos | 14 mos<br>14 mos | Early thalamic densities, cerebral atrophy, subcortical cysts | Severe global retardation, spastic (14 mos) |
| 8 | 3,240 | 40 | $^1H/^{31}P$ | 2 days | 4 days | | | Moderate birth asphyxia, hypoglycemia, subcortical cysts | Increased muscle tone (1 mo) |
| Group B: moderate birth asphyxia and/or localized ischemic disease | | | | | | | | | |
| 9 | 2,100 | 37 | $^1H$ | 18 days | 24 days | 8 wks | 12 wks | Moderate birth asphyxia, thalamic densities | Increased muscle tone, severe developmental delay (4 mos), died (6 mos) |
| 10 | 2,530 | 35 | $^1H$ | 10 days | | 8 mos | | Moderate birth asphyxia, polycythemia, left thalamic hemorrhage, porencephalic dilatation of left ventricles | Mild motor delay, slight hypotonia (8 mos) |
| 11 | 1,860 | 35 | $^1H$ | 10 days | | 8 mos | | Mild birth asphyxia, anemia, bilateral germinal layer hemorrhage | Mild increased tone (8 mos) |
| 12 | 2,760 | 39 | $^1H/^{31}P$ | 10 wks | | | | Moderate birth asphyxia, mild irregular ventricular dilation | Increased muscle tone, very irritable (6 mos) |
| 13 | 4,000 | 42 | $^1H/^{31}P$ | 4 wks | | | | Moderate birth asphyxia, myelofibrosis | Moderate developmental delay (3 mos) |
| 14 | 0820 | 25 | $^1H$ | 10 wks | | 14 mos | | Periventricular leukomalacia, left thalamic hemorrhage, right intraventricular hemorrhage | Left facial palsy, quadriplegia, motor delay (13 mos) |
| 15 | 1,570 | 35 | $^1H$<br>$^{31}P$ | 2 wks | <br>3 wks | 11 mos | | Left intraventricular hemorrhage, marked periventricular densities, possible venous infarction | Mild diplegia (12 mos) |
| 16 | 2,000 | 35 | $^1H$ | 25 days | | 11 mos | | Persistent parenchymal echodensities, mild ventricular dilation | Normal (11 mos) |
| Group C: no birth asphyxia or ischemic disease but other neurological disease | | | | | | | | | |
| 17 | 2,800 | 40 | $^1H$ | 2 days | | | | Abnormal facies | Hurler syndrome (3 mos) |

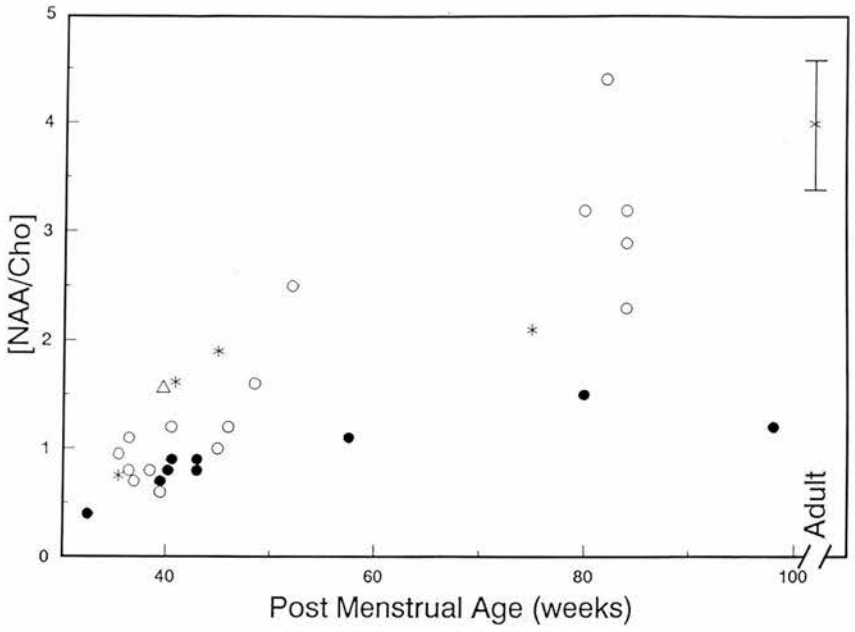



**FIG. 1.** NAA/Cho ratios plotted against postmenstrual age in weeks. The means and SD of 11 adult values are shown for comparison. (*), neurologically normal; (●), Group A—severe birth asphyxia and/or extensive parenchymal disease; (○), Group B—moderate birth asphyxia and/or localized parenchymal disease; (△), Group C—infant with Hurler syndrome.

parenchymal involvement on ultrasound scan) fell below those of the normal infants and the majority of infants in Group B (moderate birth asphyxia and/or localized brain involvement) of comparable age. These differences become more obvious with increasing age.

The NAA/Cho value for the neurologically normal infant (Case 1) was very close to that of the moderately abnormal preterm infants. The NAA/Cho values from the other normal infant (Case 2) at term and 45 weeks PMA were higher than those of the abnormal infants of the same age. The follow-up on Case 1 at 9 months gave an NAA/Cho ratio of 2.1.

The infant with Hurler syndrome (Case 17) had an NAA/Cho ratio of 1.6, which was similar to that of neurologically normal infants of the same age as shown in Fig. 1.

Spectra from the two neurologically normal infants of PMA 36 weeks (Case 1) and 40.5 weeks (Case 2) are shown in Figs. 2 and 3 together with a normal adult spectrum (Fig. 4). There was an increase in the NAA/Cho ratio (0.75 to 5.1) and NAA/Cr ratio (2.0 to 3.7) and a decrease in the Cho/Cr ratio (2.7 to 0.7) with increasing age.

Figures 5 and 6 compare the spectra of normal (Case 2) and abnormal (Case 9) twins at 45 weeks PMA. The abnormal twin had moderate birth asphyxia. The abnormal twin's spectrum has lower NAA/Cho and NAA/Cr ratios than the normal twin's (1.0:1.9 and 1.3:2.5, respectively).

The proton spectrum acquired on follow-up at 9 months PNA of a child in Group A (Case 5) with severe neurological abnormality (Fig. 7) is compared with the follow-up proton spectrum of a child at 10 months PNA in Group B (Case 15) with minor neurological problems (Fig. 8). The first child's proton spectrum had an NAA/Cho ratio of 1.5. In comparison, the spectrum of Case 15 had an NAA/Cho ratio of 4.4, which was within the normal adult range.

### Comparison of Proton and Phosphorus Spectra at Varying Postnatal Ages

Figure 9 shows proton and phosphorus spectra obtained at 48 h after birth from a term infant (Case

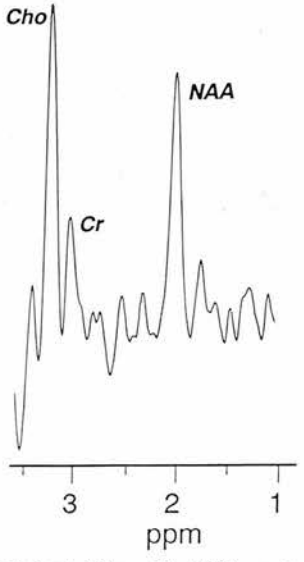



**FIG. 2.** Normal infant (Case 1) at 36 weeks postmenstrual age. Proton spectrum acquired from 27 $cm^3$ voxel, TR 2,000 ms, TE 270 ms, 128 data collections. The NAA/Cho ratio is 0.75. For this and subsequent figures, NAA, *N*-acetyl aspartate; Cr, creatine plus phosphocreatine; Cho, choline containing compounds. The spectra are not scaled vertically for comparison.

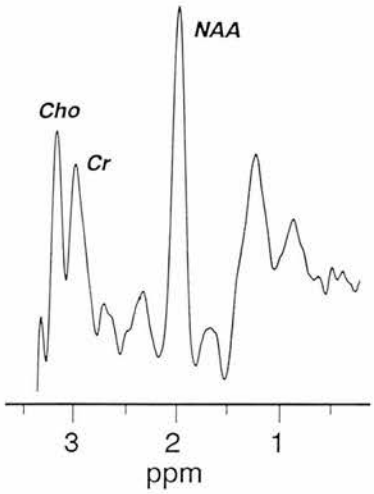



**FIG. 3.** Normal infant (Case 2) at 40.5 weeks postmenstrual age. Proton spectrum acquired from a 64 $cm^3$ voxel. The peak present between 1 and 1.5 ppm is probably due to lipid from skull fat. The NAA/Cho ratio is 1.6.

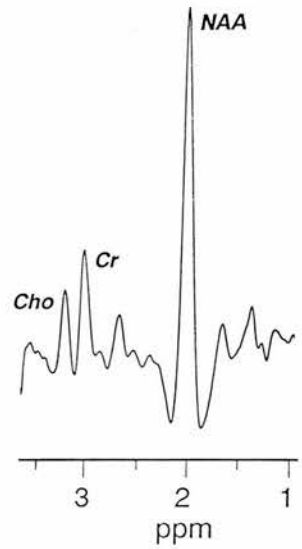



**FIG. 4.** Normal adult. Proton spectrum acquired from a 64 $cm^3$ voxel, TR 2,000 ms, TE 270 ms, 128 data collections. The NAA/Cho ratio is 5.1.

8) with moderate birth asphyxia, hypoglycemia, and later extensive parenchymal cystic lesions on ultrasound scan. The proton spectrum has an NAA/Cho ratio of 0.8, which was very close to that of other less affected infants. The phosphorus spectrum was very abnormal, with a $PCr/P_i$ ratio of 0.5 and pH of 7.28, in comparison with spectra from other infants we have investigated and with the normal data from other groups (1,2).

Figure 10 shows the phosphorus and proton spectra acquired at 13 and 18 days PNA from a term infant (Case 4) who became extremely neurologically abnormal. The NAA/Cho ratio of 0.9 and NAA/Cr ratio of 1.4 from the proton spectrum (Fig. 10a) were very similar to those of the infant illustrated in Fig. 9. The phosphorus spectrum (Fig. 10b) of this infant at 18 days was still abnormal with a $PCr/P_i$ ratio of 0.7 and pH of 7.28.

Figure 11 shows two proton spectra acquired from Case 7 with extensive subcortical cysts, cerebral atrophy, microcephaly, and hypsarrhythmia at 5 and 14 months (Fig. 11a and b) together with a phosphorus spectrum obtained at 14 months (Fig. 11c). The proton spectrum at 5 months (Fig. 11a) shows an NAA/Cho ratio of 1.1 and an NAA/Cr ratio of 1.3, which were reduced in comparison with available normal data. There is little change in these ratios in the proton spectrum (Fig. 11b) obtained 9

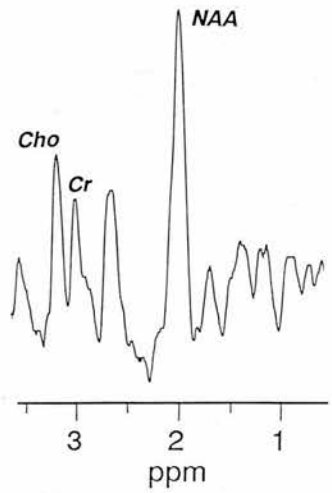



**FIG. 5.** Normal twin (Case 2) at 45 weeks postmenstrual age. Proton spectrum acquired from a 64 $cm^3$ voxel, TR 2,000 ms, TE 270 ms, 128 data collections. The NAA/Cho ratio is 1.9.

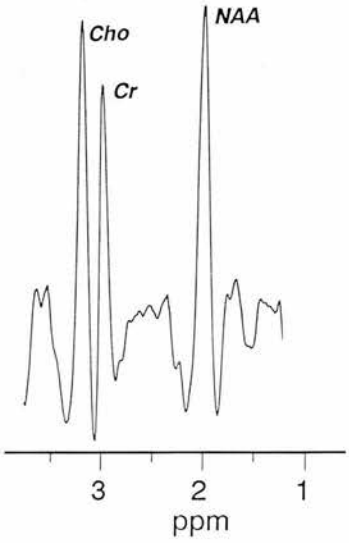



**FIG. 6.** Abnormal twin (Case 9) at 45 weeks postmenstrual age. Proton spectrum acquired from a 64 $cm^3$ voxel, TR 2,000 ms, TE 270 ms, 128 data collections. The NAA/Cho ratio is 1.0.

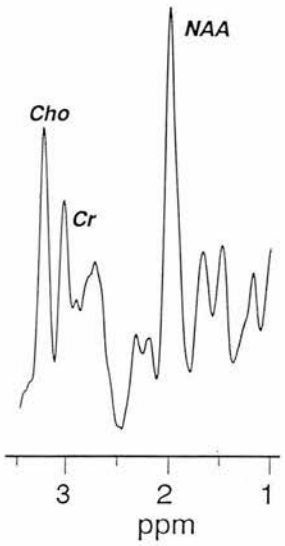



**FIG. 7.** Infant (Case 5) at 80 weeks postmenstrual age (9 months postnatal age). Proton spectrum acquired from a 64 $cm^3$ voxel, TR 2,000 ms, TE 270 ms, 128 data collections. The NAA/Cho ratio is 1.5.

months later. However, the phosphorus spectrum (Fig. 11c) obtained at this stage has a pH of 7.12 and a $PCr/P_i$ ratio of 2.5, within normal limits.

### Saturation Factors

The peak height ratios of the normal infants (Cases 1 and 7) and seven abnormal infants (Cases 5, 7, 8, 10, 11, 14, and 16) at 5,000 and 2,000 ms were used to assess the effects of saturation. These

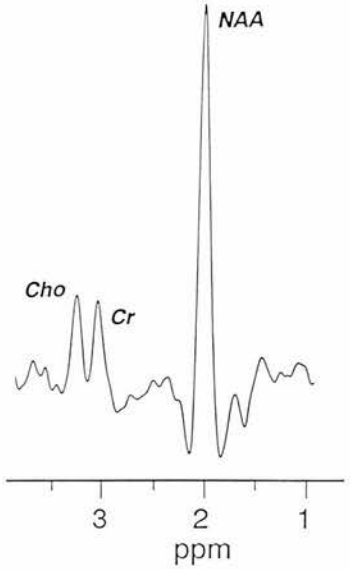



**FIG. 8.** Infant (Case 15) at 82 weeks postmenstrual age (11 months postnatal age). Proton spectrum acquired from a 64 $cm^3$ voxel, TR 2,000 ms, TE 270 ms, 128 data collections. The NAA/Cho ratio is 4.4.

are shown in Table 2; there is little difference observed from adults.

## DISCUSSION

This study has demonstrated increasing NAA/Cho and NAA/Cr ratios with age in the normal and abnormal neonatal brain. There was little difference in saturation factors between adults and normal and abnormal infants so these changes are unlikely to arise from T1 differences. The fact that these changes could arise from T2 differences must be borne in mind, but it was not possible to measure T2 parameters in the limited examination time available.

A similar increase in NAA/Cho and NAA/Cr ratios in the normal infant brain with age has previously been reported by van der Knaap et al. (12). This work and our data are consistent with proton MRS studies of the developing rat brain. One study by Nakada et al. (13) of the fetal rat brain demonstrated Cho and Cr resonances, but virtually no NAA. In another study of the developing rat brain, the concentration of NAA increased from ~0.5 to 5 μmol/g wet weight during the first 21 days of life. Creatinine plus phosphocreatine also increased from ~2 to 5 μmol/g wet weight, while Cho decreased by ~50% from its initial value of 0.7 μmol/g wet weight (14). The greatest change in metabolite ratios was in NAA/Cho, which is in agreement with our data shown in Figs. 1–3.

On the basis of animal studies, it appears that the rise in NAA/Cho with age is due at least partly to an increase in the concentration of NAA. The increase in NAA coincides with myelination (14,15), although any direct causal relationship between the two remains to be established.

Little is known of the function of NAA, but it does appear to be located primarily in neurons rather than in glial cells and its concentration is known to be greater in gray rather than white matter (16). This factor is likely to affect results as the infants grow when voxel placement may result in relatively different amounts of gray and white matter in the volume of study.

The changing NAA/Cho ratio during development may also reflect a reduction in the Cho signal. This signal appears to contain contributions from phosphorylcholine and glycerophosphorylcholine (3,14). A decrease in the Cho signal with age may be analogous to the reduction in phosphorylethanolamine, a constituent of the phosphomonoester peak that is seen with phosphorus MRS in the developing brain (17).

The principal change seen in the spectra of the neurologically abnormal infants was a lower NAA/Cho ratio than in the normal subjects. However, at present we have few normal data and only one

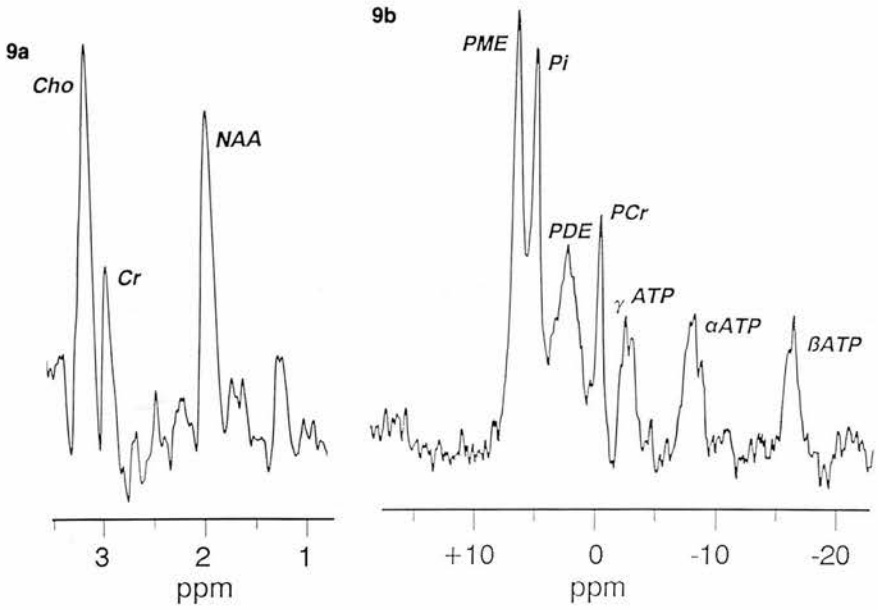



**FIG. 9.** Infant (Case 8) at 40 weeks postmenstrual age. **a:** Proton spectrum acquired from a 64 $cm^3$ voxel, TR 2,000 ms, TE 270 ms, 128 data collections. The NAA/Cho ratio is 0.8. **b:** Phosphorus spectrum acquired from the whole brain at a TR of 5 s with 64 data collections. The $PCr/P_i$ ratio is 0.5. The pH is 7.28. For this and subsequent phosphorus spectra, PCr, phosphocreatine; $P_i$, inorganic phosphate; PME, phosphomonoester; PDE, phosphodiester; ATP, adenosine triphosphate. The phosphorus spectra are not scaled vertically for comparison.

value for a normal infant under 40 weeks PMA. His result is indistinguishable from that of the similarly aged abnormal infants. After 40 weeks PMA the severely abnormal infants have NAA/Cho ratios that are lower than those of the normals and most of the moderately affected infants. This difference becomes more apparent with increasing age. There are several possible explanations for this. The premature brain has relatively little NAA (13), and therefore there may be very little difference in NAA/Cho ratios between normal and abnormal brains at this stage. In addition, NAA is thought to be located principally in neurons and so the reduction in the NAA/Cho ratios in the abnormal infants could be due to loss of neurons or delayed development, which would become more apparent with increasing age. A relative reduction in the number of neurons in the lesion has been proposed to account for the reduction in NAA that has been seen in brain tumors (3–5), in cerebrovascular disease (6), and in a child with herpes simplex encephalitis (10).

No obvious lactate peaks were seen in any of the spectra that we obtained from either normal or abnormal infants (the peaks occasionally seen in the region 1.0–1.5 ppm may be attributed to fat). Though this does not preclude the possibility of a modest increase in lactate in the abnormal infants, our spectra provide no evidence for a dramatic elevation in the lactate. This may be because the earliest study of a hypoxically damaged baby was performed at 40 h PNA, which is relatively remote

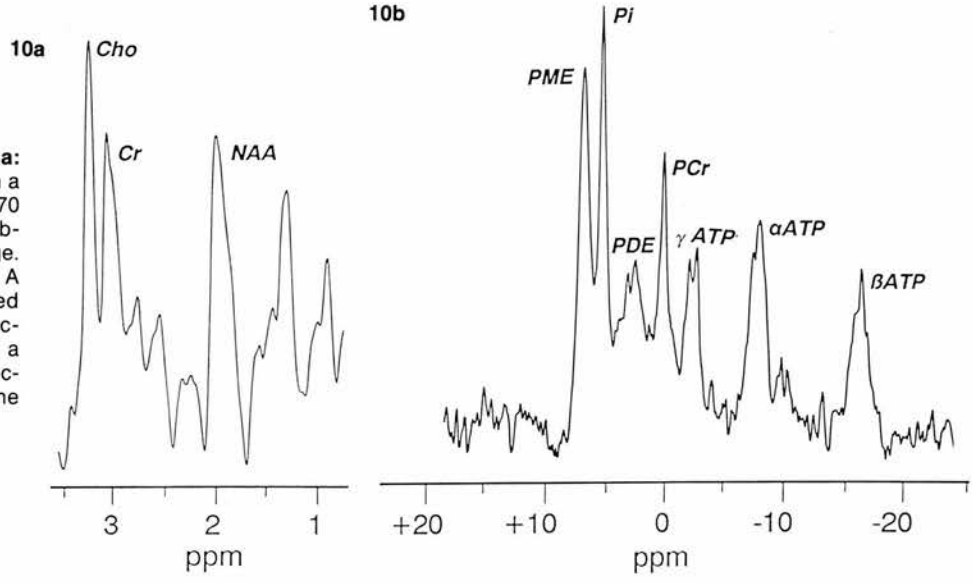



**FIG. 10.** Term infant (Case 4). **a:** Proton spectrum acquired from a 64 $cm^3$ voxel, TR 2,000 ms, TE 270 ms, 128 data collections, obtained at 18 days postnatal age. The NAA/Cho ratio is 0.8. **b:** A phosphorus spectrum obtained at 13 days postnatal age, acquired from the whole brain at a TR of 20 s with 64 data collections. The $PCr/P_i$ ratio is 0.7. The pH is 7.28.

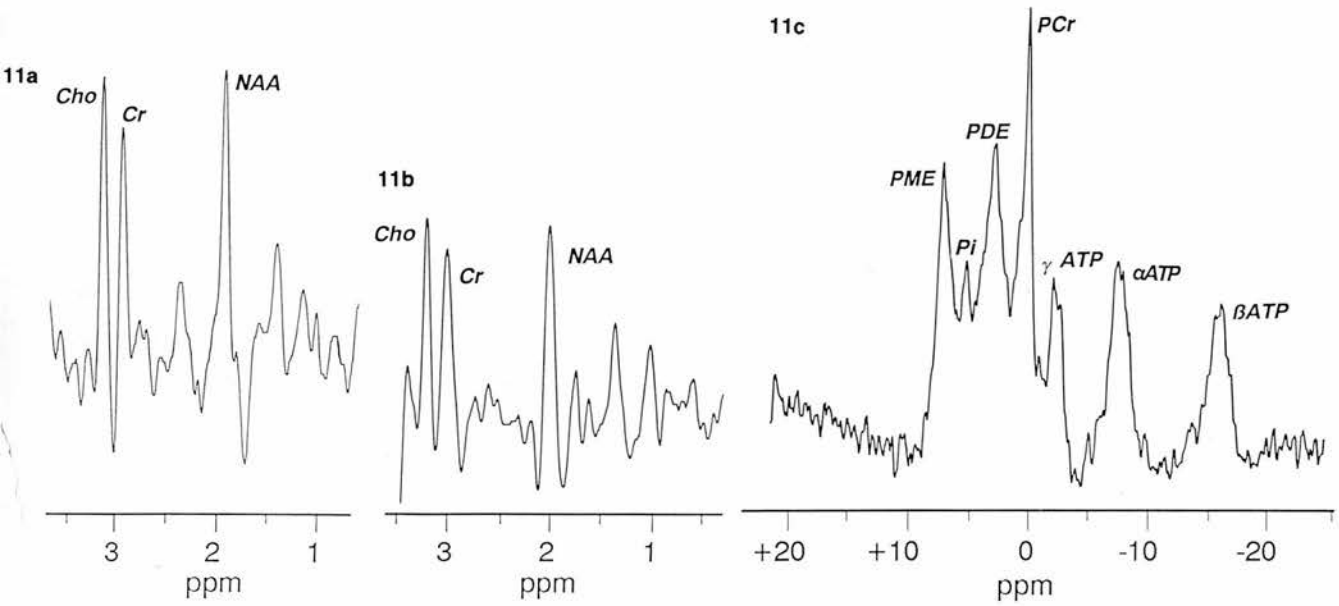



**FIG. 11.** *Case 7.* **a:** Proton spectrum acquired from a 64 $cm^3$ voxel, TR 2,000 ms, TE 270 ms, 128 data collections, obtained at 57 weeks postmenstrual age (5 months postnatal age). The NAA/Cho ratio is 1.1. **b:** Proton spectrum at 97 weeks postmenstrual age (14 months postnatal age), acquired from a 64 $cm^3$ voxel, TR 2,000 ms, TE 270 ms, 128 data collections. The NAA/Cho ratio is 1.2. **c:** Phosphorus spectrum at 97 weeks postmenstrual age (14 months postnatal age), acquired from the whole brain at a TR of 20 s, 32 data collections. The $PCr/P_i$ ratio is 2.5 and the pH is 7.12.

from the insult. A study of hypoxic-ischemic brain damage in the immature rat showed that lactate levels declined rapidly in the first hour of recovery to only marginally above control values (18). Other factors such as the immature blood–brain barrier and the ability of the immature brain to utilize lactate (19) support the fact that the lactate concentrations decline rapidly. The lack of detectable lactate may also reflect the low capacity of the immature brain to produce this compound. In a study of neural activity and high energy phosphate in adult and immature rat brain, Kawai et al. (20) demonstrated that lactate production in response to injury was markedly reduced in the 4-day-old rat compared with an adult rat exposed to the same insult.

It is interesting to compare the phosphorus and proton spectra during the progression from the subacute to the chronic phase of injury. For example, the phosphorus spectra in Fig. 9 acquired at 2 days PNA and in Fig. 10 acquired at 13 days PNA are very abnormal, while the proton spectra obtained from the same infants at 2 and 18 days, respectively, show only a moderate decrease in the NAA/Cho ratio when compared with other values from infants of the same age. In Case 7 with extensive parenchymal damage (Fig. 11), proton spectra at 5 and 14 months are very abnormal, with NAA/Cho ratios markedly lower than those of the moderately abnormal infants of comparable age. However, his phosphorus spectra at 8 and 14 months appear normal.

The acute and subacute effects that are observed by phosphorus MRS are characteristic of energy failure. Presumably, the subsequent return to normal of the phosphorus metabolite ratios reflects complete loss of severely damaged cells, the remaining viable cells showing a normal metabolite profile. This is consistent with previous clinical studies showing that in the majority of infants who survive hypoxic-ischemic injury the phosphorus metabolite ratios return to normal within a few weeks (1).

**TABLE 2.** *Signal-to-height ratios (SHRs) at TR of 5,000 and 2,000 ms with TE of 270 ms*

| | | NAA | Cr | Cho |
|---|---|---|---|---|
| Normal infants (Cases 1 and 2) | Mean | 1.2 | 1.5 | 1.5 |
| (n = 4) | Range | 1.0–1.3 | 1.0–2.0 | 1.0–1.8 |
| Abnormal infants (Groups A and B; | Mean | 1.2 | 1.3 | 1.3 |
| Cases 5, 7, 8, 10, 11, 14, and 16) | Range | 1.0–1.6 | 1.0–2.0 | 1.0–2.1 |
| (n = 11) | | | | |
| Normal adults (n = 6) | Mean | 1.3 | 1.5 | 1.5 |
| | Range | 1.2–1.5 | 1.0–1.7 | 1.2–2.2 |

n, no. of examinations.

The abnormalities that are seen on the proton spectra become more marked with time. This reflects a relative loss of NAA, which could be associated with failure of neurons to develop normally or with areas of neuronal loss and gliosis resulting from hypoxic-ischemic damage. Such a change in the relative populations of the different cell types from neurons to glia would have little effect on the $^{31}P$ spectra if, as studies of cell cultures have suggested, neurons and glia have similar phosphorus metabolite ratios (21).

Our observations suggest that in the majority of infants with hemorrhagic and/or ischemic brain damage, the phosphorus spectrum will be of most diagnostic and prognostic use in the acute and subacute phase of injury, whereas the proton spectrum may provide more useful information in the chronic phase. Improvements in the signal-to-noise ratio and spectral resolution of the data will further enhance the utility of this technique.

We conclude that phosphorus and proton spectroscopy can be combined to provide clinically useful complementary information on the development of the brain in the neurologically abnormal infant.

**Acknowledgment:** We would like to thank the Medical Research Council and the Department of Health for their financial support.

## REFERENCES

1. Azzopardi D, Wyatt JS, Cady EB, et al. Prognosis of newborn infants with hypoxic-ischemic brain injury assessed by phosphorus magnetic resonance spectroscopy. *Pediatr Res* 1989;25:445–51.
2. Laptook AR, Corbett RJT, Uauy R, Mize C, Mendelsohn D, Nunnally RL. Use of $^{31}P$ magnetic resonance spectroscopy to characterize evolving brain damage after perinatal asphyxia. *Neurology* 1989;39:709–12.
3. Gill SS, Thomas DGT, van Bruggen N, et al. Proton MR spectroscopy of intracranial tumours: in vitro and in vivo studies. *J Comput Assist Tomogr* 1990;14:497–504.
4. Bruhn H, Frahm J, Gyngell ML, et al. Noninvasive differentiation of tumors with use of localized H-1 MR spectroscopy in vivo: initial experience in patients with cerebral tumors. *Radiology* 1989;172:541–8.
5. Langhowski JH, Wieland J, Bomsdorf H, et al. Preoperative localized in vivo proton spectroscopy in cerebral tumours at 4.0 Tesla—first results. *Magn Res Imag* 1989; 7:547–55.
6. Bruhn H, Frahm J, Gyngell NM, Merboldt KD, Hanicke W, Sauter R. Cerebral metabolism in man after acute stroke: new observations using localised proton NMR spectroscopy. *Magn Res Med* 1989;9:126–31.
7. Sarnat HB, Sarnat MS. Neonatal encephalopathy following fetal distress. A clinical and electroencephalographic study. *Arch Neurol* 1976;33:696–705.
8. Levene MI, Kornberg J, Williams THC. The incidence and severity of post asphyxial encephalopathy in full term infants. *Early Hum Dev* 1985;11:21–6.
9. Lampman D, Hurst G, McNally J, Paley M. Volume selective $^{1}H$ NMR spectroscopy with solvent suppression. *Magn Res Imag* 1986;4:115.
10. Menon DK, Sargentoni J, Peden CJ, et al. Proton MR spectroscopy in herpes simplex encephalitis: assessment of neuronal loss. *J Comput Assist Tomogr* 1990;14:449–52.
11. Petroff OAC, Prichard JW, Behar KL, Alger JR, den Hollander JA, Shulman RG. Cerebral intracellular pH by $^{31}P$ magnetic resonance spectroscopy. *Neurology* 1985;35: 781–8.
12. van der Knaap MS, van der Grond J, van Rijan PR, Luyten PR, Valk J. Age dependent changes in localised proton and phosphorus spectra of the brain in healthy children from birth till sixteen years. Book of Abstracts, Society of Magnetic Resonance in Medicine, Amsterdam meeting, 1989: 376.
13. Nakada T, Kwee IL, Suzuki SR, Houkin K. Intrauterine fetal brain NMR spectroscopy: $^{1}H$ and $^{31}P$ studies in rats. *Magn Res Med* 1989;12:172–80.
14. Bates TE, Bell JD, Williams SR, Small RK, Iles RA, Gadian DG. A $^{1}H$ NMR study of cerebral development in the rat. *NMR Biomed* 1989;2:225–9.
15. Valk J, van der Knaap MS. White matter and myelin. In: *Magnetic resonance of myelin, myelination and myelin disorders*. Berlin: Springer-Verlag, 1989:9–21.
16. Birken DL, Oldendorf WH. *N*-Acetyl-L-aspartic acid: a literature review of a compound prominent in $^{1}H$ NMR spectroscopic studies of brain. *Neurosci Biobehav Rev* 1989; 13:23–31.
17. Brenton DP, Garrow PJ, Krywawych S, et al. Phosphoethanolamine is a major constituent of phosphomonoester peak detected by $^{31}P$ NMR in the newborn brain. *Lancet* 1985; 1:115.
18. Palmer C, Brucklacher RM, Christensen MA, Vannucci RC. Carbohydrate and energy metabolism during the evolution of hypoxic-ischemic brain damage in the immature rat. *J Cereb Blood Flow Metab* 1990;10:227–35.
19. Johanson CE. Ontogeny and phylogeny of the blood-brain barrier. In: Neuwelt EA, ed. *Implications of the blood–brain barrier and its manipulation*, vol 1. New York: Plenum, 1989:157–98.
20. Kawai S, Yonetani M, Nakamura H, Okada Y. Effects of deprivation of oxygen and glucose on the neural activity and the level of high energy phosphates in the hippocampal slices of immature and adult rat. *Dev Brain Res* 1989;48:11–8.
21. Gill SS, Small RK, Thomas DGT, et al. Brain metabolites as $^{1}H$ NMR markers of neuronal and glial disorders. *NMR Biomed* 1989;2:196–200.

# PROTON SPECTROSCOPY OF THE NEONATAL BRAIN FOLLOWING HYPOXIC–ISCHAEMIC INJURY

*C. J. Peden*
*M. A. Rutherford*
*J. Sargentoni*
*I. J. Cox*
*D. J. Bryant*
*L. M. S. Dubowitz*

Magnetic resonance spectroscopy (MRS) is unique in its ability to allow non-invasive visualisation of cellular metabolism in the brain, and therefore ideally suited as a research tool to study changes in the brains of infants with hypoxic–ischaemic encephalopathy (HIE). Previous proton spectroscopy studies have identified the principal peaks seen in spectra from the human brain; namely *N*-acetylaspartate (NAA), choline-containing compounds (Cho) and creatine plus phosphocreatine (Cr) (Peden *et al.* 1990, van der Knaap *et al.* 1990, Huppi *et al.* 1991). Changes in these peaks and the appearance of a lactate peak have been reported in disease states such as ischaemia, demyelinating disorders and inborn errors of metabolism (Peden *et al.* 1990, Grodd *et al.* 1991). Interpretation of proton spectra from the abnormal infant brain is complicated by age-related changes, which are most rapid during the first months of life (Peden *et al.* 1990, van der Knaap *et al.* 1990, Grodd *et al.* 1991, Huppi *et al.* 1991), and regional metabolite variations known to occur within the brain of both children and adults (Frahm *et al.* 1989, Connelly *et al.* 1991).

The aim of this preliminary study was to observe the changes produced in the proton spectrum from a standardised region of the brain of infants with HIE, and to correlate these findings with neurodevelopmental outcome at one year. To minimise spectral changes produced by age differences, only infants born at term and post-term (37 to 42 weeks) were studied within the first month of life.

## Patients and method

Permission for this study was obtained from the Research Ethics Committee of the Royal Postgraduate Medical School, Hammersmith Hospital. Informed consent was obtained from a parent in each case.

### *Patients*

Infants born at term and post-term (37 to 42 weeks) were studied. The earliest study was performed two days after birth, the latest at 27 (mean 13·6) days. Neurological evaluation included serial neurological examinations, imaging (magnetic resonance imaging (MRI) and cranial ultrasound scans) and Doppler blood flow studies. The severity of HIE was graded according to Sarnat and Sarnat's classification (1976). At one year, all infants had a structured neurological examination and the Griffiths developmental scale was administered. On the basis of this examination, the infants were divided into three outcome categories:

NORMAL

Infants who were normal at one year, but who may have had transient abnormalities of tone before this.

TABLE I
**Clinical details of all infants with hypoxic–ischaemic encephalopathy**

| *Case* | *Birthweight (g)* | *GA at birth (wks)* | *Fetal distress*[1] | *Delivery*[2] | *Apgar score (score, mins)* | *HIE score*[3] | *Clinical outcome at one year* |
|---|---|---|---|---|---|---|---|
| A | 3530 | 42 | Type II dips | Emergency LSCS | 0,0 | II | Normal |
| B | 3090 | 42 | Type II dips/MSL | Forceps | 1,4 | I | Normal |
| C | 2285 | 40 | Type II dips | NVD | 7,8 | II | Normal |
| D | 3450 | 40 | Type II dips/MSL | Forceps | 9,10 | II | Normal |
| E | 3500 | 40 | Not recorded. Postnatal collapse at 1½ hours, severe hypoxia | NVD | 9,10 | II | Normal |
| F | NA[4] | 38 | Type II dips | Emergency LSCS | 0,2 | III | Spastic quadriplegia, fits, severe developmental delay |
| G | 3805 | 40 | Not recorded | NVD | 3,9 | II | Spastic quadriplegia |
| H | 3590 | 40 | Bradycardia | Emergency LSCS | 0,5 | II | Spastic quadriplegia, fits, severe developmental delay |
| I | 3240 | 42 | Type II dips | NVD | 3,9 | II | Microcephaly, fits, severe developmental delay |
| J | 3010 | 40 | Type II dips | Emergency LSCS | 3,4 | II | Spastic quadriplegia, severe developmental delay |

[1]MSL = meconium-stained liquor; [2]LSCS = lower-segment caesarean section, NVD = normal vaginal delivery; [3]graded according to classification of Sarnat and Sarnat (1976); [4]not available.

MODERATE
Infants who had persisting mild abnormalities of tone or delay in development at one year. No infants had an outcome in this category.

SEVERE
Infants with signs of hemiplegia or quadriplegia and/or severe developmental delay at one year.

In addition, one normal infant who had no history of birth asphyxia and who was completely normal on clinical neurological examination was studied as a control. He was examined at one year of age to ensure that his neurodevelopment was normal.

A summary of the clinical details is given in Table I.

*Proton spectroscopy*

All infants were examined unsedated during natural sleep, after a feed. They were monitored with an EEG (Marquette Electronics, Inc.) and pulse oximeter (Nellcor N-200). The total MR examination (imaging and spectroscopy) lasted between one and 2½ hours.

A 1·6 Tesla Picker prototype magnet system was used, with a bore size of one metre. An enveloping saddle-shaped receiver coil operating at 68MHz was used with a separate saddle-shaped transmitter coil. MRI using a spin-echo sequence (500/22) was performed first, in at least two orthogonal planes, to visualise the region for spectroscopic study. To reduce spectral variability, spectra were acquired from the same region in each infant. A 27 or 64cm$^3$ volume in the parieto-occipital region of the brain at the mid-ventricular level was selected. Choice of this region minimised contamination of the spectrum from overlying fat in the skull and was easier to shim than a similar volume in the frontal lobes; it included cortical grey matter, as well as periventricular white matter. The parieto-occipital region is commonly involved in hypoxic–ischaemic brain injury. Spectroscopic localisation was by multiple spin-echoes, using slice-selective 180° pulses in three orthogonal planes. The multiple spin-echo sequence incorporated a binomial pulse ($1\bar{3}3\bar{1}$) optimised for detection of NAA to suppress the larger water peak (Lampman *et al.* 1986). All spectra were acquired with an echo time (TE) of 270ms and repetition time (TR) of 2000ms. 128 data collections were acquired from all infants. Spectra were processed using an exponential line-broadcasting filter of 2·7Hz.

Chemical shifts were referenced to NAA (chemical shift 2ppm). The line widths of the NAA, Cho and Cr peaks varied from patient to patient as a result of differences

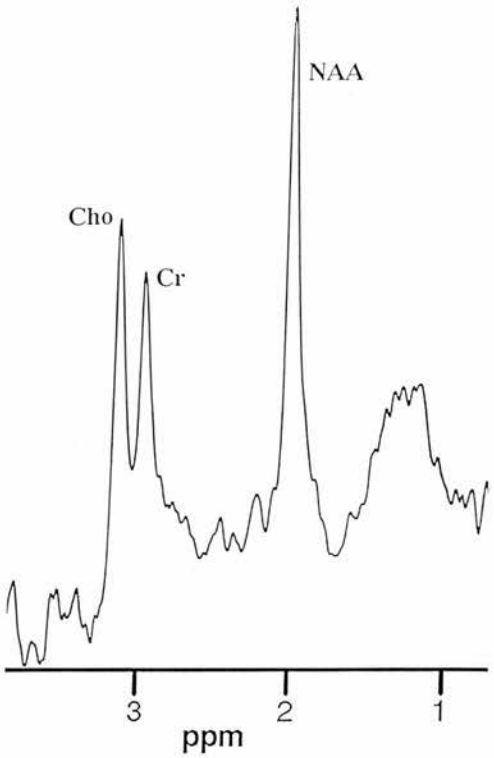
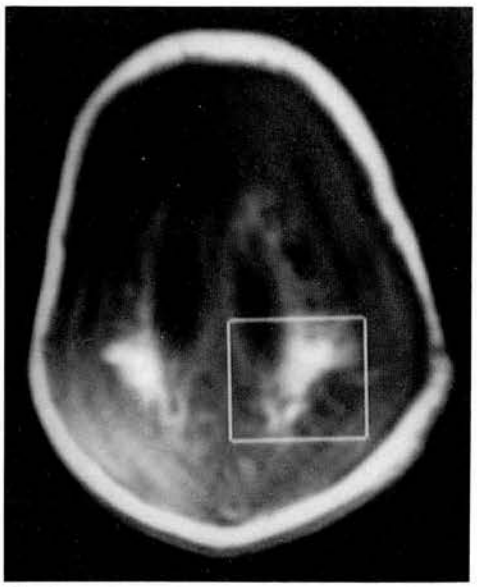



*Fig. 1. Proton spectrum of an infant with hypoxic–ischaemic encephalopathy who was neurologically normal at one year (infant E). Spectrum was acquired with a TE of 270ms and a TR of 2000ms, with 128 data collections. NAA/Cho ratio is 1·5, NAA/Cr ratio is 1·9 and Cho/Cr ratio is 1·5.*



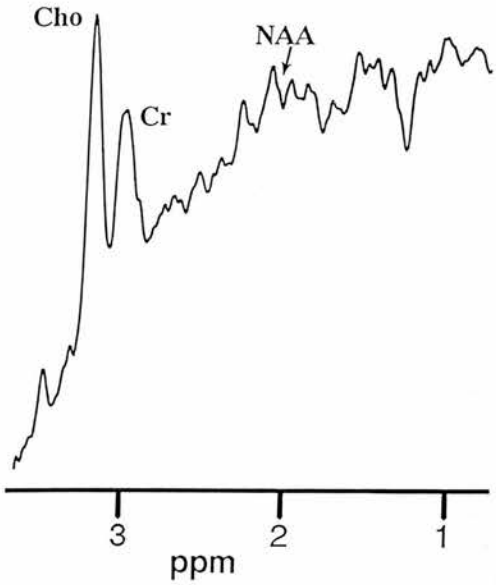



*Fig. 2.* (left) *Transverse $T_1$-weighted spin-echo image (TR 500ms, TE 22ms), showing voxel from which spectra were acquired. There are large bilateral subdural fluid collections; ventricles are dilated and there is extensive subcortical cystic change.* (right) *Proton spectrum of an infant with hypoxic–ischaemic encephalopathy who was clinically neurologically abnormal at one year (infant F). Spectrum was acquired with a TE of 270ms and a TR of 2000ms, with 128 data collections. NAA/Cho ratio is 0·2, NAA/Cr ratio is 0·3 and Cho/Cr ratio is 1·9.*

TABLE II
**Gestational age, postnatal age at time of examination and metabolite ratios calculated from proton spectra**

| *Case* | *GA at birth (wks)* | *Postnatal age at examination (days)* | *NAA/Cho ratio*[1] | *NAA/Cr ratio*[2] | *Cho/Cr ratio* |
|---|---|---|---|---|---|
| Control | 37 | 24 | 1·9 | 2·3 | 1·2 |
| A | 42 | 2 | 1·0 | 1·8 | 1·9 |
| B | 42 | 7 | 1·1 | 1·6 | 1·5 |
| C | 40 | 7 | 1·1 | 1·6 | 1·5 |
| D | 40 | 10 | 1·7 | 2·7 | 1·6 |
| E | 40 | 18 | 1·5 | 1·9 | 1·5 |
| F | 38 | 27 | 0·2 | 0·3 | 1·9 |
| G | 40 | 7 | 0·3 | 1·1 | 3·3 |
| H | 40 | 20 | 0·8 | 1·1 | 1·4 |
| I | 42 | 4 | 0·7 | 0·7 | 1·2 |
| J | 40 | 10 | 0·7 | 0·9 | 1·2 |

[1]NAA = *N*-acetylaspartate, Cho = choline-containing compounds; [2]Cr = creatine and phosphocreatine.

in magnetic-field homogeneity, but were similar in each individual case; therefore peak heights were used to compare metabolite ratios. To measure the peak height, a chord was drawn between the two extremes of each peak and the height was measured with respect to this. The chord was not usually parallel to the baseline, due to imperfections in water suppression. In addition, the ratios obtained were influenced by the water-suppression sequence used, which effectively reduces the Cho and Cr signals in relation to NAA. The spectra were analysed blind by four individuals, then the results were averaged to obtain a mean value and standard deviation to give an assessment of the error introduced by inter-observer variation.

## Results

A proton spectrum from an infant who was neurologically normal at one year is shown in Figure 1. The proton spectrum acquired from an infant with HIE who was severely abnormal at one year is shown, with the corresponding image in Figure 2. The MR image in Figure 2 shows large ventricles and multiple cystic lesions, and the corresponding proton spectrum has virtually no identifiable NAA peak.

Table II shows the infants' gestational ages at birth, their postnatal ages at the time of examination and the mean values of the metabolite ratios calculated from the spectra.

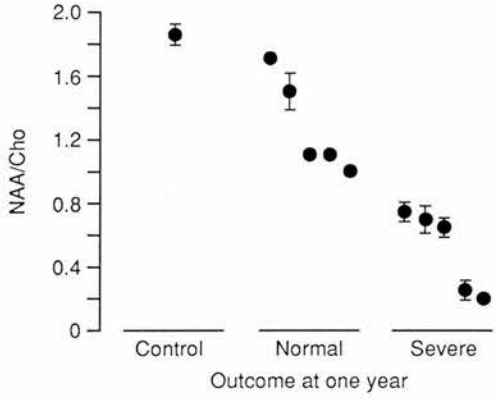
The means and one standard deviation of the NAA/Cho, NAA/Cr and Cho/Cr ratios measured from the 11 proton spectra are shown in Figures 3 to 5, in relation to the infants' clinical outcome at one year. Spectra with a high signal-to-noise ratio produced little disagreement in observer measurement, resulting in little or no standard deviation from the mean. Spectra with a lower signal-to-noise ratio, for example caused by patient movement during the examination, resulted in much higher inter-observer variability.

The NAA/Cho ratios show a clear trend, with the highest value seen in the control infant and the lowest in the infants with an abnormal outcome. There was no overlap between the values obtained from the normal and severe groups. The NAA/Cr ratios also showed a decline in the values obtained between the control and normal infants and those infants with a severe outcome at one year. Again, there was no overlap between the two

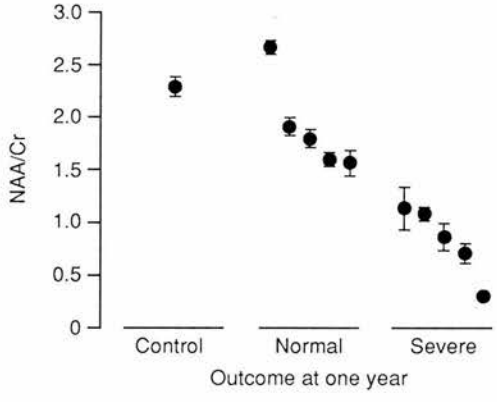


*Developmental Medicine and Child Neurology*, 1993, 35, 502–510

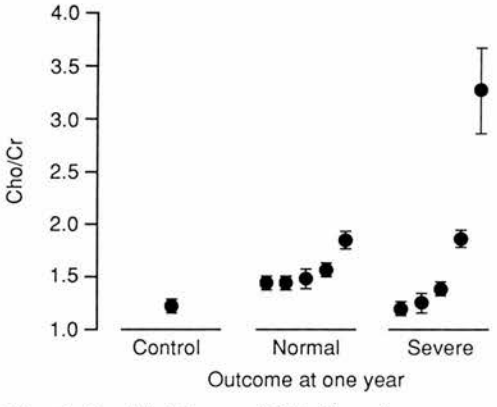
3




4




5




***Figs. 3, 4 and 5.*** *Mean and 1SD (from four 'blind' observer measurements) of NAA/Cho, NAA/Cr and Cho/Cr ratios, respectively, from all infant spectra, shown against outcome at one year.*

groups. The Cho/Cr ratios showed a slight increase in the mean value of the group with the severe outcome compared with that of the control infant, but the spread of the values was very large.

## Discussion

In this preliminary study, we have demonstrated changes in the proton spectrum associated with HIE and have shown that some of these changes correlate with later outcome. The number of infants in this study is small, so our findings can only suggest what may be confirmed by a larger study. However, there were eight infants examined with grade II HIE (Sarnat and Sarnat classification 1976), and the proton spectroscopy findings (NAA/Cho and NAA/Cr ratios) correlated well with their clinical neurological state at one year. It is for this intermediate group of infants, for whom outcome is most uncertain, that non-invasive predictive studies may be of greatest value. Our findings are in agreement with those of Roth *et al.* (1992), who demonstrated that changes in the phosphorus spectra of neonates, with a clinical and biochemical diagnosis of birth asphyxia, were directly related to outcome at one year.

Changes in metabolite ratios can be due to $T_1$ and $T_2$ differences. In a previous study (Peden *et al.* 1990), we found little difference in $T_1$ values between the adult brain and the normal and abnormal infant brain, so it is unlikely that the observed changes in metabolite ratios arise from $T_1$ differences. The changes could arise from $T_2$ differences. The TE we used (270ms) is relatively long, compared with the $T_2$ of the metabolites visualised (Frahm *et al.* 1989). The $T_2$ of creatinine is shortest, and therefore the loss in peak height of creatine is greatest. We have been unable to measure $T_2$ parameters because of technical difficulties and limited examination time.

The quantitation of *in vivo* proton spectra is controversial. We, and other authors of clinical proton spectroscopy papers (van der Knaap *et al.* 1990), have used peak height ratios as opposed to peak area ratios, because we felt that this minimised variability between spectra. However, peak areas may provide more

accurate analysis of the differences in peaks within one spectrum.

Unfortunately, we were able to study only one infant who was neurologically normal at birth. We approached mothers antenatally to discuss entering their infants, after birth, into the study, but few consented. Of those who did, some found the environment of our prototype magnet daunting and withdrew consent; on other occasions, there was inadequate time to perform the examination before the mother left hospital; and on two occasions, normal infants were put into the magnet bore for the study but would not keep still, so the examination had to be terminated. We did not have permission from the Research Ethics Committee to sedate or anaesthetise normal infants.

The proton spectrum changes with age: the NAA/Cho and NAA/Cr ratios increase and the Cho/Cr ratio decreases (Peden *et al.* 1990, van der Knaap *et al.* 1990, Grodd *et al.* 1991, Huppi *et al.* 1991). This study examined infants within the first month of life at times ranging from two to 27 days after birth, so the infants examined at three and four weeks of age are very likely to have slightly higher NAA/Cho and NAA/Cr ratios and slightly lower Cho/Cr ratios than the younger infants. The normal control infant was at the upper end of the age-range (24 days). Huppi and colleagues (1991) demonstrated a two-fold increase in NAA in the preterm (31 to 37 weeks post-conceptional age) to term infant's brain (38 to 45 weeks post-conceptional age) and a two-fold increase of NAA from term to adult brain in humans. Therefore, it appears that rapid changes in NAA concentration in preterm infants are considerably slower in term infants, so we hoped to minimise the spectral changes in NAA/Cr and NAA/Cho due to age by studying only term infants. Ideally, we wished to examine all infants at the same postnatal age, but for many reasons this was not possible.

There are two advantages to using proton spectroscopy to predict outcome, rather than the more established technique of phosphorus spectroscopy (Hope *et al.* 1984, Younkin *et al.* 1984, Azzopardi *et al.* 1989, Roth *et al.* 1992). First, while changes in the metabolite ratios of the abnormal phosphorus spectra return to within normal limits at about two weeks after birth (Hope *et al.* 1984, Azzopardi *et al.* 1989), proton spectra remain abnormal for much longer after the insult (Peden *et al.* 1990), thus abnormal biochemical information can be obtained even when infants are referred weeks or months after birth. Second, it may be possible to perform proton spectroscopy on the rapidly increasing number of commercial imaging systems operating at a magnetic field strength of 1·0 Tesla or greater with additional software only, while phosphorus spectroscopy requires additional hardware so is likely to remain confined to a small number of research centres.

Interpretation of a spectrum relies on a thorough understanding of the roles of the individual metabolites. While the function of the phosphocreatine, inorganic phosphate and ATP peaks of the phosphorus spectrum are well known, the precise roles of the metabolites seen in the proton spectrum—particularly those represented by the NAA and Cho peak resonances—remain unclear.

Proton MRS has stimulated research into *N*-acetylaspartate, since the NAA peak is so dominant in the proton spectrum and is seen to change in many disease states. NAA is one of the most abundant amino acids in free solution in the mammalian brain, and it has been suggested that it is a specific marker of neuronal viability (Birken and Oldendorf 1989). As development and myelination of the normal infant brain coincide with an increase in the concentration of NAA (Peden *et al.* 1990, van der Knaap *et al.* 1990, Huppi *et al.* 1991), abnormal myelination has been proposed as another reason for the changes seen in NAA (Grodd *et al.* 1991). However, Small and colleagues (1990) have shown that NAA concentrations in hypomyelinated mouse mutants, although taking longer to reach normal values, reach the same concentrations as in normally myelinated mice.

Not only is there uncertainty about the exact roles of the metabolites in the proton spectrum, but there is also confusion in the literature about the timing of the changes that take place with hypoxic–ischaemic injury. In earlier live animal experiments lasting several hours

(Crockard *et al.* 1987, Hope *et al.* 1987) and postmortem studies (Tews *et al.* 1963, Petroff *et al.* 1988), the concentration of NAA appeared to be so constant during hypoxia and ischaemia that it was used as an internal reference for analysis of proton spectra (Tews *et al.* 1963, Crockard *et al.* 1987, Hope *et al.* 1987, Petroff *et al.* 1988). More recent experiments show that this is not the case. Van Rijen and colleagues (1991) found a significant decrease in the NAA/Cr ratio from rat brain at five and 15 minutes of ischaemia, which failed to recover during perfusion. They attributed this to a decrease in the concentration of NAA, as they assumed no gross changes in the total Cr pool. Rosenberg and colleagues (1991) suggested that since NAA itself has been shown to be stable in earlier biochemical studies of hypoxia (Tews *et al.* 1963, Crockard *et al.* 1987, Hope *et al.* 1987, Petroff *et al.* 1988), it is the other compounds that make up this peak which are decreasing. Another component of the NAA peak is *N*-acetylaspartylglutamate, which can be enzymatically cleaved to NAA and glutamate. Glutamate has been observed to persist in ischaemic regions in which NAA has decreased (Higuchi *et al.* 1991).

Proton spectroscopy studies of the human brain to date have observed the effects of hypoxia and ischaemia in localised regions of the brain of adults who have had cerebrovascular accidents (Berkelbach van der Sprenkel *et al.* 1988, Bruhn *et al.* 1989, Fernstermacher and Narayana 1990). These proton spectra showed a persistent decrease in the NAA peak, but the spectra were not acquired until several days after the stroke had occurred. In our study, the most abnormal spectra recorded—with little or no NAA peak visible—were acquired one to four weeks after birth. Sequential studies commencing within hours of birth are required to establish the time course of the decrease in NAA.

The change in the NAA/Cho and NAA/Cr ratios after HIE may be due not only to a decrease in NAA, but also to increases in Cho and Cr. Some studies assume that the total brain creatine pool remains stable during hypoxia (Petroff *et al.* 1988); others show a decrease in Cr in pathological states such as focal ischaemia (Higuchi *et al.* 1991). A rise in the choline peak after hypoxic–ischaemic injury is consistent with the findings of Scremin and Jenden (1989), who demonstrated an increase in free brain choline after ischaemia; this may explain the slight increase in the Cho/Cr ratio of those infants with a severe outcome. Other authors report no change (Fenstermacher and Narayana 1990) or a fall in Cho (Higuchi *et al.* 1991) in infarcted regions. The wide distribution of Cho/Cr values, acquired between 96 hours and four weeks after birth in our severe-outcome group, may indicate that the Cho concentration alters with time after injury, perhaps rising acutely in the first few hours and then falling to normal or low levels. Again, frequent sequential studies commencing as soon as possible after birth are required to establish the time course of these changes.

Proton spectroscopy, like phosphorus spectroscopy, may not only become a useful prognostic tool, but also may lead to a greater understanding of those changes which result in permanent neurological damage—or those that aid recovery—following hypoxic–ischaemic events in infants. Further work to clarify the role of metabolites and the nature of the changes in their concentration observed with proton spectroscopy may lead to a better understanding of the biochemical changes caused by hypoxia and provide, in the future, a more widely available MRS technique to monitor therapy non-invasively.

*Accepted for publication 12th November 1992.*

*Acknowledgements*
This work was supported by the Department of Health and Social Security, the Medical Research Council and The Spastics Society.

*Authors' Appointments*
*Carol J. Peden, Medical Research Council Research Fellow, NMR Unit;
Mary A. Rutherford, M.R.C.Paed., Spastics Society Fellow, Department of Paediatrics and NMR Unit;
Janet Sargentoni, D.C.R(R).M.U., Senior Radiographer, NMR Unit;
I. Jane Cox, Ph.D., Lecturer Department of Radiology;
David J. Bryant, Ph.D., Senior Lecturer, NMR Unit;
Lilly M. S. Dubowitz, M.D., Medical Research Council Research Fellow, Department of Paediatrics

and NMR Unit;
Royal Postgraduate Medical School and Hammersmith Hospital, London.

*Correspondence to first author* at Sir Humphry Davy Department of Anaesthesia, Bristol Royal Infirmary, Bristol BS2 8HW.

SUMMARY
Proton magnetic resonance spectroscopy was used to examine, within the first month of life, the brains of 11 infants born at term—10 with signs of hypoxic-ischaemic encephalopathy (HIE) and one who was neurologically normal at birth. All the infants had peak resonances on their spectra which could be assigned to *N*-acetylaspartase (NAA), choline-containing compounds (Cho) and creatine plus phosphocreatine (Cr). When neurodevelopmental outcome at one year was correlated with initial spectroscopy findings, the NAA/Cho and NAA/Cr ratios reflected clinical outcome. This study suggests that proton spectroscopy not only provides new information about biochemical changes occurring in the brains of infants with HIE, but also may help to predict outcome within the first month of life.

RÉSUMÉ
*Spectroscopie protonique du cerveau à la naissance, à la suite d'une agression hypoxique ischémique*
La spectroscopie de résonance magnétique protonique a été utilisée pour examiner, durant le premier mois de vie, les cerveaux de 11 nourrissons nés à terme, 10 avec des signes d'une encéphalopathie hypoxique (HIE) et un qui était neurologiquement normal à la naissance. Tous les nourrissons présentaient des pics de résonance sur leur spectre qui pouvaient être attribués à la *N*-acetylaspartase (NAA), à des composés de choline (Cho) et à la créatine plus phosphocréatine (CR). Quand le devenir neurodéveloppemental à l'âge d'un an fut corrélé avec les données spectroscopiques initiales, les rapports NAA/Cho et NAA/CR apparurent caractériser le devenir clinique. Les enfants neurologiquement normaux à un an présentaient les rapports les plus bas. Cette étude suggère que la spectroscopie protonique, non seulement fournit des informations nouvelles sur les modifications biochimiques survenant dans les cerveaux de nourrissons ayant présenté une HIE, mais peut également aider à prédire le devenir dès le premier mois de vie.

ZUSAMMENFASSUNG
*Magnet-Resonanz-Spektroskopie des neonatalen Gehirns nach hypoxisch-ischämischem Insult*
Bei 11 zum Termin geborenen Kindern—10 mit hypoxisch-ischämischer Enzephalopathie (HIE) und einem bei der Geburt unauffälligen Kind—wurden im ersten Lebensmonat Hirnuntersuchungen mit der Magnet-Resonanz-Spektroskopie durchgeführt. Alle Kinder hatten Peak Resonanzen für *N*-acetylasparatase (NAA), Cholin enthaltende Verbindungen (Cho) und Kreatin plus Phosphokreatin (Cr) in ihren Spektren. Korrelierte man den entwicklungsneurologischen Outcome im Alter von einem Jahr mit den anfänglichen Spektroskopiebefunden, so spiegelten die NAA/Cho und die NAA/Cr Verhältnisse den klinischen Befund wider. Die Kinder, die mit einem Jahr neurologisch unauffällig waren, hatten die niedrigsten gehabt. Diese Studie zeigt, daß die Magnet-Resonanz-Spektroskopie nicht nur neue Informationen über biochemische Veränderungen im Gehirn von Kindern mit HIE liefert, sondern auch prognostsich für den Outcome im ersten Lebensmonat von Bedeutung sein kann.

RESUMEN
*Espectroscopia por protones de cerebros de recién nacidos después de una lesión hipóxico-isquémica*
La espectroscopia con resonancia magnética con protones se utilizó para examinar, dentro del primer mes de vida, los cerebros de 11 lactantes, de los cuales 10 tenían signos de encefalopatia hupóxica-isquémica (EHI) y uno era neurológicamente normal al nacer. Todos los niños tenían picos de resonancia en sus espectros que podían asignarse a la *N*-acetilasparatasa (NAA), compuestos continentes de colina (Co) y creatina más fosfocreatina. Cuando el curso neuroevolutivo al año de edad se correlacionó con los hallazgos espectroscópicos iniciales, las relaciones NAA/Co y NAA/Cr reflejaban el curso clínico. Los lactantes que eran neurológicamente normales al año de edad tenían las relaciones más bajas. Este estudio sugiere que la espectroscopia protónica no sólo proporciona nueva información sobre los cambios bioquímicos ocurridos en los cerebros de niños con EHI, si no que también puede ayudar a predecir el curso que seguirá a lo largo del primer año de vida.

*References*

Azzopardi, D., Wyatt, J. S., Cady, E. B., Delpy, D. T., Baudin, J., Stewart, A. L., Hope, P. L., Reynolds, E. O. R. (1989) 'Prognosis of newborn infants with hypoxic-ischemic brain injury assessed by phosphorus magnetic resonance spectroscopy.' *Pediatric Research,* **25,** 445–451.

Berkelbach van der Sprenkel, J. W., Luyten, P. R., van Rijen, P. C., Tulleken, C. A., den Hollander, J. A. (1988) 'Cerebral lactate detected by regional proton magnetic resonance spectroscopy in a patient with cerebral infarction.' *Stroke,* **19,** 1556–1560.

Birken, D. L., Oldendorf, W. H. (1989) '*N*-Acetyl-L-aspartic acid: a literature review of a compound prominent in $^{1}$H NMR spectroscopic studies of brain.' *Neuroscience and Biobehavioural Reviews,* **13,** 23–31.

Bruhn, H., Frahm, J., Gyngell, M. L., Merboldt, K. D., Hänicke, W., Sauter, R. (1989) 'Cerebral metabolism in man after acute stroke: new observations using localized proton NMR spectroscopy.' *Magnetic Resonance in Medicine,* **9,** 126–131.

Connelly, A., Austin, S. J., Gadian, D. G. (1991) 'Localised $^{1}$H MRS in the paediatric brain: age

*Journal of Computer Assisted Tomography*
14(4):497–504, July/August
© 1990 Raven Press, Ltd., New York

# Proton MR Spectroscopy of Intracranial Tumours: In Vivo and In Vitro Studies

Steven S. Gill, David G. T. Thomas, Nicholas Van Bruggen, David G. Gadian, Carol J. Peden, Jimmy D. Bell, I. Jane Cox, David K. Menon, Richard A. Iles, David J. Bryant, and Glyn A. Coutts

**Abstract:** Proton magnetic resonance spectroscopy ($^1$H MRS) was used to investigate intracranial tumours in vitro and in vivo. Biopsy specimens were studied from 47 patients, 11 of whom were also examined in vivo. Analysis was based on the signals from *N*-acetylaspartate (NAA), phosphocreatine plus creatine (Cr), choline-containing compounds (Cho), alanine (Ala), and lactate. Biopsy data from 26 astrocytomas showed that the NAA/Cr ratio differs significantly in all grades from its value in normal white matter and that the Cho/Cr ratio differs significantly in grade IV tumours from its value in the other grades. Meningiomas have an unusually high Ala/Cr ratio. Spectra obtained in vivo are consistent with in vitro results from the same patients, and their lactate signal provides additional information about abnormal metabolism. We conclude that $^1$H MRS has a clear role in the diagnosis and biochemical assessment of intracranial tumours and in the evaluation and monitoring of therapy. **Index Terms:** Spectroscopy—Meningioma—Astrocytoma—Magnetic resonance imaging, techniques.

Proton magnetic resonance spectroscopy ($^1$H MRS) provides a noninvasive method of examining a wide variety of metabolites in the human brain (1–7). These include *N*-acetylaspartate (NAA), an amino acid derivative believed to be located in neurons (8,9), choline-containing compounds (Cho) such as phosphoryl- and glycerophosphoryl-choline, which participate in membrane synthesis and degradation (10), as well as phosphocreatine and creatine, which play a major role in energy metabolism (11). In addition, elevated lactate levels may be detected in areas of infarction (12,13) or in tumours (14,15) as a result of increased anaerobic glycolysis.

The interpretation of spectra obtained in vivo can be greatly facilitated by parallel nuclear magnetic resonance (NMR) spectral analysis of tissue extracts obtained from biopsy specimens. These latter studies have the advantages that they can be performed over many hours using a very high magnetic field, yielding spectra that are much better resolved than those obtained in vivo. These spectra are particularly useful for identification of peaks and concentration measurements.

In comparison, in vivo NMR is totally noninvasive, but the quantification of metabolite levels, particularly for proton spectroscopy, is not straightforward within the time constraints of a clinical examination. In addition, even with the use of modern localisation techniques, it is extremely difficult to exclude nontumourous tissue from the volume of study, and this may significantly affect the observed spectral intensities.

The aim of the present study was to use in vitro spectroscopy in conjunction with in vivo MRS to study the biochemical features of intracranial tumours and to assess the clinical value of in vivo $^1$H MRS in diagnosis.

From the Neurosurgery Department, National Hospitals for Nervous Diseases (S. S. Gill and D. G. T. Thomas), Neurosurgery Department, Royal Free Hospital, (S. S. Gill), Hunterian Institute, Royal College of Surgeons (N. Van Bruggen and D. G. Gadian), NMR Unit, Royal Postgraduate Medical School, Hammersmith Hospital (C. J. Peden, J. D. Bell, I. J. Cox, and D. K. Menon), Medical Unit, London Hospital Medical College (R. A. Iles) London, and Picker International, Middlesex (D. J. Bryant and G. A. Coutts), England. Address correspondence and reprint requests to Prof. D. G. Gadian at Hunterian Institute, Royal College of Surgeons of England, 35-43 Lincoln's Inn Fields, London WC2A 3PN, England.

## MATERIALS AND METHODS

Permission for this study was obtained from the Research Ethics Committee of Hammersmith Hospital.

### Patients

The 47 patients in this study were admitted to a neurosurgical unit (National Hospitals for Nervous Diseases or Royal Free Hospital). The patients ranged in age from 30 to 77 years; there were 26 men and 21 women. In all cases a contrast enhanced CT scan (third or fourth generation) displayed a low attenuation focal lesion with evidence of a mass effect, consistent with the presence of an intracranial tumour. All patients underwent biopsy (open or serial stereotaxic) or tumour resection. Tissue histology revealed astrocytoma (grades I–IV) in 26 cases, metastatic tumour in 7 cases, meningioma in 9 cases, and 5 other miscellaneous tumours (1 gemistocytic astrocytoma, 2 oligodendrogliomas, 1 neuroblastoma, 1 schwannoma). In seven of these cases, normal white matter was available from one of the serial biopsies or from normal brain resected at surgery.

### In Vitro $^1$H MRS

The biopsy samples ranged in weight from 5 mg to 2.6 g. Each sample was frozen in liquid nitrogen within 30 s of surgical removal and then extracted into 12% perchloric acid, using standard procedures for extraction and neutralisation.

For 41 of the patients, sodium 3-(trimethylsilyl)2,2,3,3-tetradeuteropropionate (TSP) was added to the samples as a chemical shift and concentration standard. Spectroscopy was carried out on lyophilised samples redissolved in deuterium oxide; comparison of spectra before and after lyophilisation showed that this procedure caused no significant loss of metabolites.

Proton spectra were accumulated at 360 MHz on a Bruker spectrometer or at 500 MHz on a JEOL spectrometer. Concentrations were determined from relative peak areas in fully relaxed spectra (or after correction for saturation) taking into account the number of protons contributing to each signal (three for phosphocreatine + creatine (Cr) and NAA, nine for Cho and TSP). This permitted measurement of absolute concentrations in millimoles per kilogram wet weight of tissue.

Data are presented as means ± SEM and statistical significance was evaluated using a two-tailed Student $t$ test.

Histology was performed on all samples, including the normal white matter. Immediate diagnosis was made on smear results and confirmed in sections of fixed and embedded material. The results were classified according to Kernohan's classification of central nervous system tumours.

### In Vivo MRS

In vivo MRS was performed on 11 of the patients 30–72 years old (5 men and 6 women) and 5 normal male volunteers (24–57 years old). The volunteers gave no significant history of neurological illness and had no abnormal findings on neurological examination.

Proton MR imaging and spectroscopy studies were carried out on a whole body Picker prototype system operating at 1.6 T. Imaging was performed in at least two orthogonal planes using a partial saturation sequence (PS 500/17). A cubic volume of interest was selected to contain the bulk of the tumour and avoid overlap with the skull and surrounding bone marrow.

Proton spectra were obtained with a multiple spin echo sequence incorporating techniques for water suppression and spatial localisation. The water signal was suppressed with a binomial pulse (1331) optimised for detection of NAA, except in one case, where optimisation was for lactate. The time to the start of data collection (echo time) was 270 ms; this value was chosen to allow observation of the proton-coupled Lac signal. A repetition time of 2 s was used. Spatial localisation was achieved by the use of slice selected 180° pulses in three orthogonal directions ($x,y,z$). Large gradient pulses were employed to dephase unwanted signals generated by out-of-slice excitation of the magnetisation. In addition, each 180° pulse was phase alternated. Static magnetic field inhomogeneities were minimized using an identical gradient pulse pattern, but with a reduced radiofrequency pulse angle in place of the binomial suppression pulse.

Proton spectra were obtained from volumes of typically 64 cm$^3$. In five patients, spectra were obtained from a radiologically normal region within the contralateral hemisphere as well as from the tumour volume. In the normal subjects spectra were obtained from volumes of interest placed either in the temporoparietal region of one hemisphere or spanning the temporoparietal regions of both hemispheres.

## RESULTS

### In Vitro MRS

Figure 1a shows a spectrum from an extract of normal white matter. The spectrum contains signals from a wide range of metabolites, including lactate (Lac), NAA, Cr, and Cho. Lactate is greatly elevated relative to its value in vivo because of the

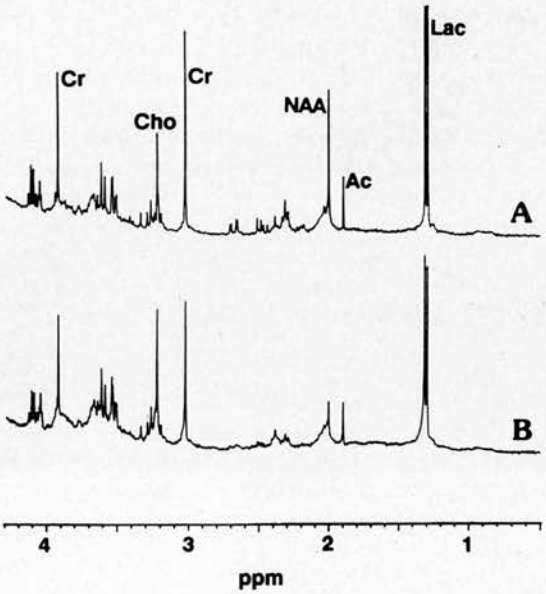



**FIG. 1.** Proton spectra obtained from perchloric acid extracts of two biopsy specimens from the same patient. **a:** normal white matter; **b:** grade III astrocytoma. Acetate (Ac) enters as an impurity in the course of extraction and storage of the specimen. For other abbreviations see the text.

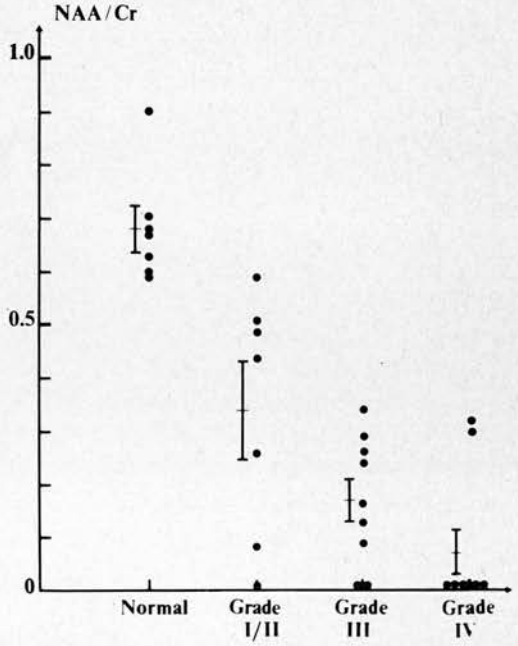



**FIG. 2.** *N*-Acetylaspartate/creatine (NAA/Cr) ratios obtained by $^1$H NMR analysis of biopsy specimens from normal white matter and astrocytomas of increasing grade of malignancy.

unavoidable anaerobic glycolysis that occurs during the short period of time between surgical removal and freezing. Similarly, because of hydrolysis of phosphocreatine to creatine during this period, the signals at 3.03 and 3.93 ppm are from the $CH_3$ and $CH_2$ groups, respectively, of creatine, with little contribution from phosphocreatine. These Cr signals therefore represent the sum of the creatine and phosphocreatine that would be present in vivo.

The spectrum from an extract of a grade III astrocytoma is shown in Fig. 1b. The spectrum differs markedly from that of normal white matter. The most noticeable difference is an elevated Cho/Cr ratio and a reduced NAA/Cr ratio. The data from normal white matter and from a series of astrocytomas are summarised in Table 1 and Figs. 2 and 3. The Cho/Cr ratio differs significantly in the grade IV tumours from its value in all other groups ($p < 0.01$). In addition, the NAA/Cr ratio differs significantly in all tumour groups from its value in normal white matter ($p < 0.01$). Excluded from the figures and the table are three cases in which the samples were necrotic; these samples produced barely any signal from NAA, Cr, or Cho, so it was not possible to measure metabolite ratios. However, lactate was still present at an average concentration of 5.4 mmol/kg wet wt.

A typical spectrum from a meningioma extract is shown in Fig. 4. This includes a relatively large signal at 1.47 ppm, which can be assigned to alanine (Ala). Biopsy samples from nine meningiomas were studied. One of these was malignant and necrotic and produced very little signal from Cho, Cr, NAA, or alanine; this made it difficult to measure ratios. In the other eight samples, NAA was not detectable, the Cho/Cr ratio was 1.58 ± 0.27, the Cr concentration was 0.54 ± 0.13 mmol/kg wet wt, and the alanine concentration was 0.91 ± 0.19 mmol/kg wet wt. In six of these eight samples, alanine was present at a higher concentration than Cr. In comparison with the astrocytomas, the unusual feature of the meningiomas is the high ratio of alanine to total Cr; only one of the astrocytomas displayed this feature.

Of the other 12 tumours that were investigated, 9 had no detectable NAA and had Cho/Cr ratios ele-

**TABLE 1.** *Metabolite ratios and Cr concentration in normal white matter and astrocytomas*

| | Cho/Cr | NAA/Cr | NAA/Cho | Cr concentration (mmol/kg wet wt) |
|---|---|---|---|---|
| Normal white matter (n = 7) | 0.22 ± 0.03 | 0.68 ± 0.04 | 3.44 ± 0.40 | 8.0 (mean of 2) |
| Grade I/II astrocytoma (n = 7) | 0.30 ± 0.04 | 0.34 ± 0.09 | 1.40 ± 0.42 | 6.09 ± 1.48 (n = 6) |
| Grade III astrocytoma (n = 9) | 0.39 ± 0.06 | 0.17 ± 0.04 | 0.63 ± 0.21 | 4.06 ± 1.08 (n = 5) |
| Grade IV astrocytoma (n = 7) | 1.12 ± 0.16 | 0.07 ± 0.04 | 0.09 ± 0.06 | 2.73 ± 0.25 (n = 6) |

Cho, choline-containing compounds; Cr, phosphocreatine + creatine; NAA, *N*-acetylaspartate.

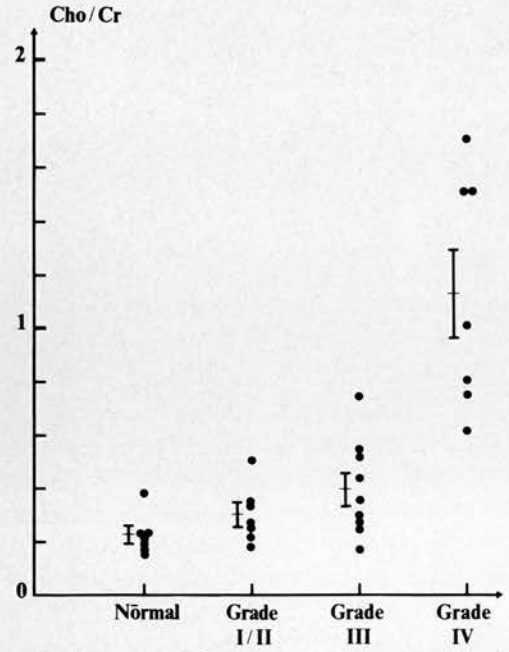



**FIG. 3.** Choline-containing compounds/creatine (Cho/Cr) ratios obtained by $^1$H NMR analysis of biopsy specimens from normal white matter and astrocytomas of increasing grade of malignancy.

vated beyond the control range. Only in the neuroblastoma, one metastatic carcinoma, and the gemistocytic astrocytoma was NAA observed. No signal from alanine was detected.

## In Vivo MRS

The proton spectrum illustrated in Fig. 5 is typical of those obtained from control subjects. The dominant peak at 2.0 ppm is from NAA, and signals from Cr (3.0 ppm) and Cho (3.2 ppm) are also observed. The peak ratios are influenced by the technique used; in this case the sequence was optimised for detection of NAA, which explains, at least in part, why the NAA/Cho and NAA/Cr ratios appear higher than in parallel studies of biopsy specimens. The spectra obtained from the radiologically normal volume of the patients' brains were similar to those of control subjects and were used for assessing the tumour spectra.

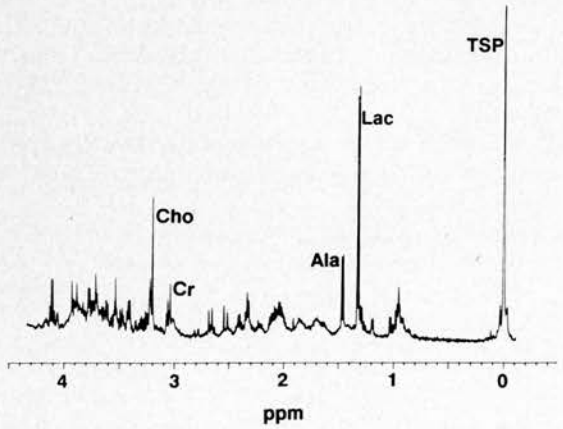



**FIG. 4.** Proton spectrum obtained from an extract of a biopsy from a meningioma. For abbreviations see the text.

Eleven patients were studied in vivo. The combined results of histology, in vitro MRS analysis, and in vivo analysis are shown in Table 2 and the main points can be summarised as follows.

### *Patient A*

The in vitro spectrum from one of five serial stereotaxic biopsies is shown in Fig. 6a. The extracts showed a moderate increase in the Cho/Cr ratio within the tumour and no detectable NAA. The main feature of the spectrum obtained in vivo (Fig. 6c) is a marked reduction in the NAA/Cr ratio. The Cho/Cr ratio was ranked as being within normal limits, but is consistent with a moderate increase. The residual NAA signal observed in vivo may reflect the presence of normal tissue, or it may be from other *N*-acetyl-containing compounds (see Discussion). Taking these possibilities into consideration, the in vivo and in vitro data are in excellent agreement with each other.

The signal at 1.3 ppm, containing contributions from lactate and fat, was ranked as within normal limits when compared with the Cr signal. Taking into account the low level of total Cr (measured from the biopsies to be 1.3 mmol/kg wet wt), there is no evidence for an elevation of lactate within this tumour.

### *Patient B*

The in vitro spectrum (Fig. 7a) showed the characteristic features of a meningioma; the abnormalities in the in vivo spectrum (Fig. 7c) were consistent with these features, showing a peak at 1.5 ppm (*) which can be assigned to alanine, and an elevated Cho/Cr ratio. The residual NAA signal may be from adjacent normal tissue or may reflect contributions from additional compounds.

### *Patient C*

The in vitro spectrum was characteristic of necrosis with a large lactate signal but very little signal from Cho, Cr, or NAA. The in vivo spectrum showed a highly elevated signal at 1.3 ppm, which contains contributions from lactate and fat, an elevated Cho/Cr ratio, and a reduced NAA/Cr ratio, consistent with a partially necrotic astrocytoma.

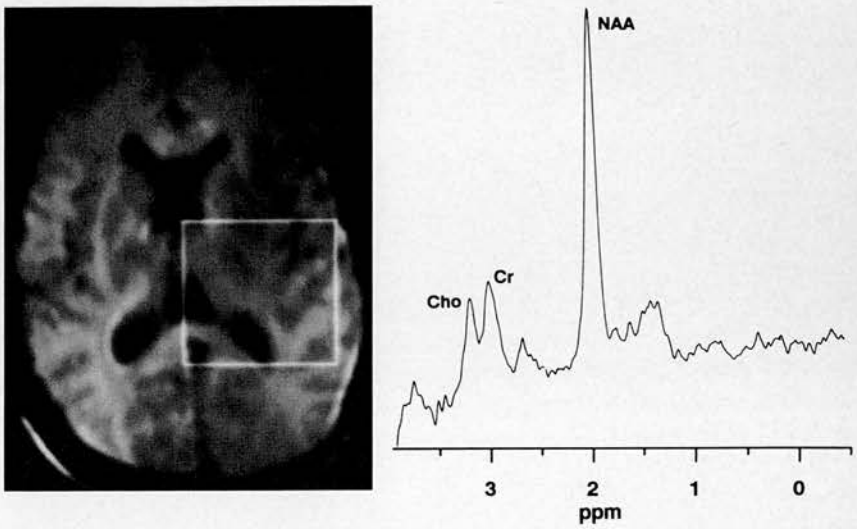



**FIG. 5.** A 29-year-old man with no significant neurological history and a normal neurological examination. **a:** Transverse proton MR image (PS 500/17 at 1.6 T) at the ventricular level; the volume of interest is indicated. **b:** Proton spectrum from the selected volume. For abbreviations see the text.

*Patient D*

The in vitro and in vivo spectra both show elevated Cho/Cr and reduced NAA/Cr ratios. This grade II astrocytoma displayed greater abnormalities of these ratios (both in vivo and in vitro) than any of the other low grade astrocytomas that we have studied.

*Patient E*

The in vitro spectrum showed elevated Cho/Cr and reduced NAA/Cr ratios; these ratios were difficult to assess in vivo because the spectra in this case were optimised for the detection of lactate. There was an elevation of the signal at 1.3 ppm in vivo.

*Patient F*

Two samples were examined in vitro: One was typical of necrosis, the dominant signal being from lactate (with barely any NAA, Cr, or Cho signal), while the other sample showed a normal Cho/Cr ratio and a small reduction in NAA/Cr. The in vivo spectrum showed Cho/Cr and NAA/Cr ratios within normal limits and an elevated signal at 1.3 ppm. As for Patient C (see Discussion), this is consistent with necrosis within the tumour.

*Patient G*

The in vitro spectrum showed a normal Cho/Cr ratio and reduced NAA/Cr ratio; in vivo the only abnormality was a moderate increase in lactate.

**TABLE 2.** *Histological diagnosis and NMR analysis of patients studied in vivo and in vitro*

| Patient/ age (yrs)/sex | Diagnosis | In vitro | | In vivo | | |
|---|---|---|---|---|---|---|
| | | Cho/Cr | NAA/Cr | Cho/Cr | NAA/Cr | Lac/Cr |
| A/68/M | Astrocytoma III | 1 | −2 | 0 | −2 | 0 |
| B/41/F | Meningioma | 2 | x | 2 | 0 | x |
| C/48/M | Recurrent astrocytoma post radiotherapy IV | x | x | 2 | −1 | 2 |
| D/44/F | Astrocytoma II | 2 | −2 | 2 | −2 | 0 |
| E/72/M | Secondary adenocarcinoma | 2 | −2 | x | x | 2 |
| F/57/F | Necrotic astrocytoma III | x<br>0 | x<br>−1 | 0 | 0 | 2 |
| G/50/M | Astrocytoma I/II | 0 | −2 | 0 | 0 | 1 |
| H/71/F | Astrocytoma IV | x | x | x | −1 | 0 |
| I/30/M | Infiltrative astrocytoma I/II | 0 | 0 | 0 | −2 | 0 |
| J/52/F | Astrocytoma IV | 2 | −2 | 0 | 0 | 0 |
| K/40/F | Astrocytoma I/II | 1 | −1 | 1 | −2 | 0 |

The in vivo spectra were ranked by four observers blinded to the histology. Cho, choline-containing compounds; Cr, phosphocreatine + creatine; NAA, *N*-acetylaspartate; Lac, lactate; (+2), definite increase; (+1), moderate increase; (0), within normal limits; (−1), moderate decrease; (−2), definite decrease; (x), no comment can be made.

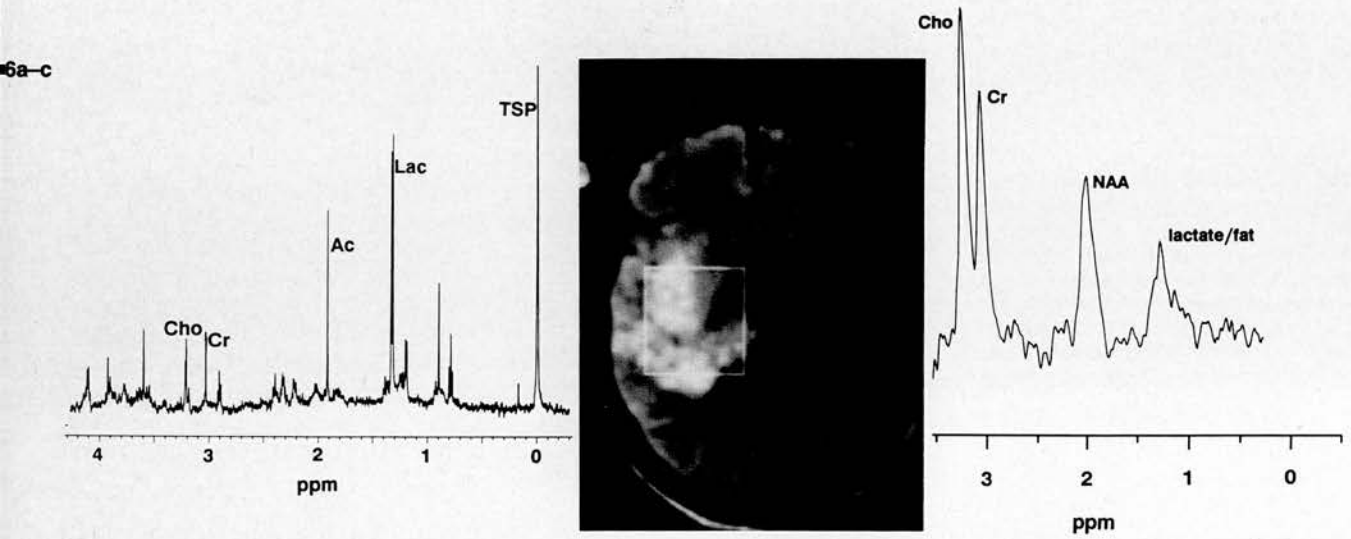



**FIG. 6.** A 68-year-old man with a grade III astrocytoma (Case A). **a:** Proton spectrum of biopsy extract from the tumour. **b:** Proton MR image (SE 1,500/80 at 0.15 T); the volume of interest is indicated. **c:** Proton spectrum from the volume of interest. For abbreviations see the text.

*Patient H*

The in vitro spectrum was typical of necrosis (very little signal from NAA, Cr, or Cho), although the histological report made no mention of this. In vivo there was a moderate decrease in the NAA/Cr ratio with no evidence of an increase in lactate. This would be consistent with only a small degree of necrosis.

*Patient I*

The in vitro spectrum showed normal metabolite ratios, whereas in vivo there was a marked reduction in the NAA/Cr ratio. This illustrates the fact that a single biopsy does not necessarily detect an overall abnormality.

*Patient J*

The in vitro spectrum showed a marked increase in Cho/Cr and a marked decrease in NAA. The lack of any detectable abnormality in vivo can be attributed to extensive contamination from normal tissue as the tumour occupied only a small percentage of the localised volume.

*Patient K*

The in vitro spectrum showed a moderate increase in Cho/Cr and decrease in NAA/Cr. The

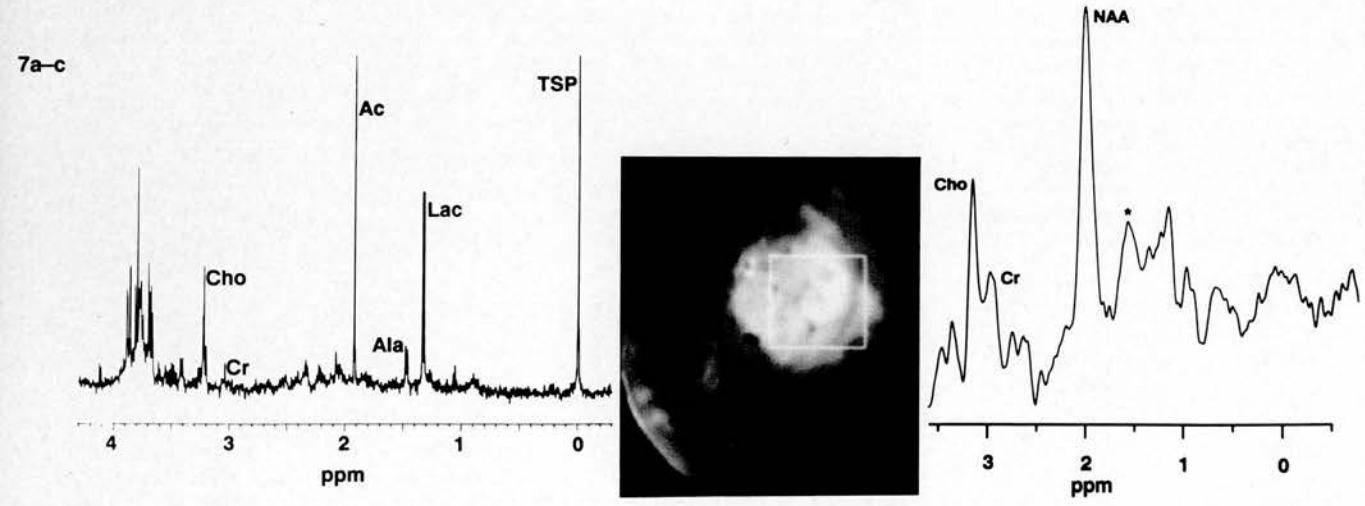



**FIG. 7.** A 41-year-old woman with a meningioma (Case B). **a:** Proton spectrum of biopsy extract from the tumour. **b:** Transverse proton MR image (PS 500/17 at 1.6 T) at the ventricular level; the volume of interest is indicated. **c:** Proton spectrum from the selected volume. Ac, acetate; for other abbreviations see the text.

changes observed in vivo were consistent with the in vitro data.

## DISCUSSION

In this study we have used in vitro spectroscopy to investigate a large number of intracranial tumours and have applied our results to evaluate clinical $^1$H MRS.

Our in vitro data for normal white matter agree well with typical metabolite levels and concentration ratios that have been measured in the mammalian brain, using both NMR and more conventional analytical techniques (8,16,17). It is interesting to note that recent proton spectra of the human brain in vivo yielded an apparent NAA/Cr ratio of ~1.7 in normal white matter (6), which is much larger than the ratio measured in our biopsy samples. A similar finding has also been noted by Hanstock et al. (4). It was suggested that the high ratio may reflect a significant contribution to the "NAA" signal from additional acetyl-containing compounds. These may include compounds such as *N*-acetylneuraminic acid and *N*-acetylgalactosamine (18). Our data add weight to this suggestion, but indicate that any such additional compounds are not extracted by perchloric acid.

Our results demonstrate several notable differences between tumour tissue and normal brain. It is known that metabolite ratios change according to location within the normal brain (6,7). However, the abnormalities we discuss here are too great to be caused by spatial variation alone.

The reduced level of total Cr that we observe in many of the tumours is consistent with the data of Lowry et al. (16), who reported a variable (and often low) total Cr concentration in gliomas in which there was no evidence of necrosis. Also, the very low content of NAA that we detect in many of the astrocytomas has previously been demonstrated by Nadler and Cooper (8) using spectrophotometric methods. Necrosis can reduce these metabolite levels even further. On the basis of their observations, Nadler and Cooper suggested that NAA is located primarily in neurons. Further evidence for this has come from the results of Koller et al. (9), who showed that NAA concentrations fell by 96% after decortication and destruction of striatal neurones in the rat. Therefore, the proton NMR signal from NAA may provide an endogenous marker for neurons.

Nadler and Cooper (8) suggested that the residual NAA that they detected in astrocytomas may have been due to extensive infiltration of normal brain by the astrocytomas and hence contamination of their samples with normal cells. Similarly, our in vivo spectra are also contaminated by signals from normal tissue. This is evident from the observation that the NAA/Cr ratio is frequently higher in vivo than in vitro, although we cannot exclude the possibility that the differences also reflect a contribution to the signal in vivo from other *N*-acetyl-containing compounds. As techniques evolve, there is scope for some improvement in spatial resolution that will tend to discriminate between these effects.

An elevated ratio of alanine to Cr and to other metabolites is noted in meningiomas, and although the reason for this is not clear, it could be of diagnostic value. The absence of NAA in the biopsy spectra is consistent with the fact that there is no neuronal tissue in meningiomas.

While the in vitro spectra provide important information about many of the tumour metabolites and their relative concentrations, these spectra cannot provide an accurate assessment of the lactate concentration present in the tumours prior to biopsy. This is because lactate accumulates during the unavoidable period between surgical removal and freezing of the tissue, so that the lactate signal is elevated in the extract spectrum. However, in the necrotic specimens, this mechanism is less likely to explain the relatively high lactate concentration of ~5 mmol/kg wet wt that we observed, as the rate of anaerobic glycolysis within these samples is likely to be very low. This suggests that necrotic tissue does indeed contain a high concentration of lactate and that it may therefore be acting as a lactate "pool," storing the lactic acid produced by surrounding cells. This would be consistent with the in vivo results. Of the astrocytomas that we studied, the largest increase in lactate relative to other metabolites was observed in the two tumours in which histology demonstrated necrosis.

The elevated lactate that is often observed in tumours could prove useful in the evaluation of therapy; for example, a fall in intracranial pressure may reduce anaerobic glycolysis, and hence the production of lactate. The important relationship of lactate to intracellular and extracellular pH (19) requires further investigation, and the combined methods of proton and phosphorus spectroscopy offer a means of doing this. However, the lactate signal may arise largely from necrotic tissue, where there may be low concentrations of the phosphorus-containing metabolites, from which the pH is calculated. Therefore, proton and phosphorus spectroscopy do not necessarily report on the same environment, so that caution may be required in making direct correlations between $^{31}$P and $^1$H data.

In evaluating the future role of $^1$H MRS in diagnosis, it is important to bear in mind that the in vivo spectrum reflects metabolite signals from the majority of the tumour volume. In contrast, diagnostic biopsies are taken from small areas of the neoplasm and may reflect localised histology rather than the overall pathology of the lesion.

At present, the possible clinical applications of

this technique, with regard to intracranial tumours, include (a) the differentiation of meningiomas from astrocytomas based largely on the Ala/Cr ratio, (b) the assessment of degree of malignancy of an astrocytoma (from the Cho/Cr ratio), and (c) the detection of a raised lactate signal implying abnormal anaerobic glycolysis. Clinical proton MR studies combine imaging and spectroscopy with ease. The same coil tuning and frequencies are used for both, and so they can be readily incorporated into one examination providing both high resolution images and a metabolic profile of the area of interest. Further clinical studies are required, but the trends shown in this article demonstrate a clear role for $^1H$ spectroscopy in the diagnosis and biochemical assessment of intracranial tumours and in the evaluation and monitoring of therapy.

**Acknowledgment:** We are grateful to the Departments of Neuropathology at the Royal Free Hospital and the National Hospitals for Nervous Diseases. We thank the Medical Research Council, Rank Foundation, and Imperial Cancer Research Fund for their support. We also thank the University of London Intercollegiate Research Service for NMR facilities at Birkbeck College (JEOL 500).

## REFERENCES

1. Barany M, Langer BG, Glick RP, Venkatasubramanian PN, Wilbur AC, Spigos DG. In vivo $^1H$ spectroscopy in humans at 1.5T. *Radiology* 1988;167:839–44.
2. Bomsdorf H, Helzel T, Kunz D, Roschmann P, Schendel OT. Spectroscopy and imaging with a 4T whole body system. *NMR Biomed* 1988;1:151–8.
3. Hanstock CC, Rothman DL, Jue T, Shulman RG. Volume selected proton spectroscopy in the human brain. *J Magn Res* 1988;77:583–8.
4. Hanstock CC, Rothman DL, Prichard JW, Jue T, Shulman RG. Spatially localized $^1H$ NMR spectra of metabolites in the human brain. *Proc Natl Acad Sci USA* 1988;85:1821–5.
5. Frahm J, Bruhn H, Gyngell ML, Merboldt KD, Hanicke W, Sauter R. Localised high resolution proton NMR spectroscopy using stimulated echoes: initial applications to human brain in vivo. *Magn Res Med* 1989;9:79–93.
6. Frahm J, Bruhn H, Gyngell ML, Merboldt KD, Hanicke W, Sauter R. Localised proton NMR spectroscopy in different regions of the human brain in vivo. Relaxation times and concentrations of cerebral metabolites. *Magn Res Med* 1989;11:1147–63.
7. Narayana PA, Fotedar LK, Jackson EF, Bohan TP, Butler IJ, Wolersky JS. Regional in vivo proton magnetic resonance spectroscopy of brain. *J Magn Res* 1989;83:44–52.
8. Nadler JV, Cooper JR. *N*-Acetyl-L-aspartic acid content of human neural tumours and bovine peripheral nervous tissues. *J Neurochem* 1972;19:313–9.
9. Koller KJ, Zaczek R, Coyle JT. *N*-Acetyl-aspartyl-glutamate: regional levels in rat brain and the effects of brain lesions as determined by a new HPLC method. *J Neurochem* 1984;43:1136–42.
10. Ansell B, Spanner S. Sources of choline for acetylcholine synthesis in the brain. In: *Nutrition and the brain, vol. 5.* New York: Raven Press, 1979:435–45.
11. Walker JB. Creatine: biosynthesis, regulation and function. *Adv Enzymol* 1979;50:177–242.
12. Luyten PR, van Rijen PC, Berkelbach v.d Sprenkel JW, Tulleken CAF, den Hollander JA. $^1H$ NMR spectroscopic detection of cerebral metabolic alterations in patients with haemodynamically significant cerebrovascular disease. Book of abstracts, Soc Magn Res Med, San Francisco meeting, 1988:619.
13. Bruhn H, Frahm J, Gyngell NM, Merboldt KD, Hanicke W, Sauter R. Cerebral metabolism in man after acute stroke: new observations using localised proton NMR spectroscopy. *Magn Res Med* 1989;9:126–31.
14. Bruhn H, Frahm J, Gyngell ML, Merboldt KD, Hanicke W, Sauter R. Localised proton spectroscopy of tumours in vivo: patients with primary and secondary cerebral tumours. Book of abstracts, Soc Magn Res Med, San Francisco meeting, 1988:253.
15. Luyten PR, den Hollander JA, Segebarth C, Baleriaux D. Localised $^1H$ NMR spectroscopy and spectroscopic imaging of human brain tumours in situ. Book of abstracts, Soc Magn Res Med, San Francisco meeting, 1988:252.
16. Lowry OH, Berger SJ, Chi MMY, Carter JG, Blackshaw A, Outlaw W. Diversity of metabolic patterns in human brain tumours—I. High energy phosphate compounds and basic composition. *J Neurochem* 1977;29:959–77.
17. Petroff OAC, Ogino T, Alger JR. High-resolution proton magnetic resonance spectroscopy of rabbit brain: regional metabolite levels and postmortem changes. *J Neurochem* 1988;51:163–71.
18. Vanier MT, Holm M, Ohman R, Svennerholm L. Developmental profiles of gangliosides in human and rat brain. *J Neurochem* 1971;18:581–92.
19. Paschem W, Djuricic B, Mies G, Schmodt-Kastner R, Linn F. Lactate and pH in the brain: association and dissociation in different pathophysiological states. *J Neurochem* 1987; 48:154–9.

*Anaesthesia*, 1992, Volume 47, pages 240–255

SPECIAL ARTICLE

# Magnetic resonance for the anaesthetist

## Part I: physical principles, applications, safety aspects

D. K. MENON, C. J. PEDEN, A. S. HALL, J. SARGENTONI AND J. G. WHITWAM

**Summary**

*Anaesthetists are being increasingly involved in magnetic resonance (MR) procedures, both in patient care and as a research tool. This paper outlines the physical basis of nuclear magnetic resonance and describes its application in magnetic resonance imaging and spectroscopy. Principles of magnet design and safety relevant to anaesthetic practice in a magnetic resonance environment are discussed and guidelines for anaesthetic practice suggested. Some recent clinical magnetic resonance studies of anaesthetic interest are reviewed.*

**Key words**

*Measurement techniques*; nuclear magnetic resonance, magnetic resonance imaging, magnetic resonance spectroscopy.

Nuclear magnetic resonance (NMR) is a phenomenon that was first described by Bloch and Purcell in 1945, and the technique was widely used as an analytical tool in chemistry and biochemistry in the following decades. In 1973, Lauterbur and his associates published the first application of NMR to imaging, and laid the foundations of what proved to be an important medical imaging tool. This application of NMR to imaging came to be known as magnetic resonance imaging (MRI), the 'nuclear' in NMR being removed to emphasise that this technique was unassociated with any radiation risk. By analogy, the application of NMR to chemical and biochemical analysis has come to be termed magnetic resonance spectroscopy (MRS). At present, MRI is the imaging modality of choice in the diagnosis of many neurological and orthopaedic conditions, and MRS has been widely used for research and may soon acquire a diagnostic role. There are more than 2500 MR installations in the USA, and though there are still only about 50 modern MR units in the UK, this number is likely to rise, and anaesthetists may find themselves increasingly involved in patient care and research in MR. It is important, therefore, that anaesthetists acquire an understanding of the technique and familiarity with patient management in an MR environment. This paper is based on the knowledge and experience acquired over 2 years in a research MR site at the Hammersmith Hospital, and is in two parts. In Part I we explain the physical basis of NMR, outline its application to spectroscopy and imaging, and discuss the safety of MR procedures. Part II

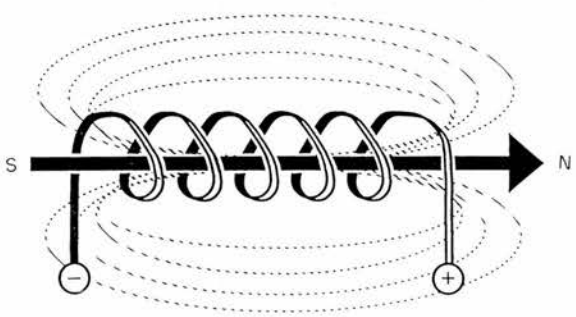



**Fig. 1.** Diagrammatic representation of current flowing through a coil and producing an electromagnetic field. N and S in this and subsequent diagrams represent the north and south poles of the magnet.

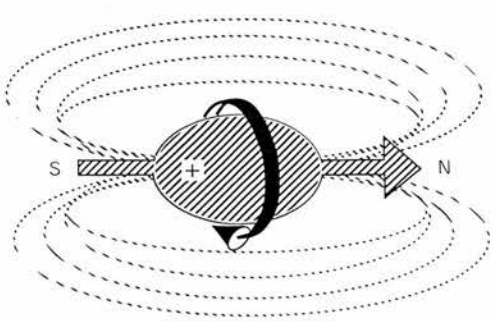



**Fig. 2.** Diagrammatic representation of a spinning atomic nucleus. Movement of the positively charged protons produces a magnetic field, causing the nucleus to behave like a baby bar magnet.

D.K. Menon, MD, MRCP, FFARCS, MRC Research Fellow, C.J. Peden, BSc, MB, ChB, FFARCS, MRC Research Fellow, A.S. Hall, PhD, Physicist, J. Sargentoni, DCRR, DMU, Radiographer, NMR Unit, Hammersmith Hospital, J.G. Whitwam, PhD, FRCP, FFARCS, Professor of Anaesthesia, Hammersmith Hospital, Du Cane Road, London W12 0HS.
Accepted 25 July 1991.

0003–2409/92/030240+16 $03.00/0
© 1992 The Association of Anaesthetists of Gt Britain and Ireland

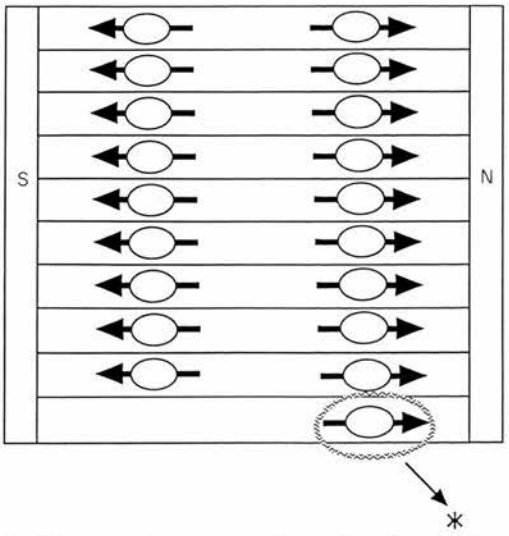



**Fig. 3.** Diagrammatic representation of NMR-sensitive nuclei aligned in a magnetic field. Nuclei are aligned either parallel or antiparallel to the field. A small excess of nuclei ($1–2/10^6$) are parallel to the field (*), and are responsible for the NMR phenomenon.

deals with monitoring systems and anaesthetic practice in MR environments.

This discussion of the principles of NMR uses a combination of quantum and classical physics, and attempts to simplify what is a complex phenomenon. In the interest of clarity, some detail is necessarily lost, and readers looking for a more comprehensive description are referred elsewhere [1].

## Physical principles

### *The basis of nuclear magnetism*

All atomic nuclei possess a charge (due to the presence of protons) and mass (due to the presence of protons and neutrons). In addition, the nuclei of some atoms possess a spin, a property that may be visualised as a rotation of the nucleus about its own axis. Just as the flow of electrons in a wire loop produces an electromagnetic field (Fig. 1), the rotation of neutrons and protons in a spinning nucleus produces a local magnetic field (Fig. 2). As a result the nucleus behaves like a miniature bar magnet. This nuclear magnetism is many times weaker than the common magnetism with which we are familiar (and which is a property of electrons).

### *Behaviour of NMR sensitive nuclei in a magnetic field*

When NMR sensitive nuclei are placed in a powerful static magnetic field (referred to as the $B_0$ field), they tend to align themselves longitudinally with the field (along an axis arbitrarily designated as 'Z'). Approximately one half of the nuclei are aligned parallel to the field and the other half antiparallel to it (Fig. 3). There is a small excess of nuclei in the lower energy parallel state, and a small net magnetisation parallel to the $B_0$ field. It is this small excess of nuclei in the parallel state (typically of the order of $1–2/10^6$) that are of interest and form the subject of the remainder of this discussion. Since such a small proportion of available nuclei are responsible for the NMR phenomenon, and since the energy transitions involved are small, magnetic resonance is basically an insensitive technique, and can only be used to study substances that are present in at least millimolar concentrations.

### *The resonant frequency of a nucleus and its determinants*

When aligned with the field, the nuclei continue to spin, and at the same time their axis of rotation rotates around the Z axis. This combination of movements is termed precession, and is a process that is best exemplified by the movement of a spinning top in the earth's gravitational field (Fig. 4). The frequency of nuclear precession ($\nu$) depends on two variables: the gyromagnetic ratio ($\gamma$), which is specific for each nucleus, and the strength of the magnetic field ($B_0$):

$$\nu = \gamma.B_0/2\pi \qquad (1)$$

Thus, each nucleus has a characteristic or resonant frequency at a given magnetic field strength. The specificity of this frequency enables the selection of a particular nucleus for study.

### *Excitation of nuclei by a second magnetic field and the production of NMR signal*

When such a population of nuclei is intermittently subjected to a second magnetic field ($B_1$), oscillating at the resonant frequency of the nucleus, and orientated at right angles to the static field ($B_0$), they tend to flip away from their longitudinal alignment and produce magnetisation in

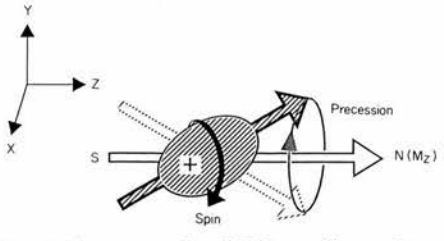



**Fig. 4.** Movement of an NMR-sensitive nucleus in a magnetic field. The nucleus spins on its own axis, and precesses about the magnetic axis.

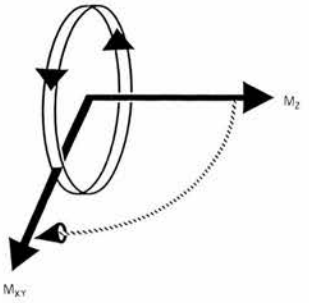



**Fig. 5.** Application of an oscillating ($B_1$) field causes the magnetisation along 'Z' to flip into the XY plane, where it continues to precess around the Z axis.

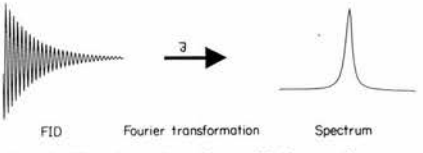



**Fig. 6.** The decaying sinusoidal waveform on the left is the free induction decay (FID) and represents the current induced in a copper wire placed in the vicinity of an excited nucleus (as in Fig. 5). Fourier transformation of the FID ( ∃ ) results in a spectrum where intensity is plotted against frequency.

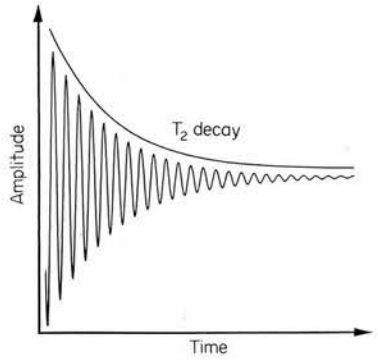



**Fig. 7.** Diagrammatic representation of the decay of an FID, which is characterised by the spin–spin relaxation time constant ($T_2$).

a plane at right angles to the Z axis (the XY plane) (Fig. 5). This magnetisation in the XY plane is still precessing around the Z axis, and decays with time after each exciting pulse. A stationary wire in the presence of such a changing magnetic field has a current induced within it. This current has a decaying sinusoidal waveform (Fig. 6), whose frequency is the same as the frequency of nuclear precession, the resonant frequency ($\nu$).

This current is related to the NMR signal and is graphically represented as the Free Induction Decay (FID), which is a plot of signal intensity against time. The FID can be subjected to a process termed Fourier Transformation to produce a spectrum, where signal intensity is plotted against signal frequency (Fig. 6). Thus, the Fournier Transform (FT) process relates signal in the time and frequency domains. When the nucleus being studied is present in very small concentrations ($\approx$ 1 millimolar), several free induction decays may need to be averaged to produce a spectrum with useful amounts of signal in relation to the background noise.

*Relaxation time constants ($T_1$ and $T_2$)*

The decay of transverse magnetisation with time is described by a time constant termed the spin–spin relaxation time constant or $T_2$ (Fig. 7). Thus, when $T_2$ is large the signal tends to decay more slowly. It is important to note that $T_2$ can be used to provide a measure of the mobility of the environment of a given nucleus, generally increasing with increasing molecular mobility, and decreasing with molecular restriction. In practice, the time frame of most biologically significant NMR experiments means that we tend to see signals that arise predominantly from small mobile molecules, since the signal from larger molecules has a very short $T_2$ (i.e. decays very rapidly) and usually goes undetected.

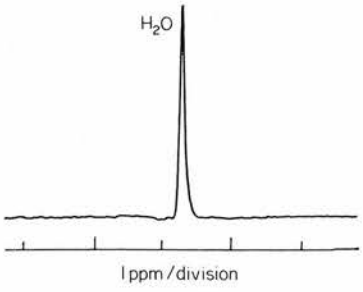



**Fig. 9.** Proton spectrum of water. All the protons are in a similar chemical environment and produce a single resonance.

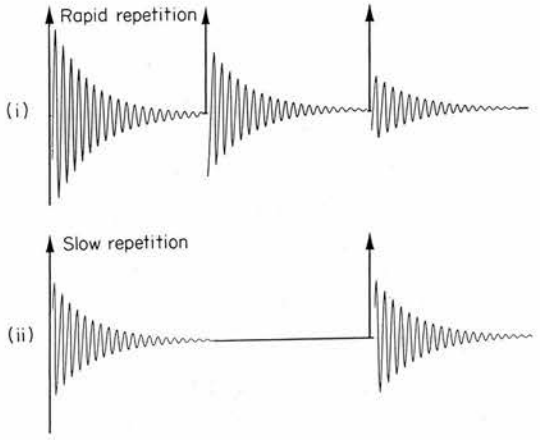



**Fig. 8.** Effect of repetition time (TR) on signal levels. Successive excitations are denoted by vertical arrows. In (i) the TR is short, recovery of magnetisation between successive pulses is incomplete and signal from successive pulses is attenuated. In (ii) the long TR allows complete recovery of magnetisation and signal strength is maintained with successive pulses.

Each time the longitudinal magnetisation along the Z axis is flipped into the XY plane, it takes a finite amount of time to recover to basal levels. This process of recovery of longitudinal magnetisation can be characterised by another time constant, termed the spin–lattice relaxation time constant or $T_1$. If the time between successive excitations is short, nuclei with a long $T_1$ will recover incompletely between excitations, resulting in decreasing amounts of NMR signal, a process termed saturation (Fig. 8).

## Chemical implications and biochemical applications

*Effects of chemical structure on resonant frequency: the chemical shift ($\delta$)*

It is clear from the above discussion that the frequency of a given signal depends on the nucleus being studied and the strength of the magnetic field that it is in. What makes NMR useful as a chemical tool is the fact that the magnetic field surrounding a given nucleus is subtly modified by the atoms that surround it, resulting in a change in resonant frequency with changing chemical composition. Thus, the proton (or hydrogen) spectrum from water consists of a single line because the two hydrogen nuclei within each $H_2O$ molecule have the same chemical environment (Fig. 9). The proton spectrum from acetic acid, on the other hand (Fig. 10), shows two peaks, each from protons in a unique chemical environment. The position of each

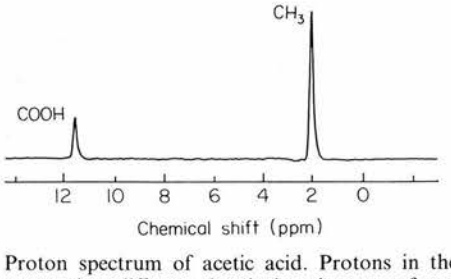



**Fig. 10.** Proton spectrum of acetic acid. Protons in the methyl ($CH_3$) group are in a different chemical environment from those in the carboxyl (−COOH) group, resulting in two separate resonances. Since there are three times as many methyl as carboxyl protons, the $CH_3$ resonance is three times the intensity of the −COOH resonance.

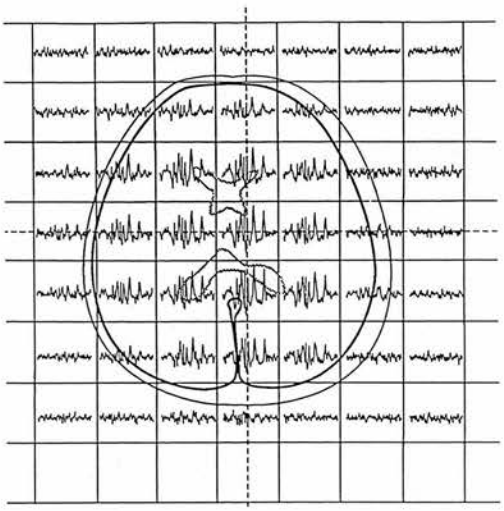


**Fig. 11.** One plane from a $^{31}P$ four-dimensional chemical shift image of the brain. $^{31}P$ MR spectra are simultaneously acquired from multiple voxels whose spatial location is shown above on an outline of a transverse image of the brain.

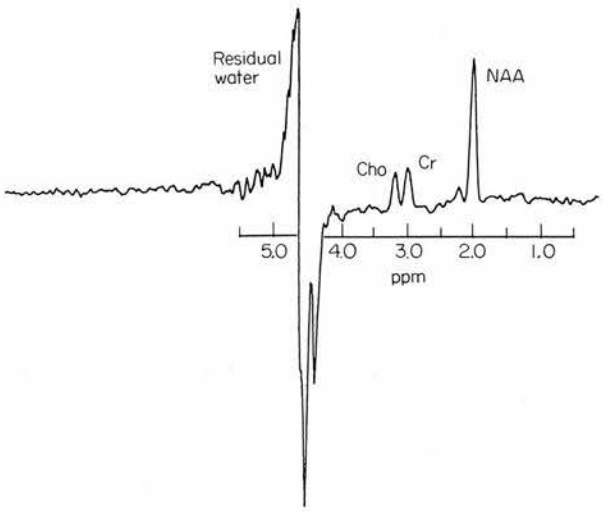



**Fig. 12.** Proton spectrum of the brain acquired from a 8 ml voxel in the parietal region of a volunteer. The complex resonance on the left arises from tissue water that has been suppressed by a factor of about 200 in order to allow visualisation of the metabolites. Abbreviations as in text.

peak on the horizontal axis can be expressed as its displacement from the resonant frequency in Hertz, but is more often expressed as its displacement from the resonance of an internal or external reference compound, and is termed its chemical shift. The chemical shift ($\delta$) is usually expressed as parts per million (ppm) of the reference frequency, an arrangement that enables comparison of chemical shifts at different field strengths. An inspection of Fig. 10 also shows that the height of each peak is related to the number of protons contributing to a particular resonance. Thus NMR, in the form of magnetic resonance spectroscopy, can provide quantitative chemical information. This application of NMR has been used *in vitro* by chemists and biochemists for many decades. What makes MRS especially useful is the fact that the phenomenon can be studied *in vivo*, thus providing what is a nondestructive, noninterventional, repeatable and nonhazardous method of acquiring chemical and biochemical information from living tissues.

Recent advances have also enabled the localisation of these signals to specific volume elements (or voxels); among the most advanced forms of such localisation is the four-dimensional chemical shift imaging (CSI) technique illustrated in Fig. 11, where a matrix of 512 voxels of 8 ml volume can be simultaneously sampled to yield spectroscopic information [2].

**Table 1.** NMR sensitive nuclei of biological interest.

| Nucleus | NMR frequency (MHz)* | Natural abundance (%) | Relative sensitivity at natural abundance |
|---|---|---|---|
| Protons ($^{1}H$) | 100.00 | 99.98 | 100.0 |
| Fluorine ($^{19}F$) | 94.08 | 100.00 | 83.3 |
| Phosphorus ($^{31}P$) | 40.48 | 100.00 | 6.6 |
| Carbon ($^{13}C$) | 25.14 | 1.11 | 0.02 |
| Sodium ($^{23}Na$) | 26.45 | 100.00 | 9.2 |

*Frequencies are arbitrarily assigned at a field strength of 2.35 tesla, chosen such that the resonant frequency for protons ($^{1}H$) is 100 MHz.

*NMR sensitive nuclei of medical/biological interest*

The nuclei that exhibit the NMR phenomenon and are of biological interest are listed in Table 1. As the table suggests, the usefulness of each of these nuclei depends on several factors, including its relative sensitivity (which depends on the gyromagnetic ratio of the nucleus and its natural abundance) and its biological importance. For purposes of comparison, the hydrogen nucleus is assigned a sensitivity of 100, and all other nuclei are compared against it. We shall now consider each of these nuclei in turn.

*Hydrogen (Protons, $^{1}H$)*

This is the most sensitive of the biologically significant nuclei, and is present in a wide variety of compounds. Body water contains approximately 100 molar $^{1}H$, and this high concentration provides the signal that is used for MR imaging. Prominent signals are also observed from fat. *In vivo* $^{1}H$ spectroscopy however, is hampered by these high proton concentrations since hardware currently in use is swamped by the signal and does not possess the dynamic range needed to study simultaneously metabolites that are only present in millimolar concentrations. $^{1}H$ spectroscopy therefore, requires the suppression of the massive water signal, which may be technically difficult to achieve. Most clinical $^{1}H$ MRS has concentrated on the brain, where a number of metabolites can be seen [3] (Fig. 12). These include N-acetyl aspartate (NAA), which seems to be a metabolic marker for normally functioning neurons, and signals from creatine and phosphocreatine (Cr), and from choline containing compounds (Cho), which are chiefly liquid substrates. Signals are also obtainable from other important metabolites such as lactate, glutamine, glutamate, taurine and inositols.

*Phosphorus-31 ($^{31}P$)*

This is a relatively insensitive nucleus, but the NMR visible isotope ($^{31}P$) does form the bulk of naturally occurring phosphorus. Many biologically important compounds

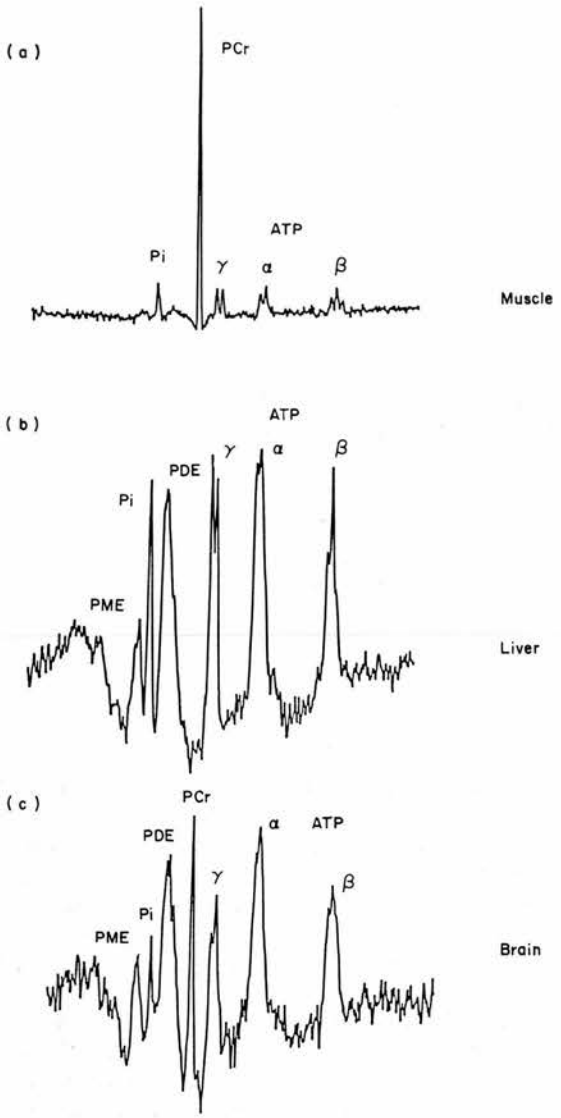



**Fig. 13.** $^{31}$P MR spectra of normal (a) muscle, (b) liver, (c) brain. Abbreviations as in text.

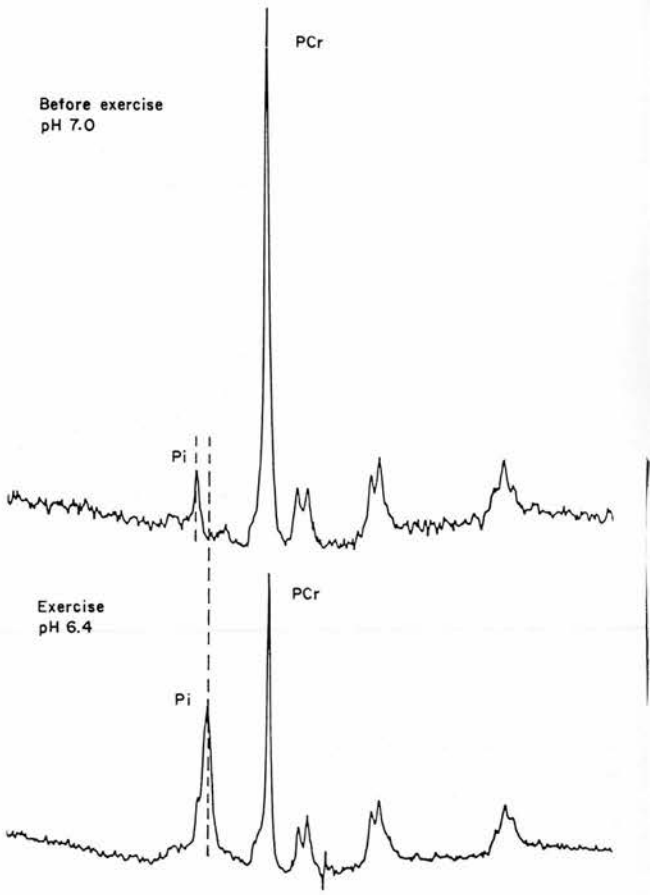



**Fig. 14.** $^{31}$P MR spectra of normal calf muscle, (a) at rest and (b) during exercise. Note the reduction in the PCr/Pi ratio and the rightward shift of the Pi resonance with exercise. The shift of the Pi resonance is due to a fall in muscle pHi.

contain phosphorus, and early *in vivo* MR spectra produced from experimental animals and man utilised the $^{31}$P nucleus [4, 5]. $^{31}$P MR spectra provide a variety of information.

1. *Energy metabolism:* $^{31}$P MR spectra from muscle and brain show prominent resonances from the three phosphate groups of adenosine triphosphate (ATP) and from phosphocreatine (PCr) while spectra from the liver contain resonances from ATP but not from PCr (Fig. 13). Both ATP and PCr are compounds that store high energy phosphate residues, and utilisation of the stored energy produces inorganic phosphate (Pi) which exhibits a separate resonance. Thus the ratios Pi/PCr and Pi/ATP provide some measure of the energy state of the cell [1] (Fig. 14).

2. *Intracellular pH (pHi):* The majority of the Pi seen in the $^{31}$P spectra is intracellular and exists in two forms ($HPO_4^{3-}$ and $H_2PO_4^{2-}$) which are in equilibrium, with relative concentrations depending on the pHi. Changes in pHi alter the relative concentrations of the two components and hence their relative effect on the position of the peak. The Pi peak is extremely sensitive to pH changes, tending to move to the right in acidosis and to the left in alkalosis, and its position can be used to measure absolute levels and relative changes of pHi (Fig. 14) with an accuracy of about 0.1 pH units [6].

3. *Phospholipid metabolism:* The resonances to the left and right of the Pi peak are termed the phosphomonoester (PME) and phosphodiester (PDE) peaks respectively. Both peaks contain contributions from more than one compound. Principally, the PME peak contains contributions from precursors of phospholipid synthesis, while products of phospholipid degradation contribute to the PDE peak. In $^{31}$P spectra from the liver, the PDE peak may also contain contributions from phospholipid headgroups in endoplasmic reticulum [7]. Thus, inspection of these peaks can provide us with information regarding membrane phospholipid metabolism. The PME peak in spectra from all organs may also contain contributions from glycolytic intermediates such as glucose 6-phosphate.

### *Carbon ($^{13}$C)*

Though carbon is present in most compounds within the human body, its most abundant isotope, $^{12}$C, does not exhibit NMR properties, and $^{13}$C, which is NMR visible, is a relatively insensitive nucleus, and constitutes less than 0.1% of naturally occurring carbon. Naturally occurring $^{13}$C is present in adequate concentrations for *in vivo* MRS only in substances like glycogen and lipid [8]. However,

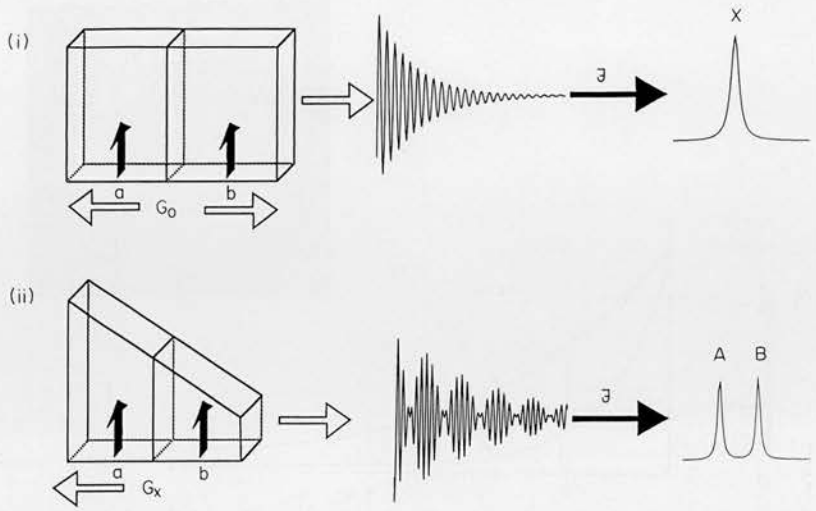



**Fig. 15.** Principles of spatial localisation using magnetic field gradients. In (i) the magnetic field is uniform and objects (a) and (b) experience the same field strength, and consequently produce a single resonance (X). In (ii) there is a gradient in the magnetic field ($G_x$). Object (a) experiences a higher magnetic field than object (b) resulting in two separate resonances (A) and (B). This difference in frequency thus encodes spatial information in the spectrum.

labelled molecules containing the stable isotope $^{13}C$ can be used in tracer studies, and provide an exiting means of charting metabolic paths *in vivo*. A word of caution. $^{13}C$ labelled compounds are extremely expensive and a single human study may cost several hundred pounds.

*Fluorine ($^{19}F$)*

There are no fluorine containing compounds present naturally that contain quantities of MR visible $^{19}F$ in concentrations that can be studied by *in vivo* MRS. However $^{19}F$ is an extremely sensitive nucleus and MRS can be used to study the pharmacokinetics and metabolism of fluorinated drugs, including volatile anaesthetics.

*Sodium ($^{23}Na$)*

Though the naturally occurring isotope of sodium is NMR visible, its sensitivity is greatly reduced by the fact that its nucleus is quadrupolar, a property that causes it to possess somewhat different spectral and relaxation properties than the other nuclei listed above. Sodium MR has been chiefly used in the imaging of experimental and clinical oedema.

## Imaging applications [9]

*Spatial localisation of NMR signal*

Magnetic resonance imaging (MRI) utilises the proton signal from water to produce high resolution images of the body. The exciting $B_1$ field is confined to one or more slices by the use of transient magnetic fields (termed gradients). The signal from individual picture elements (or pixels) within this slice are 'encoded' for recognition by the use of gradient magnetic fields that are applied during data acquisition. This enables the data collection process to assign the signal from different parts of the body slice studied to appropriate parts of the pixel matrix on the screen or film (Fig. 15).

*Production of image contrast*

The intensity of signal in any given pixel depends on the density of water protons in the region, the delay between excitation and data collection, and the time allowed for recovery between successive excitations. If the delay between excitation and signal collection is long (a $T_2$ weighted image), the process will tend to produce contrast between areas where water protons have a short $T_2$ (relatively low signal) and areas where the water protons have a long $T_2$ (relatively high signal) (Fig. 16). Similarly, manipulation of the interval between successive repetitions can produce contrast between regions with different proton $T_1$ values (a $T_1$ weighted image). Other processes, too complicated to discuss here, also contribute to image contrast and their manipulation can reveal subtle differences between areas with different anatomy, physiology and pathology, to an extent not possible with other imaging techniques. An additional advantage of MRI is the fact that unlike X ray computed tomography, images can be obtained in any plane — transverse, sagittal, coronal or oblique (Fig. 17).

Three other aspects of MRI are worth mentioning. First, images can be sensitised to detect and quantify molecular diffusion and, in principle at least, tissue perfusion. Such imaging is still in its infancy but holds great promise for the future. Second, although conventional MRI does take minutes to acquire images, newer methods of fast imaging enable the production of tomographic snapshots with subsecond imaging times. This greatly improves the ability to perform dynamic scanning, and reduces respiratory, cardiac and peristaltic motion artifact. Finally, there are now increasing numbers of MR contrast agents which can improve the clinical utility of MRI. These alter image contrast by their ability to alter local magnetic field. For example, one such agent, gadopentate dimeglumine (Gd-DTPA, Magnevist), increases signal intensity on $T_1$ weighted scans. Since it does not cross the intact blood brain barrier, local increase in signal can demonstrate breakdown of the blood brain barrier, and fast imaging after intravenous administration can follow its passage

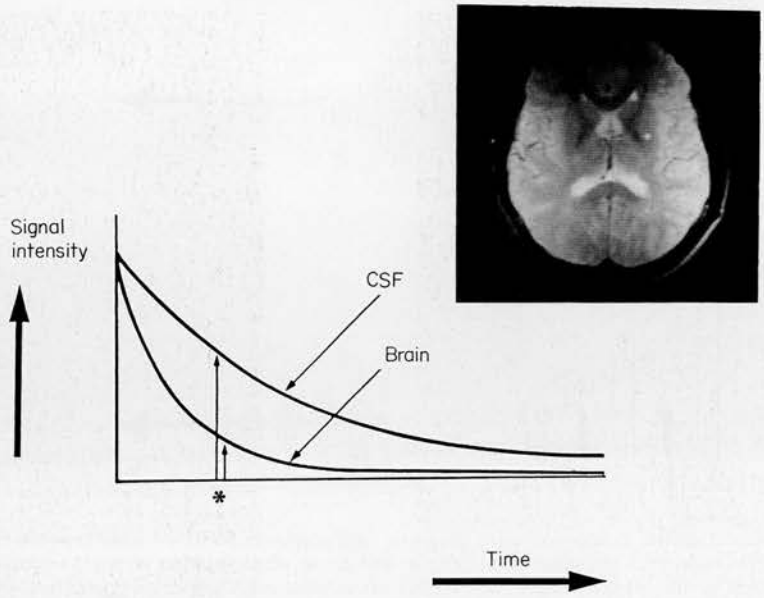



**Fig. 16.** Superimposed $T_2$ decay curves for signal from CSF and brain. The signal intensity from both structures is initially similar, but decays more rapidly with time in brain (where the $T_2$ is less). As a result, at the time of data collection (*) CSF exhibits a more intense signal than surrounding brain due to in the $T_2$ weighting in the image shown (SE 3000/80 at 1.6 tesla).

through the cerebral circulation and produce images that reflect cerebral perfusion.

## Practical aspects

### *Field strengths in use for clinical MR*

Magnetic field strengths in use for MRI and MRS are measured in units called tesla (T). One tesla equals 10 000 Gauss, and the earth's magnetic field at the surface is of the order of 0.5–1.0 Gauss. Field strengths in use for imaging range between 0.05 and 2.0 tesla, increasing strengths being associated with better spatial resolution, but also with greater expense and some technical problems. The higher field ( $\geqslant$ 0.5 tesla) systems tend to be based on cryogenic magnets with superconducting coils operating in liquid helium (4.22°K), while the lower field systems may be based on resistive (room temperature) electromagnets or permanent magnets. *In vivo* spectroscopy generally requires field strengths of 1.5 tesla or higher, although proton spectra have been acquired at 1.0 tesla.

### *Hardware for MR studies*

In practical terms, the whole body magnet consists of a long tube, usually about 2 m in length (Fig. 18). The items of hardware required for imaging and spectroscopy are contained within the magnet bore, leaving a free bore diameter for patient examination that ranges from 50–65 cm. The part of the body to be examined (e.g the head) may be enclosed within a smaller coil, which can

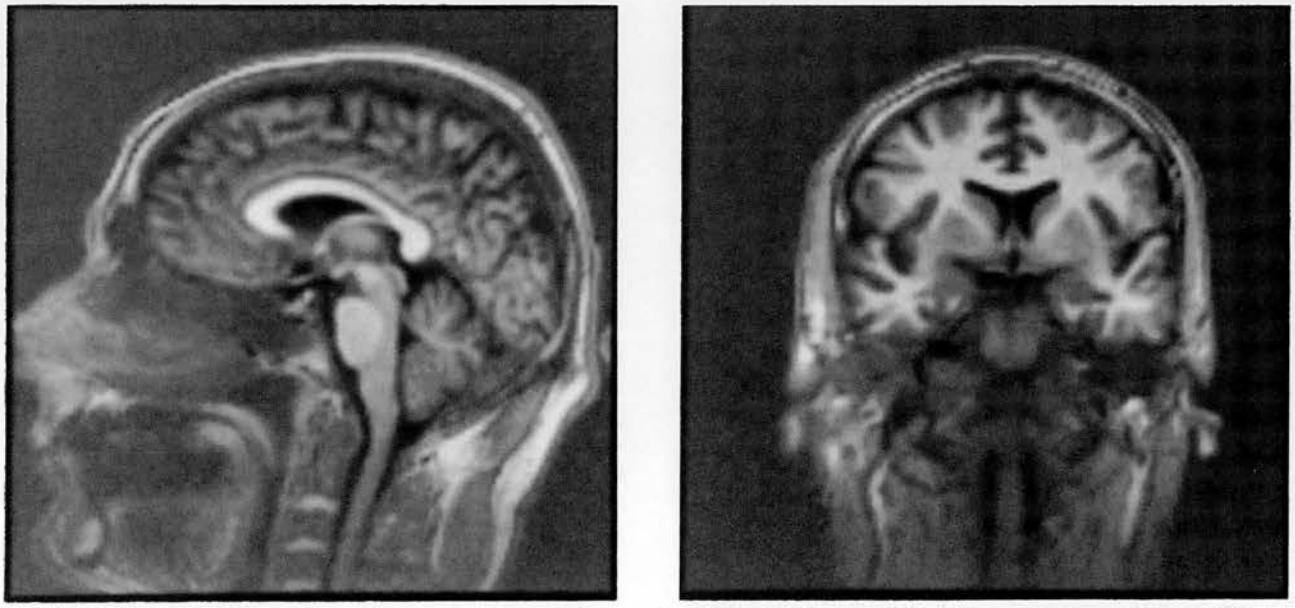


**Fig. 17.** Sagittal and coronal inversion recovery images of normal brain showing the excellent soft tissue detail possible with MRI.




**Fig. 18.** A modern MR imaging system (courtesy Picker, UK). Note the relatively small dimensions of the magnet bore, and the imaging head coil which further restricts patient access.

substantially restrict access to patients. Access during scanning is further reduced by the fact that the portion to be examined is in the middle of the magnet (i.e. approximately 1 m from the end of the tube). The bore space of some of the lower strength noncryogenic magnets may be substantially larger, and some of the newer low field strength open magnet systems have greatly reduced problems of patient access.

*The need for radiofrequency screens and filters*

Since the NMR signals being studied are of very low intensity, they can be interfered with by stray high frequency electromagnetic radiation (such as radio waves transmitted by FM radio stations) or interference arising from electrical equipment or monitoring devices. It is common practice therefore, to enclose the scanning area in a radiofrequency (RF) shield or Faraday cage which may be either built into the fabric of the MR imaging room or immediately surround the magnet, in order to prevent the ingress of contaminating signals. Nonconductive devices such as ventilator tubing can safely be passed through the

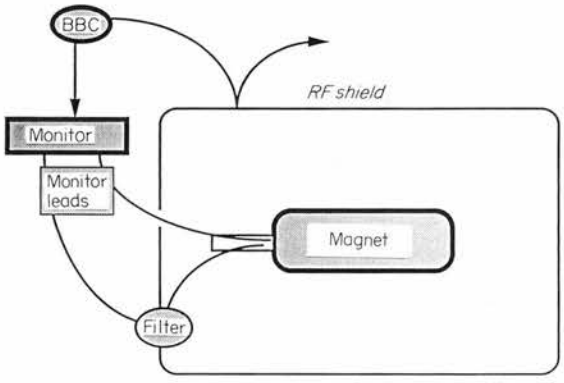



**Fig. 19.** Radiofrequency interference from external sources (labelled BBC) and monitoring equipment is prevented from entering the imaging area by the RF shield. This shield is breached by monitoring cables that can pick up and carry interference into the scanner. The interposition of low pass filters in the circuit prevents this.

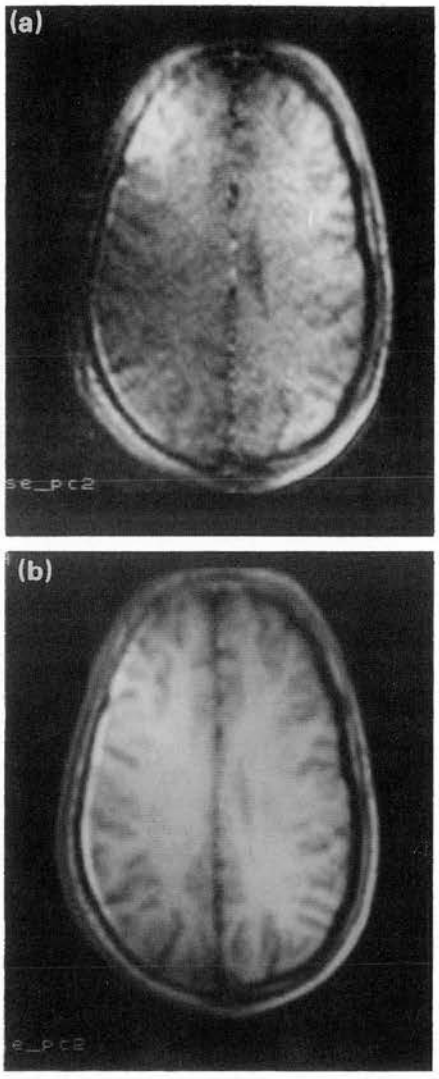



**Fig. 20.** Transverse $T_1$ weighted images of the brain of a normal volunteer demonstrating (a) the interference produced by an unfiltered pulse oximetry lead. In (b) the monitor lead has been filtered through a low pass RF filter, thus excluding the interference.

shield (using specially constructed copper lined RF ports), but wires that transgress the Faraday cage act as aerials and feed noise from the external environment into the examination area (Fig. 19). This problem is overcome by filtering wires that run in and out of the Faraday cage (Fig. 20) in one of several ways. Standard [10] or ECG gated [11] bandpass electronic filters are most commonly used, but the area within the cage can be isolated by using an optical [12] or radio link (employing frequencies that are far from the one being studied) [13]. An alternative method is to house the monitoring equipment within a small Faraday cage which is situated within the radiofrequency shield [14]. If standard radiofrequency Pi ($\pi$) filters are used, care must be taken to match filters to specific monitors. We have found that the readings from the Nellcor N-200 pulse oximeter, for example, are falsely high when the signal is passed through filters that seem acceptable for ECG and arterial waveform signals (Murata–Erie 9001–100–1021; STC Mercator, Great Yarmouth); accurate readings can however be obtained if somewhat less stringent filtering is used (Oxley FTLM/P/5000; Oxley

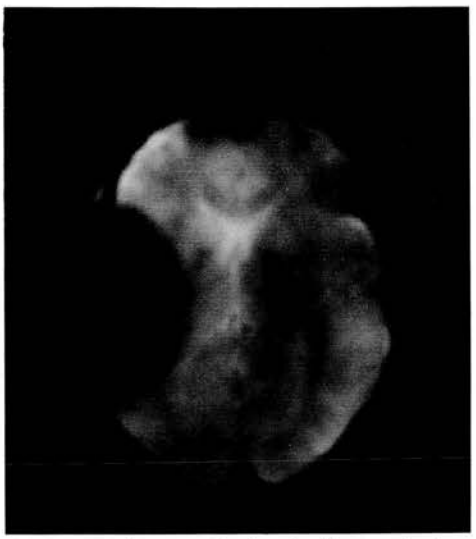


**Fig. 21.** Transverse images of a head with standard precordial stethoscope placed on the left infraclavicular region, demonstrating the imaging artifact produced by metal objects.

Developments, Ulverston, Cumbria). This may be due to the fact that the former filter distorts the leading edge of the signal from the pulse oximeter. It must be remembered that mains wiring can also carry interference into the Faraday cage. This obviously has implications for power supply to anaesthetic monitoring equipment within the Faraday cage; such devices will need to have an adequately filtered and isolated power source or be run by batteries. If the former option is chosen, it must be remembered that the small leakage currents present in $\pi$ filters may activate isolation fault detector circuits in medical equipment, even though the device may continue to function normally [10]. If the latter option is chosen, it must be ensured that the batteries, which are usually strongly magnetic, are adequately secured to prevent them becoming dangerous projectiles (see below).

## Safety considerations [15]

### *Ferromagnetic metal objects*

The attractive force of the magnet exerts a substantial pull on ferromagnetic objects and, when free, these can move towards the magnet centre with dangerous speed. The attractive force on a ferromagnetic object can be several times that of the earth's gravitational field by the time it reaches the centre of a high field magnet, and there are anecdotal reports of impalement by runaway forklift trucks during construction near an MR imaging facility. In practical terms, however, scissors, paging devices and oxygen cylinders probably constitute a less dramatic but more frequent risk to patients.

These attractive forces also affect implanted prosthetic devices such as joints, cardiac valves or vascular clips. This problem is less prominent than it first appears because a large proportion of implantable metallic devices used in medical practice are nonferromagnetic [16]. The presence or absence of ferromagnetism in a given metal object depends on a number of factors, including its composition and manufacture [15]. Individual objects can be tested for ferromagnetism with a powerful hand held magnet or by suspending them by a string in the magnet bore, and observing whether the string is deflected from the vertical.

Objects that are ferromagnetic may still be safe because their mass is too small for the forces involved to be significant, and/or because they are firmly anchored in position. As an example, many prosthetic cardiac valves are attracted, to some extent, by magnetic fields, but the magnetic forces acting on most of these valves, even during high field imaging, are less than those produced by the beating heart [16]. Similarly, surgical clips that have been *in situ* for years are well anchored by surrounding scar tissue, and even newly inserted sternal sutures are sufficiently immobilised to be safe in the magnet. However, metallic objects in vulnerable positions such as cerebral aneurysm clips and intra-ocular foreign bodies must not be risked within the magnet field unless they are unequivocally known to be constructed of nonferromagnetic material, however long they have been in position. Patients may suffer major intracranial or vitreous haemorrhage if this guideline is ignored [17]. Plain X rays of the orbit probably constitute adequate screening for intra-ocular foreign bodies in high risk subjects [17, 18], though some centres use thin slice X ray CT [19]. Less than 5% of MR sites in the USA use metal detectors for screening patients, and it is generally agreed that such devices are insensitive and have little, if any, role to play in screening patients prior to MR examinations [11].

### *Nonferromagnetic metal objects*

Even nonferromagnetic implants must be treated with care if they are in close proximity to the region to be scanned. This is for two reasons. First, metal objects (including anaesthetic apparatus [20] and tattoos [21] or cosmetics [22] that contain metal) can distort the field sufficiently to cause degradation of image quality (Fig. 21). Second, the application of intermittent radiofrequency $B_1$ fields to metallic objects can lead to heating and the danger of burns. Standard practice in such situations is for the patient to inform the operator if the area in question feels warm or uncomfortable, but this cannot apply to anaesthetised or unconscious patients. It is the anaesthetist's duty in such situations to obtain an assessment of risk from radiological or scientific staff in the MR unit. Electrical current induced in conductors may cause arcing, and currents in a pulse oximeter probe have been recorded as a cause of patient injury [23]. However, the risk of such burns is small and can be further reduced by simple safety precautions (see practice guidelines). In the current medicolegal climate it is important to record the fact that the above dangers have been guarded against, and that monitoring sites have been checked for injury at the end of the procedure (see below).

### *Fringe fields and medical equipment*

The field strength of a magnet is quantified in the middle of the magnet where imaging and spectroscopy are undertaken. However, this field does extend beyond the margins of the magnet, decreasing in strength with distance from the magnet bore. This peripheral or fringe field can be responsible for malfunction of electrical or electronic equipment, erase magnetic tape (such as that on credit cards) or computer discs, or cause pacemakers to dysfunction. It is important therefore, that anaesthetists are aware of the extent of fringe fields of the MRI installations that

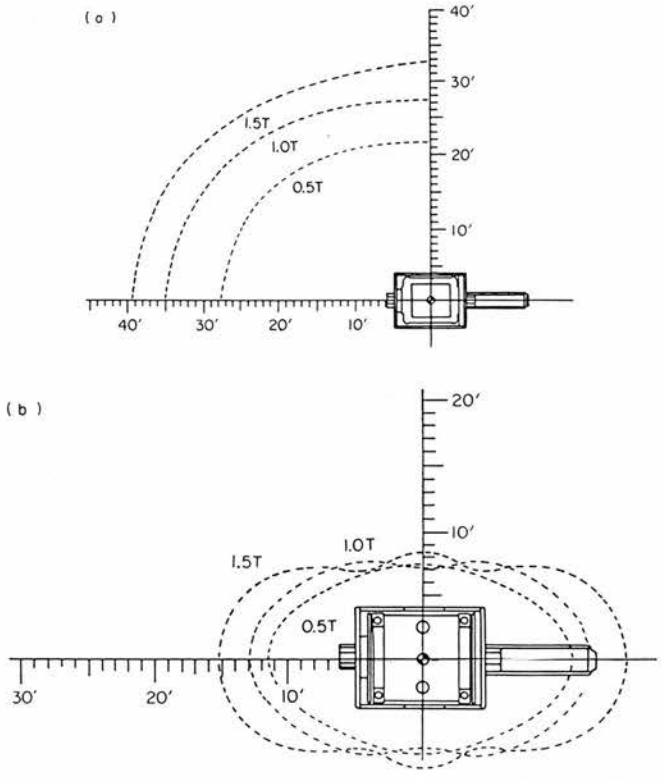



**Fig. 22.** Diagrammatic representation of 5 Gauss lines for (a) unshielded, and (b) actively shielded MR systems of different field strengths. Courtesy of Picker International Inc. Axes are calibrated in feet.

they work in. The most important determinant of the extent of such fields is magnet strength (Fig. 22(a)), but recent technical innovations have produced actively shielded magnets whose fringe fields are substantially reduced. In the case of standard high field cryogenic magnets the fringe field may extend for several metres away from the magnet, but may be much more compact in the case of low field resistive magnets or electromagnets. Developments in magnet technology have enabled the production of high field magnets with fringe fields that fall away very rapidly (Fig. 22(b)), thus enabling ferromagnetic equipment to be sited relatively close to the magnet. However, it must be remembered that such fringe fields also tend to rise rapidly as the magnet is approached, and great care must be taken to prevent ferromagnetic equipment from being inadvertently taken dangerously close to the magnet.

### *Practice guidelines*

In practice, the anaesthetist needs to ascertain where the 5 Gauss and 50 Gauss lines on the fringe field are. The reed switch on demand pacemakers malfunctions at field strengths above 5 Gauss [24] and patients with pacemakers should not be subjected to MR examination or allowed to cross a 5 Gauss line. Pacemaker malfunction in magnetic fields has been documented in animal models [25], and has been cited as causing death from arrhythmia in patients [26]. The situation with other implantable battery driven devices is less well recognised. Some cochlear implants may actually use cobalt samarium magnets to retain external coils [27]; most of these devices are electronically controlled. Similarly, implantable infusion pumps, neurostimulators and automatic implantable cardiac defibrillators have electronic control circuitry which may dysfunction in magnetic fields, and the motors of infusion pumps may not operate accurately at fields in excess of 100 Gauss. It seems prudent therefore, to suggest that patients with such devices *in situ* should not undergo MR examinations [15]. Concerns have been expressed that epicardial pacemaker wires and intracardiac catheters may act as aerials and deliver high frequency currents to the myocardium. Although there is no evidence to support such fears, some authors have suggested that patients with such devices should not be exposed to MR examination [15]. The uneventful examination at the Hammersmith of over 20 patients with epicardial pacing wires *in situ* within 24 h of open cardiac surgery suggests that the risks are not great, at least at low field strengths (0.15 tesla). It is essential, however, that the ends of the two pacing wires are well separated by insulating material, thus preventing the formation of a conducting loop.

The attractive force on ferromagnetic objects tends to become significant at field strengths of about 50 Gauss, and it is generally agreed that objects such as ferromagnetic gas cylinders are stationed outside the 50 Gauss line.

This risk of burns from monitoring cables can be minimised by following some simple precautions: (1) check that the insulation on all monitoring wires and MR cables is intact; (2) do not form loops within the magnet bore, and minimise contact between cables; (3) remove any wires or leads not in use; (4) separate cables from skin (by padding if necessary); (5) keep the cable and sensor away from the examination area e.g. place a pulse oximeter on the toe of a patient whose head is being examined.

### *Effects on monitoring devices*

Other electronic and electrical equipment may also be affected. Colour cathode ray screens are distorted by fields that exceed 1–2 Gauss, while monochrome screens may function reasonably well up to 5 Gauss. Magnetic tape and computer disks are corrupted by fields of 30 Gauss or higher. Most monitoring and infusion devices function normally at fields of 50 Gauss or less (field strength inferred from Karlik *et al.* [10]).

We have noted that many devices operated by rechargeable batteries tend to switch off and blank their screen when magnetic gradients operate. This effect, in fact, limits how close we can get to our MR system with pulse oximeters and monitoring display screens. We are as yet, unsure of the reason for this, but such malfunction may be due to the effects of the rapidly changing magnetic fields on either microprocessor circuitry or current inverters within the instrument.

### *Auditory considerations*

Operation of gradient coils often produces a loud thumping or tapping noise. The levels of noise permitted by regulatory bodies is clearly defined, and most commerical MR systems do not exceed these [15]. However, there have been reports of temporary and permanent hearing loss following MR examinations [15]. Furthermore, even levels of noise that do not produce hearing loss may necessitate deeper levels of anaesthesia than otherwise needed for MR exam-

inations. Magnet compatible earplugs are commercially available and can provide a simple solution to this problem [15]. An ingenious new method to reduce noise levels during MR imaging involves the feeding of noise in antiphase to produce noise cancellation [15].

*Contrast agents in MRI [15]*

The pharmacology and toxicology of such agents is substantially different from conventional radiographic contrast media. The most common of the MRI contrast agents, gadopentate dimeglumine (Gd-DTPA, Magnevist) has a high therapeutic ratio and a low incidence of side effects (2.4%) when compared with iodinated contrast agents. Side effects that have been reported include headache, nausea, vomiting, burning at the site of injection (the preparation is hyperosmolar) and hives. There have also been reports of transient severe hypertension and anaphylactoid reactions (with an incidence of about 1:100 000). Although there have been isolated reports of fatalities temporally related to administration of the drug, no causal effect has been demonstrated. Other MR contrast agents are being introduced into practice, and anaesthetists may need to acquire familiarity with these drugs.

*Cryogens and quenches*

All superconducting systems are based on cryogenic magnets operating in an environment of liquid helium at 4.22°K, while many older magnets also have a cryostat buffer consisting of liquid nitrogen at 77.3°K. These gases are normally maintained in their liquid state by insulation and losses due to evaporation are usually small. If the temperature of the cryostat rises suddenly for any reason however, these gases may 'boil off' rapidly in an explosive event known as a quench. Helium vapour (which resembles steam) is lighter than air and will rise, whereas gaseous nitrogen is approximately the same density as air. The distribution of the gases during a quench will reflect their physical properties, and have two potential hazardous effects. First, dilution of available oxygen by inert gas can result in asphyxiation. Second, the condensing vapour can result in frostbite and/or cryogenic burns. Most superconducting MR systems should have efficient ventilation systems to cope with such an eventuality, and witnessed quenches have usually been relatively gradual events. However the onset of asphyxia may be extremely rapid, with little or no warning [15], and more gradual reductions in ambient oxygen levels due to slow leaks may be difficult to detect. It has been suggested that oxygen monitors (e.g. the Sabre CM 610; Sabre Gas Detection, Aldershot, Hants GU12 4DL) be sited within areas at risk of quenches, and set to sound an alarm when levels drop below 19–20% [15].

## Biological effects [15]

*Effects of static magnetic fields*

Fears of biohazard associated with exposure to magnetic fields have prompted a number of studies in unicellular organisms, cell systems, animals and humans. Isolated studies have demonstrated effects of magnetic fields on embryogenesis, insulin release, blood–brain barrier permeability, haemostasis, plasma enzyme levels, and other biological functions. Other experiments and the vast majority of human data to date however, suggest that static magnetic fields do not have any significant deleterious effects on patients or health care professionals exposed to MR procedures.

Blood is a conductive medium, and when it flows in a magnetic field, tends to induce a voltage across the vessel. This voltage is maximal when flow is at right angles to the lines of magnetic flux, and is hence most prominently seen in the arch of the aorta in patients who are in the magnet. Such potential differences can distort the electrocardiogram and theoretical extrapolation of results from animal experiments suggest that the voltages induced in myocardiac vessels may reach depolarisation thresholds above 2.5 tesla [28]. Clinical experience and further animal work (at up to 4.7 tesla [29]) have failed to confirm these fears.

*Effects of rapidly switched gradient fields*

Gradient fields switch at rates of around 1–5 tesla.s$^{-1}$ [15] (up to 100 tesla.s$^{-1}$ with newer fast imaging sequences) and may induce currents in biological tissue. These currents do not generate enough heat to cause concern about thermal effects, but they may have electrophysiological consequences. Recent studies have reported peripheral muscle stimulation by gradient fields in volunteers at thresholds of 60 tesla.s$^{-1}$ and the stimulation of retinal receptors with the production of visual sensations (termed magnetophosphenes) have been reported at field strengths above or around 2 tesla. Theoretical and experimental evidence indicates that gradient switch rates of 1 tesla.s$^{-1}$ result in tissue current densities of around 1 $\mu$A.cm$^{-2}$. Extrapolation of these results would suggest that switch rates in excess of 300 tesla.s$^{-1}$ would be required to induce ventricular fibrillation [30]. Many reports suggest that noncardiac excitable tissue is excited at a lower threshold value, thus providing a relatively sensitive marker of dangerously high gradient switch rates [30]. There are some 4 tesla MR systems in use now, and there are documented instances of metallic taste, nausea or vertigo being produced when subjects are pushed rapidly into these magnets [15].

*Effects of radiofrequency time varying magnetic fields ($B_1$ fields)*

These are magnetic fields that oscillate at the resonant frequency, and can produce electrical currents in tissue. In contrast to the currents produced by gradient fields, the currents produced by radiofrequency time varying fields have no significant electrophysiological effects, but can cause significant heating. The occurrence of heating in metallic implants has been discussed, but thermal effects may also be seen in biological tissue. Rises in temperature depend not only on thermal energy deposition, but also on the rate at which heat is lost. There are clear guidelines for permissible levels of heat deposition prescribed by the National Radiological Protection Board in the UK and by the FDA in the USA [31, 32]. Similar recommendations exist for Canadian MR sites [33]. Special concerns have been expressed regarding the effects of scrotal heating on spermatogenesis, and the possible generation of cataracts by ocular heating; studies to date suggest that such fears are unjustified in the context of radiofrequency fields used for clinical examination [15].

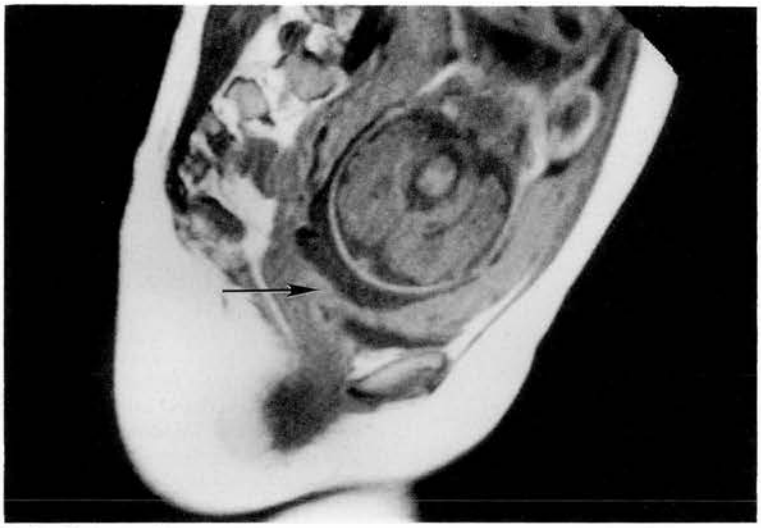


**Fig. 23.** Sagittal image of the pelvis in a pregnant female at term demonstrating a placenta praevia (→). Image courtesy of Miss H.A. Case, Bristol MRI Centre.

*Carcinogenic and teratogenic risks*

The potential of radiofrequency magnetic fields in producing cancer or developmental abnormalities is an area of critical debate. The interested reader is referred to reviews by Adey [34] and Beers [35]. There appears to be no evidence to suggest that exposure to the fields used in MR imaging and spectroscopy is associated with any significant increase in the risk of developing cancer. Similarly, there is little hard evidence to support the suggestion that routine clinical exposure to MR examinations may cause developmental abnormality, and authorities in the field suggest that MR is the imaging procedure of choice at any stage of pregnancy if ultrasound is inappropriate or provides inadequate information [15] (Fig. 23). Occupational exposure to MR procedures (radiologists, radiographers, nurses) is however, minimised by many MR units [11], and it has been suggested that pregnant personnel are not exposed to time varying magnetic fields or to static fields in excess of 10 Gauss [15].

## Recording information during MR studies

The long list of contraindications and hazards listed above makes it important that patient assessment and procedure planning prior to MR examinations be formalised in some way. Many MR units use a checklist, which is often given to patients to fill in while they await their MR study. If patients are unconscious, such information may need to be acquired from several sources, and filled in by medical or paramedical staff. In any case, before an anaesthetist accepts responsibility for caring for a patient in an MR scanner he or she must ensure that a suitable checklist has been filled in (Table 2), since we have found that verbal assurances of safety from referring clinicians can be misleading. For anaesthetised or sedated patients, an additional 'anaesthetist's MR checklist' may be valuable (Table 3). The combination of these two checklists provides the basis of safe anaesthetic practice in an MR environment for the individual anaesthetist, who may be infrequently involved in MR studies. Anaesthetists may come into contact with MR in two other situations. First, there is the anaesthetist who is responsible for setting up equipment for monitoring and anaesthesia in an MR unit; issues which are dealt with in Part II of this paper, along with details of anaesthetic practice. Second, there is the anaesthetist who may use MR as a research tool as exemplified by the studies listed in the next section.

## Some clinical MR studies of special anaesthetic interest

The last decade has seen an explosion of research employing MRI and MRS. We would like here to touch upon some of the clinical studies which may be of special interest to anaesthetists and intensivists.

*Phosphorus spectroscopy of the brain in birth-asphyxiated neonates*

The physiological changes associated with neonatal hypoxic–ischaemic injury result in changes in energy metabolism within the brain that have been studied using $^{31}P$ MRS [36–38]. In the hyperacute stage there is an intracellular acidosis but no other change in the phosphorus spectrum. Over the first 48 h cerebral PCr levels drop while Pi levels rise, suggesting a worsening energy state within the cell (Fig. 24). These changes revert to normal over 10–14 days. The initially acid pH normalises at first, but then exhibits an alkaline overshoot. The clinical relevance of these changes lies in their proven ability to provide a noninvasive index of outcome [37], and they show great potential in the assessment of neuroprotective agents. We have, more recently, used $^{1}H$ MRS to study neonatal injury at longer intervals after birth asphyxia [38].

*Phosphorus spectroscopy in the diagnosis of malignant hyperpyrexia*

Studies of muscle from patients with malignant hyperthermia (MH) have shown that the abnormal muscle metabolism in this condition can be diagnosed with a high degree of accuracy using $^{31}P$ MR spectroscopy [39] (98%

**Table 2.** Checklist for patients undergong magnetic resonance imaging/spectroscopy.

It is the responsibility of the NMR Unit staff member who puts the patient in the magnet to satisfy himself or herself that the following checklist is completed. This may involve obtaining information from the patient or patient notes, from the referring doctor, or in some cases, obtaining previous or fresh radiographs to exclude metallic objects.

| Device category | Yes | No | Unsure |
|---|---|---|---|
| 1 Heart pacemaker (any type). | ___ | ___ | ___ |
| 2 Cerebral aneurysm or other haemostatic clips.* | ___ | ___ | ___ |
| 3 Metal fragments in head/eyes — postoperative/post-trauma. | ___ | ___ | ___ |
| 4 Shrapnel. | ___ | ___ | ___ |
| 5 Prosthetic heart valves (Starr Edwards pre 6000).* | ___ | ___ | ___ |
| 6 Orthopaedic implants (pins, plates, wires).* | ___ | ___ | ___ |
| 7 Cochlear implants.* | ___ | ___ | ___ |
| 8 Neurostimulators (Chronic pain therapy or spasticity).* | ___ | ___ | ___ |
| 9 Implantable pumps.* | ___ | ___ | ___ |
| 10 Penile implants (Omniphase, Decomed Corp).* | ___ | ___ | ___ |
| 11 Contraceptive diaphragms/IUCDs.* | ___ | ___ | ___ |
| 12 Coloured contact lenses.* | ___ | ___ | ___ |
| 13 Ocular prostheses (false eyes).* | ___ | ___ | ___ |
| 14 Interventional radiology devices (coils, filters, stents).* | ___ | ___ | ___ |
| 15 Dentures or removable bridgework. | ___ | ___ | ___ |
| *Other information* | | | |
| 16 Has the patient ever been a machinist or metal worker? | ___ | ___ | ___ |
| 17 Is there any possibility that the patient may be pregnant? | ___ | ___ | ___ |

*Note: Some devices in this category may be safe while others are not. Listings are incomplete. A device not known to be safe must be assumed to be unsafe. In the case of devices operated by microprocessors (e.g. implantable pumps) device malfunction caused by field effects on circuitry must be considered. Other devices such as ventricular shunts, orthodontic braces may be safe, but may degrade image quality significantly. Images may also be degraded by metal containing tattoos or cosmetics. (See *Radiology* 1991; **180:** 541.

This is to confirm that the above checklist has been completed.

Signed:_____(Patient)_____(NMR Unit Personnel)
Dated: ____/____/____

**Table 3.** Anaesthetic checklist for MR procedures.

Remove metallic objects (including paging devices), nondigital watches and credit cards, check your pockets for dangerous metallic objects (scissors, artery forceps, pens, needles, paper clips etc). Do not take credit cards, computer floppy discs, or other magnetic data storage devices near the magnet.

| | |
|---|---|
| 1 Ensure that (a) anaesthetic/monitoring equipment is working | [ ] |
| (b) there is a suitable area for induction/recovery | [ ] |
| (c) the breathing system in the magnet area is long enough to allow transfer from the oxygen cylinder outside the 50 Gauss line. | [ ] |
| 2 Consent form signed. | [ ] |
| 3 Day case criteria satisfied if needed. | [ ] |
| 4 MR safety checklist completed; contraindications excluded. | [ ] |
| 5 Magnetic and metallic objects removed from patient, including eye makeup and prosthetic devices if appropriate. | [ ] |
| 6 Placement of MR compatible monitoring leads. If patient already has monitoring on, these leads may need to be removed. | [ ] |
| 7 Interposition of appropriate lengths of extension line to i.v. access site (and infusion pumps, if appropriate). | [ ] |
| 8 Induction of anaesthesia on an MR compatible trolley. | [ ] |
| 9 Move patient to magnet area and position for examination. CHECK THAT FERROUS OXYGEN CYLINDER IS REMOVED AND INFUSION PUMPS ARE AT A SAFE DISTANCE FROM THE MAGNET. | [ ] |
| 10 Connect monitoring devices and anaesthetic breathing system and check function. | [ ] |
| 11 Ensure that i.v. access will still be available when the patient goes into the magnet bore. | [ ] |
| 12 Patient moved into magnet bore. Monitoring and receiver coil leads are separate, and there are no non-essential cables or potentially dangerous inductive loops. | [ ] |
| 13 MR procedure complete. Remove patient to induction/recovery area, with transfer to cylinder gases outside 50 Gauss line. | [ ] |
| 14 Reversal of anaesthesia and recovery. Check monitoring sites for burns and record their presence or absence in the notes. | [ ] |

sensitivity, 96% specificity *vs* muscle biopsy contracture tests with halothane and caffeine). $^{31}P$ MR spectra from patients with MH show a higher Pi/PCr ratio than controls and exhibit a slower recovery in PCr levels after exercise. These studies provide not only a noninvasive means of diagnosing MH, but also an opportunity to study the pathophysiology and biochemistry of the disease [40].

### *Fluorine spectroscopy of volatile anaesthetics*

Many authors have published $^{19}F$ MRS studies of halothane, enflurane and isoflurane in animals. These studies have mapped the distribution of halothane in the head [41], identified two discrete physicochemical environments for halothane binding [42, 43], and studied the uptake and elimination of volatile anaesthetics from the brain [44, 45]. Recent work at this centre has duplicated many of these studies in humans [46]. $^{19}F$ MRS may provide us with a powerful tool to study the pharmacokinetics and metabolism of fluorinated volatile anaesthetics.

### *MR imaging of patients after anaesthesia*

Many authors have used *in vitro* proton spectroscopy to study the effects of general anaesthetic agents on the mobility of macromolecules [47] and model lipid bilayers [48]. Whitfield and Douglas used $T_2$ weighted MR imaging to assess tissue molecular mobility in the brain after general anaesthesia [49]. One to 3 h after general anaesthesia, patients showed small increases in cerebral $T_2$ values as measured by imaging on a 0.2 tesla MR system. These changes show how MR imaging may be used to study, and perhaps validate theories of general anaesthesia *in vivo*.

## Conclusion

Clinical magnetic resonance imaging has been in use for over a decade, and its availability and use is increasing. Our experience suggests that ideally no anaesthetised or

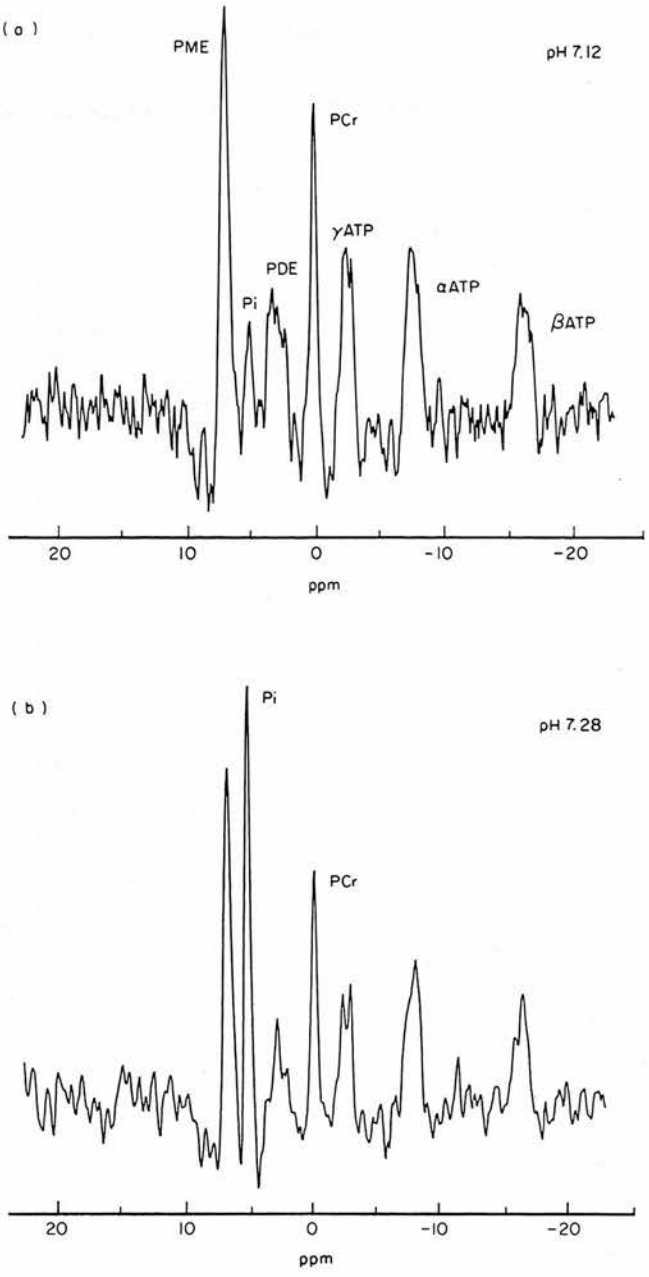



**Fig. 24.** $^{31}$P MR spectra of the brain from (a) a normal neonate, and (b) a baby with birth asphyxia, at 4 days postnatal age. Note the reduction in PCr/Pi ratio and the relatively alkaline pHi in (b), both of which are characteristic of the subacute phase of hypoxic-ischaemic neonatal CNS birth injury.

critically ill patient should be subjected to MR procedures without adequate monitoring and continuous supervision by an anaesthetist who is fully conversant with the potential problems and risks of the procedure. An understanding of the basic principles involved will facilitate the acquisition of the knowledge needed for this process, and provide an opportunity to consider the application of this exciting technique to answer questions that interest anaesthetists.

**Acknowledgments**

Financial support for these studies was provided by the Medical Research Council of the UK, and by Picker International.

We thank Dr J. Lumley, Dr D. Zideman and Mr M. Chakrabarti from the Department of Anaesthetics, and Dr R. Stillman from the Department of Medical Physics at the Hammersmith Hospital for their help. Advice and suggestions from colleagues in the NMR unit were of great value; in particular, we would like to thank Professor Bydder in this regard.

**References**

[1] GADIAN DG. *Nuclear magnetic resonance and its applications to living systems*. Oxford: Clarendon, 1982.

[2] COUTTS GA, BRYANT DJ, COLLINS AG, COX IJ, SARGENTONI J, GADIAN DG. $^{31}$P magnetic resonance spectroscopy of the

normal human brain: approaches using four dimensional chemical shift imaging and phase mapping techniques. *NMR in Biomedicine* 1989; **1:** 190–7.

[3] WEINER MW, HETHERINGTON HP. The power of the proton. *Radiology* 1989; **172:** 318–20.

[4] ROSS BD, RADDA GK, GADIAN DG, ROCKER G, ESIRI M, FALCONER-SMITH J. Examination of a case of suspected McArdle's syndrome by $^{31}$P nuclear magnetic resonance. *New England Journal of Medicine* 1981; **304:** 1338–42.

[5] ACKERMAN JJH, GROVE TH, WONG GG, GADIAN DG, RADDA GK. Mapping of metabolities in whole animals by $^{31}$P NMR using surface coils. *Nature* 1980; **283:** 167–70.

[6] GARLICK PB, RADDA GK, SEELY PJ. Studies of acidosis in the ischaemic heart by phosphorus nuclear magnetic resonance. *Biochemical Journal* 1979; **184:** 547–54.

[7] MURPHY EJ, RAJAGOPALAN B, BRINDLE KM, RADDA GK. Phospholipid bilayer contribution to $^{31}$P NMR spectra in vivo. *Magnetic Resonance in Medicine* 1989; **12:** 282–9.

[8] SHULMAN GI, ROTHMAN DL, JUE T, STEIN P, DEFRONZO RA, SHULMAN RG. Quantitation of muscle glycogen synthesis in normal subjects and subjects with non-insulin-dependent diabetes by $^{13}$C nuclear magnetic resonance spectroscopy. *New England Journal of Medicine* 1990; **322:** 223–8.

[9] VILLAFANA T. Fundamental physics of magnetic resonance imaging. *Radiologic Clinics of North America* 1988; **26:** 701–15.

[10] KARLIK SJ, HEATHERLEY T, PAVAN F, STEIR J, LEBRON F, RUTT B, CAREY L, WEXLER R, GELB A. Patient anesthesia and monitoring at a 1.5T MRI installation. *Magnetic Resonance in Medicine* 1988; **7:** 210–21.

[11] ROKEY R, WENDT RE, JOHNSTON DL. Monitoring of acutely ill patients during nuclear magnetic resonance imaging: use of a time-varying filter electrocardiographic gating device to reduce gradient artifacts. *Magnetic Resonance in Medicine* 1988; **6:** 240–5.

[12] HENNEBERG S, HOK B, WIKLUND L, SJODIN G. Remote auscultatory patient monitoring during magnetic resonance imaging. *Journal of Clinical Monitoring* 1992; **8:** 37–43.

[13] REJGER VS, COHN BF, VIELVOYE GJ, DE RAADT FB. A simple anaesthetic and monitoring system for magnetic resonance imaging. *European Journal of Anaesthesiology* 1989; **6:** 373–8.

[14] BOESCH C, MARTIN E. Combined application of MR imaging and spectroscopy in neonates and children: installation and operation of a 2.35-T system in a clinical setting. *Radiology* 1988; **168:** 481–8.

[15] KANAL E, SHELLOCK FG, TALAGALA L. Safety considerations in MR imaging. *Radiology* 1990; **176:** 593–606.

[16] SHELLOCK FG, CURTIS JS. MR imaging and biomedical implants, materials and devices: an updated review. *Radiology* 1991; **180:** 541–50.

[17] KELLY WM, PAGLEN PG, PEARSON JA, SAN DEIGO AG, SOLOMAN MA. Ferromagnetism of intraocular foreign body causes unilateral blindness after MR study. *American Journal of Neuroradiology* 1986; **7:** 243–5.

[18] WILLIAMS S, CHAR DH, DILLON WP, LINCOFF N, MOSELEY M. Ferrous intraocular foreign bodies and magnetic resonance imaging. *American Journal of Ophthalmology* 1988; **105:** 398–401.

[19] MANI RL. In search of an effective screening system for intraocular metallic foreign bodies prior to MR: an important issue of patient safety. *American Journal of Neuroradiology* 1988; **9:** 1032.

[20] NIXON C, HIRSCH NP, ORMEROD IEC, JOHNSON G. Nuclear magnetic resonance. Its implication for the anaesthetist. *Anaesthesia* 1986; **41:** 131–7.

[21] LUND G, WIRTSCHAFTER JD, NELSON JD, WILLIAMS PA. Tattooing of eyelids: magnetic resonance imaging artifacts. *Ophthalmic Surgery* 1986; **17:** 550–3.

[22] SACCO DC STEIGER DA, BELLON EM, COLEMAN PE, HAACKE EM. Artifacts caused by cosmetics in MR imaging of the head. *American Journal of Roentgenology* 1987; **148:** 1001–4.

[23] SHELLOCK FG, SLIMP GL. Severe burn of the finger caused by using a pulse oximeter during MR imaging. *American Journal of Roentgenology* 1989; **153:** 1105.

[24] PAVLICEK W, GEISINGER M, CASTLE L, BORKOWSKI GP, MEANEY TF, BREAM BL, GALLAGHER JH. The effects of nuclear magnetic resonance on patients with cardiac pacemakers. *Radiology* 1983; **147:** 148–53.

[25] HAYES DL, HOLMES DR, GRAY JE. Effect of 1.5 tesla nuclear magnetic resonance imaging scanner on implanted permanent pacemakers. *Journal of the American College of Cardiology* 1987; **10:** 782–6.

[26] Centre for Devices and Radiological Health MR product reporting program and medical device report program. Washington, DC: U.S. Food and Drug Administration, 1989.

[27] DORMER KJ, RICHARD GL, HOUGH JVD, NORDQUIST RE. The use of rare earth magnet couplers in cochlear implants. *Laryngoscope* 1981; **91:** 1812–20.

[28] BEISCHER DE, KNEPTON JC. Influence of strong magnetic fields on the electrocardiogram of squirrel monkeys *(Saimiri sciureus)*. *Aerospace Medicine* 1964; **35:** 939–44.

[29] DOHERTY JU, WHITMAN GJR, ROBINSON MD, HARKEN AH, SIMSON MB, SPEAR JF, JOSEPHSON ME. Changes in cardiac excitability and vulnerability in NMR fields. *Investigative Radiology* 1985; **20:** 129–35.

[30] BUDINGER TF. Nuclear magnetic resonance (NMR) In vivo studies: known thresholds for health effects. *Journal of Computer Assisted Tomography* 1981; **5:** 800–11.

[31] Board statement on Clinical Magnetic Resonance Diagnostic Procedures. National Radiological Protection Board (NRPB). *Documents of the NRPB* 1991; **2:** 1.

[32] Guidance for content and review of a magnetic resonance diagnostic device 510(k) application. Federal Register (USA), August 2, 1988.

[33] PRATO FS, NICHOLSON RL, SMITH M, DROST DJ. Hazards and associated recommendations for Canadian MR imaging sites. *Journal of the Canadian Association of Radiologists* 1986; **37:** 233–7.

[34] ADEY WR. Tissue interactions with nonionizing electromagnetic fields. *Physiological Reviews* 1981; **61:** 435–514.

[35] BEERS GJ. Biological effects of weak electromagnetic fields from 0 Hz to 200 MHz: a survey of the literature with special emphasis of possible magnetic resonance effects. *Magnetic Resonance Imaging* 1989; **7:** 309–31.

[36] YOUNKIN DP, DELIVORIA-PAPADOPOULOS M, LEONARD JC, SUBRAMANIAN VH, ELEFF S, LEIGH JS, CHANCE B. Unique aspects of human newborn cerebral metabolism evaluated with phosphorus nuclear magnetic resonance spectroscopy. *Annals of Neurology* 1984; **16:** 581–6.

[37] AZZOPARDI D, WYATT JS, CADY EB, DELPY DT, BAUDIN J, STEWART AL, HOPE PL, HAMILTON PA, REYNOLDS EOR. Prognosis of newborn infants with hypoxic-ischemic brain injury assessed by phosphorus magnetic resonance spectroscopy. *Pediatric Research* 1989; **25:** 445–51.

[38] PEDEN CJ, COWAN FM, BRYANT DJ, SARGENTONI J, COX IJ, MENON DK, GADIAN DG, BELL JD, DUBOWITZ LM. Proton MR spectroscopy of the brain in infants. *Journal of Computer Assisted Tomography* 1990; **14:** 886–94.

[39] OLGIN J, ROSENBERG H, ALLEN G, SEESTEDT R, CHANCE B. A blinded comparison of noninvasive, in vivo phosphorus nuclear magnetic resonance spectroscopy and the in vitro halothane/caffeine contracture test in the evaluation of malignant hyperthermia susceptibility. *Anesthesia and Analgesia* 1991; **72:** 36–47.

[40] OLGIN J, ARGOV Z, ROSENBERG H, TUCHLER M, CHANCE B. Non-invasive evaluation of malignant hyperthermia susceptibility with phosphorus nuclear magnetic resonance spectroscopy. *Anesthesiology* 1988; **68:** 507–13.

[41] WYRWICZ AM, CONBOY CB. Determination of halothane distribution in the rat head using $^{19}$F NMR technique. *Magnetic Resonance in Medicine* 1989; **9:** 219–28.

[42] EVERS AS, BERKOWITZ BA, D'AVIGNON DA. Correlation between the anaesthetic effect of halothane and saturable binding in brain. *Nature* 1987; **328:** 157–60.

[43] EVERS AS, BERKOWITZ BA, D'AVIGNON DA. Correlation between the anaesthetic effect of halothane and saturable binding in brain. *Nature* 1989; **341:** 766.

[44] LITT L, GONZÁLEZ-MÉNDEZ R, JAMES TL, SESSLER DI, MILLS P, CHEW W, MOSELEY M, PEREIRA B, SEVERINGHAUS JW, HAMILTON WK. An *in vivo* study of halothane uptake and elimination in the rat brain with fluorine nuclear magnetic resonance spectroscopy. *Anesthesiology* 1987; **67:** 161–8.

[45] MILLS P, SESSLER DI, MOSELEY M, CHEW W, PEREIRA B, JAMES TL, LITT L. An *in vivo* $^{19}$F nuclear magnetic resonance

study of isoflurane elimination from the rabbit brain. *Anesthesiology* 1987; **67:** 169–73.

[46] MENON DK, LOCKWOOD GG, PEDEN CJ, COX IJ, BELL J, BRYANT DJ, SARGENTONI J, WHITWAM JG. $^{19}F$ MRS studies of brain halothane in humans. *British Journal of Radiology* 1991; **64:** 79.

[47] BARKER RW, BROWN FF, DRAKE R, HALSEY MJ, RICHARDS RE. Nuclear magnetic resonance studies of anaesthetic interactions with haemoglobin. *British Journal of Anaesthesia* 1975; **47:** 25–9.

[48] SHIEH DD, UEDA I, LIN HC, EYRING H. Nuclear magnetic resonance studies of the interaction of general anesthetics with 1, 2-dihexadecyl-sn-glycero-3-phosphorylcholine bilayer. *Proceedings of the National Academy of Sciences* 1976; **73:** 3999–4002.

[49] WHITFIELD A, DOUGLAS RHB. Effect of general anaesthesia on the magnetic resonance imaging signal from the brain. *British Journal of Anaesthesia* 1989; **62:** 694–6.

*Anaesthesia*, 1992, Volume 47, pages 508–517

SPECIAL ARTICLE

# Magnetic resonance for the anaesthetist

## Part II: anaesthesia and monitoring in MR units

C. J. PEDEN, D. K. MENON, A. S. HALL, J. SARGENTONI AND J. G. WHITWAM

**Summary**

*Anaesthetists are increasingly involved in patient care during magnetic resonance imaging and spectroscopy. This paper describes a system which has been developed for the management of critically ill patients and the conduct of anaesthesia in a magnetic resonance unit with a 1.6 tesla whole body magnet. Difficulties which arise from working in a confined space in a high magnetic field are highlighted. Different approaches to anaesthesia, sedation and the modification of equipment for use in this environment are reviewed. The problems associated with patient monitoring within a magnetic field are discussed and some solutions are suggested. A transport system for critically ill patients is described and a protocol for management is outlined.*

**Key words**

*Measurement techniques*; nuclear magnetic resonance.
*Anaesthesia*; magnetic resonance imaging.
*Monitoring*; blood pressure, carbon dioxide; electrocardiography, oxygen.
*Equipment*; anaesthesia machines.

Magnetic resonance imaging (MRI) is now established as a valuable imaging technique, particularly for the investigation of the central nervous system. Magnetic resonance spectroscopy (MRS), which is based on the same physical principles as MRI, is used to provide biochemical information from a variety of different nuclei ($^{1}H$, $^{19}F$, $^{31}P$, $^{13}C$) [1]. The number of MR systems is increasing and new applications for the technique are still being developed; in 1990 approximately 100 000 examinations were performed in the UK. The requirement for anaesthetists to provide sedation or anaesthesia and to manage critically ill patients in the difficult environment of a magnetic field is also likely to increase.

In this paper we discuss the problems of administering anaesthesia for MRI and review the existing literature on the subject. On the basis of our experiences of MRI and MRS in a 1.6 tesla (T) magnet system, we suggest how these problems may be solved using, wherever possible, commercially available equipment.

### General considerations

*Indications for anaesthesia and sedation (Table 1)*

*The need for immobility*. The images and spectra are composed of multiple data acquisitions which are averaged by the system computer to give the final image or spectrum. At present, some individual scans may take up to 20 min and the whole examination may last over an hour. Movement of the patient at any point during the multiple acquisitions which make up one scan will result in faulty spatial allocation of signal and so degrade the quality of the final image by the production of movement artifacts. In addition, if the patient changes position at any time during the examination the homogeneity of the magnetic field, which has been maximised to his original position, is reduced and this may also degrade the quality of all the subsequent scans obtained. This factor is of more importance in MRS than during an MRI examination.

*Patient anxiety*. Severe anxiety may be a significant problem for which the examination may have to be aborted. The confined space, the loud noises which occur during the scans, the temperature of the magnet bore and the length of the procedure were found to be the principle causes of distress [2]. Flaherty and Hoskinson [3] investigated 210 patients undergoing MRI and found that 4% became too anxious to complete the procedure. Sedation or anaesthesia is an extreme solution to this particular problem. Education and counselling, the presence of a companion, gradual familiarisation with the enclosed space and prone positioning [4] should be tried first.

C.J. Peden, BSc, MB, ChB, FFARCS, MRC Research Fellow, D.K. Menon, MD, MRCP, FFARCS, MRC Research Fellow, A.S. Hall, PhD, Physicist, J. Sargentoni, DCRR, DMU, Radiographer, NMR Unit, Hammersmith Hospital and JG Whitwam, PhD, FRCP, FFARCS, Professor of Anaesthesia, Hammersmith Hospital, Du Cane Road, London W12 0HS.
Correspondence to: Dr C.J. Peden, Sir Humphry Davy Department of Anaesthesia, Bristol Royal Infirmary, Bristol BS2 8HW.
Accepted 25 July 1991.

0003–2409/92/060508 + 10 $03.00/0
© 1992 The Association of Anaesthetists of Gt Britain and Ireland

**Table 1.** Indications for sedation or general anaesthesia for a magnetic resonance examination.

| Indication | Patient group | Action |
|---|---|---|
| Reduce patient movement | Infants and small children.<br>Confused, intellectually subnormal, mentally ill adults. | Sedation or anaesthesia. |
| Airway protection | Unconscious patients.<br>Critically ill patients receiving IPPV. | Anaesthesia<br>Anaesthesia and IPPV |
| Control of ventilation | Head injuries.<br>Patients with raised ICP where $Paco_2$ has to be controlled. | Anaesthesia and IPPV |
| Anxiety and claustrophobia | Adults. | Reassurance, education, counselling, prone position.<br>Sedation.<br>Anaesthesia only if necessary and examination essential. |

IPPV, intermittent positive pressure ventilation.
ICP, intracranial pressure.

Table 1 summarises the types of patients who may require anaesthesia or sedation in order to undergo MR examination.

*Problems of anaesthesia in the MR environment*

Anaesthesia and monitoring of patients in an MR system present several problems which have been discussed in detail elsewhere [1]. In summary, these are: (1) the need to exclude ferromagnetic equipment from the magnetic field; (2) limited access to and view of the patient within the magnet bore; (3) malfunction of monitoring equipment, or interference, produced by the changing magnetic field gradients and rapidly switching radiofrequency currents;. (4) degradation of image and spectral quality arising from stray radiofrequency currents produced by monitoring equipment and leads.

*Location of the anaesthetic equipment*

The principal decision to be made by the anaesthetist concerns the location of the anaesthetic machine, ventilator and monitoring equipment in relation to the magnet. This will depend upon the strength of the magnetic field and the type of magnetic field shielding in use [1].

At present, however, there are two possible options, the choice of which may be dictated by the layout of the magnet suite.

*Outside the magnetic field.* All anaesthetic and monitoring equipment may be kept outside the magnetic field (or Gauss) line at which attraction of ferromagnetic items is likely to occur. This is normally between the 30 and 50 Gauss lines. The distance of these lines from the centre of the magnet depends on field strength and shielding [1]. If the anaesthetic machine, monitoring equipment and ventilator are sited several metres from the magnet face, long monitoring leads and ventilation tubing, with a large compressible volume in the circuit, are required. There is an increased risk of disconnection and ideally two anaesthetists should be present, one by the magnet bore close to the patient and the other to observe the equipment. If two anaesthetists are not available, the second person should be an appropriately trained anaesthetic assistant.

*Close to the magnet.* The anaesthetic and monitoring equipment may be sited close to the magnet bore, in which case the anaesthetic machine and its components must be non-ferromagnetic. Monitoring equipment powered by an unfiltered mains supply may introduce interference. If battery powered units are used they should be in a permanently fixed, secure position since batteries are strongly magnetic. Once the examination has started, the position of the anaesthetic machine should not be changed because the repositioning of a large metallic mass may degrade magnetic field homogeneity.

New developments in magnet design are likely to help the anaesthetist in future. The trend in imaging is to move to lower field strengths. Open magnets are being built, in which the patient is placed between pillars within the field, rather than into the enclosed tube of a magnet bore. In these open systems, access, visualisation and monitoring of the patient will be greatly improved.

*Review of existing literature*

Authors from a number of MRI centres have described various modifications to existing anaesthetic equipment. The first report of anaesthesia in an MR scanner was from Geiger and Cascorbi [5] who sited the anaesthetic machine in the MR control room distant from the magnet and allowed the patient to breathe spontaneously while anaesthesia was maintained by the intravenous route. A simple breathing system for manual ventilation of children, composed of corrugated tubing up to 16 m long, connected to a Laerdal self-inflating bag with a nonrebreathing valve, was described by Liao *et al.* [6]. Boutros and Pavlicek reported the use of a Mapleson D system, with oxygen delivered from 6 m away by several connected tubes [7]; coaxial Mapleson D circuits have been used elsewhere [8,9]. Neumark *et al.* used a Siemens Servo 900-D ventilator placed more than 7 m away, in both adults and children and employed nomograms to calculate the volume of compressed gas lost in the 9 m long tubing [10].

Mirvis *et al.* used an unmodified Siemens Servo 900-C ventilator, placed 1.2 m from the bore of a 1.5 T magnet, for both adults and children. The positive end-expiratory pressure (PEEP) valve of the Servo 900-C is of a solenoidal

type which may be affected by the magnetic field and can malfunction if placed closer than this to the magnet [11].

Cady *et al.*, who were investigating birth asphyxiated infants, modified a conventional transport incubator and its ventilator to stand 3 m away from a 1.9 T magnet [12]. McGowan and Erenberg ventilated neonates with a modified Bio-Med Devices MVP-10 ventilator which was sited 3 m away in a 0.5 T magnet [13].

Prien *et al.* used a commercial anaesthetic machine and breathing system with minor modifications, situated close to the magnet bore [14].

Rejger *et al.* sited their anaesthetic machine close to the 100 Gauss line and ventilated the patient through a specially adapted breathing system attached to a Drager Oxylog ventilator which has no ferromagnetic components [15].

Dunn *et al.* used a fluidic ventilator close to the magnet bore to passively ventilate the lungs of volunteers [16]. This ventilator was subsequently modified to become the MRI compatible (Monoghan Medical Corp., Plattsburg, NY) which Smith and colleagues used in conjunction with anaesthesia maintained using a total intravenous technique [17]. This ventilator has also been used in other centres [18–20]. Barnett *et al.* incorporated a Puritan–Bennet ventilatory pressure alarm [19] which has magnetic components, therefore the ventilator was sited outside the magnet room. This modified ventilator was also used by Karlik *et al.*, who, in addition, modified an Ohmeda anaesthetic machine. Magnetic parts were replaced with nonmagnetic grade stainless steel and ferromagnetic oxygen cylinders with aluminium ones [20].

A modified Foregger Model BC anaesthetic machine has also been used within 1 m of a 1.5 T magnet [21]. Ferromagnetic castors and support struts were replaced with stainless steel and aluminium counterparts and again, aluminium cylinders were used.

A fully integrated ventilatory and monitoring system, complete within its own Faraday shield to reduce radiofrequency electromagnetic emission, for use with a 2.35 T magnet was described by Boesch *et al.* [22,23].

### Current management of anaesthesia and sedation

We have experiences of imaging patients at two different magnetic field strengths, 0.15 T and 1.6 T. The latter system is a prototype magnet which is used principally for spectroscopy research, and our practice has been developed mainly around this system. This account is intended to assist those anaesthetists who wish to purchase or modify equipment for regular use in an MR unit. However, patient management in a situation in which no specialised equipment is available is also described.

#### *Anaesthetic machine and mechanical ventilator*

We have sited the anaesthetic machine and monitoring equipment between the 5 Gauss and 30 Gauss lines (8–9 m from the patient's head) because of the design of this prototype 1.6 T magnet. We use an unmodified Excel 210 (Ohmeda: Hatfield, UK) anaesthetic machine which is supplied by a piped gas installation. Ohmeda now make a modified version of the Ohmeda XL 210 for MRI use which is nonmagnetic. It is 99.1% nonmagnetic by weight, has aluminium cylinders and includes an MRI compatible oxygen monitor. It has been tested with a 1.5 T system at a field of approximately 2300 G and its performance, and that of the Fluotec 4 vaporizers, were within normal limits [24,25]. No degradation of image quality was noted. The system, which costs about £9500 (May 1991), is now available in the UK. However, at present, aluminium gas cylinders are not readily available in the UK (written communication to Ohmeda/BOC March 1991). Penlon, PneuPac (Luton, Bedfordshire, England) and Siare Hospital (S.R.L., Bologna, Italy) are also manufacturing nonmagnetic anaesthetic apparatus.

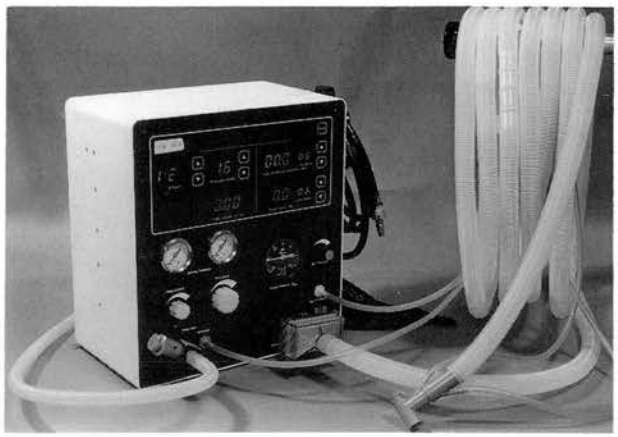


**Fig. 1.** The CW 200A ventilator with extended disposable tubing.

We have used either a Penlon Nuffield Series 200 or the new CW 200 ventilator [26] (Fig. 1). Both ventilators are suitable for adults, children and neonates (with the addition of a Newton valve to the Nuffield 200). The Nuffield 200 behaves as a pressure generator [27], therefore any reduction in compliance or increase in resistance at the patient end of the system leads to a reduction in ventilatory volume. This is of particular concern in the MR environment when the patient's chest wall movement is not visible, and very long breathing circuits are being used. We found that the maximum mouth pressure generated by the Nuffield 200 attached to a 10 m long Bain system was 45 $cmH_2O$. Since the safety valve blows off at pressures above this, the system is unsuitable for use in adults with noncompliant lungs. The CW 200 has the advantage of being a valveless ventilator, therefore if the casing was plastic, it could be taken safely to the edge of the magnet bore. The CW 200 has the characteristics of a pressure generator, but with features which increase its safety. Tidal and minute volumes are continuously displayed and calculated from the expired volume and the machine maintains a constant volume using a servo system. Variable PEEP can be applied without the addition of a separate valve, therefore it is more suitable for use in critically ill patients in whom PEEP is required. Hatch *et al.* [28] compared the Nuffield 200 and the CW 200 for use with a T-piece in paediatric anaesthesia. They found that the CW 200 caused a greater reduction in end-tidal $CO_2$ values at the same tidal volumes as the Nuffield 200. This may have the additional advantage of avoiding barotrauma [26].

#### *Breathing systems*

We have used a noncoaxial Mapleson D system, and a coaxial Mapleson D (Bain) system, both of which were approximately 10 m long. The extended Bain system

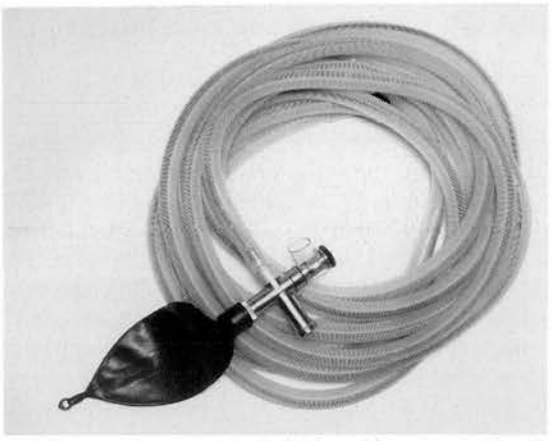


**Fig. 2.** A coaxial Mapleson D (Bain) breathing system, 10 m long.

(Fig. 2) was supplied by the manufacturer (Penlon Limited, Abingdon, UK). Concern has been expressed about increased expiratory resistance with the Bain system [18]. We measured expiratory pressures both in the noncoaxial Mapleson D system and the Bain system and found them to be 0.33 $cmH_2O.m^{-1}$ and 0.5 $cmH_2O.m^{-1}$ respectively. Therefore, at a length of 10 m an extra 1.7 $cmH_2O$ expiratory resistance is generated by the Bain system. When the Heidbrink valve was included in the Bain system the expiratory resistance rose to 0.6 $cmH_2O.m^{-1}$. These pressures were measured at a flow of 60 $l.min^{-1}$ which can be achieved in critically ill patients with high minute volume requirements. We have used the Bain system only in conjunction with the Penlon-Nuffield 200 ventilator to ventilate adults.

A modified T-piece system will permit either spontaneous respiration or manual ventilation in adults. This may be the method of choice when the environment of an

**Table 2.** Anaesthesia and ventilation in a magnetic resonance unit which is without modified ventilatory and monitoring equipment.

1. Do not administer anaesthesia until you are satisfied that there are no patient contraindications to an MR examination (Table 2, Part I of this paper [1]).
2. Ensure that you are familiar with the MR installation, including the extent of fringe fields and RF shielding (Table 2, Part I of this paper [1]).
3. Ensure that the equipment needed for the technique chosen (such as the one below) is available. You may need time to modify existing equipment (see 7 below).
4. Position the anaesthetic machine well outside the 50 Gauss line.
5. Induce anaesthesia and intubate the patient's trachea outside the magnetic field.
6. Allow the patient to breathe spontaneously or ventilate by hand with oxygen and air, or oxygen and nitrous oxide using a modified T-piece system.
7. Maintain anaesthesia with either a volatile agent or with intermittent drug doses or an infusion. Infusion pump must be sited outside the 30 Gauss line and extension tubing is required. If possible, avoid moving metallic equipment once the scan has begun.
8. Monitor with an oesophageal stethoscope, a finger on the pulse if possible (the dorsalis pedis is usually accessible), a clearly visible marker object placed on the chest to observe respiratory movement, and, if a second trained person is available, a capnograph with extended tubing sited on the anaesthetic machine. Try to acquire extended tubing and plastic connectors for an automated BP monitor.
9. Remove the patient from the magnet bore before reversing neuromuscular blockers or discontinuing anaesthesia.

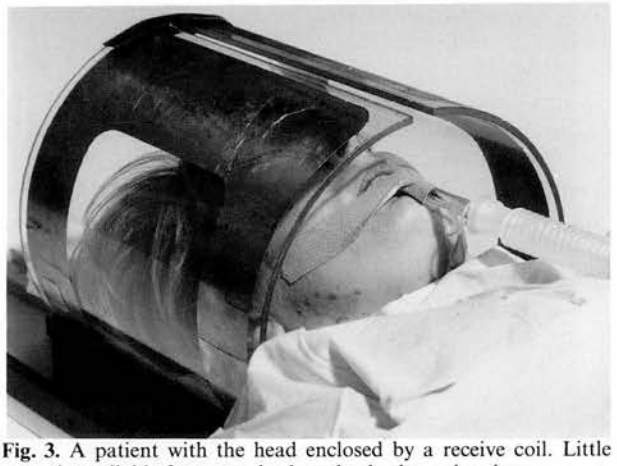


**Fig. 3.** A patient with the head enclosed by a receive coil. Little space is available for a standard tracheal tube and catheter mount, a RAE tube minimises this problem and facilitates placement of anaesthetic tubing.

MR unit is unfamiliar and no provision has been made for anaesthesia (Table 2). A T-piece system and a length of disposable oxygen tubing can be attached to the fresh gas outlet of an anaesthetic machine sited well outside the 50 Gauss line. We have had no problems with lengths up to 10 m and at this distance from the magnet oxygen cylinders can be changed safely if piped gases are unavailable. Further management is discussed elsewhere in the text. Other centres have used an extended Bain system [8,9]. Both the coaxial Mapleson D and noncoaxial Mapleson D breathing systems are cumbersome to store and, because of the long lengths of tubing, should be meticulously checked before use.

### *Airway management*

We consider that the airways of anaesthetised or unconscious individuals should be maintained with a tracheal tube since the patient is not visible in the magnet bore and the head is inaccessible. The use of a RAE tube facilitates the placement of ventilation tubing [18]. In some magnet systems, in which a receive coil encloses the patient's head (Fig. 3), there may be insufficient space for a standard tracheal tube and catheter mount to be used. All catheter mounts and connectors should be plastic to avoid the production of artifacts on images. The use of the laryngeal mask has been reported but this requires further evaluation [29].

### *Miscellaneous equipment*

Once the patient is in the magnet bore there is no movement of any part of the magnet system, but the patient may be disturbed by the banging noise produced by gradient operation during the scan. Magnet compatible headphones or ear plugs are available, and some form of ear protection may be advisable for the unconscious patient since there have been reports of hearing loss [30]. Patient comfort is important. We have adaped a 'Spenco' mattress (Spenco-Medical, Haywards Heath, Sussex) to minimise the possibility of pressure sores developing in critically ill patients during prolonged examinations.

*Needles and intravenous cannulae.* Most are made of high grade stainless steel which is not attracted by the magnetic



**Fig. 4.** Transverse magnetic resonance image of the head of a spontaneously breathing, intubated patient, who is using accessory muscles for ventilation. Artifacts result from head movement secondary to respiratory effort.

field. However, any new items of unknown content should be carefully tested for magnetic attraction before use.

*Infusion pumps.* The motor of an infusion pump may be damaged by the high magnetic field and result in pump malfunction. Karlik *et al.* tested an IVAC 530 pump and found this to be accurate to within 1% when sited 2 m from the face of a 1.5 T magnet [20]. We have used IVAC 710/711 and IMED 960/960A infusion pumps, in a magnetic field of approximately 30 Gauss, and found them to function accurately. The use of Vygon Lectro-Spiral (Vygon (UK) Ltd, Cirencester) extension sets eliminates the problems of trailing lines but permits them to be stretched.

*Anaesthetic techniques*

Anaesthesia can be maintained by a total intravenous technique [5,15,17], and we have had experience with propofol infusions. A volatile agent may also be used [15] although there is a possibility that general anaesthesia itself may alter the MRI signal from the brain [31]. The output of Cyprane TEC III and Fluotec-4 vaporizers have been tested and appear to be unaffected by the magnetic field [20,25]. The choice of spontaneous or controlled ventilation can be made by the individual anaesthetist. It is important to incorporate some form of disconnection alarm (airway pressure and end-tidal $CO_2$), since there is always a danger of distant disconnection.

In patients with ventilatory problems, neuromuscular blockade and controlled ventilation is preferable, not only for the benefit of improved gas exchange. Excessive neck and head movements associated with obstructed or inadequate respiration may render the imaging examination useless (Fig. 4).

The need for sedative premedication should be reviewed on an individual basis. Many seriously ill patients may be referred to the unit as day cases and may have raised intracranial pressure. Removal of secretions will not be possible when the patient is in the magnet bore. The use of glycopyrronium should be considered since it is a more effective antisialogogue than atropine, has a longer duration of action and produces less tachycardia.

*Sedation*

Sedation is used in many centres to facilitate examination in children. Keeter *et al.*, in a review of current practices of paediatric sedation for computerised tomography (CT) in the USA, suggest that more than 80% of toddlers are sedated for CT [32]. An anaesthetist was involved in less than 1% of cases and in 47% of responding hospitals the sedation was prescribed by the radiologist. Commonly, the sole form of monitoring of both lightly and deeply sedated children was visual inspection from the control room and in only 11% of hospitals was any type of electromechanical monitoring device used. Current practice therefore appears to be far from ideal and has been the subject of two recent editorials [33,34]. It is probable that an even higher percentage of children will be sedated for MRI, since the examination time is longer than for CT. For reasons already stated, monitoring during MRI is difficult. Resuscitation equipment and an oxygen supply should be at hand, but for safety reasons may be inaccessible, so that when required, oxygen tubing and leads may be of insufficient length.

In this department, only two critical incidents have been recorded, out of a total of 600 or more infants and small children who have received sedation for MRI or MRS. It is usual practice for the sedation to be prescribed by the referring paediatrician, using oral chloral hydrate in a dose ranging from 30–100 $mg.kg^{-1}$ [35,36]. Although this dose is in excess of that recommended by the *British National Formulary* (20–30 $mg.kg^{-1}$) it does produce a predictable level of sedation, mostly without complications. This is an important consideration in a busy radiological unit. The institution of adequate monitoring has generally confirmed, and improved, the safety of this regimen. Temazepam syrup may provide equally satisfactory levels of sedation.

In this department, neonates are not sedated, but are fed before the examination, wrapped well and placed prone within the magnet. The majority settle quickly and sleep through the study. Infants are also placed prone or on their side. Older children and adults may be examined in the supine position, but if there is concern over the airway the possibility of lateral positioning should be discussed with the radiologist. Radiologists should consult an anaesthetist about problem patients and there may be situations in which anaesthesia may be considered the safest option. Initially, examinations in this department were performed with an apnoea alarm only. Pulse oximetry and ECG is now applied by the radiographers and more than 100 infants have been monitored (with the use of radiofrequency filters) without any deterioration in the quality of images produced. The case for giving supplementary oxygen to sedated infants has been convincingly argued [34].

## Cardiopulmonary resuscitation

It is impossible to manage a cardiopulmonary arrest in the bore of a magnet, therefore the patient must immediately be removed from the bore and out of the magnetic field. It is essential that staff in an MR unit practice a cardiac arrest

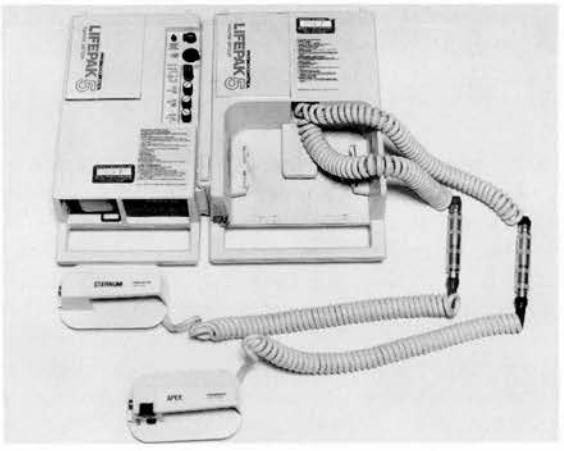


**Fig. 5.** Defibrillator, (Lifepak 5, Physio Control International) with leads to the paddle modified by the manufacturer, to double their length to 4 m.

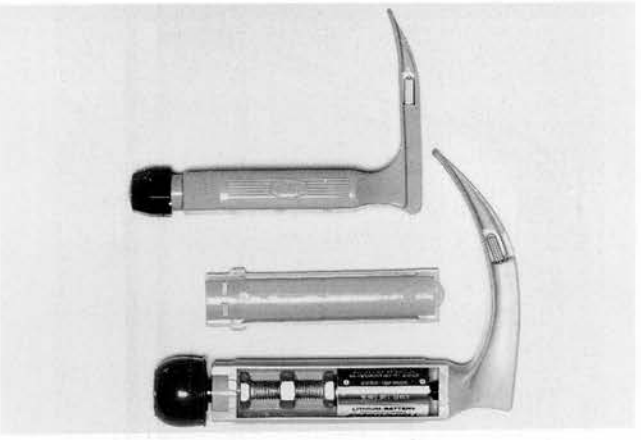


**Fig. 6.** Plastic laryngoscopes (Penlon) powered by a single paper covered, nonmagnetic 3 V lithium battery. A nonmagnetic aluminium spacer is required to hold the single battery in place.

drill and that each member is assigned to a particular rôle. If the hospital cardiac arrest team is called, all ferromagnetic items must be removed from them before they are allowed into the magnet suite.

*Defibrillators*

The unit used in this department (Lifepak 5, Physio-Control International, Basingstoke) is sited just outside the 5 Gauss line, since the batteries are ferromagnetic. The leads to the paddles have been lengthened to 4 m by the manufacturer and this has not decreased the power output (Fig. 5). The patient can be defibrillated within the magnetic field, but the defibrillator is kept at a safe distance from the magnet bore. There has been one report of defibrillator failure, when the defibrillator was kept at the edge of the magnetic field [37]. Regular testing has not revealed any reduction in its reliability or power output in the range of 20–360 J.

The cathode ray oscilloscope ECG trace on the defibrillator is distorted by the magnetic field but, in our experience, still provides adequate clinical data.

*Laryngoscopes*

Standard Macintosh laryngoscopes are metallic not ferromagnetic and therefore in high magnetic fields they undergo a degree of torque. The batteries, however, are highly magnetic. It has been suggested that a DC light source be used to solve this problem [20], but a simpler solution is to use a plastic Penlon laryngoscope (adult and paediatric) with a paper covered 3 V lithium battery. A nonmagnetic aluminium spacer is necessary to hold the single battery in place (Fig. 6). This adaptation is completely nonmagnetic and can be used even at the centre of the magnetic field.

*Resuscitators*

The Laerdal (Laerdal Medical Ltd, Orpington, Kent) adult and paediatric self-inflating silicone bags are valveless and have no magnetic working parts, therefore they can be safely used within a magnetic field.

*Suction apparatus*

A hand-held emergency suction apparatus (Vitalograph Ltd, Maids Moreton House, Buckingham, UK) is nonferromagnetic. The wall-mounted suction unit (Ohmeda) with 10 m extension tubing can also be used.

## Monitoring

Reliable and accurate monitoring is an essential component of the safe examination of an unconscious individual in an MR system, since the patient cannot be seen adequately and is not readily accessible to the anaesthetist.

The use of monitoring equipment is hindered by the problems already outlined and solutions to some of these have been discussed in previous papers [38,39]. Many manufacturers of MR equipment now make ECG and respiratory monitors compatible with their own systems, which are primarily used for respiratory and cardiac gating of imaging sequences but may in addition be used for monitoring. Although many of these cannot be relied on to provide any qualitative assessment of the ECG (manufacturers' product information will specifically disclaim any diagnostic attributes), they can still be used to provide an index of heart rate and serve as a gating signal for other monitoring equipment (e.g. pulse oximeters: see below). The use of fibreoptic [40] and telemetry systems [41] avoids the hazards of trailing cables.

*Burns.* Recent reports of burns resulting from current induction by the oscillating radiofrequency fields in monitoring leads are of concern [42,43], and adherence to the safe practice guidelines suggested in Part I is important [1].

*ECG*

The ECG of an individual situated within a static magnetic field shows significant changes [44]. According to Faraday's law, a voltage is induced across a column of conducting fluid (in this case blood) flowing through a magnetic field. The changes are maximal when the fluid flow is at 90° to the field, which occurs in a supine patient when blood flows through the transverse aorta, hence the changes are principally in leads I, II, $V_1$ and $V_2$ [45]. These superimposed potentials are greatest in the early T waves, and late ST

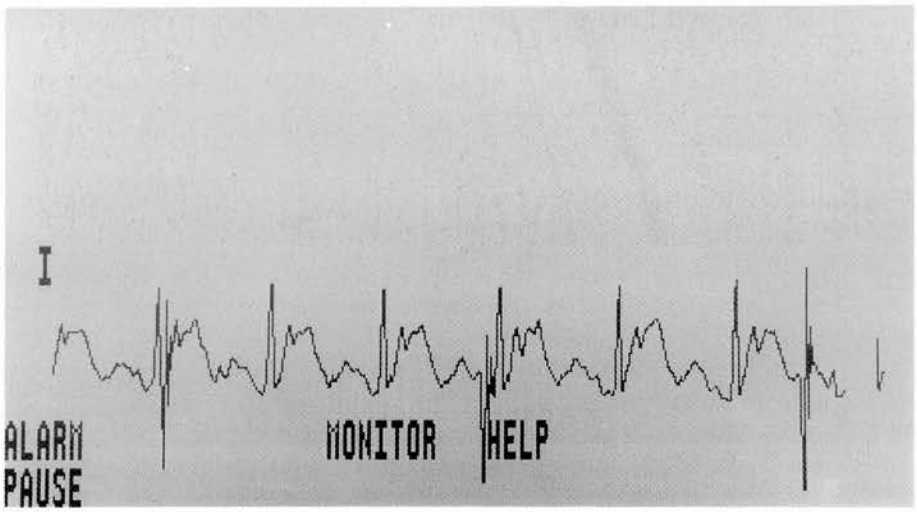



**Fig. 7.** ECG recorded from a healthy volunteer within the bore of a 1.6 T magnet. The T wave and ST abnormalities, caused by the voltage induced by blood flow, are clearly shown. The changing magnetic fields of the imaging gradients have produced spike artifacts superimposed on the ECG.

segments and can mimic the ECG changes of conditions such as hyperkalaemia and pericarditis (Fig. 7). They are related to field strength and hence increase as this increases.

The rapidly changing magnetic fields of the imaging gradients also induce potential differences across the loops formed by the ECG leads. Artifacts produced by the pulsing of the gradients can appear as spikes on the ECG and can be of sufficient magnitude to be detected and interpreted as an R wave. They cause interference with cardiac gating and an artificially elevated heart rate on the ECG monitor (Fig. 7).

The radiofrequency currents used to excite the nuclei during MRI can cause induction of currents within leads and cables and produce artifacts on the ECG. This problem can be ameliorated by the use of shielded cables [1]. Another solution is to transmit the ECG data by telemetry [41], lossy transmission lines [46] or a fibreoptic system [40].

The use of electrodes or leads which contain metal will exacerbate the problem of current induction in addition to producing image artifacts [47]. We have successfully used carbon fibre leads (NDM Division, American Hospital Supply Corporation, Dayton, Ohio, USA), similar to those described by van Genderingen *et al.* [48]. Some ECG electrodes are magnetic, but 'Red Dot' (3M Medical, St. Paul, Minnesota) and Medicotest (Medicotest A/S, Olstykke, Denmark) do not appear to cause interference.

Careful placement of the ECG electrodes and leads can minimise the ECG changes produced by the static and changing magnetic fields. The recommendations of Wendt *et al.* [47] and Dimick *et al.* [45] are summarised here: (1) braid or twist the leads to reduce the loops across which potential differences can be generated; (2) place the ECG electrodes as close as possible to the centre of the magnetic field since the gradients should be changing least at this point; (3) if possible keep the limb electrodes close together and in the same plane; (4) when using the chest leads, $V_5$ and $V_6$ are least likely to develop and record artifacts because they are close to the QRS axis, and far from the voltage induced by blood flow through the transverse aorta.

Two other points are worth noting. The relative length of ECG leads may be critical in preventing gradient-induced artifact, therefore many manufactures advise against modifying ECG leads supplied with MR systems. If a cathode ray tube ECG monitor is used the magnetic field will pull the beam of electrons off centre and distort the trace. A liquid crystal display screen, such as that used in the Marquette (Marquette Electronics Inc., Bewdly, Worcs.) 'TRAM' system, does not undergo distortion and provides a clear backlit display.

Pulse plethysmography [49] and standard vascular Doppler systems [39] have also been used to show heart rate and assess peripheral perfusion.

### *Pulse oximetry*

Pulse oximetry has proved to be the most difficult monitor to use within magnetic fields. The problems and possible solutions are summarised in Table 3.

We originally tested four pulse oximeters in our 1.6 T magnet; the Nellcor N-100, the Nellcor N-200, the Datex OSP-200 and the Ohmeda Biox 3700. The Nellcor N-200 consistently gave the best performance, and we have now used it on approximately 100 patients, including preterm neonates and adults with poor peripheral perfusion.

There are several reasons that may account for the Nellcor N-200's performance in the MR environment. All the pulse oximeter leads were passed through radiofrequency filters. The Nellcor is the only oximeter in which the signal is amplified by a nonmagnetic pre-amplifier before it is passed through the filters, therefore there is less loss of signal during filtering. It also has an ECG locking facility which improves detection of the pulse waveform when interference is present (Fig. 8). In addition, the standard Nellcor probes have no magnetic components, therefore they do not require modification.

McArdle *et al.* used Nellcor N-100 and Ohmeda Biox pulse oximeters for neonates [36]. They found slight image degradation with the Nellcor and significant loss of quality with the Ohmeda Biox. We noted no change in spectral or image quality when the leads were passed through the




**Fig. 8.** Nellcor N-200 pulse oximeter in use during a magnetic resonance imaging examination. The ECG lock facility (QRS complex symbol) is in use, helping to detect the pulse waveform when interference is present.

radiofrequency filters. Aluminium foil has been used to increase the shielding of the pulse oximeter probe [50]. We originally used variable length plastic radiofrequency shielding (Alpha Wire Corporation, USA) to enclose leads. However, we found the use of radiofrequency filters alone to be satisfactory, provided that an ECG signal was available to gate out gradient artifact.

Karlik *et al.* tested Nellcor, Sensormedics and Ohmeda Biox pulse oximeters and, in contrast to our experience, found the Ohmeda Biox 3700 to give the best results. They noted radiofrequency interference even with the oximeter cable shielded and suggested using an optical link for the infrared signal [20].

The Nonin 8604 (Cardiokinectics, Salford) is a new MR-compatible pulse oximeter. After limited testing we found it performed well. It provided continuous data during imaging and there was no image degradation. This unit is now available with a fibreoptic sensor (8604FO) which should further improve data quality and reduce the risk of radiofrequency-induced burns.

### *Capnography*

We have successfully used an Ohmeda 5200 capnograph sited at a distance of 11 m from the patient's head, although the lag and alarm times are about 10 s. The wave form shows a prolonged upslope (Fig. 9), even in individuals with healthy lungs, because of the long gas pathway. Although end-tidal concentrations of $CO_2$ are not accurate, trends can be observed and the respiratory rate estimated.

A nasal catheter has been used to monitor end-tidal carbon dioxide in spontaneously breathing patients [51]. We have found this technique useful in sedated infants. A 14-gauge cannula inserted into one limb of nasal oxygen prongs has also been used to monitor expired $CO_2$, in sedated patients [52]. The use of a commercially available capnograph (8800 Capnometer, Biochem International) and respiration monitor (515 Respiration monitor, Biochem International) has also been described [53].

### *Noninvasive blood pressure*

Satisfactory NIBP readings are obtained if the ferrous connections on a standard automated (Dinamap) cuff are changed to nylon and the tubing is lengthened as necessary.

### *Invasive pressure monitoring*

Direct pressure readings can be obtained if the lead from the pressure transducer is passed through a radiofrequency filter. The transducers must be kept close to the patient (within 1.5 m) so that damping caused by excessively long saline filled columns, is prevented [19]. The waveforms are displayed on our Marquette 'TRAM' monitor liquid crystal display, without any loss of accuracy of reading or damping of the trace. This is to be expected since the radiofrequency filters are filtering from the kilohertz range upwards, while the clinical waveforms have harmonics below 100 Hz. Intracranial pressure monitoring has been described using nonmetallic subarachnoid bolts [19].

### *Precordial/oesophageal stethoscopes*

These may be unsatisfactory because of the length of tubing required and the fact that the noise made by the gradients changing during the examination may obscure the heart and breath sounds.

**Table 3.** Problems encountered in the use of pulse oximetry with magnetic resonance systems and some possible solutions.

| | |
|---|---|
| 1. *Degradation of pulse oximetry signal by MR* | |
| *Problem* | *Solution* |
| Poor signal due to movement | Careful selection of site and placement of probe. |
| Poor perfusion or contact | |
| Induced currents in cable | Screen cable.<br>Minimise cable length. |
| Poor signal/noise ratio | Amplify signal early. |
| 2. *Degradation of MRI by pulse oximeter* | |
| *Problem* | *Solution* |
| Metallic artifact on images | Remove all magnetic components from probe or use plastic/disposable probes. |
| Interference due to switched pulses | Screen cable. |
| Introduction of stray radiofrequency current by leads acting as aerials | Screen lead. Pass through radiofrequency filters, or keep unit within radiofrequency screened room. |

[12] CADY EB, DAWSON MJ, HOPE PL, TOFTS PS, COSTELLO A MDEL, DELPY DT, REYNOLDS EOR, WILKIE DR. Non-invasive investigation of cerebral metabolism in newborn infants by phosphorus nuclear magnetic resonance spectroscopy. *Lancet* 1983; **1:** 1059–62.
[13] MCGOWAN JE, ERENBERG A. Mechanical ventilation of the neonate during magnetic resonance imaging. *Magnetic Resonance Imaging* 1989; **7:** 145–8.
[14] PRIEN T, MIELE B, BONGARTZ G, WENDT M. Magnetresonanztomographie: ein patientennahes System für Beatmung und Überwachung. *Anaesthesist* 1989; **38:** 323–6.
[15] REJGER VS, COHN BF, VIELVOYE GJ, DE RAADT FB. A simple anaesthetic and monitoring system for magnetic resonance imaging. *European Journal of Anaesthesiology* 1989; **6:** 373–8.
[16] DUNN V, COFFMAN CE, MCGOWAN JE, EHRHARDT JC. Mechanical ventilation during magnetic resonance imaging. *Magnetic Resonance Imaging* 1985; **3:** 169–72.
[17] SMITH DS, ASKEY P, YOUNG ML, KRESSEL HY. Anesthetic management of acutely ill patients during magnetic resonance imaging. *Anesthesiology* 1986; **65:** 710–11.
[18] NIXON C, HIRSCH NP, ORMEROD IEC, JOHNSON G. Nuclear magnetic resonance. Its implications for the anaesthetist. *Anaesthesia* 1986; **41:** 131–7.
[19] BARNETT GH, ROPPER AH, JOHNSON KA. Physiological support and monitoring of critically ill patients during magnetic resonance imaging. *Journal of Neurosurgery* 1988; **68:** 246–50.
[20] KARLIK SJ, HEATHERLEY T, PAVAN F, STEIN J, LEBRON F, RUTT B, CAREY L, WEXLER R, GELB A. Patient anesthesia and monitoring at a 1.5-T MRI installation. *Magnetic Resonance in Medicine* 1988; **7:** 210–21.
[21] RAO CC, MCNIECE WL, EMHARDT J, KRISHNA G, WESTCOTT R. Modification of an anesthesia machine for use during magnetic resonance imaging. *Anesthesiology* 1988; **68:** 640–1.
[22] BOESCH C, MARTIN E. Combined application of MR imaging and spectroscopy in neonates and children: installation and operation of a 2.35-T system in a clinical setting. *Radiology* 1988; **168:** 481–8.
[23] BOESCH C, LUESCHER K, BRUNNER P, DANGEL P, MARTIN E, KEWITZ G, KIKINIS R. A comprehensive scheme for the care and surveillance of critically ill, premature and anaesthetised patients during high field MR examinations. Society for Magnetic Resonance in Medicine 1989 meeting, Amsterdam. Book of Abstracts p. 999.
[24] RAO CC, KRISHNA G, EMHARDT J. Anesthesia machine for use during magnetic resonance imaging. *Anesthesiology* 1990; **73:** 1054–5.
[25] RAO CC, KRISHNA G, BALDWIN S, ROBBELOTH R. Ohmeda (R) Fluotec-4 vaporizer output near MRI magnet. *Anesthesiology* 1990; **73:** A476.
[26] WHITWAM JG, CHAKRABARTI MK, KONARZEWSKI WH, ASKITOPOULOU H. A new valveless all purpose ventilator: clinical evaluation. *British Journal of Anaesthesia* 1983; **55:** 1017–23.
[27] NEWTON NI, HILLMAN KM, VARLEY JG. Automatic ventilation with the Ayre's T-piece. A modification of the Nuffield series 200 ventilator for neonatal and paediatric use. *Anaesthesia* 1981; **36:** 22–36.
[28] HATCH DJ, CHAKRABARTI MK, WHITWAM JG, BINGHAM RM, MACKERSIE AM. Comparison of two ventilators used with the T-piece in paediatric anaesthesia. *British Journal of Anaesthesia* 1990; **65:** 262–7.
[29] RAFFERTY C, BURKE AM, COSSAR DF, FARLING PA. Laryngeal mask and magnetic resonance imaging. *Anaesthesia* 1990; **45:** 590–1.
[30] BRUMMETT RE, TALBOT JM, CHARUHAS P. Potential hearing loss resulting from MR imaging. *Radiology* 1988; **169:** 539–40.
[31] WHITFIELD A, DOUGLAS RHB. Effect of general anaesthesia on the magnetic resonance imaging signal from the brain. *British Journal of Anaesthesia* 1989; **62:** 694–6.
[32] KEETER S, BENATOR RM, WEINBERG SM, HARTENBERG MA. Sedation in pediatric CT: national survey of current practice. *Radiology* 1990; **175:** 745–52.
[33] COHEN MD. Pediatric sedation. *Radiology* 1990; **175:** 611–2.
[34] FISHER DM. Sedation of pediatric patients: an anesthesiologist's perspective. *Radiology* 1990; **175:** 613–5.
[35] LEVENE MI, WHITELAW A, DUBOWITZ V, BYDDER GM, STEINER RE, RANDELL CP, YOUNG IR. Nuclear magnetic resonance imaging of the brain in children. *British Medical Journal* 1982; **285:** 774–6.
[36] MCARDLE CB, NICHOLAS DA, RICHARDSON CJ, AMPARO EG. Monitoring of the neonate undergoing MR imaging: technical considerations. *Radiology* 1986; **159:** 223–6.
[37] SNOWDON SL. Defibrillator failure in a magnetic resonance unit. *Anaesthesia* 1989; **44:** 359.
[38] SHELLOCK FG. Monitoring during MRI. An evaluation of the effect of high-field MRI on various patient monitors. *Medical Electronics* 1986; **17:** 93–7.
[39] ROTH JL, NUGENT M, GRAY JE, JULSRUD PR, BERQUIST TH, SILL JC, KISPERT DB. Patient monitoring during magnetic resonance imaging. *Anesthesiology* 1985; **62:** 80–3.
[40] LEGENDRE JP, MISNER R, FORESTER GV, GEOFFRION Y. A simple fiber optic monitor of cardiac and respiratory activity for biomedical magnetic resonance applications. *Magnetic Resonance in Medicine* 1986; **3:** 953–7.
[41] ROKEY R, WENDT RE, JOHNSTON DL. Monitoring of acutely ill patients during nuclear magnetic resonance imaging: use of a time-varying filter electrocardiograph gating device to reduce gradient artifacts. *Magnetic Resonance in Medicine* 1988; **6:** 240–5.
[42] SHELLOCK FG, SLIMP GL. Severe burn of the finger caused by using a pulse oximeter during MR imaging. *American Journal of Roentgenology* 1989; **153:** 1105.
[43] KANAL E, SHELLOCK FG. Burns associated with clinical MR examinations. *Radiology* 1990; **175:** 585.
[44] MEZRICH R, REICHECK N, KRESSEL HY. ECG effects in high-field MR imaging. *Radiology* 1985: **157**(P): 219.
[45] DIMICK RN, HEDLUND LW, HERFKENS RJ, FRAM EK, UTZ J. Optimizing electrocardiograph electrode placement for cardiac-gated magnetic resonance imaging. *Investigative Radiology* 1987; **22:** 17–22.
[46] DAMJI AA, SNYDER RE, ELLINGER DC, WITKOWSKI FX, ALLEN PS. RF interference suppression in a cardiac synchronization system operating in a high magnetic field NMR imaging system. *Magnetic Resonance Imaging* 1988; **6:** 637–40.
[47] WENDT RE, ROKEY R, VICK GW, JOHNSTON DL. Electrocardiographic gating and monitoring in NMR imaging. *Magnetic Resonance Imaging* 1988; **6:** 89–95.
[48] VAN GENDERINGEN HR, SPRENGER M, DE RIDDER JW, VAN ROSSUM AC. Carbon-fiber electrodes and leads for electrocardiography during MR imaging. *Radiology* 1989; **171:** 872.
[49] SELLDÉN H, DE CHATEAU P, EKMAN G, LINDER B, SÄÄF J, WAHLUNDL-O. Circulatory monitoring of children during anaesthesia in low-field magnetic resonance imaging. *Acta Anaesthesiologica Scandinavica* 1990; *34:* 41–3.
[50] WAGLE WA. Technique for RF isolation of a pulse oximeter in a 1.5 T MR unit. *American Journal of Neuroradiology* 1989; **10:** 208.
[51] BONSU AK, TAMILARASAN A, BROMAGE PR. A nasal catheter for monitoring tidal carbon dioxide in spontaneously breathing patients. *Anesthesiology* 1989; **71:** 318.
[52] ROY J, MCNULTY S, TORJMAN M. An improved nasal prong apparatus for end-tidal carbon dioxide monitoring in the awake sedated patient. *Anesthesiology* 1989; **71:** A356.
[53] SHELLOCK FG. Monitoring sedated pediatric patients during MR imaging. *Radiology* 1990; **177:** 586–7.
[54] HÖK B, BYTHELL V, BENGTSSON M. Development of a wireless stethoscope for ausculatory monitoring during anaesthesia. *Medical and Biological Engineering and Computing* 1988; **26:** 317–20.
[55] HENNEBERG S, HÖK B, WIKLUND L, SJÖDIN G. Remote auscultatory patient monitoring during magnetic resonance imaging. *Journal of Clinical Monitoring* 1992; **8:** 37–43.